

# LAMINAR FLOW THROUGH SINUSOIDAL CHANNELS AND PIPES

by

PRABODH KUMAR MAJI

TH  
me/1986/m

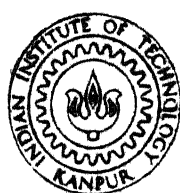
M288e

ME  
1986

M

MAJ

WAM



DEPARTMENT OF MECHANICAL ENGINEERING  
INDIAN INSTITUTE OF TECHNOLOGY KANPUR  
MAY, 1986

# **LAMINAR FLOW THROUGH SINUSOIDAL CHANNELS AND PIPES**

*A Thesis Submitted*  
**in Partial Fulfilment of the Requirements**  
**for the Degree of**

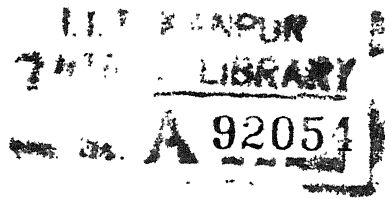
**MASTER OF TECHNOLOGY**

*by*  
**PRABODH KUMAR MAJI**

*to the*  
**DEPARTMENT OF MECHANICAL ENGINEERING**  
**INDIAN INSTITUTE OF TECHNOLOGY KANPUR**  
**MAY, 1986**

167 86

TH  
532.515  
M288l



ME-1986-M-MAJ-LAM

CERTIFICATE

Certified that the thesis entitled "Laminar Flow Through Sinusoidal Channels and Pipes" has been carried out by Prabodh Kumar Maji under my supervision and that it has not been submitted elsewhere for award of a degree.

I.I.T. Kanpur  
April, 1986.

( Dr.Vijay K. Garg )  
Professor  
Department of Mechanical Engineering  
INDIAN INSTITUTE OF TECHNOLOGY  
KANPUR

## ACKNOWLEDGEMENT

I have great pleasure to express my deep regards, whole-hearted gratitude and thanks to my respected teacher and thesis supervisor Dr. V.K. Garg, Professor, Department of Mechanical Engineering, I.I.T. Kanpur, for initiating me into this interesting problem and giving necessary guidance, constant inspiration and encouragement throughout my stay at I.I.T. Kanpur. I was deeply impressed by his meticulousness, systematic approach and above all total devotion into his work.

I wish to thank the members of the Mechanical Engineering faculty for their kind interest and encouragement.

The author is also indebted to his friend Mr. N.Chowdhury Mr. B.K. Rakshit, and Mr. K. Sen for their kind help. He also thanks all his friends for helping him throughout his stay over here.

Finally the author wants to thank Mr. G.L. Misra for his excellent typing of the manuscript.



( Prabodh Kumar Maji )

I.I.T. Kanpur  
April 1986.

## CONTENTS

| Chapter |   | Page No. |
|---------|---|----------|
|         | NOMENCLATURE  | v        |
|         | LIST OF FIGURES                                     | xii      |
|         | ABSTRACT  | xviii    |
| 1       | INTRODUCTION  | 1        |
| 2       | ANALYTICAL FORMULATION                              | 5        |
| 2.1     | Description of the Problem                          | 5        |
| 2.2     | Conservation Equations                              | 7        |
| 2.3     | Formulation for Symmetric Channel and Pipe          | 8        |
| 2.4     | Formulation for Non-symmetric Channel               | 28       |
| 3       | FINITE DIFFERENCE SOLUTION                          | 35       |
| 3.1     | Domain Discretization                               | 35       |
| 3.2     | Discretized Equations for Symmetric Channel or Pipe | 37       |
| (a)     | Discretization of U-momentum equation               | 37       |
| (b)     | Discretization of $U_\xi$ -momentum equation        | 51       |
| (c)     | Discretization of energy equation                   | 58       |
| (d)     | Discretization of Continuity equation               | 62       |
| (e)     | Under-relaxation                                    | 62       |
| (f)     | Derivation of pressure-correction equation          | 64       |
| 3.3     | Discretized Equations for the Non-symmetric Channel | 70       |
| (a)     | Discretization of U-momentum equation               | 70       |
| (b)     | Discretization of $U_\xi$ -momentum equation        | 72       |
| (c)     | Discretization of energy equation                   | 75       |
| (d)     | Discretization of Continuity equation               | 77       |
| (e)     | Pressure Correction equation                        | 77       |

| Chapter | Page No.                     |
|---------|------------------------------|
| 4       | RESULTS AND DISCUSSION 79    |
| 4.1     | For Symmetric Channel 80     |
| 4.2     | For Pipe 82                  |
| 4.3     | For Non-Symmetric Channel 84 |
| 5       | CONCLUSIONS 147              |
|         | APPENDIX 150                 |
|         | REFERENCES 153               |

## NOMENCLATURE

|                             |   |
|-----------------------------|---|
| A                           | Convection diffusion function [e.g. Eq. (3.2.14)]   |
| a                           | Coefficient of different equations; also a vector quantity  |
| B                           | Source term for pressure correction equation<br>[e.g. Eq. (3.2.91)]   |
| b                           | Source term   |
| $b_u$                       | Source term for U-momentum equation   |
| $b_v$                       | Source term for $U_\xi$ -momentum equation  |
| $b_H$                       | Source term for energy equation   |
| $C_p$                       | Specific heat of the fluid at constant pressure   |
| D                           | Diffusion coefficient; also coefficient of different equations  |
| DPIPE                       | Dimensionless width or diameter of a channel or pipe respectively   |
| d                           | Factor multiplying the pressure difference  |
| DXG(IX)                     | Difference in the $\eta$ -coordinate values between two adjacent grid nodes on a $\xi$ -constant line           |
| DXU(IX)                     | Difference in the $\eta$ -coordinate values between two adjacent U-locations on a $\xi$ -constant line          |
| DYG(IY)                     | Difference in $\xi$ -coordinate values between two adjacent grid nodes on an $\eta$ -constant line              |
| DYV(IY)                     | Difference in the $\xi$ -coordinate values between two adjacent $U_\xi$ -locations on an $\eta$ -constant line. |
| E                           | Relaxation factor ( $= \frac{\alpha_R}{1-\alpha_R}$ ) recommended by Van Doormaal and Raithby [12]              |
| $\vec{e}_x, \vec{e}_y$      | Unit vectors in X-Y directions  |
| $\vec{e}_\eta, \vec{e}_\xi$ | Unit vectors in $\eta - \xi$ directions   |
| F                           | Flow rate [e.g. Eq.(3.2.8)]   |

|          |  |
|----------|--|
| $F_1$    | Expansion factor (i.e. > 1) for grid step-length<br>in the $\eta$ -direction   |
| $F_2$    | Contraction or expansion factor for grid step<br>length in the $\xi$ -direction. < 1 for symmetric channel<br>> 1 for non-symmetric channel            |
| H        | Dimensional enthalpy ( $= \frac{h - h_w}{h_o - h_w}$ )   |
| h        | Dimensional enthalpy   |
| $h_o$    | Enthalpy at entrance to the duct   |
| $h_w$    | Wall enthalpy  |
| IX       | Grid line number for an $\eta$ -constant line  |
| IXM1     | IX-1   |
| IXP1     | IX+1   |
| IY       | Grid line number for a $\xi$ -constant line  |
| IYM1     | IY-1   |
| IYP1     | IY+1   |
| J        | Total heat flux, convection plus diffusion   |
| K        | Control index for Cartesian or cylindrical polar<br>(axi-symmetric) coordinate<br>= 1 for Cartesian coordinate<br>= 2 for cylindrical polar coordinate |
| $\kappa$ | Thermal conductivity of the fluid  |
| L        | Reference length   |
| LAMBDA   | Non-dimensional wall amplitude ( $= \lambda/L$ )   |
| $L_c$    | Cycle length of the wavy boundary  |
| NX       | Number of $\eta$ -constant grid lines in the flow domain   |
| NXM1     | NX-1   |
| NXM2     | NX-2   |

|                                     |  |
|-------------------------------------|--|
| $NX_1$                              | Number of non-uniformly spaced grid points in the $\eta$ -direction  |
| $NX_2$                              | Number of uniformly spaced grid points in the $\eta$ -direction  |
| $NY$                                | Number of $\xi$ -constant grid lines in the flow domain  |
| $NYD2$                              | $NY/2$   |
| $NYM1$                              | $NY-1$   |
| $NYM2$                              | $NY-2$   |
| $\vec{n}$                           | Unit vector along normal to surface  |
| $P, p$                              | dimensionless and dimensional pressure respectively  |
| $Pe$                                | Peclet number ( $= Pr \cdot Re$ )  |
| $Pr$                                | Prandtl number ( $= \mu C_p / K$ )   |
| $P_o$                               | Pressure at entrance to the duct   |
| $P^*$                               | Estimated Pressure   |
| $P'$                                | Pressure Correction  |
| $P'^o$                              | Best estimate of $P'$  |
| $Re$                                | Reynolds number ( $= \frac{\rho U_o L}{\mu}$ )   |
| $RPIPE$                             | Half width or radius of a channel or pipe respectively   |
| $S$                                 | Source containing pseudodiffusion terms; also control surface  |
| $S_b$                               | Combined source term ( $= S + b$ )   |
| $SHE, SHW,$<br>$SHN, SHS,$<br>$SHP$ | Source terms for energy equation, respectively, at east, west, north, south faces and at centre of a main control volume |
| $SPRIME_1,$<br>$SPRIME_2$           | Coefficient of $(U_\xi)_P$ , in linearized source term.  |
| $SUE, SUW,$<br>$SUN, SUS,$<br>$SUP$ | Source terms for U-momentum equation, respectively at east, west, north, south faces and at centre of a U-control volume |

|   |   |
|---|---|
| SVE, SVW,<br>SVN, SVS   | Source terms for $U_\xi$ -momentum equation at east, west, north and south faces of a $U_\xi$ -control volume |
| SVP, SVP <sub>1</sub> ,<br>SVP <sub>2</sub> , SVP <sub>3</sub> ,<br>SVP <sub>4</sub> , SVP <sub>5</sub> ,<br>SVP <sub>6</sub> | Source terms for $U_\xi$ -momentum equation at centre P* of a $U_\xi$ -control volume                         |
| SXG(IX)   | Distance separating the two constant $\eta$ cell walls of a cell around a node                                |
| SXU(IX)   | Distance separating the two constant $\eta$ cell-walls of a U-cell  |
| SYG(IY)   | Distance separating the two constant $\xi$ cell walls of a cell around a node                                 |
| SYV(IY)   | Distance separating the two constant $\xi$ cell-walls of a $U_\xi$ -cell                                      |
| $S_1, S_2, S_3, S_4$  | East, north, west and south face of a control volume (Fig. 2)   |
| $S_u, S_{U_\xi}, S_H$   | Source terms for U-momentum, $U_\xi$ momentum and energy equations respectively                               |
| $S_c'', S_c', S_c$  | Constant part of linearized source term for U-momentum, $U_\xi$ -moment and energy equation respectively      |
| $s_p'', s_p', s_p$  | Coefficient of $U_p''$ , $(U_\xi)_p'$ , $H_p$ in linearized source term respectively                          |
| $U, U_{X_1}$  | Velocity component in $X_1$ direction; dimensionless and dimensional respectively                             |
| $\vec{U}$   | Velocity vector   |
| $U_\eta, U_\xi$   | Velocity components in $\eta - \xi$ directions  |
| $U^*, U_\xi^*$  | Velocity based on P*  |
| $U', U_\xi'$  | Velocity correction   |
| $U_{X_2}, V$  | Velocity component in $X_2$ direction; dimensional and dimensionless, respectively                            |
| $\nabla$  | Control volume  |
| X, Y  | Dimensionless generalized Coordinates   |

|                                 |   |
|---------------------------------|---|
| XPIPE                           | Length of the pipe or channel   |
| X(IX)                           | $\eta$ -coordinate values of the $\eta$ -constant grid lines  |
| X(IXM1)                         | X(IX-1)   |
| X(IXP1)                         | X(IX+1)   |
| XU(IX)                          | $\eta$ -coordinate values of the $\eta$ -constant lines through the U-locations   |
| XU(IXM1)                        | XU(IX-1)  |
| XU(IXP1)                        | XU(IX+1)  |
| X <sub>1</sub> , X <sub>2</sub> | Generalized coordinate  |
| Y(IY)                           | $\xi$ -coordinate values of the $\xi$ -constant grid lines  |
| Y(IYM1)                         | Y(IY-1)   |
| Y(IYP1)                         | Y(IY+1)   |
| YV(IY)                          | $\xi$ -coordinate values of the $\xi$ -constant lines through the U <sub><math>\xi</math></sub> -locations                                    |
| YV(IYM1)                        | YV(IY-1)  |
| YV(IYP1)                        | YV(IY+1)  |
| $\alpha$                        | Geometric function ( $= 1+\beta^2$ )  |
| $\alpha_R$                      | Under-relaxation factor   |
| $\beta$                         | Geometric function<br><br>$= \xi \frac{d\delta}{d\eta}$ for symmetric channel and pipe<br>$= \frac{d\delta}{d\eta}$ for non-symmetric channel |
| $\beta_0$                       | Value of $\beta$ at entrance to the duct  |
| $\Gamma$                        | diffusion coefficient<br><br>$= 1/Re$ for momentum equations<br>$= 1/Pe$ for energy equations   |
| $\gamma$                        | Diffusion term ( $= -\delta \frac{\partial \psi}{\partial \eta}$ for symmetric channel)   |

|                |  |
|----------------|--|
| $\nabla$       | Delta operator   |
| $\Delta P$     | Percycle pressure drop   |
| $\delta'(x_1)$ | Function representing the wall of the duct   |
| $\delta(x)$    | Dimensionless form of $\delta'(x_1)$   |
|                | $= \frac{\delta'(x_1)}{L}$ for symmetric channel or pipe   |
|                | $= \frac{\delta'(x)}{L}$ for non-symmetric channel   |
| $\eta$         | Transformed coordinate ( $= x$ )   |
| $\Lambda$      | Pseudodiffusion term ( $= \beta \frac{\partial \phi}{\partial \eta}$ )   |
| $\mu$          | Viscosity  |
| $\xi$          | Transformed coordinate<br>$= Y/\delta(x)$ for symmetric channel or pipe<br>$= Y-\delta(x)$ for non-symmetric channel |
| $\rho$         | Density  |
| $\phi$         | General dependent variable   |
| $\Psi$         | Pseudodiffusion term ( $= \beta \frac{\partial \phi}{\partial \xi}$ )  |
| $\Omega$       | Diffusion term ( $= -\frac{\alpha}{\delta} \frac{\partial \phi}{\partial \xi}$ for symmetric channel)                |

### Subscripts

P, E, W, S, N, Main grid point locations  
SE, SW, NE, NW

P', E', W', S', U <sub>$\xi$</sub> -grid point locations  
N', SW', SE',  
NW', NE'

P'', E'', W'', S'', U-grid point location  
N'', SW'', SE'',  
NW'', NE''

e, w, n, s Main control volume faces (Fig. 10)

|             |   |
|-------------|---|
| s'', n''    | South and north faces of a U-control volume<br>(Fig. 8)   |
| w', e'      | West and east faces of a $U_\xi$ -control volume [Fig. 9] |
| nb          | neighbour points  |
| Superscript |   |
| ,           | $U_\xi$ -velocity locations                               |
| ''          | U-velocity locations                                      |

## LIST OF FIGURES

| Figure<br>No. |  | Page No. |
|---------------|--|----------|
| 1             | Types of channels and pipe<br>considered (one cycle only)  | 6        |
| a)            | Converging-diverging symmetric<br>channel  | 6        |
| b)            | Non-symmetric curved channel   | 6        |
| c)            | Converging-diverging pipe  | 6        |
| 2             | Shape of Control Volume for a<br>Symmetric Channel or Pipe   | 14       |
| a)            | Shape of Control Volume in<br>Physical Space   | 14       |
| b)            | Shape of Control Volume in<br>$\eta-\xi$ plane   | 14       |
| c)            | Shape of Control Volume Element<br>in Cartesian Coordinate ( $dZ = \text{unity}$ )   | 14       |
| d)            | Shape of Control Volume Element in<br>Cylindrical Coordinate ( $d\theta = \text{unity}$ )  | 14       |
| 3             | Shape of Control Volume for non-<br>symmetric Channel  | 30       |
| a)            | Shape of Control Volume in Physical<br>Space   | 30       |
| b)            | Shape of Control Volume element<br>( $dZ = \text{unity}$ )   | 30       |
| 4             | Type of Control Volume Considered  | 38       |
| 5             | Type of Control Volume at the<br>Boundary  | 38       |
| 6             | a) Complete picture of the Discretized<br>Computational Domain   | 39       |
| b)            | Various Grid Quantities  | 40       |
| 7             | a) Discretized Physical Domain for a<br>Symmetric Channel or Pipe (for 1st<br>Cycle only) With $\lambda/L = 0.10$ ,<br>$F_1=1.02$ , $F_2=0.98$ , $NX=58$ , and $NY=20$ | 41       |
| b)            | Discretized Physical domain for a<br>Non-Symmetric Channel (for 1st Cycle<br>only) with $\lambda/L=0.10$ , $F_1=1.02$ , $F_2=1.01$ ,<br>and $NY=20$                    | 41       |

| Figure<br>No.   | Page No. |
|---|----------|
| 8      U-Control Volume   | 43       |
| 9 $U_{\xi}$ -Control Volume   | 43       |
| 10     Main Control Volume  | 43       |
| 11     U-Velocity Profiles for a Symmetric Channel with $\lambda=0.10$ and $Re=100$   | 86       |
| 12     V-Velocity profiles for a Symmetric Channel with $\lambda=0.10$ and $Re=100$   | 87       |
| 13     Velocity Vectors in a Symmetric Channel with $\lambda=0.10$ and $Re=100$       | 88       |
| 14     Enthalpy Profiles for a Symmetric Channel with $\lambda=0.10$ and $Re=100$     | 89       |
| 15     U-Velocity Profiles for a Symmetric Channel with $\lambda = 0.10$ and $Re=500$ | 90       |
| 16     V-Velocity Profiles for a Symmetric Channel with $\lambda=0.10$ and $Re=500$   | 91       |
| 17     Velocity Vectors in a Symmetric Channel with $\lambda=0.10$ and $Re=500$       | 92       |
| 18     Enthalpy Profiles for a Symmetric Channel with $\lambda=0.10$ and $Re=500$     | 93       |
| 19     U-Velocity Profiles for a Symmetric Channel with $\lambda=0.20$ and $Re=100$   | 94       |
| 20     V-Velocity Profiles for a Symmetric Channel with $\lambda=0.20$ and $Re=100$   | 95       |
| 21     Velocity vectors in a Symmetric Channel with $\lambda=0.20$ and $Re=100$       | 96       |
| 22     Enthalpy Profiles for a Symmetric Channel with $\lambda=0.20$ and $Re=100$     | 97       |
| 23     U-Velocity Profiles for a Symmetric Channel with $\lambda=0.25$ and $Re=100$   | 98       |
| 24     V-Velocity Profiles for a Symmetric channel with $\lambda=0.25$ and $Re=100$   | 99       |

| Figure<br>No. | Page No.   |     |
|---------------|--|-----|
| 25            | Velocity Vectors in a Symmetric Channel with LAMBDA=0.25 and Re=100                  | 100 |
| 26            | Enthalpy Profiles for a Symmetric Channel with LAMBDA=0.25 and Re=100                | 101 |
| 27            | Velocity Vectors in a Symmetric Channel with LAMBDA=0.20 and Re=500                  | 102 |
| 28            | a) Pressure Distribution along X for a Symmetric Channel with LAMBDA=0.10 and Re=100 | 103 |
|               | b) Pressure Distribution along X for a Symmetric Channel with LAMBDA=0.10 and Re=500 | 103 |
| 29            | a) Pressure Distribution along X for a Symmetric Channel with LAMBDA=0.20 and Re=100 | 104 |
|               | b) Pressure Distribution along X for a Symmetric Channel with LAMBDA=0.25 and Re=100 | 104 |
| 30            | U-Velocity Profiles for a Pipe with LAMBDA=0.10 and Re=100                           | 105 |
| 31            | V-Velocity Profiles for a Pipe with LAMBDA=0.10 and Re=100                           | 106 |
| 32            | Velocity Vectors in a Pipe with LAMBDA=0.10 and Re=100                               | 107 |
| 33            | Enthalpy Profiles for a Pipe with LAMBDA=0.10 and Re=100                             | 108 |
| 34            | U-Velocity Profiles for a Pipe with LAMBDA=0.10 and Re=500                           | 109 |
| 35            | V-Velocity Profiles for a Pipe with LAMBDA=0.10 and Re=500                           | 110 |
| 36            | Velocity Vectors in a Pipe with LAMBDA=0.10 and Re=500                               | 111 |
| 37            | Enthalpy Profiles for a Pipe with LAMBDA=0.10 and Re=500                             | 112 |

| Figure<br>No.  | Page No. |
|--|----------|
| 38      U-Velocity Profiles for a pipe<br>with LAMBDA=0.20 and Re=100              | 113      |
| 39      V-Velocity Profiles for a Pipe<br>with LAMBDA=0.20 and Re=100              | 114      |
| 40      Velocity Vectors in a Pipe with<br>LAMBDA=0.20 and Re=100                  | 115      |
| 41      Enthalpy Profiles for a Pipe with<br>LAMBDA=0.20 and Re=100                | 116      |
| 42      U-Velocity Profiles for a Pipe with<br>LAMBDA=0.20 and Re=500              | 117      |
| 43      V-Velocity Profiles for a Pipe with<br>LAMBDA=0.20 and Re=500              | 118      |
| 44      Velocity Vectors in a Pipe with<br>LAMBDA=0.20 and Re=500                  | 119      |
| 45      Enthalpy Profiles for a Pipe with<br>LAMBDA=0.20 and Re=500                | 120      |
| 46      U-Velocity Profiles for a Pipe with<br>LAMBDA=0.25 and Re=100              | 121      |
| 47      V-Velocity Profiles for a Pipe with<br>LAMBDA=0.25 and Re=100              | 122      |
| 48      Velocity Vectors in a Pipe with<br>LAMBDA=0.25 and Re=100                  | 123      |
| 49      Enthalpy Profiles for a Pipe with<br>LAMBDA=0.25 and Re=100                | 124      |
| 50      a) Pressure Distribution along X for a<br>pipe with LAMBDA=0.10 and Re=100 | 125      |
| b) Pressure Distribution along X for a<br>pipe with LAMBDA=0.10 and Re=500         | 125      |
| 51      a) Pressure Distribution along X for a<br>pipe with LAMBDA=0.20 and Re=100 | 126      |
| b) Pressure Distribution along X for a<br>pipe with LAMBDA=0.20 and Re=500         | 126      |
| 52      Pressure Distribution along X for a<br>pipe with LAMBDA=0.25 and Re=100    | 127      |

| Figure<br>No.   | Page No. |
|---|----------|
| 53      U-Velocity Profiles for a non-Symmetric Channel with LAMBDA=0.10 and Re=100 | 128      |
| 54      V-Velocity Profiles for a Non-Symmetric Channel with LAMBDA=0.10 and Re=100 | 129      |
| 55      Velocity Vectors in a Non-Symmetric Channel with LAMBDA=0.10 and Re=100     | 130      |
| 56      Enthalpy Profiles for a Non-Symmetric Channel with LAMBDA=0.10 and Re=100   | 131      |
| 57      U-Velocity Profiles for a Non-Symmetric Channel with LAMBDA=0.10 and Re=500 | 132      |
| 58      V-Velocity Profiles for a Non-Symmetric Channel with LAMBDA=0.10 and Re=500 | 133      |
| 59      Velocity Vectors in a non-Symmetric Channel with LAMBDA=0.10 and Re=500     | 134      |
| 60      Enthalpy Profiles for a non-Symmetric Channel with LAMBDA=0.10 and Re=500   | 135      |
| 61      U-Velocity Profiles for a Non-Symmetric Channel with LAMBDA=0.20 and Re=100 | 136      |
| 62      V-Velocity Profiles for a Non-Symmetric Channel with LAMBDA=0.20 and Re=100 | 137      |
| 63      Velocity Vectors in a Non-Symmetric Channel with LAMBDA=0.20 and Re=100     | 138      |
| 64      Enthalpy Profiles for a Non-Symmetric Channel with LAMBDA=0.20 and Re=100   | 139      |
| 65      U-Velocity Profiles for a non-Symmetric Channel with LAMBDA=0.20 and Re=500 | 140      |
| 66      V-Velocity Profiles for a Non-Symmetric Channel with LAMBDA=0.20 and Re=500 | 141      |
| 67      Velocity Vectors in a Non-Symmetric Chennel with LAMBDA=0.20 and Re=500     | 142      |

| Figure<br>No. | Page No.  |     |
|---------------|---|-----|
| 68            | Enthalpy Profiles for a Non-Symmetric Channel with LAMBDA=0.20 and Re=500             | 143 |
| 69 a)         | Pressure Distribution along X for a Non-Symmetric Channel with LAMBDA=0.10 and Re=100 | 144 |
| b)            | Pressure Distribution along X for a Non-Symmetric Channel with LAMBDA=0.10 and Re=500 | 144 |
| 70 a)         | Pressure Distribution along X for a Non-Symmetric Channel with LAMBDA=0.20 and Re=100 | 145 |
| b)            | Pressure Distribution along X for a Non-Symmetric Channel with LAMBDA=0.20 and Re=500 | 145 |
| 71            | Pressure Distribution along Y for a Non-Symmetric Channel with LAMBDA=0.20 and Re=100 | 146 |

## ABSTRACT

A finite-difference solution for laminar viscous flow through a short wavelength sinusoidal symmetric as well as non-symmetric channel and through a converging-diverging pipe is presented here. The physical wavy domain is transformed into a rectangular computational domain in order to simplify the application of boundary conditions on the walls. The discretized conservation equations for mass, momentum and energy are derived on a control volume basis. The resulting discretized equations are solved using the SIMPLEC method suggested by Van Doormaal and Raithby [12]. We also follow their other suggestions regarding i) the use of E-factor in place of the usual under-relaxation factor, and ii) the solution of the pressure correction equation. The latter was found to be very effective in reducing the number of iterations as compared to the procedure suggested by Patankar [7]. Results are obtained for both the developing and the fully-developed flow for a Prandtl number ( $\text{Pr}$ ) of 0.72, for the Reynolds number ( $\text{Re}$ ) ranging from 100 to 500, and for non-dimensional wall amplitude ( $\lambda/L$ ) = 0.10 to 0.25. Solutions are obtained for constant fluid properties and for a prescribed wall enthalpy only. It is found that the separated flow region grows with increase of  $\text{Re}$  and  $\lambda/L$  and is mainly confined to the diverging part of the symmetric channel or pipe. However, for higher  $\text{Re}$  and  $\lambda/L$  it occurs in the converging portion as well. In the non-symmetric channel flow separates near the upper boundary in one

section whereas it separates near the lower boundary in the adjacent section. Per-cycle pressure drop in the fully-developed region is same and increases with increase of Re and  $\lambda/L_p$ . A point of inflection in the enthalpy profiles is observed in the separated region whereas in the non-separated region the enthalpy distribution is almost parabolic.

## Chapter 1

### INTRODUCTION

A lot of effort has been expended during the last few years to employ boundary fitted coordinates in conjunction with finite-difference techniques to solve fluid flow problems in and around wavy surfaces. The analysis of such problem finds application in different areas such as generation of wind waves on water, formation of sedimentary ripples in river channels and dunes in deserts, transpiration cooling of re-entry vehicles and rocket boosters, stability of liquid film in contact with a gas stream, rippling of melting surfaces, cross hatching on ablative surfaces and film vapourization in combustion chambers. This type of configuration is also used in heat exchangers in order to enhance the convective heat transfer characteristics. Physiologists are also interested in it trying to explain blood and urinary flow and to apply the results for optimal design of artificial organs.

#### - Earlier development

One of the earliest studies on viscous flow in sinusoidally varying channels and pipes is that of Burns and Parks [1]. They carried out the solution for small amplitude channels and pipes by expressing the stream function in a Fourier cosine series under the assumption that the Reynolds number is small enough for the Stokes approximation to be valid.

Tsangaris and Leiter [2] solved the same problem by expressing the stream function in a Fourier series not in the physical plane but in the transformed plane where the wavy boundary is transformed into a straight one. Their above proposed analytical perturbation method for creeping flow was extended to laminar flow for higher Reynolds numbers by the same authors [3] and results are presented for an amplitude to wavelength ratio of  $0.1/\pi$ . Steady and unsteady flow through furrowed channels has been studied numerically by Sobey [4]. He especially concentrated on the Reynolds number effect for separated flow. Fluid flow connected with heat transfer in wavy channels was calculated by Vajravelu [5] by the perturbation method for long-wavelength channels. Heat transfer effect has also been studied by Prata and Sparrow [6] for laminar flow in an annular duct having a streamwise-periodic variation of the cross-sectional area. They obtained the solution by using the SIMPLE algorithm of Patankar [7] for Reynolds number ranging from 50 to 1000 and Prandtl number ranging from 2 to 10. The viscous flow in a circular pipe whose radius has slight sinusoidal variation was treated by Belinfante [8] using the power series method. Some experimental work has also been carried out by Hsu and Kennedy [9] to find the variation of pressure and shear stress along a wavy pipe for turbulent non-separated flow. Stephanoff, Sobey and Bellhouse[10] Compared the results of Sobey's calculation with experimental observations by visualization techniques.

Present Work :

In the present work, a finite-difference solution for two-dimensional, viscous laminar flow in sinusoidally varying channels and pipe is presented. To solve such problems, both orthogonal and non-orthogonal grids have been generated numerically in the physical domain so that the boundaries are grid lines. The governing transport equations are then solved in the generalized coordinate system. In the present development, however, suitable non-orthogonal algebraic transformation are used in order to transform the physical wavy domain into a rectangular computational domain. The discretized conservation equations are then derived on a control volume basis [11]. This approach has two attractive features. One is that it facilitates physical interpretation of the terms that result from the coordinate transformation. Thus for example pseudodiffusion terms that result from the non-orthogonal nature of transformation can be easily identified. The second attractive feature of the control volume is that it ensures global conservation of mass, momentum and energy.

The resulting discretized equations are solved using the SIMPLEC method recently developed by Van Doormaal and Raithby [12]. This method is superior to the SIMPLE or SIMPLER method suggested by Patankar [7]. It is consistent in terms of approximation made and avoids the task of searching for optimal values of under relaxation factor since in this method

the relaxation factor for pressure is simply unity. Their other suggestions regarding use of E-factor in place of the usual under-relaxation factor and the solution of pressure correction equation are also adopted here. The latter was found to be very effective in reducing the number of iterations required for convergence as compared to the procedure suggested by Patankar. This reduces the solution cost considerably.

## Chapter 2

### ANALYTICAL FORMULATION

#### 2.1 Description of the Problem :

We are concerned with two-dimensional, viscous, laminar flow through a wavy channel and a wavy pipe formed by alternating converging and diverging cross-sections defined by a sinusoidal function as well as through a wavy channel formed by a sinusoidal function but having a constant cross-sectional area in the flow direction. For all the above three cases, the solid boundaries are curved and do not lie along a coordinate line. A schematic view of the types of physical domains being considered is shown in Fig. 1. The walls of the channels or pipe are denoted by a sinusoidal function. For the non-symmetric channel the sinusoidal function is different from that for the symmetric channel or pipe. These are given by

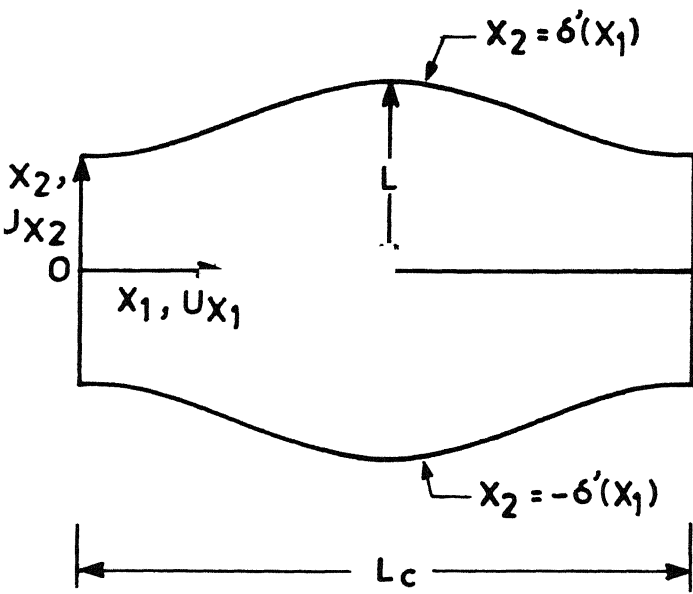
For the symmetric channel or pipe

$$\delta'(x_1) = L - \lambda(1 + \cos(\pi x_1/L)) \quad (2.1.1)$$

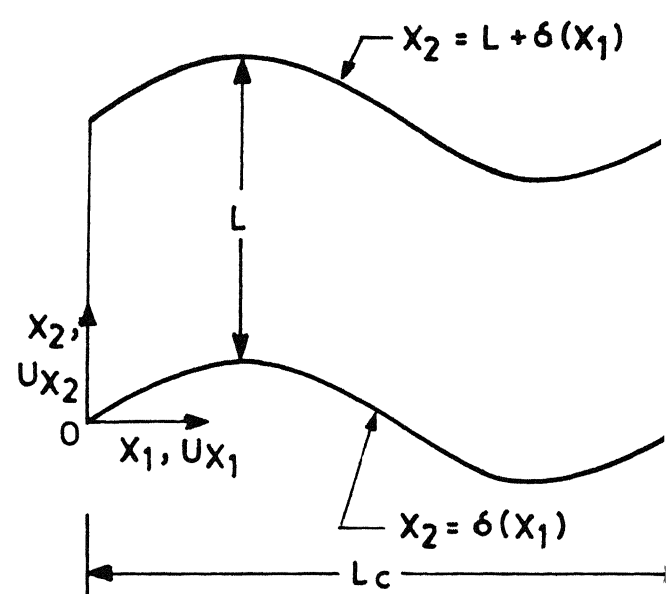
For the non-symmetric channel

$$\delta'(x_1) = \lambda \sin(\pi x_1/L) \quad (2.1.2)$$

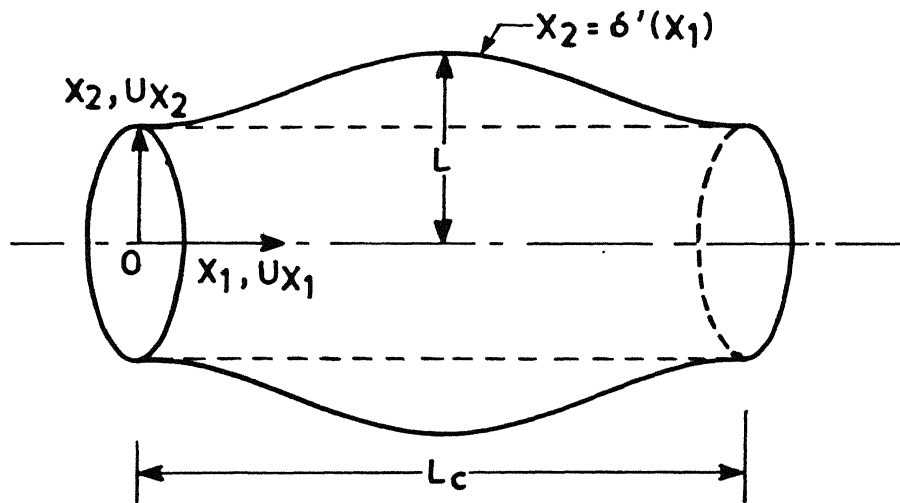
where  $L$  is a reference length and  $\lambda$  is the amplitude of the channels or pipe. The origin of the coordinate system is placed on the entrance plane of the duct as shown in Fig. 1. Here  $x_1$  and  $x_2$  are used as the generalized coordinates. For the Cartesian coordinate system used for channels  $x_1$  and  $x_2$  represent the



(a) Converging and diverging  
symmetric channel



(b) Non symmetric curved  
channel



(c) Converging diverging pipe

Fig. 1 Types of channels and pipe considered  
(one cycle only)

x- and y- coordinates respectively, whereas in the cylindrical coordinate system used for pipe  $x_1$  represents the z-coordinate and  $x_2$  represents the r-coordinate.

Other types of problems, like external flow over a wavy boundary can be dealt with by the present methodology but these will not be considered here.

## 2.2 Conservation Equations :

The governing equations to be considered here are the continuity, momentum and energy equations. Constant thermo-physical properties are assumed and viscous dissipation is neglected in the energy equation. Moreover, the flow is either two-dimensional or axisymmetric, i.e., the flow parameters are independent of the z-direction in the case of a channel and independent of the  $\theta$ -direction in the case of a pipe. Using these assumptions the governing equations become :

### a) For channel :

continuity equation :

$$\frac{\partial U_{x_1}}{\partial x_1} + \frac{\partial U_{x_2}}{\partial x_2} = 0 \quad (2.2.1)$$

$x_1$ -momentum equation :

$$U_{x_1} \frac{\partial U_{x_1}}{\partial x_1} + U_{x_2} \frac{\partial U_{x_1}}{\partial x_2} = - \frac{1}{\rho} \frac{\partial p}{\partial x_1} + \frac{\mu}{\rho} \left( \frac{\partial^2 U_{x_1}}{\partial x_1^2} + \frac{\partial^2 U_{x_1}}{\partial x_2^2} \right) \quad (2.2.2)$$

$x_2$ -momentum equation :

$$U_{x_1} \frac{\partial U_{x_2}}{\partial x_1} + U_{x_2} \frac{\partial U_{x_2}}{\partial x_2} = - \frac{1}{\rho} \frac{\partial p}{\partial x_2} + \frac{\mu}{\rho} \left( \frac{\partial^2 U_{x_2}}{\partial x_1^2} + \frac{\partial^2 U_{x_2}}{\partial x_2^2} \right) \quad (2.2.3)$$

**energy equation :**

$$U_{X_1} \frac{\partial h}{\partial X_1} + U_{X_2} \frac{\partial h}{\partial X_2} = \frac{k}{\rho C_p} \left( \frac{\partial^2 h}{\partial X_1^2} + \frac{\partial^2 h}{\partial X_2^2} \right) \quad (2.2.4)$$

b) For pipe :

**continuity equation :**

$$\frac{\partial U_{X_1}}{\partial X_1} + \frac{\partial U_{X_2}}{\partial X_2} + \frac{U_{X_2}}{X_2} = 0 \quad (2.2.5)$$

$X_1$ -momentum equation :

$$U_{X_1} \frac{\partial U_{X_1}}{\partial X_1} + U_{X_2} \frac{\partial U_{X_1}}{\partial X_2} = - \frac{1}{\rho} \frac{\partial p}{\partial X_1} + \frac{\mu}{\rho} \left( \frac{\partial^2 U_{X_1}}{\partial X_1^2} + \frac{\partial^2 U_{X_1}}{\partial X_2^2} + \frac{1}{X_2} \frac{\partial U_{X_1}}{\partial X_2} \right) \quad (2.2.6)$$

$X_2$ -momentum equation :

$$U_{X_1} \frac{\partial U_{X_2}}{\partial X_1} + U_{X_2} \frac{\partial U_{X_2}}{\partial X_2} = - \frac{1}{\rho} \frac{\partial p}{\partial X_2} + \frac{\mu}{\rho} \left( \frac{\partial^2 U_{X_2}}{\partial X_1^2} + \frac{\partial^2 U_{X_2}}{\partial X_2^2} + \frac{1}{X_2} \frac{\partial U_{X_2}}{\partial X_1} - \frac{U_{X_2}}{X_2^2} \right) \quad (2.2.7)$$

**energy equation :**

$$U_{X_1} \frac{\partial h}{\partial X_1} + U_{X_2} \frac{\partial h}{\partial X_2} = \frac{k}{\rho C_p} \left( \frac{\partial^2 h}{\partial X_1^2} + \frac{\partial^2 h}{\partial X_2^2} + \frac{1}{X_2} \frac{\partial h}{\partial X_2} \right) \quad (2.2.8)$$

Boundary conditions for the above problems will be discussed later.

### 2.3 Formulation For Symmetric Channel and Pipe :

Since both the converging-diverging channel and pipe are symmetric about their respective centre lines, the total solution domain can be folded at the centre line with certain

modifications in the boundary conditions to get the numerical solution of the problem. The coordinate transformation described later for this channel and pipe is also of the same type. This is made possible by introducing a factor K which is unity for the Cartesian coordinate system and 'two' for the cylindrical coordinate system in such a way that the same mathematical analysis can be applied to both the cases.

Therefore with the insertion of factor K, the governing equations take the form

continuity equation :

$$\frac{\partial U_{X_1}}{\partial X_1} + \frac{\partial U_{X_2}}{\partial X_2} + (K-1) \frac{U_{X_2}}{X_2} = 0 \quad (2.3.1)$$

$X_1$ -momentum equation :

$$U_{X_1} \frac{\partial U_{X_1}}{\partial X_1} + U_{X_2} \frac{\partial U_{X_1}}{\partial X_2} = - \frac{1}{\rho} \frac{\partial p}{\partial X_1} + \frac{\mu}{\rho} (\nabla^2 U_{X_1}) \quad (2.3.2)$$

$X_2$ -momentum equation :

$$U_{X_1} \frac{\partial U_{X_2}}{\partial X_1} + U_{X_2} \frac{\partial U_{X_2}}{\partial X_2} = - \frac{1}{\rho} \frac{\partial p}{\partial X_2} + \frac{\mu}{\rho} (\nabla^2 U_{X_2} - (K-1) \frac{U_{X_2}}{X_2^2}) \quad (2.3.3)$$

energy equation :

$$U_{X_1} \frac{\partial h}{\partial X_1} + U_{X_2} \frac{\partial h}{\partial X_2} = \frac{k}{\rho C_p} \nabla^2 h \quad (2.3.4)$$

where the Laplacian ( $\nabla^2$ ) operator is

$$\nabla^2 = \frac{\partial^2}{\partial X_1^2} + \frac{\partial^2}{\partial X_2^2} + (K-1) \frac{1}{X_2} \frac{\partial}{\partial X_2} \quad (2.3.5)$$

The boundary conditions (except those at exit) are

$$U_{X_1}(0, X_2) = U_o \quad (\text{assumed constant here, although a function of } X_2 \text{ is also permissible})$$

$$U_{X_1}(x_1, \delta'(x_1)) = 0, \quad \frac{\partial U_{X_1}}{\partial X_2}(x_1, 0) = 0$$

$$U_{X_2}(x_1, 0) = 0 \quad , \quad U_{X_2}(x_1, \delta'(x_1)) = 0$$

(2.3.6a)

$$p(0, X_2) = p_o \quad , \quad h(0, X_2) = h_o$$

$$h(x_1, \delta'(x_1)) = h_w \quad , \quad \frac{\partial h}{\partial X_2}(x_1, 0) = 0$$

where  $U_o$ ,  $p_o$ , and  $h_o$  are the velocity, pressure and enthalpy at entrance to the duct and  $h_w$  is the enthalpy at the wall.

#### Boundary conditions at exit

The characteristics of velocity and temperature (or enthalpy) in a periodic fully developed regime are discussed in [6]. The periodicity conditions of velocity can be expressed as

$$U_{X_1}(x_1^*, X_2) = U_{X_1}(x_1^* - L_c, X_2)$$

(2.3.6b)

$$U_{X_2}(x_1^*, X_2) = U_{X_2}(x_1^* - L_c, X_2)$$

where  $x_1^*$  is an arbitrary station in the fully developed region and  $L_c$  is the cycle length.

For a periodic thermally developed regime with constant wall enthalpy, we have

$$(a) \quad H(x_1^*, X_2) = H(x_1^* - L_c, X_2)$$

(2.3.6c)

if the dimensionless enthalpy  $H$  is defined as

$$H = \frac{h - h_w}{h_b - h_w}$$

where the bulk enthalpy  $h_b$  is given by

$$h_b = h_w + \frac{\int_A U_{X_1} (h - h_w) dA}{\int_A U_{X_1} dA}$$

and

$$(b) \quad \frac{H(X_1^*, X_2)}{H(X_1^* - L_c, X_2)} = \frac{H(X_1^* - L_c, X_2)}{H(X_1^* - 2L_c, X_2)} \quad (2.3.6d)$$

if  $H$  is defined as

$$H = \frac{h - h_w}{h_o - h_w}$$

Now using the following non-dimensional variables

$$\begin{aligned} X &= \frac{X_1}{L}, \quad Y = \frac{X_2}{L}, \quad U = \frac{U_{X_1}}{U_o}, \quad V = \frac{U_{X_2}}{U_o} \\ H &= \frac{h - h_w}{h_o - h_w}, \quad P = \frac{P - P_o}{\rho U_o^2} \end{aligned} \quad (2.3.7)$$

the governing equations take the form

$$\frac{\partial U}{\partial X} + \frac{\partial V}{\partial Y} + (K-1) \frac{V}{Y} = 0 \quad (2.3.8)$$

$$U \frac{\partial U}{\partial X} + V \frac{\partial U}{\partial Y} = - \frac{\partial P}{\partial X} + \frac{1}{Re} \left\{ \frac{\partial^2 U}{\partial X^2} + \frac{\partial^2 U}{\partial Y^2} + (K-1) \frac{1}{Y} \frac{\partial U}{\partial Y} \right\} \quad (2.3.9)$$

$$U \frac{\partial V}{\partial X} + V \frac{\partial V}{\partial Y} = - \frac{\partial P}{\partial Y} + \frac{1}{Re} \left\{ \frac{\partial^2 V}{\partial X^2} + \frac{\partial^2 V}{\partial Y^2} + (K-1) \frac{1}{Y} \frac{\partial V}{\partial Y} - (K-1) \frac{V}{Y^2} \right\} \quad (2.3.10)$$

$$U \frac{\partial H}{\partial X} + V \frac{\partial H}{\partial Y} = \frac{1}{Pe} \left\{ \frac{\partial^2 H}{\partial X^2} + \frac{\partial^2 H}{\partial Y^2} + (K-1) \frac{1}{Y} \frac{\partial H}{\partial Y} \right\} \quad (2.3.11)$$

where Reynolds number,  $Re = \frac{\rho U_o L}{\mu}$  and Peclet number,  $Pe = Re \cdot Pr$ ;  
 $Pr = \mu C_p / k$ .

The boundary conditions become

$$U(0, Y) = 1.0 \quad , \quad U(X, \delta(X)) = 0.0$$

$$\frac{\partial U}{\partial Y}(X, 0) = 0.0 \quad , \quad V(X, 0) = 0.0$$

$$V(X, \delta(X)) = 0.0 \quad , \quad U(X^*, Y) = U(X^* - L_C^*, Y)$$

$$V(X^*, Y) = V(X^* - L_C^*, Y), \quad P(0, Y) = 0.0 \quad (2.3.12)$$

$$H(0, Y) = 1.0 \quad , \quad H(X, \delta(X)) = 0.0$$

$$\frac{\partial H}{\partial Y}(X, 0) = 0.0 \quad , \quad \frac{H(X^*, Y)}{H(X^* - L_C^*, Y)} = \frac{H(X^* - L_C^*, Y)}{H(X^* - 2L_C^*, Y)}$$

$$\text{where } X^* = \frac{x_1}{L}, \quad L_C^* = L_C/L \text{ and } \delta(X) = 2 \frac{\delta'(X)}{L}.$$

Equations (2.3.9) and (2.3.10) are the X- and Y- components of the vector momentum equation. Therefore, the momentum equations (2.3.9) and (2.3.10) may be expressed as

$$\begin{aligned} & \{ U \frac{\partial U}{\partial X} + V \frac{\partial U}{\partial Y} + \frac{\partial P}{\partial X} - \frac{1}{Re} \left( \frac{\partial^2 U}{\partial X^2} + \frac{\partial^2 U}{\partial Y^2} + (K-1) \frac{1}{Y} \frac{\partial U}{\partial Y} \right) \} \vec{e}_X \\ & + \{ U \frac{\partial V}{\partial X} + V \frac{\partial V}{\partial Y} + \frac{\partial P}{\partial Y} - \frac{1}{Re} \left( \frac{\partial^2 V}{\partial X^2} + \frac{\partial^2 V}{\partial Y^2} + (K-1) \frac{1}{Y} \frac{\partial V}{\partial Y} \right. \\ & \left. - (K-1) \frac{V}{Y^2} \right) \} \vec{e}_Y = 0 \end{aligned} \quad (2.3.13)$$

where  $\vec{e}_X$  and  $\vec{e}_Y$  are the unit vectors in the X- and Y-directions respectively. The need for writing the momentum equation in vector form will be justified later.

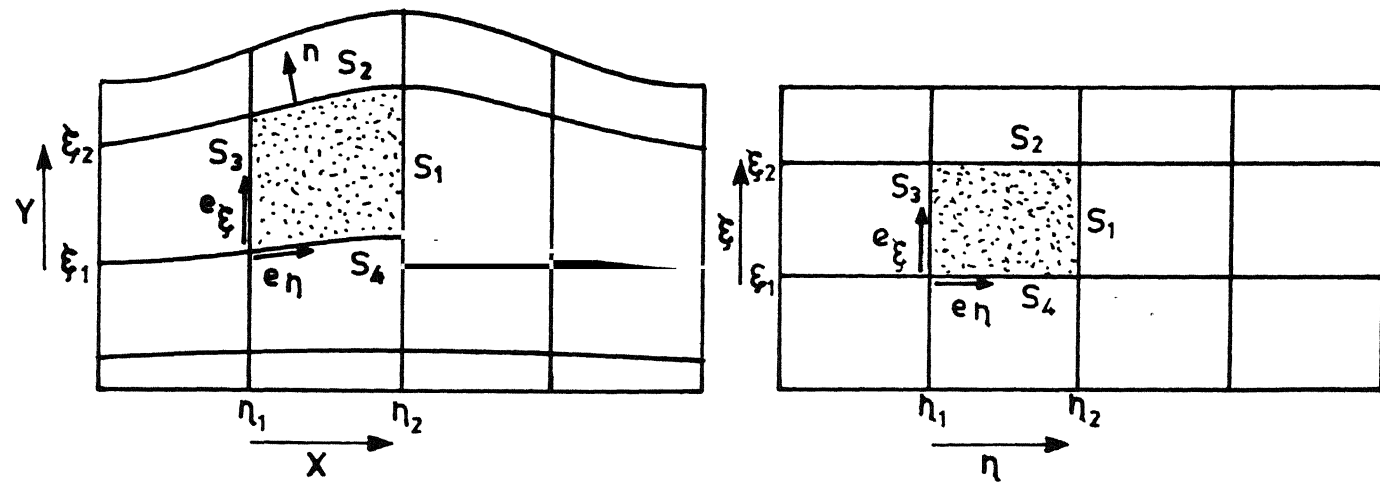
The next step in the analysis is to introduce a transformation of coordinates in order to transform the non-rectangular physical domain into a rectangular computational domain so as to avoid the task of numerically generating the boundary fitted coordinates and also to simplify the application of boundary conditions at the walls.

Specifically, the X and Y coordinates are transformed to  $\eta$  and  $\xi$  coordinates respectively by the relations

$$\eta = X, \quad \xi = Y/\delta(X) \quad (2.3.14)$$

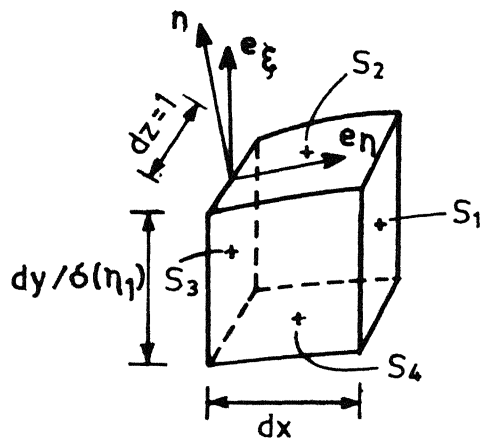
such that  $\xi = 0.5$  at all points on the curved boundaries.

The lines of constant  $\eta$  and  $\xi$  for a given boundary shape are illustrated in Fig. 2a. It is evident that a control volume contained between lines  $\eta = \eta_1$ ,  $\eta = \eta_2$  and  $\xi = \xi_1$ ,  $\xi = \xi_2$  is a curvilinear element with non-orthogonal sides. The quantities  $\vec{e}_\eta$  and  $\vec{e}_\xi$  are unit vectors in the physical coordinate system, which lie along the lines of constant  $\xi$  and constant  $\eta$  respectively. It is evident from the figure that the direction of  $\vec{e}_\eta$  changes with position. This is in contrast to the unit vectors  $\vec{e}_X$  and  $\vec{e}_Y$ , which do not change direction throughout the solution domain. The shape of the control volume element both in Cartesian coordinates and in cylindrical coordinates is shown in Fig. 2c and Fig. 2d respectively. Now the vector momentum equation (2.3.13) is recast in terms of the unit vectors  $\vec{e}_\eta$  and  $\vec{e}_\xi$  and the coefficients of the respective unit vectors are identified as the momentum equations in the  $\eta$  and  $\xi$

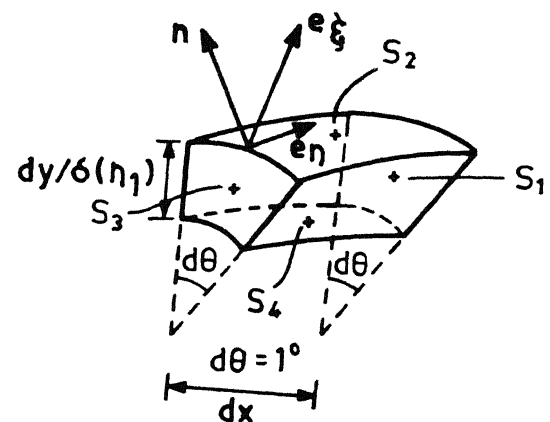


(a) Shape of control volume  
in physical space

(b) Shape of control volume  
in  $\eta - \xi$  plane



(c) Shape of control volume  
element in cartesian  
co ordinates ( $dz = \text{unity}$ )



(d) Shape of control volume  
element in cylindrical  
co ordinates ( $d\theta = \text{unity}$ )

Fig. 2 Shape of control volume for a symmetric  
channel or pipe.

direction. These momentum equations are used to replace the X- and Y-momentum equations. The continuity and energy equations are scalars and remain as they are.

In order to resolve the momentum equation along  $\eta$ ,  $\xi$  directions, the unit vectors  $\vec{e}_\eta$  and  $\vec{e}_\xi$  illustrated in Fig. 2 are used. Since lines of constant  $\eta$  coincide with lines parallel to the Y-coordinate, we have

$$\vec{e}_\xi = \vec{e}_Y \quad (2.3.15)$$

To determine  $\vec{e}_\eta$ , consideration is first given to the unit vector  $\vec{n}$  which is normal to a line (or surface) of constant  $\xi$ . Since the gradient of  $\xi$  is normal to a line of constant  $\xi$ , we have

$$\vec{n} = \frac{\text{grad } \xi}{|\text{grad } \xi|} = \frac{\nabla \xi}{|\nabla \xi|} .$$

$$\text{Now } \nabla \xi = \vec{e}_X \frac{\partial \xi}{\partial X} + \vec{e}_Y \frac{\partial \xi}{\partial Y} .$$

From the definition of  $\xi$  (Eq. (2.3.14)), we get

$$\frac{\partial \xi}{\partial Y} = \frac{1}{\delta}$$

$$\text{and } \frac{\partial \xi}{\partial X} = - \frac{Y}{\delta^2} \frac{d\delta}{dX} = - \frac{\xi}{\delta} \frac{d\delta}{d\eta} = - \frac{\beta}{\delta}$$

$$\text{where } \beta = \xi \frac{d\delta}{d\eta} \quad (2.3.16)$$

$$\therefore \nabla \xi = \frac{1}{\delta} (-\beta \vec{e}_X + \vec{e}_Y)$$

$$\text{and } \vec{n} = \frac{-\beta \vec{e}_X + \vec{e}_Y}{\sqrt{1 + \beta^2}} = \frac{-\beta \vec{e}_X + \vec{e}_Y}{\alpha^{1/2}} \quad (2.3.17)$$

$$\text{where } \alpha = 1 + \beta^2 \quad (2.3.18)$$

Since the unit vector  $\vec{e}_\eta$  is perpendicular to the vector  $\vec{n}$ , we have

$$\vec{e}_\eta \cdot \vec{n} = 0, \text{ which gives}$$

$$\vec{e}_\eta = \frac{\vec{e}_X + \beta \vec{e}_Y}{\alpha^{1/2}} \quad (2.3.19)$$

This unit vector is not constant, but it is a function of position.

The following inverse relations can be obtained directly from Eqs. (2.3.15) and (2.3.19).

$$\begin{aligned} \vec{e}_X &= \alpha^{1/2} \vec{e}_\eta - \beta \vec{e}_\xi \\ \vec{e}_Y &= \vec{e}_\xi \end{aligned} \quad (2.3.20)$$

Now any vector  $\vec{a}$  can be expressed as

$$\vec{a} = a_\eta \vec{e}_\eta + a_\xi \vec{e}_\xi \quad \text{or} \quad \vec{a} = a_X \vec{e}_X + a_Y \vec{e}_Y$$

so that

$$\begin{aligned} a_Y &= \vec{a} \cdot \vec{e}_Y = (a_\eta \vec{e}_\eta + a_\xi \vec{e}_\xi) \cdot \vec{e}_Y \\ &= [a_\eta \alpha^{-1/2} (\vec{e}_X + \beta \vec{e}_Y) + a_\xi \vec{e}_Y] \cdot \vec{e}_Y \\ &= a_\eta \alpha^{-1/2} \beta + a_\xi \end{aligned} \quad (2.3.21a)$$

and

$$\begin{aligned} a_X &= \vec{a} \cdot \vec{e}_X = (a_\eta \vec{e}_\eta + a_\xi \vec{e}_\xi) \cdot \vec{e}_X \\ &= [a_\eta \alpha^{-1/2} (\vec{e}_X + \beta \vec{e}_Y) + a_\xi \vec{e}_Y] \cdot \vec{e}_X \\ &= a_\eta \alpha^{-1/2} \end{aligned} \quad (2.3.21b)$$

From Eqs. (2.3.21) we get

$$a_\eta = \alpha^{1/2} a_X, \quad a_\xi = -\beta a_X + a_Y \quad (2.3.22)$$

Therefore, if  $\vec{a} = \vec{U} = U \vec{e}_X + v \vec{e}_Y = U_\eta \vec{e}_\eta + U_\xi \vec{e}_\xi$

$$\text{Then } U_\eta = \alpha^{1/2} U, \quad U_\xi = v - \beta U \quad (2.3.23)$$

Substituting  $\vec{e}_X$  and  $\vec{e}_Y$  in terms of  $\vec{e}_\eta$  and  $\vec{e}_\xi$  from equation (2.3.20), equation (2.3.13) becomes

$$\left\{ U \frac{\partial U}{\partial X} + v \frac{\partial U}{\partial Y} + \frac{\partial P}{\partial X} - \frac{1}{Re} \left( \frac{\partial^2 U}{\partial X^2} + \frac{\partial^2 U}{\partial Y^2} + (K-1) \frac{1}{Y} \frac{\partial U}{\partial Y} \right) \right\} (\alpha^{1/2} \vec{e}_\eta - \beta \vec{e}_\xi) \\ + \left\{ U \frac{\partial V}{\partial X} + v \frac{\partial V}{\partial Y} + \frac{\partial P}{\partial Y} - \frac{1}{Re} \left( \frac{\partial^2 V}{\partial X^2} + \frac{\partial^2 V}{\partial Y^2} + (K-1) \frac{1}{Y} \frac{\partial V}{\partial Y} - (K-1) \frac{V}{Y^2} \right) \right\} \vec{e}_\xi = 0$$

or

$$\left\{ U \frac{\partial U}{\partial X} + v \frac{\partial U}{\partial Y} + \frac{\partial P}{\partial X} - \frac{1}{Re} \left( \frac{\partial^2 U}{\partial X^2} + \frac{\partial^2 U}{\partial Y^2} + (K-1) \frac{1}{Y} \frac{\partial U}{\partial Y} \right) \right\} \alpha^{1/2} \vec{e}_\eta \\ + \left\{ U \left( \frac{\partial V}{\partial X} - \beta \frac{\partial U}{\partial X} \right) + v \left( \frac{\partial V}{\partial Y} - \beta \frac{\partial U}{\partial Y} \right) - \left( \beta \frac{\partial P}{\partial X} - \frac{\partial P}{\partial Y} \right) - \frac{1}{Re} \left( \frac{\partial^2 V}{\partial X^2} + \frac{\partial^2 V}{\partial Y^2} \right. \right. \\ \left. \left. + (K-1) \frac{1}{Y} \frac{\partial V}{\partial Y} - (K-1) \frac{V}{Y^2} + \beta \left( \frac{\partial^2 U}{\partial X^2} + \frac{\partial^2 U}{\partial Y^2} + (K-1) \frac{1}{Y} \frac{\partial U}{\partial Y} \right) \right) \right\} \vec{e}_\xi = 0.$$

From this vector equation it is possible to write

i) momentum equation in the  $\eta$ -direction :

$$U \frac{\partial U}{\partial X} + v \frac{\partial U}{\partial Y} = - \frac{\partial P}{\partial X} + \frac{1}{Re} \left( \frac{\partial^2 U}{\partial X^2} + \frac{\partial^2 U}{\partial Y^2} + (K-1) \frac{1}{Y} \frac{\partial U}{\partial Y} \right) \quad (2.3.24)$$

ii) momentum equation in the  $\xi$ -direction :

$$U \left( \frac{\partial V}{\partial X} - \beta \frac{\partial U}{\partial X} \right) + v \left( \frac{\partial V}{\partial Y} - \beta \frac{\partial U}{\partial Y} \right) = \left( \beta \frac{\partial P}{\partial X} - \frac{\partial P}{\partial Y} \right) + \frac{1}{Re} \\ \left\{ \frac{\partial^2 V}{\partial X^2} + \frac{\partial^2 V}{\partial Y^2} + (K-1) \frac{1}{Y} \frac{\partial V}{\partial Y} - (K-1) \frac{V}{Y^2} - \beta \left( \frac{\partial^2 U}{\partial X^2} + \frac{\partial^2 U}{\partial Y^2} + (K-1) \frac{1}{Y} \frac{\partial U}{\partial Y} \right) \right\} \\ (2.3.25)$$

Since  $V = U_\xi + \beta U$ , we get

$$\frac{\partial V}{\partial X} = \frac{\partial U_\xi}{\partial X} + U \frac{\partial \beta}{\partial X} + \beta \frac{\partial U}{\partial X},$$

$$\frac{\partial V}{\partial Y} = \frac{\partial U_\xi}{\partial Y} + U \frac{\partial \beta}{\partial Y} + \beta \frac{\partial U}{\partial Y},$$

$$\frac{\partial^2 V}{\partial X^2} = \frac{\partial}{\partial X} \left( \frac{\partial U_\xi}{\partial X} + U \frac{\partial \beta}{\partial X} + \beta \frac{\partial U}{\partial X} \right)$$

$$= 2 \frac{\partial U}{\partial X} \cdot \frac{\partial \beta}{\partial X} + U \frac{\partial^2 \beta}{\partial X^2} + \beta \frac{\partial^2 U}{\partial X^2} + \frac{\partial^2 U_\xi}{\partial X^2},$$

and

$$\frac{\partial^2 V}{\partial Y^2} = 2 \frac{\partial U}{\partial Y} \cdot \frac{\partial \beta}{\partial Y} + U \frac{\partial^2 \beta}{\partial Y^2} + \beta \frac{\partial^2 U}{\partial Y^2} + \frac{\partial^2 U_\xi}{\partial Y^2}.$$

Using these derivatives,  $\xi$ -momentum equation becomes

$$\begin{aligned} U(U \frac{\partial \beta}{\partial X} + \frac{\partial U_\xi}{\partial X}) + V(U \frac{\partial \beta}{\partial Y} + \frac{\partial U_\xi}{\partial Y}) &= \beta \frac{\partial P}{\partial X} - \frac{\partial P}{\partial Y} \\ &+ \frac{1}{Re} \{ 2 \frac{\partial U}{\partial X} \frac{\partial \beta}{\partial X} + U \frac{\partial^2 \beta}{\partial X^2} + \beta \frac{\partial^2 U}{\partial X^2} + \frac{\partial^2 U_\xi}{\partial X^2} + 2 \frac{\partial U}{\partial Y} \frac{\partial \beta}{\partial Y} \\ &+ U \frac{\partial^2 \beta}{\partial Y^2} + \beta \frac{\partial^2 U}{\partial Y^2} + \frac{\partial^2 U_\xi}{\partial Y^2} + (K-1) \frac{1}{Y} (U \frac{\partial \beta}{\partial Y} + \beta \frac{\partial U}{\partial Y} + \frac{\partial U_\xi}{\partial Y}) \\ &- (K-1) \frac{1}{Y^2} (U_\xi + \beta U) - \beta (\frac{\partial^2 U}{\partial X^2} + \frac{\partial^2 U}{\partial Y^2} + (K-1) \frac{1}{Y} \frac{\partial U}{\partial Y}) \} \end{aligned}$$

or

$$\begin{aligned} U \frac{\partial U_\xi}{\partial X} + V \frac{\partial U_\xi}{\partial Y} &= \beta \frac{\partial P}{\partial X} - \frac{\partial P}{\partial Y} + \frac{1}{Re} \left( \frac{\partial^2 U_\xi}{\partial X^2} + \frac{\partial^2 U_\xi}{\partial Y^2} + (K-1) \frac{1}{Y} \frac{\partial U_\xi}{\partial Y} \right) \\ &- U(U \frac{\partial \beta}{\partial X} + V \frac{\partial \beta}{\partial Y}) + \frac{1}{Re} \{ U(\frac{\partial^2 \beta}{\partial X^2} + \frac{\partial^2 \beta}{\partial Y^2} + (K-1) \frac{1}{Y} \frac{\partial \beta}{\partial Y}) \\ &+ 2 \frac{\partial U}{\partial X} \frac{\partial \beta}{\partial X} + 2 \frac{\partial U}{\partial Y} \frac{\partial \beta}{\partial Y} - (K-1) \frac{1}{Y^2} (U_\xi + \beta U) \} \end{aligned} \quad (2.3.26)$$

The form of Eq. (2.3.26) is attractive because it displays

$U_\xi$  as the primary dependent variable instead of the clumsy

combination of  $U$  and  $V$  that appears in the convective and diffusive terms of Eq. (2.3.25). On the other hand Eq. (2.3.24) wherein  $U$  plays the role of the dependent variable, is much simpler than the transformed version having  $U_\eta$  as the dependent variable. Therefore it is advantageous to retain Eq. (2.3.24) and to use  $U$  rather than  $U_\eta$ .

The boundary conditions for Eqs. (2.3.8), (2.3.24), (2.3.26) and (2.3.11) are

$$U(0, \xi) = 1.0, \quad U(\eta, 0.5) = 0.0, \quad \frac{\partial U}{\partial \xi}(\eta, 0) = 0.0$$

$$U(\eta^*, \xi) = U\{(\eta^* - L_C^*), \xi\}, \quad U_\xi(0, \xi) = -\beta_0 U(0, \xi) = -\beta_0$$

$$U_\xi(\eta, 0) = 0.0, \quad U_\xi(\eta, 0.5) = 0.0, \quad U_\xi(\eta^*, \xi) = U_\xi\{(\eta^* - L_C^*), \xi\}$$

$$P(0, \xi) = 0.0, \quad H(0, \xi) = 1.0, \quad H(\eta, 0.5) = 0.0, \quad \frac{\partial H}{\partial \xi}(\eta, 0) = 0.0,$$

$$\frac{H(\eta^*, \xi)}{H\{(\eta^* - L_C^*), \xi\}} = \frac{H\{(\eta^* - L_C^*), \xi\}}{H\{(\eta^* - 2L_C^*), \xi\}}$$

where  $\eta^* = X^*$  and  $\beta_0$  is the value of  $\beta$  at entrance to the channel or pipe.

#### Control volume form of the conservation equations :

At this point, the governing equations [Eqs. (2.3.24), (2.3.26), (2.3.11), and (2.3.8)] are integrated over a control volume in physical space bounded by lines of constant  $\eta$  and constant  $\xi$ . Such a control volume is illustrated in Fig. 2a. This is done with a view to obtain the discretization equations. Equations obtained in this manner express the conservation

principle for the dependent variable for the finite control volume, just as the differential equation expresses it for an infinitesimal control volume. Thus the resulting solution will exactly satisfy the integral conservation of quantities such as mass, momentum, and energy over any group of control volumes, and thus over the whole domain.

The term-by-term integration of Eq. (2.3.26), using the divergence theorem, will now follow.

$$\int_V (U \frac{\partial U_\xi}{\partial X} + V \frac{\partial U_\xi}{\partial Y}) dV = \int_V (\vec{U} \cdot \nabla U_\xi) dV = \int_S (\vec{U} \cdot \vec{n}) U_\xi dS \quad (2.3.27)$$

and

$$\begin{aligned} \int_V \left( \frac{\partial^2 U_\xi}{\partial X^2} + \frac{\partial^2 U_\xi}{\partial Y^2} + (K-1) \frac{1}{Y} \frac{\partial U_\xi}{\partial Y} \right) dV \\ = \int_V \nabla^2 U_\xi dV = \int_V \nabla \cdot \nabla U_\xi dV = \int_S \vec{n} \cdot \nabla U_\xi dS \end{aligned} \quad (2.3.28)$$

With these, Eq. (2.3.26) becomes

$$\begin{aligned} \int_S (\vec{U} \cdot \vec{n}) U_\xi dS - \frac{1}{Re} \int_S (\vec{n} \cdot \nabla U_\xi) dS &= \int_V (\beta \frac{\partial P}{\partial X} - \frac{\partial P}{\partial Y}) dV \\ - \int_V U (\vec{U} \cdot \nabla \beta) dV + \frac{1}{Re} \int_V \{ U \nabla^2 \beta + 2\nabla U \cdot \nabla \beta - (K-1) \frac{1}{Y^2} (U_\xi + \beta U) \} dV \end{aligned} \quad (2.3.29)$$

Using the vector identities similar to those in Eqs. (2.3.27) and (2.3.28), Eqs. (2.3.24), (2.3.11), and (2.3.8) become

$$\int_S (\vec{U} \cdot \vec{n}) U dS - \frac{1}{Re} \int_S (\vec{n} \cdot \nabla U) dS = - \int_V \frac{\partial P}{\partial X} dV \quad (2.3.30)$$

$$\int_S (\vec{U} \cdot \vec{n}) H dS - \frac{1}{Pe} \int_S (\vec{n} \cdot \nabla H) dS = 0 \quad (2.3.31)$$

$$\int_S (\vec{n} \cdot \vec{U}) dS = 0 \quad (2.3.32)$$

where  $\Psi$  and  $S$  represent, respectively, the dimensionless volume and surface of the control volume.

For evaluation of the surface integrals expressions are needed for the area  $dS$  of the surface, the gradient operator  $\nabla$ , and the unit vector  $\vec{n}$ . To derive these quantities, it is necessary to consider a formal transformation between derivatives with respect to  $X$ ,  $Y$  and those with respect to  $\eta$ ,  $\xi$  where  $\eta$  and  $\xi$  have been defined in Eq. (2.3.14). This transformation is

$$\frac{\partial}{\partial X} = \frac{\partial}{\partial \eta} \cdot \frac{\partial \eta}{\partial X} + \frac{\partial}{\partial \xi} \cdot \frac{\partial \xi}{\partial X} = \frac{\partial}{\partial \eta} - \frac{\beta}{\delta} \frac{\partial}{\partial \xi} \quad (2.3.33)$$

$$\frac{\partial}{\partial Y} = \frac{\partial}{\partial \eta} \cdot \frac{\partial \eta}{\partial Y} + \frac{\partial}{\partial \xi} \cdot \frac{\partial \xi}{\partial Y} = \frac{1}{\delta} \frac{\partial}{\partial \xi} \quad (2.3.34)$$

The surface integrals which appear in Eqs. (2.3.29) - (2.3.32) are evaluated with reference to the control volume shown in Fig. 2. Also the total surface integral is subdivided into a sum of four surface integrals over the segments  $S_1$ ,  $S_2$ ,  $S_3$  and  $S_4$ .

The first surface integral in Eq. (2.3.29) will now be evaluated.

For surface  $S_1$

Unit normal vector  $\vec{n} = \vec{e}_X$

$$\text{Therefore, } \vec{U} \cdot \vec{n} = (U \vec{e}_X + V \vec{e}_Y) \cdot \vec{e}_X = U \quad (2.3.35)$$

$$\text{Elemental surface area } dS = Y^{K-1} dY.$$

Now from Eq. (2.3.14),  $Y = \xi \delta(\eta)$

$$\therefore dY = \delta d\xi \quad (\text{since } \eta \text{ is constant along } S_1) \quad (2.3.36)$$

$$\text{Thus } dS = (\delta \xi)^{K-1} \delta d\xi \quad (2.3.37)$$

For surface  $S_2$

$$\text{Unit normal vector } \vec{n} = \alpha^{-1/2} (-\beta \vec{e}_X + \vec{e}_Y)$$

$$\begin{aligned} \therefore \vec{U} \cdot \vec{n} &= (U \vec{e}_X + V \vec{e}_Y) \cdot (-\beta \vec{e}_X + \vec{e}_Y) \alpha^{-1/2} \\ &= (-\beta U + V) \alpha^{-1/2} = U_{\xi} \alpha^{-1/2} \end{aligned} \quad (2.3.38)$$

Elemental surface area

$$dS = Y^{K-1} (dx^2 + dy^2)^{1/2}$$

Since  $\eta = X$  and  $Y = \xi \cdot \delta(\eta)$ , therefore  $d\eta = dX$  and

$$dY = \xi \frac{d\delta}{d\eta} \cdot d\eta \quad (\because \xi \text{ is constant along } S_2)$$

$$= \beta d\eta$$

$$\text{Thus } dS = (\delta \xi)^{K-1} (1+\beta^2)^{1/2} d\eta = (\delta \xi)^{K-1} \alpha^{1/2} d\bar{\eta} \quad (2.3.39)$$

For surfaces  $S_3$  and  $S_4$ ,  $dS$  is identical to those for  $S_1$  and  $S_2$ , with the exception that the outward normal  $\vec{n}$  has the opposite sign.

Thus, the first integral in Eq. (2.3.29) is

$$\begin{aligned} \int_S (\vec{U} \cdot \vec{n}) U_{\xi} dS &= \int_{S_1} (\vec{U} \cdot \vec{n}) U_{\xi} dS + \int_{S_2} (\vec{U} \cdot \vec{n}) U_{\xi} dS + \int_{S_3} (\vec{U} \cdot \vec{n}) U_{\xi} dS \\ &\quad + \int_{S_4} (\vec{U} \cdot \vec{n}) U_{\xi} dS = \int_{S_1} U U_{\xi} (\delta \xi)^{K-1} \delta d\xi \\ &\quad + \int_{S_2} U_{\xi} U_{\xi} (\delta \xi)^{K-1} d\eta - \int_{S_3} U U_{\xi} (\delta \xi)^{K-1} \delta d\xi \\ &\quad - \int_{S_4} U_{\xi} U_{\xi} (\delta \xi)^{K-1} d\eta \end{aligned} \quad (2.3.40)$$

From the above, it is observed that the term  $\vec{U} \cdot \vec{n}$  yields only one velocity component. This is because the unit vectors  $\vec{e}_\eta$  and  $\vec{e}_\xi$  were chosen to be tangent to the coordinate lines and the velocities were resolved in those directions; otherwise  $\vec{U} \cdot \vec{n}$  for surfaces  $S_2$  and  $S_4$  would have involved both velocity components  $U$  and  $V$ .

The  $\nabla$  operator appearing in the integral has its standard form in X-Y coordinates as

$$\nabla = \vec{e}_X \frac{\partial}{\partial X} + \vec{e}_Y \frac{\partial}{\partial Y} \quad (2.3.41)$$

which, after substitution for  $\frac{\partial}{\partial X}$  and  $\frac{\partial}{\partial Y}$  from equation (2.3.33) and (2.3.34), becomes

$$\nabla = \left( \frac{\partial}{\partial \eta} - \frac{\beta}{\delta} \frac{\partial}{\partial \xi} \right) \vec{e}_X + \frac{1}{\delta} \frac{\partial}{\partial \xi} \vec{e}_Y \quad (2.3.42)$$

Therefore, for surface  $S_1$ ,

$$\begin{aligned} \vec{n} \cdot \nabla U_\xi &= \vec{e}_X \cdot \left( \frac{\partial U_\xi}{\partial X} \vec{e}_X + \frac{\partial U_\xi}{\partial Y} \vec{e}_Y \right) \\ &= \frac{\partial U_\xi}{\partial X} = \frac{\partial U_\xi}{\partial \eta} - \frac{\beta}{\delta} \frac{\partial U_\xi}{\partial \xi} \end{aligned} \quad (2.3.43)$$

For surface  $S_2$ ,

$$\begin{aligned} \vec{n} \cdot \nabla U_\xi &= \alpha^{-1/2} (-\beta \vec{e}_X + \vec{e}_Y) \cdot \left( \frac{\partial U_\xi}{\partial X} \vec{e}_X + \frac{\partial U_\xi}{\partial Y} \vec{e}_Y \right) = \alpha^{-1/2} (-\beta \frac{\partial U_\xi}{\partial X} + \frac{\partial U_\xi}{\partial Y}) \\ &= \alpha^{-1/2} \left( -\beta \frac{\partial U_\xi}{\partial \eta} + \frac{\beta^2}{\delta} \frac{\partial U_\xi}{\partial \xi} + \frac{1}{\delta} \frac{\partial U_\xi}{\partial \xi} \right) = \frac{\alpha^{1/2}}{\delta} \frac{\partial U_\xi}{\partial \xi} - \beta \alpha^{-1/2} \frac{\partial U_\xi}{\partial \eta} \end{aligned} \quad (\because \alpha = 1+\beta^2) \quad (2.3.44)$$

Aside from a minus sign,  $\vec{n} \cdot \nabla U_\xi$  for surfaces  $S_3$  and  $S_4$  is identical to those for  $S_1$  and  $S_2$  respectively.

With the aid of the above, the second surface integral of Eq. (2.3.29) may now be expressed as

$$\begin{aligned} \int_S (\vec{n} \cdot \nabla U_\xi) dS &= \int_{S_1} (\vec{n} \cdot \nabla U_\xi) dS + \int_{S_2} (\vec{n} \cdot \nabla U_\xi) dS + \int_{S_3} (\vec{n} \cdot \nabla U_\xi) dS \\ &+ \int_{S_4} (\vec{n} \cdot \nabla U_\xi) dS = \int_{S_1} \left( \frac{\partial U_\xi}{\partial \eta} - \beta \frac{\partial U_\xi}{\partial \xi} \right) (\delta \xi)^{K-1} \delta d\xi + \int_{S_2} \left( \frac{\alpha}{\delta} \frac{\partial U_\xi}{\partial \xi} \right. \\ &\quad \left. - \beta \frac{\partial U_\xi}{\partial \eta} \right) (\delta \xi)^{K-1} d\eta - \int_{S_3} \left( \frac{\partial U_\xi}{\partial \eta} - \beta \frac{\partial U_\xi}{\partial \xi} \right) (\delta \xi)^{K-1} \delta d\xi \\ &- \int_{S_4} \left( \frac{\alpha}{\delta} \frac{\partial U_\xi}{\partial \xi} - \beta \frac{\partial U_\xi}{\partial \eta} \right) (\delta \xi)^{K-1} d\eta \end{aligned} \quad (2.3.45)$$

In the above equation the terms  $\beta \frac{\partial U_\xi}{\partial \xi}$  and  $\beta \frac{\partial U_\xi}{\partial \eta}$  are cross-diffusion terms across surfaces  $S_1$  or  $S_3$  and  $S_2$  or  $S_4$  driven respectively by velocity gradients in the  $\xi$  and  $\eta$  directions. They originate from the non-orthogonal nature of control volume boundaries that appear through the transformation given by Eq. (2.3.33).

Attention will now be focussed on the volume integrals that appear on the right side of Eq. (2.3.29).

The volume element  $dV$  may be expressed as

$$dV = Y^{K-1} dY dX = (\delta \xi)^{K-1} \delta d\xi d\eta \quad (2.3.46)$$

Now various terms related to the right side of Eq. (2.3.29) are evaluated as follows :

$$\vec{U} \cdot \nabla \beta = (U \vec{e}_X + V \vec{e}_Y) \cdot (\frac{\partial \beta}{\partial X} \vec{e}_X + \frac{\partial \beta}{\partial Y} \vec{e}_Y) = U \frac{\partial \beta}{\partial X} + V \frac{\partial \beta}{\partial Y} .$$

Since  $\beta = \xi \frac{d\delta}{d\eta} = \frac{Y}{\delta} \frac{d\delta}{d\eta}$ , therefore  $\frac{\partial \beta}{\partial Y} = \frac{1}{\delta} \frac{d\delta}{d\eta}$

$$\text{and } \frac{\partial \beta}{\partial X} = - \frac{Y}{\delta^2} \frac{d\delta}{d\eta} \cdot \frac{d\delta}{d\eta} + \xi \frac{d^2 \delta}{d\eta^2} = \xi \frac{d^2 \delta}{d\eta^2} - \frac{\beta}{\delta} \frac{d\delta}{d\eta}$$

$$\begin{aligned} \text{Thus } \vec{U} \cdot \nabla \beta &= U \xi \frac{d^2 \delta}{d\eta^2} - \frac{U \beta}{\delta} \frac{d\delta}{d\eta} + V \frac{d\delta}{d\eta} = \frac{1}{\delta} (V - \beta U) \frac{d\delta}{d\eta} + U \xi \frac{d^2 \delta}{d\eta^2} \\ &= \frac{U}{\delta} \frac{d\delta}{d\eta} + U \xi \frac{d^2 \delta}{d\eta^2} \end{aligned} \quad (2.3.47)$$

$$\nabla^2 \beta = \frac{\partial^2 \beta}{\partial X^2} + \frac{\partial^2 \beta}{\partial Y^2} + (K-1) \frac{1}{Y} \frac{\partial \beta}{\partial Y}$$

$$\begin{aligned} \text{Now } \frac{\partial^2 \beta}{\partial X^2} &= \frac{\partial}{\partial X} \left( \frac{\partial \beta}{\partial X} \right) = \frac{\partial}{\partial X} \left\{ \xi \frac{d^2 \delta}{d\eta^2} - \frac{\xi}{\delta} \left( \frac{d\delta}{d\eta} \right)^2 \right\} \\ &= \xi \frac{d^3 \delta}{d\eta^3} + \frac{d^2 \delta}{d\eta^2} \left( -\frac{\xi}{\delta} \right) \frac{d\delta}{d\eta} - \left\{ \frac{\xi}{\delta} \right\} 2 \frac{d\delta}{d\eta} \frac{d^2 \delta}{d\eta^2} + \left( \frac{d\delta}{d\eta} \right)^2 \left( -\frac{2\xi}{\delta^2} \right) \frac{d\delta}{d\eta} \\ &= \xi \frac{d^3 \delta}{d\eta^3} + \frac{2\xi}{\delta^2} \left( \frac{d\delta}{d\eta} \right)^3 - \frac{3\xi}{\delta} \frac{d\delta}{d\eta} \frac{d^2 \delta}{d\eta^2} . \end{aligned}$$

Similarly

$$\frac{\partial^2 \beta}{\partial Y^2} = \frac{\partial}{\partial Y} \left( \frac{\partial \beta}{\partial Y} \right) = \frac{\partial}{\partial Y} \left( \frac{1}{\delta} \frac{d\delta}{d\eta} \right) = 0$$

$$\frac{1}{Y} \frac{\partial \beta}{\partial Y} = \frac{1}{\delta \xi} \frac{1}{\delta} \frac{d\delta}{d\eta} = \frac{1}{\xi \delta^2} \frac{d\delta}{d\eta}$$

$$\therefore \nabla^2 \beta = \xi \frac{d^3 \delta}{d\eta^3} + \frac{2\xi}{\delta^2} \left( \frac{d\delta}{d\eta} \right)^3 - \frac{3\xi}{\delta} \frac{d\delta}{d\eta} \frac{d^2 \delta}{d\eta^2} + (K-1) \frac{1}{\xi \delta^2} \frac{d\delta}{d\eta} \quad (2.3.48)$$

$$\begin{aligned} \nabla U \cdot \nabla \beta &= \left( \frac{\partial U}{\partial X} \vec{e}_X + \frac{\partial U}{\partial Y} \vec{e}_Y \right) \cdot \left( \frac{\partial \beta}{\partial X} \vec{e}_X + \frac{\partial \beta}{\partial Y} \vec{e}_Y \right) \\ &= \frac{\partial U}{\partial X} \cdot \frac{\partial \beta}{\partial X} + \frac{\partial U}{\partial Y} \cdot \frac{\partial \beta}{\partial Y} \end{aligned}$$

$$\begin{aligned}
&= (\frac{\partial U}{\partial \eta} - \frac{\beta}{\delta} \frac{\partial U}{\partial \xi}) (\xi \frac{d^2 \delta}{d\eta^2} - \frac{\beta}{\delta} \frac{d\delta}{d\eta}) + \frac{1}{\delta} \frac{\partial U}{\partial \xi} \cdot \frac{1}{\delta} \frac{d\delta}{d\eta} \\
&= \frac{\partial U}{\partial \eta} (\xi \frac{d^2 \delta}{d\eta^2} - \frac{\beta}{\delta} \frac{d\delta}{d\eta}) + \frac{\partial U}{\partial \xi} (\frac{1+\beta^2}{\delta^2} \frac{d\delta}{d\eta} - \frac{\beta \xi}{\delta} \frac{d^2 \delta}{d\eta^2}) \\
&= \frac{\partial U}{\partial \eta} (\xi \frac{d^2 \delta}{d\eta^2} - \frac{\beta}{\delta} \frac{d\delta}{d\eta}) + \frac{\partial U}{\partial \xi} (\frac{\alpha}{\delta^2} \frac{d\delta}{d\eta} - \frac{\beta \xi}{\delta} \frac{d^2 \delta}{d\eta^2}) \tag{2.3.49}
\end{aligned}$$

$$\beta \frac{\partial P}{\partial X} - \frac{\partial P}{\partial Y} = \beta (\frac{\partial P}{\partial \eta} - \frac{\beta}{\delta} \frac{\partial P}{\partial \xi}) - \frac{1}{\delta} \frac{\partial P}{\partial \xi} = \beta \frac{\partial P}{\partial \eta} - \frac{\alpha}{\delta} \frac{\partial P}{\partial \xi} \tag{2.3.50}$$

and

$$\frac{1}{Y^2} (U_\xi + \beta U) = \frac{1}{\xi^2 \delta^2} (U_\xi + \beta U) \tag{2.3.51}$$

All the ingredients needed to evaluate the right side of Eq. (2.3.29) have been derived. Therefore, their sum, denoted by  $b$ , is given by

$$\begin{aligned}
b &= \int_U (\beta \frac{\partial P}{\partial \eta} - \frac{\alpha}{\delta} \frac{\partial P}{\partial \xi}) (\delta \xi)^{K-1} \delta d\xi d\eta \\
&\quad - \int_U \{U(\frac{U_\xi}{\delta} \frac{d\delta}{d\eta} + U_\xi \frac{d^2 \delta}{d\eta^2})\} (\delta \xi)^{K-1} \delta d\xi d\eta \\
&\quad + \frac{1}{Re} \int_U \{U(\xi \frac{d^3 \delta}{d\eta^3} + \frac{2\xi}{\delta^2} (\frac{d\delta}{d\eta})^3 - \frac{3\xi}{\delta} \frac{d\delta}{d\eta} \frac{d^2 \delta}{d\eta^2} + (K-1) \frac{1}{\xi \delta^2} \frac{d\delta}{d\eta})\} \\
&\quad (\delta \xi)^{K-1} \delta d\xi d\bar{\eta} + \frac{2}{Re} \int_U \{\frac{\partial U}{\partial \eta} (\xi \frac{d^2 \delta}{d\eta^2} - \frac{\beta}{\delta} \frac{d\delta}{d\eta}) \\
&\quad + \frac{\partial U}{\partial \xi} (\frac{\alpha}{\delta^2} \frac{d\delta}{d\eta} - \frac{\beta \xi}{\delta} \frac{d^2 \delta}{d\eta^2})\} (\delta \xi)^{K-1} \delta d\xi d\bar{\eta} \\
&\quad - \frac{1}{Re} \int_U \{(K-1) \frac{1}{\xi^2 \delta^2} (U_\xi + \beta U)\} (\delta \xi)^{K-1} \delta d\xi d\bar{\eta} \tag{2.3.52}
\end{aligned}$$

Now with the aid of expressions in Eqs. (2.3.40), (2.3.45), and (2.3.52), Eq.(2.3.29) becomes

$$\begin{aligned}
 & \int_{S_1} \left\{ UU_\xi \delta - \frac{1}{Re} \left( \delta \frac{\partial U_\xi}{\partial \eta} - \beta \frac{\partial U_\xi}{\partial \xi} \right) \right\} (\delta \xi)^{K-1} d\xi \\
 & - \int_{S_3} \left\{ UU_\xi \delta - \frac{1}{Re} \left( \delta \frac{\partial U_\xi}{\partial \eta} - \beta \frac{\partial U_\xi}{\partial \xi} \right) \right\} (\delta \xi)^{K-1} d\xi \\
 & + \int_{S_2} \left\{ U_\xi U_\xi - \frac{1}{Re} \left( \alpha \frac{\partial U_\xi}{\partial \xi} - \beta \frac{\partial U_\xi}{\partial \eta} \right) \right\} (\delta \xi)^{K-1} d\eta \\
 & - \int_{S_4} \left\{ U_\xi U_\xi - \frac{1}{Re} \left( \alpha \frac{\partial U_\xi}{\partial \xi} - \beta \frac{\partial U_\xi}{\partial \eta} \right) \right\} (\delta \xi)^{K-1} d\eta = b \quad (2.3.53)
 \end{aligned}$$

Because of similarity among Eqs. (2.3.29) - (2.3.31), it is possible to rewrite them in a common compact form by introducing the following parameters :

$$\begin{aligned}
 Q &= -\frac{\alpha}{\delta} \frac{\partial \Psi}{\partial \xi}, \quad \gamma = -\delta \frac{\partial \Psi}{\partial \eta}, \\
 \Lambda &= \beta \frac{\partial \Psi}{\partial \eta}, \quad \Psi = \beta \frac{\partial \Psi}{\partial \xi}
 \end{aligned} \quad (2.3.54)$$

where  $\Psi$  stands for  $U, U_\xi$  or  $H$ . Using the above parameters, the common form of Eqs. (2.3.29) - (2.3.31) is

$$\begin{aligned}
 & \int_{S_1} \left\{ U\Psi \delta + \Gamma(\gamma + \Psi) \right\} (\delta \xi)^{K-1} d\xi - \int_{S_3} \left\{ U\Psi \delta + \Gamma(\gamma + \Psi) \right\} (\delta \xi)^{K-1} d\xi \\
 & + \int_{S_2} \left\{ U_\xi \Psi + \Gamma(Q + \Lambda) \right\} (\delta \xi)^{K-1} d\eta - \int_{S_4} \left\{ U_\xi \Psi + \Gamma(Q + \Lambda) \right\} (\delta \xi)^{K-1} d\eta \\
 & = b \quad (2.3.55)
 \end{aligned}$$

where  $\Gamma$  is the diffusion co-efficient and is equal to  $1/Re$  for momentum equations and  $1/Pe$  for the energy equation. The  $b$ -term for  $\xi$ -momentum equation is given by Eq. (2.3.52). For  $\eta$ -momentum equation,  $b$  is obtained from the right side of Eq. (2.3.30) and is given by

$$b = - \int_{\Psi} \frac{\partial P}{\partial X} d\Psi = - \int_{\Psi} \left( \frac{\partial P}{\partial \eta} - \frac{\beta}{\delta} \frac{\partial P}{\partial \xi} \right) (\delta \xi)^{K-1} \delta d\xi d\eta \quad (2.3.56)$$

For energy equation [Eq. (2.3.31)] b is simply zero.

The terms  $U\varphi$  and  $U_\xi\varphi$  in Eq. (2.3.55) are usual convective fluxes crossing the control volume surface. The quantities  $\gamma$  and  $Q$  are, respectively, proportional to diffusive heat or momentum fluxes in the  $\eta$  and  $\xi$  directions. The  $\Lambda$  and  $\Psi$  terms can also be thought of as representing pseudodiffusion fluxes. Thus,  $\Lambda$  denotes diffusion driven across a  $\xi$ -face by a gradient in the  $\eta$ -direction, while  $\Psi$  represents diffusion across an  $\eta$ -face driven by a  $\xi$ -gradient.

Finally, the continuity Eq. (2.3.32) can be written as

$$\int_{S_1} (\vec{n} \cdot \vec{U}) dS + \int_{S_2} (\vec{n} \cdot \vec{U}) dS + \int_{S_3} (\vec{n} \cdot \vec{U}) dS + \int_{S_4} (\vec{n} \cdot \vec{U}) dS = 0$$

or

$$\begin{aligned} \int_{S_1} U(\delta \xi)^{K-1} \delta d\xi + \int_{S_2} U_\xi(\delta \xi)^{K-1} d\eta - \int_{S_3} U(\delta \xi)^{K-1} \delta d\xi \\ - \int_{S_4} U_\xi(\delta \xi)^{K-1} d\eta = 0 \end{aligned} \quad (2.3.57)$$

If velocities are retained in terms of physical components  $U$  and  $V$ , the resulting continuity equation would have involved two extra mass flux terms on surfaces  $S_2$  and  $S_4$ .

## 2.4 Formulation for Non-symmetric Channel

Using the same assumptions and same non-dimensional parameters the governing equations are the same as earlier [Eqs. (2.3.8), (2.3.9), (2.3.10) and (2.3.11) with  $K = 1$ ].

The boundary conditions in this case are,

$$\begin{aligned}
 U(0, Y) &= 1.0 & V(0, Y) &= 0.0 \\
 U(X, \delta(X)) &= 0.0 & V(X, \delta(X)) &= 0.0 \\
 U\{X, (1+\delta(X))\} &= 0.0 & V\{X, (1+\delta(X))\} &= 0.0 \\
 H(0, Y) &= 1.0 & & (2.4.1) \\
 H(X, \delta(X)) &= 0.0 \\
 H\{X, (1+\delta(X))\} &= 0.0 \\
 P(0, Y) &= 0.0
 \end{aligned}$$

The boundary conditions at exit are the same as those for the symmetric channel.

In this case the X, Y coordinates are transformed to  $\eta$ ,  $\xi$  coordinates by the relations

$$\eta = X, \quad \xi = Y - \delta(X) \quad (2.4.2)$$

where  $\delta(X) = \delta'(X)/L$  instead of  $\delta(X) = 2 \frac{\delta'(X)}{L}$  as earlier.

Following the same mathematical steps as in Sec. 2.3, the following expressions are obtained with reference to Fig. 3.

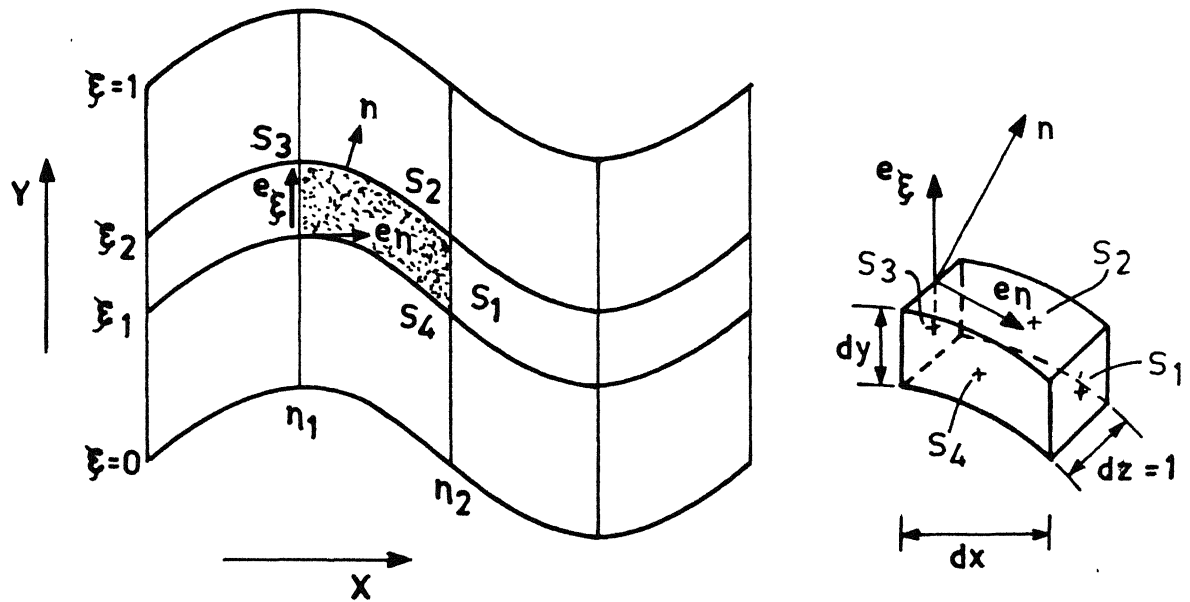
i) Unit normal vector perpendicular to  $\xi$ -constant lines

$$\vec{n} = \frac{-\beta \vec{e}_X + \vec{e}_Y}{\alpha^{1/2}} \quad (2.4.3)$$

$$\text{where } \beta = \frac{d\delta}{d\eta} \quad (2.4.4)$$

$$\text{and } \alpha = 1 + \beta^2 \quad (2.4.5)$$

ii) Unit normal vector tangent to the  $\eta$ -constant and  $\xi$ -constant lines respectively



(a) Shape of control volume  
in physical space

(b) Shape of control  
volume element  
( $dz = \text{unit}$ )

Fig. 3 Shape of control volume for non-symmetric channel.

$$\vec{e}_\xi = \vec{e}_Y, \quad \vec{e}_\eta = \frac{\vec{e}_X + \beta \vec{e}_Y}{\alpha^{1/2}} \quad (2.4.6)$$

iii) The velocity components, in the  $\eta$ - and  $\xi$ -directions, respectively, are

$$U_\eta = \alpha^{1/2} U, \quad U_\xi = -\beta U + V \quad (2.4.7)$$

iv) The momentum equations in the  $\eta$ - and  $\xi$ -directions, respectively, are

$$U \frac{\partial U}{\partial X} + V \frac{\partial U}{\partial Y} = - \frac{\partial P}{\partial X} + \frac{1}{Re} \left( \frac{\partial^2 U}{\partial X^2} + \frac{\partial^2 U}{\partial Y^2} \right) \quad (2.4.8)$$

$$\begin{aligned} U \frac{\partial U_\xi}{\partial X} + V \frac{\partial U_\xi}{\partial Y} &= \beta \frac{\partial P}{\partial X} - \frac{\partial P}{\partial Y} + \frac{1}{Re} \left( \frac{\partial^2 U_\xi}{\partial X^2} + \frac{\partial^2 U_\xi}{\partial Y^2} \right) \\ &- U(U \frac{d\beta}{dX}) + \frac{1}{Re} (U \frac{d^2 \beta}{dX^2} + 2 \frac{\partial U}{\partial X} \frac{d\beta}{dX}) \end{aligned} \quad (2.4.9)$$

v) Control volume form of the governing equations :

$\xi$ -momentum equation :

$$\begin{aligned} \int_S (\vec{U} \cdot \vec{n}) U_\xi dS - \frac{1}{Re} \int_S (\vec{n} \cdot \nabla U_\xi) dS &= \int_V (\beta \frac{\partial P}{\partial X} - \frac{\partial P}{\partial Y}) dV \\ - \int_V U(U \frac{d\beta}{dX}) dV + \frac{1}{Re} \int_V (U \frac{d^2 \beta}{dX^2} + 2 \frac{\partial U}{\partial X} \frac{d\beta}{dX}) dV \end{aligned} \quad (2.4.10)$$

$\eta$ -momentum equation :

$$\int_S (\vec{U} \cdot \vec{n}) U dS - \frac{1}{Re} \int_S (\vec{n} \cdot \nabla U) dS = - \int_V \frac{\partial P}{\partial X} dV \quad (2.4.11)$$

energy equation :

$$\int_S (\vec{U} \cdot \vec{n}) H dS - \frac{1}{Pe} \int_S (\vec{n} \cdot \nabla H) dS = 0 \quad (2.4.12)$$

continuity equation :

$$\int_S (\vec{n} \cdot \vec{U}) dS = 0 \quad (2.4.13)$$

vi) The quantities needed to evaluate the surface and volume integral in Eq. (2.4.10) are

$$\nabla = \left( \frac{\partial}{\partial \eta} - \beta \frac{\partial}{\partial \xi} \right) \vec{e}_X + \frac{\partial}{\partial \xi} \vec{e}_Y$$

$$\text{volume element } dV = d\eta d\xi$$

For surface  $S_1$

$$\text{Unit normal vector } \vec{n} = \vec{e}_X$$

$$\vec{U} \cdot \vec{n} = U,$$

$$\vec{n} \cdot \nabla U_\xi = \frac{\partial U_\xi}{\partial \eta} - \beta \frac{\partial U_\xi}{\partial \xi} \text{ and } dS = d\xi$$

For surface  $S_2$

$$\vec{n} = \alpha^{-1/2} (-\beta \vec{e}_X + \vec{e}_Y), \text{ therefore } \vec{U} \cdot \vec{n} = U_\xi \alpha^{-1/2}$$

$$\vec{n} \cdot \nabla U_\xi = \alpha^{1/2} \frac{\partial U_\xi}{\partial \xi} - \beta \alpha^{-1/2} \frac{\partial U_\xi}{\partial \eta} \text{ and } dS = \alpha^{1/2} d\eta$$

For surface  $S_3$  and  $S_4$ ,  $dS$  is identical to those for  $S_1$  and  $S_2$ , with the exception that the outward normal  $\vec{n}$  has the opposite sign.

With the aid of above expressions, the first and second surface integrals in Eq. (2.4.10) become

$$\begin{aligned} \int_S (\vec{U} \cdot \vec{n}) U_\xi dS &= \int_{S_1} U U_\xi d\xi + \int_{S_2} U_\xi U_\xi d\eta - \int_{S_3} U U_\xi d\xi - \int_{S_4} U_\xi U_\xi d\eta, \\ \int_S (\vec{n} \cdot \nabla U_\xi) dS &= \int_{S_1} \left( \frac{\partial U_\xi}{\partial \eta} - \beta \frac{\partial U_\xi}{\partial \xi} \right) d\xi + \int_{S_2} \left( \alpha \frac{\partial U_\xi}{\partial \xi} - \beta \frac{\partial U_\xi}{\partial \eta} \right) d\eta \\ &\quad - \int_{S_3} \left( \frac{\partial U_\xi}{\partial \eta} - \beta \frac{\partial U_\xi}{\partial \xi} \right) d\xi - \int_{S_4} \left( \alpha \frac{\partial U_\xi}{\partial \xi} - \beta \frac{\partial U_\xi}{\partial \eta} \right) d\eta \end{aligned}$$

and the right side of the same equation becomes

$$\begin{aligned} b = & - \int_{\Psi} (-\beta \frac{\partial P}{\partial \eta} + \alpha \frac{\partial P}{\partial \xi}) d\eta d\xi - \int_{\Psi} U^2 \frac{d^2 \delta}{d\eta^2} d\eta d\xi + \frac{1}{Re} \int_{\Psi} U \frac{d^3 \delta}{d\eta^3} d\eta d\xi \\ & + \frac{2}{Re} \int_{\Psi} \frac{\partial U}{\partial \eta} \frac{d^2 \delta}{d\eta^2} d\eta d\xi - \frac{2}{Re} \int_{\Psi} \beta \frac{\partial U}{\partial \xi} \frac{d^2 \delta}{d\eta^2} d\eta d\xi \end{aligned} \quad (2.4.14)$$

Due to the same reason as before, the common form of Eqs. (2.4.10), (2.4.11), and (2.4.12) becomes

$$\begin{aligned} \int_{S_1} \{ (U \varphi + \Gamma(\gamma + \Psi)) \} d\xi - \int_{S_3} \{ (U \varphi + \Gamma(\gamma + \Psi)) \} d\xi + \int_{S_2} \{ U_\xi \varphi \\ + \Gamma(\Omega + \Lambda) \} d\eta - \int_{S_4} \{ U_\xi \varphi + \Gamma(\Omega + \Lambda) \} d\eta = b \end{aligned} \quad (2.4.15)$$

where  $\varphi$  stands for  $U$  or  $U_\xi$  or  $H$ ,

$$\begin{aligned} \Gamma &= 1/Re \text{ for momentum equations} \\ &= 1/Pe \text{ for the energy equation,} \end{aligned}$$

and

$$\Omega = -\alpha \frac{\partial \varphi}{\partial \xi}, \quad \gamma = -\frac{\partial \varphi}{\partial \eta}, \quad \Lambda = \beta \frac{\partial \varphi}{\partial \eta}, \quad \Psi = \beta \frac{\partial \varphi}{\partial \xi} \quad (2.4.16)$$

For  $\xi$ -momentum equation  $b$  is given by Eq. (2.4.14). For  $\eta$ -momentum equation  $b$  is given by

$$b = - \int_{\Psi} \frac{\partial P}{\partial X} d\Psi = - \int_{\Psi} (\frac{\partial P}{\partial \eta} - \beta \frac{\partial P}{\partial \xi}) d\eta d\xi \quad (2.4.17)$$

For energy equation  $b$  is zero. Finally, the continuity equation Eq. (2.4.13) may be expressed as

$$\int_{S_1} U d\xi + \int_{S_2} U_\xi d\eta - \int_{S_3} U d\xi - \int_{S_4} U_\xi d\eta = 0 \quad (2.4.18)$$

The control-volume formulation for the flow through channels and pipe is now complete. In the next chapter attention will be focussed on the finite-difference approximation of the control volume form of the governing equations derived here.

## Chapter 3

### FINITE-DIFFERENCE SOLUTION

#### 3.1 Domain Discretization :

For the derivation of finite-difference equation, the computational domain in the  $\eta - \xi$  coordinate system (which is rectangular in the  $\eta - \xi$  plane and non-rectangular in the X-Y plane) is first discretized. Only gradients of pressure appear in the momentum equations and pressure does not appear explicitly in the continuity equation, although it is the continuity constraint that is used to determine the pressure. Thus if the velocity components and pressure are computed at the same location and interpolated linearly for evaluation at the control volume faces, the resulting discretization equations can permit a physically unrealistic solution [7]. This possibility of an unrealistic solution can be prevented by using different grids for the velocity components and pressure and suitably staggering them relative to each other. The locations where the pressure and other dependent variables (except the velocity components) are calculated are designated as main grid points. In practice, for computational domain discretization, the main control volume boundaries are first drawn in an arbitrarily nonuniform manner and the main grid points are then placed at their geometric centres. In the above practice, the main control volume faces are not located

midway between adjacent grids points, which represents less accurate finite difference representation of the derivatives. In spite of this, the above practice is adopted here due to the following desirable features :

- a) the grid point at the geometric centre of the control volume represents the control volume better than any other point,
- b) half control volume does not occur adjacent to a boundary,
- c) discontinuities in thermophysical properties, boundary conditions and the source terms are easier to handle.

Due to mathematical singularity, the grid spacing near the entrance to the channels or pipe should be small. Also smaller grid spacing is needed near the walls because of larger gradient of the flow parameters in the direction normal to the wall.

The grid points corresponding to the velocity components are displaced with respect to the main grid points in such a way that they are located on the faces of the main control volume. The U-control volumes are staggered horizontally (i.e., in the  $\eta$ -direction) with respect to the main control volume, while the  $U_\xi$ -control volumes are staggered vertically (i.e., in the  $\xi$ -direction). This staggering is done in such a way that the displaced faces pass through the main grid points, while non-displaced faces lie along the main control volume faces. Hence the resultant shape of the control volume used to compute

velocity components and other dependent variables becomes L-shaped as shown in Fig. 4. In this figure the main grid points are denoted by dots identified by letters, P, W, E, S, N, SW, SE, NW, and NE whereas U-velocity locations are denoted by arrows ( $\rightarrow$ ) identified by P'', W'', E'', S'', N'', SW'', NW'' and NE'' and  $U_\xi$ -velocity locations are denoted by arrows ( $\rightarrow$ ) identified by P', W', E', S', N', SW', SE', NW', and NE'. The U and  $U_\xi$  locations are referred to as staggered points. In the same figure (Fig. 4) the main control volume, U-control volume, and  $U_\xi$ -control volume are, respectively, identified by inclined, vertical, and horizontal hatch lines. The type of control volume used for velocities near the boundaries is different as shown in Fig. 5. A complete picture of the discretized computational domain used is shown in Fig. 6a, in which NX and NY are the total no. of main grid points used for discretizing the computational domain, respectively, in the  $\eta$ - and  $\xi$ -directions. In this figure boundaries of the main control volume are shown as dashed lines. Discretized form of physical domain for both symmetric channel or pipe and for non-symmetric channel are also shown in Figs. 7a and 7b. The various geometrical quantities needed for discretizing the governing equations are also shown in Figs. 4, 5, and 6 in FORTRAN variables. Attention will now be focussed on deriving the discretized form of Eqs. (2.3.55) and (2.4.15).

### 3.2 Discretized Equations For Symmetric Channel Or Pipe

#### a) Discretization of U-momentum equation

The control volume form of the U-momentum equation is

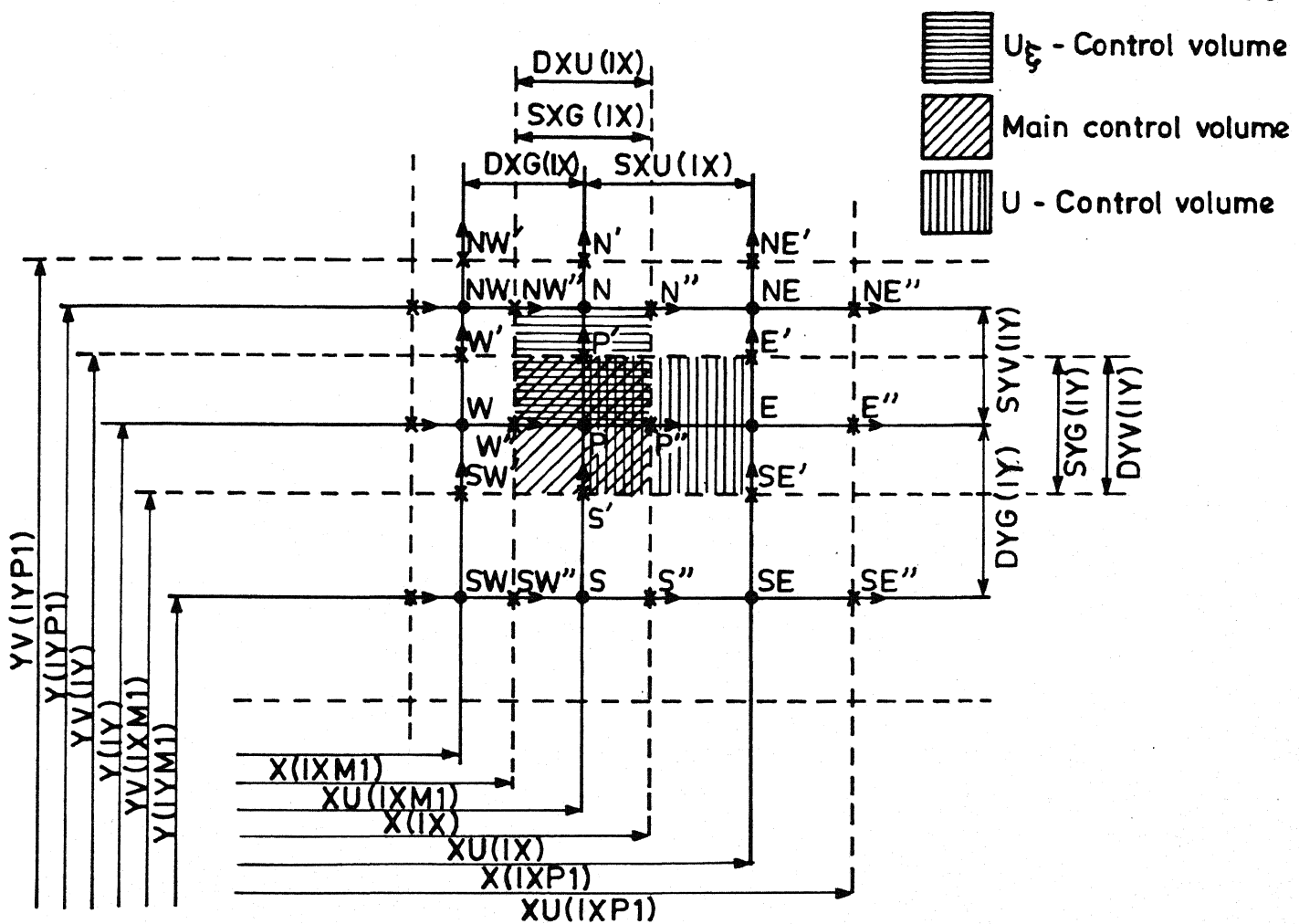


Fig. 4 Type of control volume considered

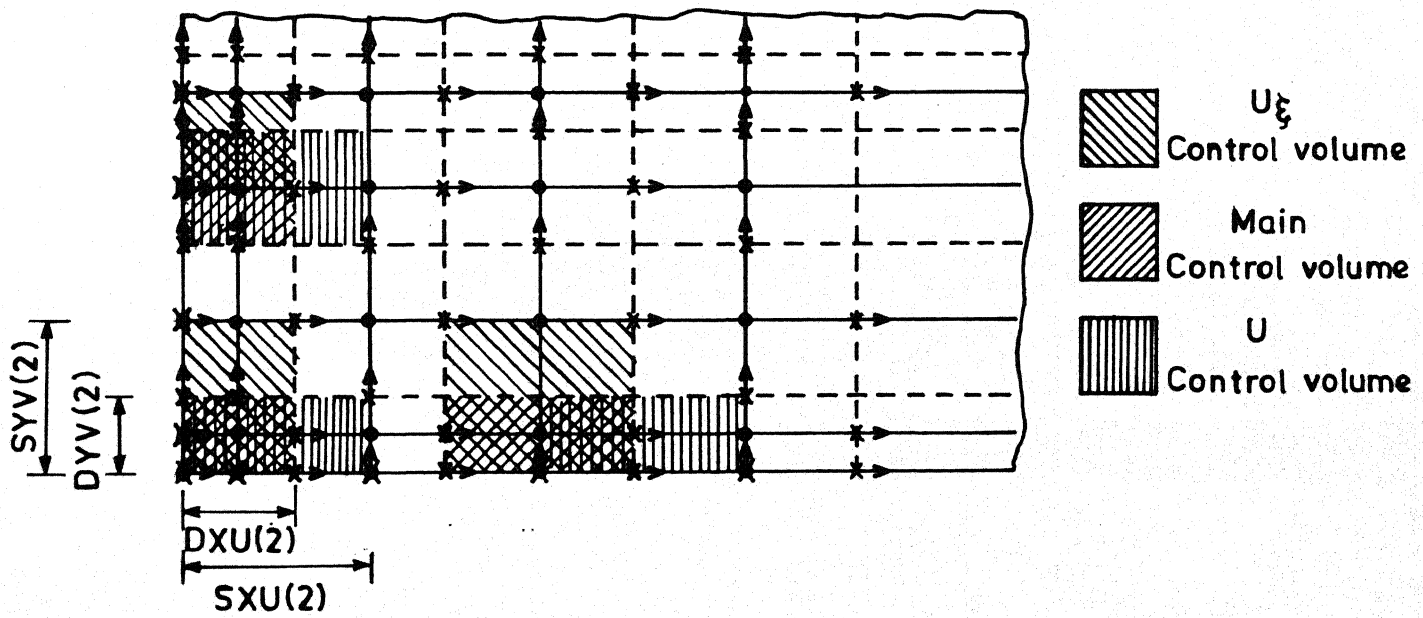


Fig. 5 Type of control volume at the boundary.

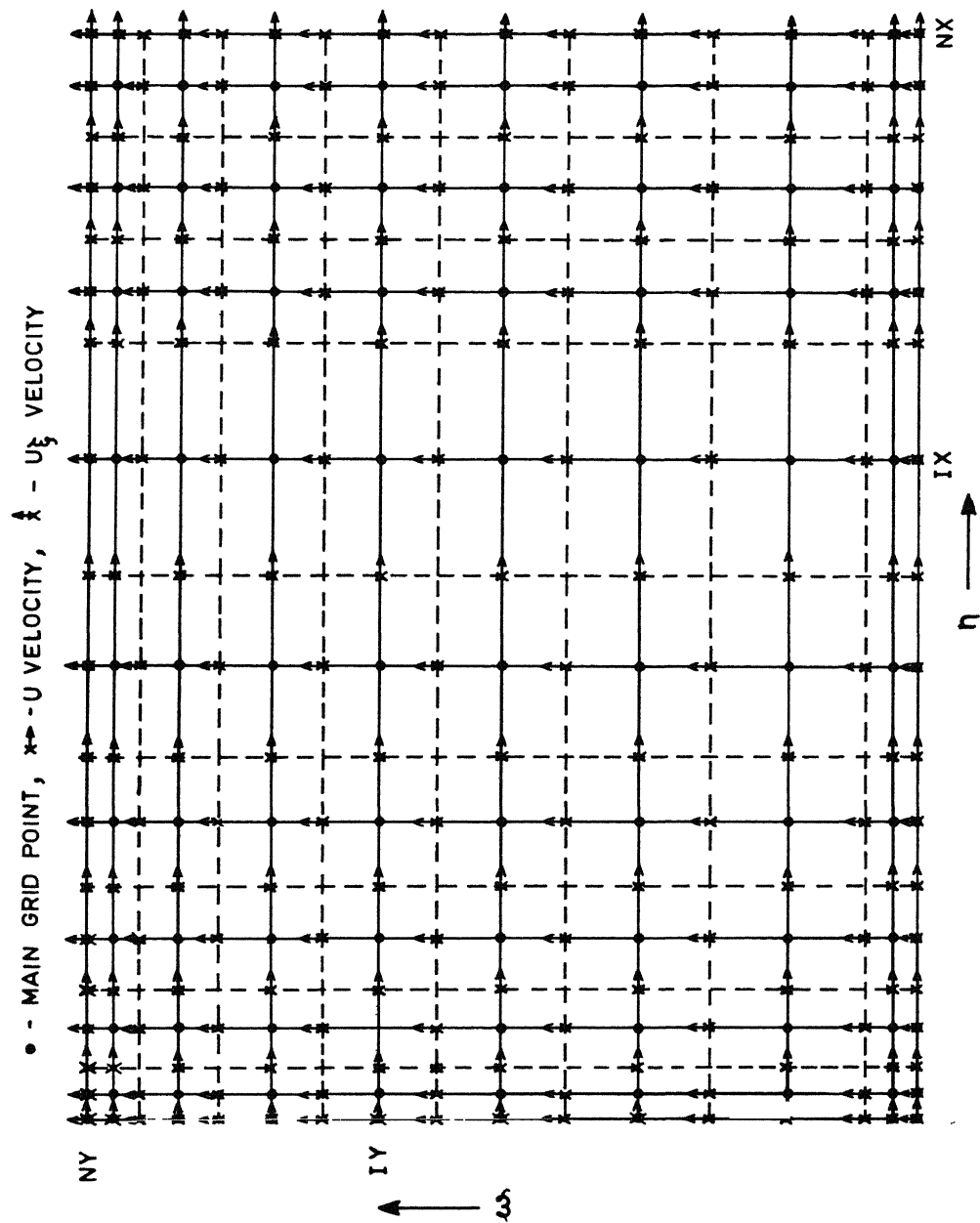


Fig. 6(a) Complete picture of the discretized computational domain.

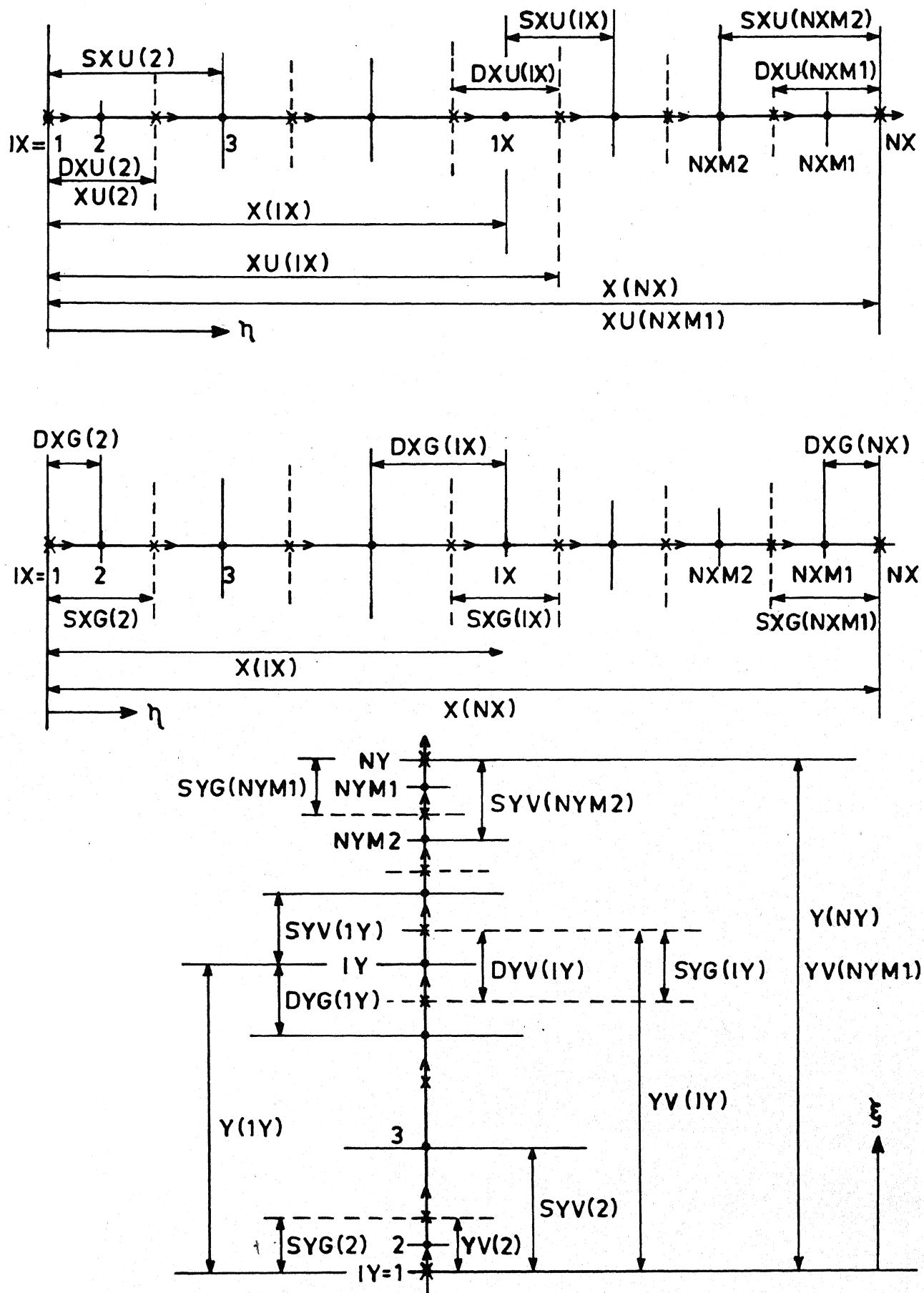


Fig. 6(b) Various grid quantities.

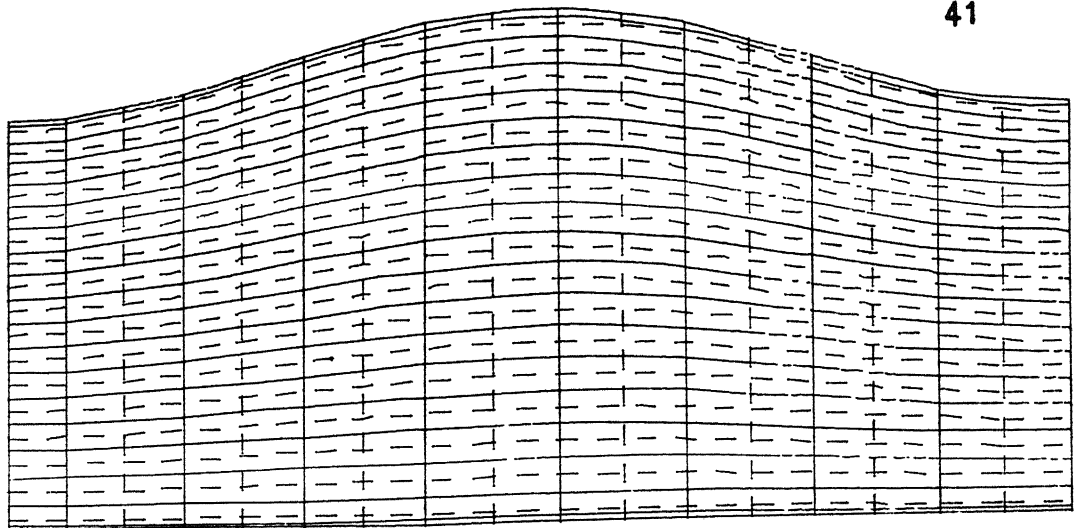


Fig. 7 a DISCRETIZED PHYSICAL DOMAIN FOR  
A SYMMETRIC CHANNEL OR PIPE ( FOR  
1st CYCLE ONLY) WITH  $\lambda L = 0.10$ ,  
 $F_1 = 1.02$ ,  $F_2 = 0.98$ ,  $NX = 58$ , and  $NY = 20$

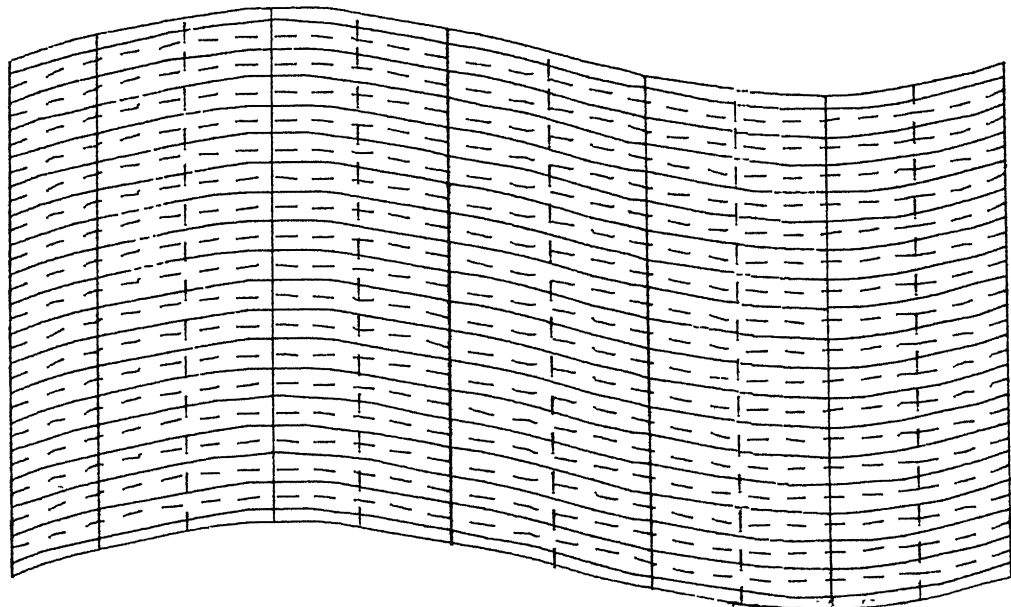


Fig. 7 b DISCRETIZED PHYSICAL DOMAIN FOR  
A NON-SYMMETRIC CHANNEL (FOR 1st  
CYCLE ONLY) WITH  $\lambda L = 0.10$ ,  $F_1 = 1.02$ ,  
 $F_2 = 1.01$ , AND  $NY = 20$ ,  $NX = 49$

given by Eq. (2.3.55) in which  $\varphi = U$ ,  $\Gamma = 1/Re$  and  $b$  is given by Eq. (2.3.56). The control volume used in this derivation is the U-control volume such as the one that surrounds the grid point  $P''$  in Fig. 8. The eight neighbouring grid points of  $P''$  are denoted by  $W'', E'', S'', N'', SW'', SE'', NW'',$  and  $NE''$ . The basic principle in the discretization of the surface integrals in Eq. (2.3.55) is to approximate  $U$  and its normal derivatives at points  $E$ ,  $n''$ ,  $P$ , and  $s''$  on each face between adjacent U-velocity grid points. Then the integration is performed by regarding those values as constant over the respective faces. With this approximation the surface integrals in Eq. (2.3.55) reduce to

$$\begin{aligned} & [(UU\delta + \frac{1}{Re} \gamma)_{E'} (\delta\xi)_{E'}^{K-1} - (UU\delta + \frac{1}{Re} \gamma)_P (\delta\xi)_P^{K-1}] \\ & \Delta\xi_u + [(U_\xi U + \frac{1}{Re} \Omega)_{n''} (\delta\xi)_{n''}^{K-1} - (U_\xi U + \frac{1}{Re} \Omega)_{s''} (\delta\xi)_{s''}^{K-1}] \Delta\xi_u \\ & (\delta\xi)_{s''}^{K-1} \Delta\xi_u = [(\frac{1}{Re} \Psi)_P (\delta\xi)_P^{K-1} - (\frac{1}{Re} \Psi)_E (\delta\xi)_E^{K-1}] \Delta\xi_u \\ & + [(\frac{1}{Re} \Lambda)_{s''} (\delta\xi)_{s''}^{K-1} - (\frac{1}{Re} \Lambda)_{n''} (\delta\xi)_{n''}^{K-1}] \Delta\eta_u + b_u \quad (3.2.1) \end{aligned}$$

$$\begin{aligned} \text{where } b_u &= \int_U \frac{\beta}{\delta} \frac{\partial P}{\partial \xi} (\delta\xi)^{K-1} \delta d\xi d\eta \\ &\quad - \int_U \frac{\partial P}{\partial \eta} (\delta\xi)^{K-1} \delta d\xi d\eta \quad (3.2.2) \end{aligned}$$

$$\text{and } \Omega = -\frac{\alpha}{\delta} \frac{\partial U}{\partial \xi}, \quad \gamma = -\delta \frac{\partial U}{\partial \eta}, \quad \Lambda = \beta \frac{\partial U}{\partial \eta}, \quad \Psi = \beta \frac{\partial U}{\partial \xi} \quad (3.2.3)$$

The choice of particular scheme for discretization of the left side of Eq. (3.2.1) depends on the relative importance of the

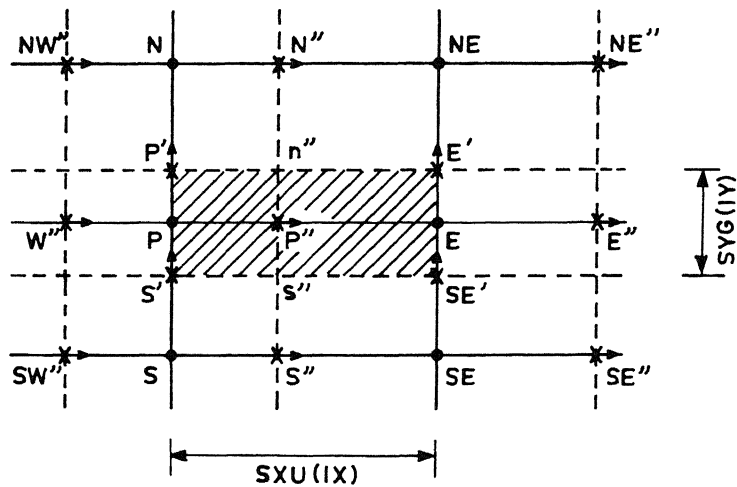


Fig. 8 U-control volume

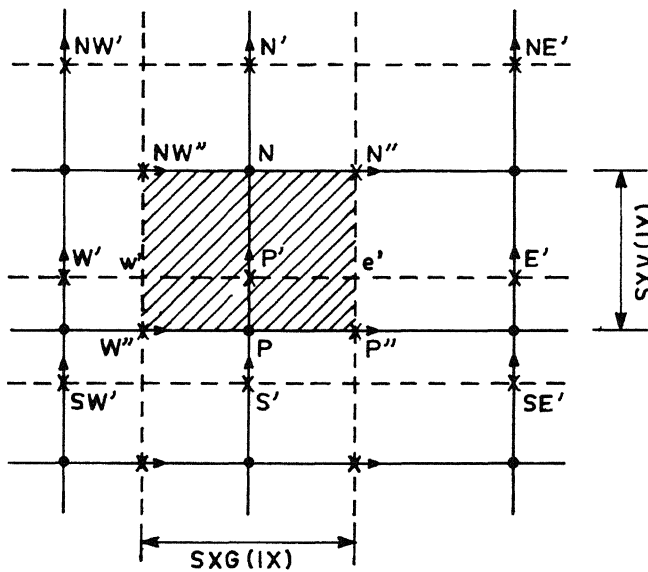
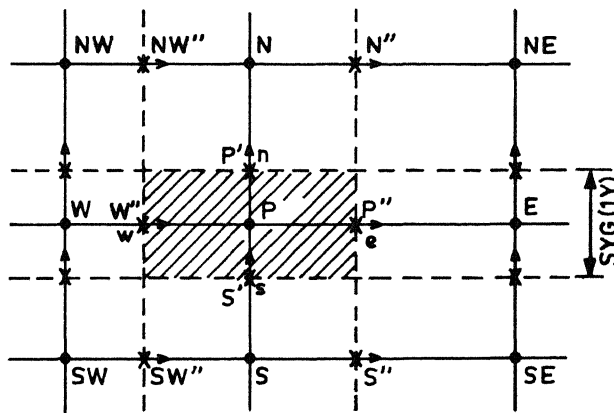
Fig. 9  $U_\xi$ -control volume

Fig. 10 Main control volume

convection and diffusion terms. When convection is small, the central difference scheme can be used to yield a result of high accuracy for a suitably small mesh size. However, for fluid flow problems, in general, convection is usually large. Therefore, the scheme should account for the special influence of the upstream values. In the presence of convection the particular discretization technique used here draws heavily from the material set forth in [ 7 ].

It is convenient to define the total (convection plus diffusion) flux  $J$  on the surfaces  $S_1$  and  $S_2$  as

$$\begin{aligned} J_E &= (UU\delta + \frac{1}{Re} \gamma)_E (\delta\xi)_E^{K-1} \Delta\xi_u \\ &= (UU\delta - \frac{\delta}{Re} \frac{\partial U}{\partial \eta})_E (\delta\xi)_E^{K-1} \Delta\xi_u \\ &= F_E U_E - D_E (U_{E''} - U_{P''}) \end{aligned} \quad (3.2.4)$$

and

$$\begin{aligned} J_{n''} &= (U_\xi U + \frac{1}{Re} Q)_{n''} (\delta\xi)_{n''}^{K-1} \Delta\eta_u \\ &= (U_\xi U - \frac{1}{Re} \frac{\alpha}{\delta} \frac{\partial U}{\partial \xi})_{n''} (\delta\xi)_{n''}^{K-1} \Delta\eta_u \\ &= F_{n''} U_{n''} - D_{n''} (U_{N''} - U_{P''}) \end{aligned} \quad (3.2.5)$$

where  $F_E$  and  $F_{n''}$  are the convective fluxes and  $D_E$  and  $D_{n''}$  are the diffusive fluxes and are given by

Convective flux :

$$F_E = (U\delta)_E (\delta\xi)_E^{K-1} \Delta\xi_u = (U\delta)_E (\delta\xi)_E^{K-1} SYG(IY) \quad (3.2.6a)$$

$$F_{n''} = (U_\xi)_{n''} (\delta \xi)_{n''}^{K-1} \Delta \eta_u = (U_\xi)_{n''} (\delta \xi)_{n''}^{K-1} SXU(IX) \quad (3.2.6b)$$

Diffusive flux :

$$D_E = \frac{1}{Re} (\delta \xi)_E^{K-1} \frac{\delta_E SYG(IY)}{DXU(IXP1)} \quad (3.2.7)$$

$$D_{n''} = \frac{1}{Re} \left(\frac{\alpha}{\delta}\right)_{n''} (\delta \xi)_{n''}^{K-1} \frac{SXU(IX)}{DYG(IYP1)}$$

where  $SYG(IY)$ ,  $SXU(IX)$ ,  $DXU(IXP1)$ , and  $DYG(IYP1)$  are the FORTRAN variables and are explained in Figs. 4. Similarly other FORTRAN variables will be introduced later.

In a similar way the total flux on faces  $S_3$  and  $S_4$  is defined as

$$J_P = F_P U_P - D_P (U_{P''} - U_{W''})$$

and  $J_{S''} = F_{S''} U_{S''} - D_{S''} (U_{P''} - U_{S''})$

where convective flux :

$$F_P = (U\delta)_P (\delta \xi)_P^{K-1} SYG(IY) \quad (3.2.8)$$

$$F_{S''} = (U_\xi)_{S''} (\delta \xi)_{S''}^{K-1} SXU(IX)$$

and diffusive flux :

$$D_P = \frac{1}{Re} (\delta \xi)_P^{K-1} \frac{\delta_P SYG(IY)}{DXU(IX)} \quad (3.2.9)$$

$$D_{S''} = \frac{1}{Re} \left(\frac{\alpha}{\delta}\right)_{S''} (\delta \xi)_{S''}^{K-1} \frac{SXU(IX)}{DYG(IY)}$$

With this definition, Eq. (3.2.1) becomes

$$J_E + J_{n''} - J_P - J_{s''} = S + b_u \quad (3.2.10)$$

where  $S$  is defined by

$$\begin{aligned} S &= \left[ \left( \frac{1}{Re} \Psi \right)_P (\delta \xi)_P^{K-1} - \left( \frac{1}{Re} \Psi \right)_E (\delta \xi)_E^{K-1} \right] \Delta \xi_u \\ &\quad + \left[ \left( \frac{1}{Re} \Lambda \right)_{s''} (\delta \xi)_{s''}^{K-1} - \left( \frac{1}{Re} \Lambda \right)_{n''} (\delta \xi)_{n''}^{K-1} \right] \Delta \eta_u \\ &= \left[ \left( \frac{\beta}{Re} \frac{\partial U}{\partial \xi} \right)_P (\delta \xi)_P^{K-1} - \left( \frac{\beta}{Re} \frac{\partial U}{\partial \xi} \right)_E (\delta \xi)_E^{K-1} \right] SYG(IY) \\ &\quad + \left[ \left( \frac{\beta}{Re} \frac{\partial U}{\partial \eta} \right)_{s''} (\delta \xi)_{s''}^{K-1} - \left( \frac{\beta}{Re} \frac{\partial U}{\partial \eta} \right)_{n''} (\delta \xi)_{n''}^{K-1} \right] SXU(IX) \end{aligned} \quad (3.2.11)$$

Also, from the continuity Eq. (2.3.57), we have

$$\begin{aligned} (U \delta)_E (\delta \xi)_E^{K-1} SYG(IY) + (U \xi)_{n''} (\delta \xi)_{n''}^{K-1} SXU(IX) \\ - (U \delta)_P (\delta \xi)_P^{K-1} SYG(IY) - (U \xi)_{s''} (\delta \xi)_{s''}^{K-1} SXU(IX) = 0 \end{aligned}$$

Using Eqs. (3.2.6) and (3.2.8), the above equation becomes

$$F_E + F_{n''} - F_P - F_{s''} = 0 \quad (3.2.12)$$

With this, Eq. (3.2.10) can be rewritten as

$$\begin{aligned} (J_E - F_E U_{P''}) + (J_{n''} - F_{n''} U_{P''}) - (J_P - F_P U_{P''}) \\ - (J_{s''} - F_{s''} U_{P''}) = S + b_u \end{aligned} \quad (3.2.13)$$

It is shown in [7] that for any  $J$  (say  $J_E$ )

$$J_E - F_E U_{P''} = a_{E''} (U_{P''} - U_{E''}) \quad (3.2.14)$$

where  $a_{E''} = D_E A \left| \frac{F_E}{D_E} \right| + [I - F_E, 0]$

where  $A \left| \frac{F_E}{D_E} \right|$  depends upon the type of scheme considered, e.g.,

for power law scheme  $A \left| \frac{F_E}{D_E} \right| = [0, (1 - 0.1 \left| \frac{F_E}{D_E} \right|)^5]$  (3.2.15)

for upwind scheme  $A \left| \frac{F_E}{D_E} \right| = 1$

The notation  $[a, b]$  means that the larger of a and b is to be used. The final form of discretized U-momentum equation may be written by substituting for  $(J_i - F_i U_{P''})$  from Eq. (3.2.14) into Eq. (3.2.13). This yields

$$\begin{aligned} a_{E''} (U_{P''} - U_{E''}) + a_{N''} (U_{P''} - U_{N''}) - a_{W''} (U_{W''} - U_{P''}) \\ - a_{S''} (U_{S''} - U_{P''}) = S + b_u \end{aligned}$$

or  $a_{P''} U_{P''} = a_{E''} U_{E''} + a_{W''} U_{W''} + a_{N''} U_{N''} + a_{S''} U_{S''} + S + b_u$  (3.2.16)

where  $a_{E''} = D_E A \left| \frac{F_E}{D_E} \right| + [I - F_E, 0]$

$$a_{W''} = D_W A \left| \frac{F_W}{D_W} \right| + [F_W, 0]$$

$$a_{N''} = D_N A \left| \frac{F_N''}{D_N''} \right| + [I - F_N, 0] \quad (3.2.16a)$$

$$a_{S''} = D_S A \left| \frac{F_S''}{D_S''} \right| + [F_S, 0]$$

$$a_{P''} = a_{E''} + a_{W''} + a_{N''} + a_{S''}$$

Again  $b_u$  can be split up in the following form assuming the value at the grid point to prevail over the control volume surrounding it

$$b_u = (\delta \xi)_P^{K-1} (P_P - P_E) \delta_{P''} \Delta \xi_u + \int_{\eta} \frac{\beta}{\delta} \frac{\partial P}{\partial \xi} (\delta \xi)_P^{K-1} \delta d\xi d\eta$$

Using the above form of  $b_u$ , Eq. (3.2.16) reduces to

$$\begin{aligned} a_{P''} U_{P''} &= a_E U_E + a_W U_W + a_N U_N + a_S U_S \\ &+ \{ (\delta \xi)_P^{K-1} \delta_{P''} \text{SYG(IY)} \} (P_P - P_E) + Sb \end{aligned} \quad (3.2.17)$$

$$\text{where } Sb = S + \int_{\eta} \frac{\beta}{\delta} \frac{\partial P}{\partial \xi} (\delta \xi)_P^{K-1} \delta d\xi d\eta \quad (3.2.18)$$

and where  $S$  is given by Eq. (3.2.11).

The last two terms in the above Eq. (3.2.17) are known as source terms. The term  $Sb$  appears due to the non-orthogonal nature of the  $\eta - \xi$  coordinate system.

For discretization of the source term  $Sb$  linear interpolation and finite-difference formulae for the variable and its derivatives which are not directly available at the location being considered are used.

Using this, the discretization form of  $Sb$  becomes

$$Sb = SUW - SUE + SUS - SUN + SUP \quad (3.2.19)$$

where

$$\begin{aligned} SUW &= \left( \frac{1}{Re} \beta \frac{\partial U}{\partial \xi} \right)_P (\delta \xi)_P^{K-1} \text{SYG(IY)} \\ &= \frac{\beta_P}{Re} \frac{1}{2} \left\{ \left( \frac{\partial U}{\partial \xi} \right)_{P''} + \left( \frac{\partial U}{\partial \xi} \right)_{W''} \right\} (\delta \xi)_P^{K-1} \text{SYG(IY)} \end{aligned}$$

$$= \frac{1}{2} \frac{\beta_P}{Re} [U_{N''} - U_{S''} + U_{NW''} - U_{SW''}] \frac{(\delta \xi)_P^{K-1} SYG(IY)}{Y(IYP1) - Y(IFYM1)} \quad (3.2.20)$$

$$SUE = \left( \frac{\beta}{Re} \frac{\partial U}{\partial \xi} \right)_E (\delta \xi)_E^{K-1} SYG(IY)$$

$$= \frac{1}{2} \frac{\beta_E}{Re} \left[ \left( \frac{\partial U}{\partial \xi} \right)_{P''} + \left( \frac{\partial U}{\partial \xi} \right)_{E''} \right] (\delta \xi)_E^{K-1} SYG(IY)$$

$$= \frac{1}{2} \frac{\beta_E}{Re} [U_{N''} - U_{S''} + U_{NE''} - U_{SE''}] \frac{(\delta \xi)_E^{K-1} SYG(IY)}{Y(IYP1) - Y(IFYM1)} \quad (3.2.21)$$

$$SUS = \left( \frac{\beta}{Re} \frac{\partial U}{\partial \eta} \right)_{S''} (\delta \xi)_{S''}^{K-1} SXU(IX)$$

$$= \frac{\beta_{S''}}{Re} \left[ \left( \frac{\partial U}{\partial \eta} \right)_{S''} + \left\{ \left( \frac{\partial U}{\partial \eta} \right)_{P''} - \left( \frac{\partial U}{\partial \eta} \right)_{S''} \right\} \frac{(1/2)SYG(IFYM1)}{DYG(IY)} \right]$$

$$(\delta \xi)_{S''}^{K-1} SXU(IX)$$

$$= \frac{\beta_{S''}}{Re} [U_{SE''} - U_{SW''} + (U_{E''} - U_{W''} - U_{SE''} + U_{SW''}) \frac{(1/2)SYG(IFYM1)}{DYG(IY)}]$$

$$\frac{(\delta \xi)_{S''}^{K-1} SXU(IX)}{XU(IXP1) - XU(IXM1)} \quad (3.2.22)$$

$$SUN = \left( \frac{\beta}{Re} \frac{\partial U}{\partial \eta} \right)_{n''} (\delta \xi)_{n''}^{K-1} SXU(IX)$$

$$= \frac{\beta_{n''}}{Re} \left[ \left( \frac{\partial U}{\partial \eta} \right)_{P''} + \left\{ \left( \frac{\partial U}{\partial \eta} \right)_{N''} - \left( \frac{\partial U}{\partial \eta} \right)_{P''} \right\} \frac{(1/2)SYG(IY)}{DYG(IYP1)} \right]$$

$$(\delta \xi)_{n''}^{K-1} SXU(IX)$$

$$= \frac{\beta_{n''}}{Re} [U_{E''} - U_{W''} + (U_{NE''} - U_{NW''} - U_{E''} + U_{W''})$$

$$\frac{(1/2)SYG(IY)}{DYG(IYP1)} ] (\delta \xi)_{n''}^{K-1} \frac{SXU(IX)}{XU(IXP1) - XU(IXM1)} \quad (3.2.23)$$

and

$$\begin{aligned}
 SUP &= \int \frac{\beta}{\delta} \left( \frac{\partial P}{\partial \xi} \right) (\delta \xi)^{K-1} \delta d\xi d\eta \\
 &= \frac{\beta_{P''}}{\delta_{P''}} \left( \frac{\partial P}{\partial \xi} \right)_{P''} (\delta \xi)_{P''}^{K-1} \delta_{P''} SYG(IY) SXU(IX) \\
 &= \frac{\beta_{P''}}{\delta_{P''}} \left[ \left( \frac{\partial P}{\partial \xi} \right)_P + \left\{ \left( \frac{\partial P}{\partial \xi} \right)_E - \left( \frac{\partial P}{\partial \xi} \right)_P \right\} \frac{(1/2)SXG(IX)}{SXU(IX)} \right] \\
 &\quad (\delta \xi)_{P''}^{K-1} \delta_{P''} SYG(IY) SXU(IX) \\
 &= \frac{\beta_{P''}}{\delta_{P''}} \left[ P_N - P_S + (P_{NE} - P_{SE} - P_N + P_S) \frac{(1/2)SXG(IX)}{SXU(IX)} \right] \\
 &\quad (\delta \xi)_{P''}^{K-1} \delta_{P''} \frac{SYG(IY) SXU(IX)}{Y(IYP1) - Y(IYM1)} \quad (3.2.24)
 \end{aligned}$$

The total source term of U-momentum equation is

$$S_u = S_b + \{(\delta \xi)_{P''}^{K-1} \delta_{P''} SYG(IY)\} (P_P - P_E) \quad (3.2.25)$$

where  $S_b$  is given by Eq. (3.2.19).

The source term  $S_u$  can be expressed in the general form [7]

$$S_u = S_C'' + S_{P''} U_{P''} \quad (3.2.26)$$

where  $S_C'' = S_b + \{(\delta \xi)_{P''}^{K-1} \delta_{P''} SYG(IY)\} (P_P - P_E)$   $(3.2.27)$

and  $S_{P''} = 0.0$   $(3.2.28)$

With these, Eq. (3.2.17) can be written as

$$\begin{aligned}
 a_{E'} &= D_{e'} A \left| \frac{F_{e'}}{D_{e'}} \right| + [ -F_{e'} , , 0 ] \\
 a_{W'} &= D_{w'} A \left| \frac{F_{w'}}{D_{w'}} \right| + [ F_{w'} , , 0 ] \\
 a_{N'} &= D_N A \left| \frac{F_N}{D_N} \right| + [ -F_N , , 0 ] \\
 a_{S'} &= D_P A \left| \frac{F_P}{D_P} \right| + [ F_P , , 0 ] \\
 a_P &= a_{E'} + a_{N'} + a_{W'} + a_{S'}
 \end{aligned} \tag{3.2.32}$$

where  $F_{e'}, F_{w'}, F_N, F_P$  and  $D_{e'}, D_{w'}, D_N, D_P$  respectively are the convective and diffusive fluxes and are given by

Convective fluxes :

$$\begin{aligned}
 F_{e'} &= (U\delta)_{e'} (\delta\xi)_{e'}^{K-1} SYV(IY) \\
 F_{w'} &= (U\delta)_{w'} (\delta\xi)_{w'}^{K-1} SYV(IY) \\
 F_N &= (U\xi)_N (\delta\xi)_N^{K-1} SXG(IX) \\
 F_P &= (U\xi)_P (\delta\xi)_P^{K-1} SXG(IX)
 \end{aligned} \tag{3.2.33}$$

where the velocity  $U_{e'}, U_{w'}, (U\xi)_N$  and  $(U\xi)_P$  are obtained from the following relation

$$U_{e'} = U_{P''} + (U_{N''} - U_{P''}) \frac{(1/2)SYG(IY)}{DYG(IYP1)} \tag{3.2.34}$$

$$U_{w'} = U_{W''} + (U_{NW''} - U_{W''}) \frac{(1/2)SYG(IY)}{DYG(IYP1)}$$

$$(U\xi)_N = (1/2) \{ (U\xi)_P + (U\xi)_N \} \tag{3.2.35}$$

$$(U\xi)_P = (1/2) \{ (U\xi)_S + (U\xi)_P \}$$

and diffusive fluxes :-

$$\begin{aligned}
 D_E &= \frac{1}{Re} (\delta \xi)^{K-1} \frac{\delta_e, SYV(IY)}{DXG(IXP1)} \\
 D_W &= \frac{1}{Re} (\delta \xi)^{K-1} \frac{\delta_w, SYV(IY)}{DXG(IX)} \\
 D_N &= \frac{1}{Re} \left(\frac{\alpha}{\delta}\right)_N (\delta \xi)^{K-1} \frac{SXG(IX)}{DYV(IYP1)} \\
 D_S &= \frac{1}{Re} \left(\frac{\alpha}{\delta}\right)_P (\delta \xi)^{K-1} \frac{SXG(IX)}{DYV(IY)}
 \end{aligned} \tag{3.2.36}$$

Eq. (3.2.30) can also be expressed as

$$\begin{aligned}
 a_p, (U_\xi)_p &= a_E, (U_\xi)_E + a_W, (U_\xi)_W + a_N, (U_\xi)_N \\
 &+ a_S, (U_\xi)_S + \left\{ \left(\frac{\alpha}{\delta}\right)_P (\delta \xi)^{K-1} \delta_p, SXG(IX) \right\} (P_p - P_N) + sb
 \end{aligned} \tag{3.2.37}$$

where

$$\begin{aligned}
 sb &= s + \int_{\Psi} \beta \frac{\partial p}{\partial \eta} (\delta \xi)^{K-1} \delta d\xi d\eta - \int_{\Psi} \left[ U \left( \frac{U_\xi}{\delta} \frac{d\delta}{d\eta} + U \xi \frac{d^2 \delta}{d\eta^2} \right) \right] \\
 &(\delta \xi)^{K-1} \delta d\xi d\eta + \frac{1}{Re} \int_{\Psi} \left[ U (\xi \frac{d^3 \delta}{d\eta^3} + \frac{2\xi}{\delta^2} (\frac{d\delta}{d\eta})^3 - \frac{3\xi}{\delta} \frac{d\delta}{d\eta} \frac{d^2 \delta}{d\eta^2}) \right. \\
 &\left. + (K-1) \frac{1}{\xi \delta} \frac{d\delta}{d\eta} \right] (\delta \xi)^{K-1} \delta d\xi d\eta + \frac{2}{Re} \int_{\Psi} \left[ \frac{\partial U}{\partial \eta} (\xi \frac{d^2 \delta}{d\eta^2} - \frac{\beta}{\delta} \frac{d\delta}{d\eta}) \right. \\
 &\left. + \frac{\partial U}{\partial \xi} (\frac{\alpha}{\delta^2} \frac{d\delta}{d\eta} - \frac{\beta \xi}{\delta} \frac{d^2 \delta}{d\eta^2}) \right] (\delta \xi)^{K-1} \delta d\xi d\eta \\
 &- \frac{1}{Re} \int_{\Psi} \left[ (K-1) \frac{1}{\xi^2 \delta^2} (U_\xi + \beta U) \right] (\delta \xi)^{K-1} \delta d\xi d\eta \tag{3.2.38}
 \end{aligned}$$

The quantity S in equation (3.2.38) is given by Eq. (3.2.31).

Using the same concept that was used for discretizing the source term in the U-momentum equation, the discretization form of  $S_b$  is given by

$$S_b = SVW - SVE + SVS - SVN + SVP1$$

$$\begin{aligned} & - SPRIME_1 (U_\xi)_P - SVP2 + SVP3 + SVP4 \\ & + SVP5 - SPRIME_2 (U_\xi)_P - SVP6 \end{aligned} \quad (3.2.39)$$

where each term on the left side of Eq. (3.2.39) is as follow:

$$\begin{aligned} SVW &= \left( \frac{\beta}{Re} \frac{\partial U_\xi}{\partial \xi} \right)_{W'} (\delta \xi)_{W'}^{K-1} SYV(IY) \\ &= \frac{\beta_{W'}}{Re} \left[ \left( \frac{\partial U_\xi}{\partial \xi} \right)_{W'} + \left\{ \left( \frac{\partial U_\xi}{\partial \xi} \right)_P - \left( \frac{\partial U_\xi}{\partial \xi} \right)_{W'} \right\} \right. \\ &\quad \left. \frac{\frac{1}{2} SXG(IXM1)}{DXG(IX)} \right] (\delta \xi)_{W'}^{K-1} SYV(IY) \\ &= \frac{\beta_{W'}}{Re} \left[ (U_\xi)_{NW'} - (U_\xi)_{SW'} + \left\{ (U_\xi)_N - (U_\xi)_S - (U_\xi)_{NW'} \right. \right. \\ &\quad \left. \left. + (U_\xi)_{SW'} \right\} \frac{\frac{1}{2} SXG(IXM1)}{DXG(IX)} \right] (\delta \xi)_{W'}^{K-1} \frac{SYV(IY)}{YV(IYP1) - YV(IXM1)} \\ SVE &= \left( \frac{\beta}{Re} \frac{\partial U_\xi}{\partial \xi} \right)_E (\delta \xi)_E^{K-1} SYV(IY) \\ &= \frac{\beta_{e'}}{Re} \left[ \left( \frac{\partial U_\xi}{\partial \xi} \right)_P + \left\{ \left( \frac{\partial U_\xi}{\partial \xi} \right)_E - \left( \frac{\partial U_\xi}{\partial \xi} \right)_P \right\} \right. \\ &\quad \left. \frac{\frac{1}{2} SXG(IX)}{DXG(IXP1)} \right] \\ &\quad \times (\delta \xi)_E^{K-1} SYV(IY) \end{aligned}$$

$$= \frac{\beta_{\xi}}{Re} [ (U_{\xi})_N - (U_{\xi})_S + \{ (U_{\xi})_{NE} - (U_{\xi})_{SE} - (U_{\xi})_N, \\ + (U_{\xi})_S \} \frac{\frac{1}{2} SXG(IX)}{DXG(IXP1)} ] (\delta \xi)_P^{K-1} \frac{SYV(IY)}{YV(IYP1) - YV(IXM1)} \quad (3.2.41)$$

$$SVS = (\frac{\beta_P}{Re} \frac{\partial U_{\xi}}{\partial \eta})_P (\delta \xi)_P^{K-1} SXG(IX) \\ = \frac{\beta_P}{Re} \frac{1}{2} \{ (\frac{\partial U_{\xi}}{\partial \eta})_P + (\frac{\partial U_{\xi}}{\partial \eta})_S \} (\delta \xi)_P^{K-1} SXG(IX) \\ = \frac{1}{2} \frac{\beta_P}{Re} [ (U_{\xi})_E - (U_{\xi})_W + (U_{\xi})_{SE} - (U_{\xi})_{SW} ] \\ (\delta \xi)_P^{K-1} \frac{SXG(IX)}{X(IXP1) - X(IXM1)} \quad (3.2.42)$$

$$SVN = (\frac{\beta_N}{Re} \frac{\partial U_{\xi}}{\partial \eta})_N (\delta \xi)_N^{K-1} SXG(IX) \\ = \frac{1}{2} \frac{\beta_N}{Re} \{ (\frac{\partial U_{\xi}}{\partial \eta})_P + (\frac{\partial U_{\xi}}{\partial \eta})_N \} (\delta \xi)_N^{K-1} SXG(IX) \\ = \frac{1}{2} \frac{\beta_N}{Re} [ (U_{\xi})_E - (U_{\xi})_W + (U_{\xi})_{NE} - (U_{\xi})_{NW} ] \\ \times (\delta \xi)_N^{K-1} \frac{SXG(IX)}{X(IXP1) - X(IXM1)} \quad (3.2.43)$$

$$SVP1 = \int_V \beta \frac{\partial P}{\partial \eta} (\delta \xi)^{K-1} \delta d\xi d\eta \\ = \beta_P (\frac{\partial P}{\partial \eta})_P (\delta \xi)_P^{K-1} \delta_P SXG(IX) SYV(IY) \\ = \beta_P [ (\frac{\partial P}{\partial \eta})_P + \{ (\frac{\partial P}{\partial \eta})_N - (\frac{\partial P}{\partial \eta})_P \} \frac{\frac{1}{2} SYG(IY)}{DYG(IYP1)} ] \\ \times (\delta \xi)_P^{K-1} \delta_P SXG(IX) SYV(IY)$$

$$= \beta_P, [P_E - P_W + (P_{NE} - P_{NW} - P_E + P_W) \frac{\frac{1}{2} SYG(IY)}{DYG(IYP1)}] (\delta\xi)_P^{K-1}$$

$$\times \frac{\delta_P, SXG(IX) SYV(IY)}{X(IXP1) - X(IXM1)} \quad (3.2.44)$$

$$SPRIME_1 \cdot (U\xi)_P = \int_U \frac{U\xi}{\delta} \frac{d\delta}{d\eta} (\delta\xi)^{K-1} \delta d\xi d\eta$$

$$= U_P, \frac{(U\xi)_P}{\delta_P}, (\frac{d\delta}{d\eta})_P, (\delta\xi)_P^{K-1} \delta_P, SXG(IX) SYV(IY)$$

$$\therefore SPRIME_1 = U_P, \frac{1}{\delta_P}, (\frac{d\delta}{d\eta})_P, (\delta\xi)_P^{K-1} \delta_P, SXG(IX) SYV(IY) \quad (3.2.45)$$

$$SVP_2 = \int_U (U\xi \frac{d^2\delta}{d\eta^2}) (\delta\xi)^{K-1} \delta d\xi d\eta$$

$$= U_P^2, \xi_P, (\frac{d^2\delta}{d\eta^2})_P, (\delta\xi)_P^{K-1} \delta_P, SXG(IX) SYV(IY) \quad (3.2.46)$$

The  $U_P$ , in Eqs. (3.2.44) and (3.2.45) is given by

$$U_P = [U_P + (U_N - U_P) \frac{\frac{1}{2} SYG(IY)}{DYG(IYP1)}]$$

$$= \frac{1}{2} [U_P'' + U_W'' + (U_{N''} + U_{NW''} - U_P'' - U_W'') \frac{\frac{1}{2} SYG(IY)}{DYG(IYP1)}]$$

$$(3.2.47)$$

$$SVP_3 = \frac{1}{Re} \int_U [U \xi \frac{d^3\delta}{d\eta^3} + \frac{2\xi}{\delta} (\frac{d\delta}{d\eta})^3 - \frac{3\xi}{\delta} \frac{d\delta}{d\eta} \frac{d^2\delta}{d\eta^2} + (K-1) \frac{1}{\xi\delta^2} \frac{d\delta}{d\eta}] (\delta\xi)^{K-1} \delta d\xi d\eta$$

$$= \frac{U_P}{Re} \{ \xi_P, (\frac{d^3\delta}{d\eta^3})_P + \frac{2\xi_P}{\delta_P^2} (\frac{d\delta}{d\eta})_P^3 - \frac{3\xi_P}{\delta_P} \times$$

$$\left( \frac{d\delta}{d\eta} \right)_{P'} \left( \frac{d^2\delta}{d\eta^2} \right)_{P'} + (K-1) \frac{1}{\xi_P \delta_P^2} \left( \frac{d\delta}{d\eta} \right)_{P'} \\ \times (\delta\xi)^{K-1} \delta_P \text{ SXG(IX) SYV(IY)} \quad (3.2.48)$$

where  $U_P$  is given by Eq. (3.2.47)

$$\begin{aligned} SVP4 &= \frac{2}{Re} \int \left[ \frac{\partial U}{\partial \eta} \left( \xi \frac{d^2\delta}{d\eta^2} - \frac{\beta}{\delta} \frac{d\delta}{d\eta} \right) \right] (\delta\xi)^{K-1} \delta d\xi d\eta \\ &= \frac{2}{Re} \left( \frac{\partial U}{\partial \eta} \right)_{P'} \left[ \xi_P \left( \frac{d^2\delta}{d\eta^2} \right)_{P'} - \frac{\beta_{P'}}{\delta_{P'}} \left( \frac{d\delta}{d\eta} \right)_{P'} \right] (\delta\xi)^{K-1} \\ &\quad \delta_P \text{ SXG(IX) SYV(IY)} \quad (3.2.49) \end{aligned}$$

$$\begin{aligned} \text{where } \left( \frac{\partial U}{\partial \eta} \right)_{P'} &= \left( \frac{\partial U}{\partial \eta} \right)_P + \left\{ \left( \frac{\partial U}{\partial \eta} \right)_N - \left( \frac{\partial U}{\partial \eta} \right)_P \right\} \frac{\frac{1}{2} \text{SYG(IY)}}{\text{DYG(IYP1)}} \\ &= \left\{ U_{P''} - U_{W''} + (U_{N''} - U_{NW''} - U_{P''} + U_{W''}) \right. \\ &\quad \left. \frac{\frac{1}{2} \text{SYG(IY)}}{\text{DYG(IYP1)}} \right\} \frac{1}{\text{SXG(IX)}} \quad (3.2.50) \end{aligned}$$

$$\begin{aligned} SVP5 &= \frac{2}{Re} \int \left\{ \frac{\partial U}{\partial \xi} \left( \frac{\alpha}{\delta^2} \frac{d\delta}{d\eta} - \frac{\beta\xi}{\delta} \frac{d^2\delta}{d\eta^2} \right) \right\} (\delta\xi)^{K-1} \delta d\xi d\eta \\ &= \frac{2}{Re} \left( \frac{\partial U}{\partial \xi} \right)_{P'} \left\{ \frac{\alpha_{P'}}{\delta_{P'}^2} \left( \frac{d\delta}{d\eta} \right)_{P'} - \frac{\beta_{P'} \xi_{P'}}{\delta_{P'}^2} \left( \frac{d^2\delta}{d\eta^2} \right)_{P'} \right\} \\ &\quad \times (\delta\xi)^{K-1} \delta_P \text{ SXG(IX) SYV(IY)} \quad (3.2.51) \end{aligned}$$

$$\text{where } \left( \frac{\partial U}{\partial \xi} \right)_{P'} = \frac{1}{2} (U_{N''} - U_{P''} + U_{NW''} - U_{W''}) \cdot \frac{1}{\text{DYG(IYP1)}} \quad (3.2.52)$$

$$\begin{aligned} SPRIME_2(U_\xi)_{P'} &= \frac{1}{Re} \int \left\{ (K-1) \frac{1}{\xi^2 \delta^2} U_\xi \right\} (\delta\xi)^{K-1} \delta d\xi d\eta \\ &= \frac{1}{Re} (K-1) \frac{1}{\xi_{P'}^2 \delta_{P'}^2} (U_\xi)_{P'} (\delta\xi)^{K-1} \delta_P \text{ SXG(IX) SYV(IY)} \quad (3.2.53) \end{aligned}$$

$$\therefore \text{SPRIME}_2 = (K-1) \frac{1}{Re} \frac{1}{(\xi_P, \delta_P)^2} (\delta \xi)_P^{K-1} \delta_P, \text{ SXG(IX) SYV(IY)} \\ (3.2.54)$$

$$\begin{aligned} \text{SVP6} &= \frac{1}{Re} \int_V \{ (K-1) \frac{1}{\xi^2 \delta^2} \beta U \} (\delta \xi)^{K-1} \delta d\xi d\eta \\ &= (K-1) \frac{1}{Re} \frac{1}{(\xi_P, \delta_P)^2} \beta_P, U_P, (\delta \xi)_P^{K-1} \delta_P, \text{ SXG(IX) SYV(IY)} \end{aligned} \\ (3.2.55)$$

$\therefore$  The total source term is

$$S_{u_\xi} = S_b + \left\{ \frac{\alpha_P}{\delta_P} (\delta \xi)_P^{K-1} \delta_P, \text{ SXG(IX)} \right\} (P_P - P_N) \quad (3.2.56)$$

In generalized form,  $S_{u_\xi}$  can be expressed as

$$S_{u_\xi} = S_c + S_P, (U_\xi)_P, \quad (3.2.57)$$

where  $S_c = SVW - SVE + SVS - SVN + SVP1 - SVP2$

$$\begin{aligned} &+ SVP3 + SVP4 + SVP5 - SVP6 + \left\{ \frac{\alpha_P}{\delta_P} (\delta \xi)_P^{K-1} \delta_P, \right. \\ &\left. \text{SXG(IX)} \right\} (P_P - P_N) \end{aligned} \quad (3.2.58)$$

$$\text{and } S_P, = -(SPRIME_1 + SPRIME_2) \quad (3.2.59)$$

With these, Eq. (3.2.37) may be written as

$$\begin{aligned} (a_P, - S_P,) (U_\xi)_P, &= a_E, (U_\xi)_E, + a_W, (U_\xi)_W, \\ &+ a_N, (U_\xi)_N, + a_S, (U_\xi)_S, + S_c, \end{aligned} \quad (3.2.60)$$

### c) Discretization of energy equation

The derivation of the discretized equation for enthalpy is based on the assumption that the flow is available *a priori*.

In this case Eq. (3.2.55) is once again considered, but now  $\phi$  is taken to be  $H$  and  $b = 0$ . The control volume of interest in this case surrounds the main grid point P as depicted in Fig. 10. The eight neighbouring points are identified by W, E, S, N, SW, SE, NW and NE.

Now using the same mathematical steps that were used for the derivation of discretized U-momentum equation, the discretized form of energy equation becomes

$$a_P H_P = a_W H_W + a_E H_E + a_S H_S + a_N H_N + S \quad (3.2.61)$$

where S is given by

$$\begin{aligned} S = & \left[ \left( \frac{\beta}{P_e} \frac{\partial H}{\partial \xi} \right)_W (\delta \xi)_W^{K-1} - \left( \frac{\beta}{P_e} \frac{\partial H}{\partial \xi} \right)_E (\delta \xi)_E^{K-1} \right] SYG(IX) \\ & + \left[ \left( \frac{\beta}{P_e} \frac{\partial H}{\partial \eta} \right)_S (\delta \xi)_S^{K-1} - \left( \frac{\beta}{P_e} \frac{\partial H}{\partial \eta} \right)_N (\delta \xi)_N^{K-1} \right] SXG(IX) \end{aligned} \quad (3.2.62)$$

and the coefficients  $a_W$ ,  $a_E$ ,  $a_S$ ,  $a_N$  and  $a_P$  are given by

$$\begin{aligned} a_W &= D_w A \left| \frac{F_w}{D_w} \right| + \left[ F_w, 0 \right] \\ a_E &= D_e A \left| \frac{F_e}{D_e} \right| + \left[ -F_e, 0 \right] \\ a_S &= D_s A \left| \frac{F_s}{D_s} \right| + \left[ F_s, 0 \right] \\ a_N &= D_n A \left| \frac{F_n}{D_n} \right| + \left[ -F_n, 0 \right] \end{aligned} \quad (3.2.63)$$

and  $a_P = a_E + a_W + a_N + a_S$ .

The convective fluxes  $F_w$ ,  $F_e$ ,  $F_s$  and  $F_n$  and the diffusive fluxes  $D_w$ ,  $D_e$ ,  $D_s$  and  $D_n$  are given by

Convective flux :

$$F_e = (U\delta)_e (\delta\xi)_e^{K-1} SYG(IY) = U_p \cdot \delta_e (\delta\xi)_e^{K-1} SYG(IY)$$

$$F_w = (U\delta)_w (\delta\xi)_w^{K-1} SYG(IY) = U_w \cdot \delta_w (\delta\xi)_w^{K-1} SYG(IY)$$

$$F_s = (U\xi)_s (\delta\xi)_s^{K-1} SXG(IX) = (U\xi)_s \cdot (\delta\xi)_s^{K-1} SXG(IX)$$

$$F_n = (U\xi)_n (\delta\xi)_n^{K-1} SXG(IX) = (U\xi)_p \cdot (\delta\xi)_n^{K-1} SXG(IX)$$

(3.2.64)

Diffusive flux :

$$D_w = \frac{1}{Pe} (\delta\xi)_w^{K-1} \frac{\delta_w SYG(IY)}{DXG(IX)}$$

$$D_e = \frac{1}{Pe} (\delta\xi)_e^{K-1} \frac{\delta_e SYG(IY)}{DXG(IXP1)}$$

(3.2.65)

$$D_s = \frac{1}{Pe} \left(\frac{\alpha}{\delta}\right)_s (\delta\xi)_s^{K-1} \frac{SXG(IX)}{DYG(IY)}$$

$$D_n = \frac{1}{Pe} \left(\frac{\alpha}{\delta}\right)_n (\delta\xi)_n^{K-1} \frac{SXG(IX)}{DYG(IYP1)}$$

The discretized form of source term S is given by

$$S = SHW - SHE + SHS - SHN \quad (3.2.66)$$

where

$$SHW = \left(\frac{\beta}{Pe} \frac{\partial H}{\partial \xi}\right)_w (\delta\xi)_w^{K-1} SYG(IY)$$

$$= \frac{\beta_w}{Pe} [H_{NW} - H_{SW} + (H_N - H_S - H_{NW} + H_{SW}) \frac{\frac{1}{2} SXG(IXM1)}{DXG(IX)}]$$

$$\times (\delta\xi)_w^{K-1} \frac{SYG(IY)}{Y(IYP1) - Y(IXM1)} \quad (3.2.67)$$

$$\begin{aligned}
 S_{HE} &= \left( \frac{\beta}{Pe} \frac{\partial H}{\partial \xi} \right)_e (\delta \xi)^{K-1} SYG(IX) \\
 &= \frac{\beta_e}{Pe} [H_N - H_S + (H_{NE} - H_{SE} - H_N + H_S) \frac{\frac{1}{2} SXG(IX)}{DXG(IYP1)}] \\
 &\quad \times (\delta \xi)^{K-1} \frac{SYG(IX)}{Y(IYP1) - Y(IXM1)} \tag{3.2.68}
 \end{aligned}$$

$$\begin{aligned}
 S_{HS} &= \left( \frac{\beta}{Pe} \frac{\partial H}{\partial \eta} \right)_S (\delta \xi)^{K-1} SXG(IX) \\
 &= \frac{\beta_s}{Pe} [H_{SE} - H_{SW} + (H_E - H_W - H_{SE} + H_{SW}) \frac{\frac{1}{2} SYG(IXM1)}{DYG(IX)}] \\
 &\quad \times (\delta \xi)^{K-1} \frac{SXG(IX)}{X(IXP1) - X(IXM1)}
 \end{aligned}$$

$$\begin{aligned}
 S_{HN} &= \left( \frac{\beta}{Pe} \frac{\partial H}{\partial \eta} \right)_N (\delta \xi)^{K-1} SXG(IX) \\
 &= \frac{\beta_n}{Pe} [H_E - H_W + (H_{NE} - H_{NW} - H_E + H_W) \frac{\frac{1}{2} SYG(IX)}{DYG(IYP1)}] (\delta \xi)^{K-1} \\
 &\quad \times \frac{SXG(IX)}{X(IXP1) - X(IXM1)} \tag{3.2.70}
 \end{aligned}$$

The total source term in this case is

$$S_H = S$$

Again the general form of  $S_H$  is given by

$$S_H = S_C + S_P H_P \tag{3.2.71}$$

where  $S_C = S$  and  $S_P = 0$  (3.2.72)

With these, Eq. (3.2.61) may be expressed as

$$(a_P - S_P) H_P = a_E H_E + a_W H_W + a_S H_S + a_N H_N + S_C \tag{3.2.73}$$

d) Discretization of continuity equation :

The control volume of specific interest in this case is that which surrounds the main grid point P in Fig. 10. The surface integrals in Eq. (2.3.57) are now approximated by evaluating the integrand at points e, n, w, and s respectively. Then the integration is performed by regarding those values as constant over each face to obtain

$$\begin{aligned} & U_e \delta_e (\delta \xi)_e^{K-1} SYG(IY) + (U_\xi)_n (\delta \xi)_n^{K-1} SXG(IX) \\ & - U_w \delta_w (\delta \xi)_w^{K-1} SYG(IY) - (U_\xi)_s (\delta \xi)_s^{K-1} SXG(IX) = 0 \end{aligned}$$

or

$$\begin{aligned} & U_p \delta_e (\delta \xi)_e^{K-1} SYG(IY) + (U_\xi)_p (\delta \xi)_n^{K-1} SXG(IX) \\ & - U_w \delta_w (\delta \xi)_w^{K-1} SYG(IY) - (U_\xi)_s (\delta \xi)_s^{K-1} SXG(IX) = 0 \end{aligned} \quad (3.2.74)$$

Using Eq. (3.2.64), the above Eq. (3.2.74) may be written as

$$F_e + F_n - F_w - F_s = 0 \quad (3.2.74a)$$

Before deriving the pressure-correction equation at this stage let us discuss the necessity of using under-relaxation factor for solving Eqs. (3.2.29), (3.2.60) and (3.2.73).

e) Under-relaxation :

The generalized form of Eqs. (3.2.20), (3.2.60) and (3.2.73) for a control volume is given by

$$(a_1 - s_1) \varphi_1 = \sum a_{nb} \varphi_{nb} + s \varphi_1 \quad (3.2.75)$$

where  $\varphi$  stands for  $U$ ,  $U_\xi$ , or  $H$ ,  $S_{\varphi_1}$  stands for  $S_C''$ ,  $S_C'$  or  $S_C$  and 1 indicates the point  $P''$ ,  $P'$  or  $P$ , respectively, for the  $U$ -momentum, the  $U_\xi$ -momentum, or the energy equation.

Equation (3.2.75) appears to be linear. However, the coefficients of Eq. (3.2.75) may themselves depend on one or more of the dependent variables represented by  $\varphi$ . To account for the resulting inter-equation linkages and nonlinearities, repeated solutions of the nominally linear form of Eq. (3.2.75) are required. Each of these iterative solutions is defined herein as a "cycle". At the beginning of each cycle, the coefficients are evaluated using the  $\varphi$  values obtained in the previous cycle. With the cycle-by-cycle change in coefficients of Eq. (3.2.75), the resulting changes in the  $\varphi$  values can be quite large, and this may cause slow convergence or even divergence. To moderate the changes in successive solutions for  $\varphi$ , and thereby improve convergence, under-relaxation is used.

Patankar [7] introduces under-relaxation into Eq. (3.2.75) through  $\alpha_R$  as follows

$$\frac{(a_1 - s_1)}{\alpha_R} \varphi_1 = \sum a_{nb} \varphi_{nb} + S_{\varphi_1} + \frac{1-\alpha_R}{\alpha_R} (a_1 - s_1) \varphi_1^o \quad (3.2.76)$$

where  $\varphi_1^o$  is the value of  $\varphi_1$  from the previous cycle, whereas Van Doormaal and Raithby [12] introduce under-relaxation through use of an E-factor according to the following revised form of Eq. (3.2.75).

$$(a_1 - s_1)(1 + \frac{1}{E}) \varphi_1 = \sum a_{nb} \varphi_{nb} + s_{\varphi_1} + \frac{1}{E} (a_1 - s_1) \varphi_1^o$$

$$\text{or } D_1 \varphi_1 = \sum a_{nb} \varphi_{nb} + s_{\varphi_1} + \frac{1}{E} (a_1 - s_1) \varphi_1^o \quad (3.2.77)$$

$$\text{where } D_1 = (a_1 - s_1)(1 + \frac{1}{E}) \quad (3.2.78)$$

From Eqs. (3.2.76) and (3.2.77) we may write

$$\alpha_R = \frac{E}{1+E}$$

Under-relaxation through the use of E-factor has better physical meaning than that using  $\alpha_R$ , as discussed by Van Doormaal and Raithby [12]. In order to accelerate convergence, values of E well in excess of unity are desirable. In fact values of E in the range 1 to 20 were found to be useful for the present problems.

#### f) Derivation of pressure-correction equation

We use the SIMPLEC procedure [12] for handling the velocity-pressure linkages. In this method the pressure field is first guessed. With this guessed pressure field, coefficients of the momentum equations can be evaluated allowing these equations to be solved to obtain the flow field. In general this flow field does not satisfy the continuity equation (3.2.74). Therefore, this guessed pressure field is corrected so that the resulting velocity field satisfies the continuity equation. This is accomplished by the pressure correction equation which is derived in accordance with [12] by combining the continuity equation with truncated forms of the momentum equation. After

solving the pressure correction equation following the recommendation given in [12], the velocity and pressure fields are corrected, and the procedure is repeated until the flow field satisfies both the continuity and momentum equations. Details for the above outline follow.

Let us say that for the guessed pressure distribution  $P^*$  the  $U^*$  and  $U_\xi^*$  velocity distribution obtained by solving the  $U$ -momentum and  $U_\xi$ -momentum equations respectively satisfies

$$D_{P''} U_{P''}^* = \sum a_{nb} U_{nb}^* + Sb_u + \{(\delta\xi)_{P''}^{K-1} \delta_{P''} \text{ SYG(IX)}\} (P_P^* - P_E^*) \\ + \frac{1}{E} (a_{P''} - S_{P''}) U_{P''}^O \quad (3.2.80a)$$

and

$$D_{P''} (U_\xi^*)_{P''} = \sum a_{nb} (U_\xi^*)_{nb} + Sb_v + \left\{ \frac{\alpha_{P'}}{\delta_{P''}} (\delta\xi)_{P''}^{K-1} \delta_{P''} \text{ SXG(IX)} \right\} \\ (P_P^* - P_N^*) + \frac{1}{E} (a_{P''} - S_{P''}) (U_\xi^*)_{P''}^O \quad (3.2.80b)$$

where  $Sb_u$  and  $Sb_v$  are given by Eqs. (3.2.19) and (3.2.39) respectively.

while the  $U$ - and  $U_\xi$ -velocities obtained from Eq. (3.2.75) using the correct (but unknown) pressure distribution  $P$  satisfy the continuity equation, the  $U^*$ - and  $U_\xi^*$ -velocities obtained from Eqs. (3.2.80) do not in general satisfy the continuity equation. Correction of the guessed pressure by  $P' = P - P^*$  is therefore necessary to correct the  $U^*$  field by  $U' = U - U^*$  and  $U_\xi^*$  field by  $U'_\xi = U_\xi - U_\xi^*$ . The relation between  $P'$  and  $U'$  is obtained by subtraction of Eq. (3.2.80a) from Eq. (3.2.75) leading to

$$D_{P''} U'_{P''} = \sum a_{nb} U'_{nb} + \{(\delta\xi)_{P''}^{K-1} \delta_{P''} \text{SYG(IY)}\} (P'_P - P'_E) \quad (3.2.81)$$

The pressure  $P$  and velocity  $U$  that satisfy both the continuity and the momentum equations are

$$U = U^* + U' \quad (3.2.82a)$$

$$P = P^* + P' \quad (3.2.82b)$$

Attention will now be given to the method used to find  $P'$ .

The exact equation for  $P'$  derived from Eqs. (3.2.81) and (3.2.82a) and the continuity constraint, is complicated and unsuitable for economic calculation. In the SIMPLE method [7] the term  $\sum a_{nb} U'_{nb}$  in Eqs. (3.2.81) is ignored whereas a term of similar magnitude on the left side of the equation is retained, leading to inconsistency of the method.

For a "consistent" approximation, leading to a suitable simple expression for  $P'$ , the term  $\sum a_{nb} U'_{P''}$  is subtracted from both sides of Eq. (3.2.81). This yields

$$(D_{P''} - \sum a_{nb}) U'_{P''} = \sum a_{nb} (U'_{nb} - U'_{P''}) + \{(\delta\xi)_{P''}^{K-1} \delta_{P''} \text{SYG(IY)}\} (P'_P - P'_E) \quad (3.2.83)$$

In this method termed "SIMPLEC" by Van Doormaal and Raithby [12] the term  $\sum a_{nb} (U'_{nb} - U'_{P''})$  is neglected. With this approximation Eq. (3.2.83) becomes

$$(D_{P''} - \sum a_{nb}) U'_{P''} = \{(\delta\xi)_{P''}^{K-1} \delta_{P''} \text{SYG(IY)}\} (P'_P - P'_E)$$

$$\text{or } U'_{P''} = d_{P''} (P'_P - P'_E)$$

$$\text{where } d_{P''} = \frac{\{(\delta\xi)_{P''}^{K-1} \delta_{P''} \text{ SYG(IY)}\}}{D_{P''} - \sum a_{nb}} \quad (3.2.84)$$

$$\text{Thus, } U_{P''} = U^*_{P''} + d_{P''} (P'_P - P'_E) \quad (3.2.85)$$

Eq. (3.2.85) is an intermediate step to link velocity with pressure, and is called the velocity correction equation. A similar expression can be obtained for  $U_{W''}$

$$U_{W''} = U^*_{W''} + d_{W''} (P'_W - P'_P) \quad (3.2.86)$$

$$\text{where } d_{W''} = \{(\delta\xi)_{W''}^{K-1} \delta_{W''} \text{ SYG(IY)}\} / (D_{W''} - \sum a_{nb}) \quad (3.2.86a)$$

Now in a manner similar to that used for deriving Eqs. (3.2.85) and (3.2.86), we have (Using Eq. (3.2.80b))

$$(U_\xi)_{P'} = (U^*_\xi)_{P'} + d_{P'} (P'_P - P'_N) \quad (3.2.87)$$

$$(U_\xi)_{S'} = (U^*_\xi)_{S'} + d_{S'} (P'_S - P'_P) \quad (3.2.88)$$

where  $d_{P'}$  and  $d_{S'}$  are given by

$$d_{P'} = \frac{\{(\frac{\alpha}{\delta})_{P'} (\delta\xi)_{P'}^{K-1} \delta_{P'} \text{ SXG(IX)}\}}{D_{P'} - \sum a_{nb}} \quad (3.2.89)$$

$$d_{S'} = \frac{\{(\frac{\alpha}{\delta})_{S'} (\delta\xi)_{S'}^{K-1} \delta_{S'} \text{ SXG(IX)}\}}{D_{S'} - \sum a_{nb}} \quad (3.2.90)$$

Substituting Eqs. (3.2.85) - (3.2.88) into the continuity Eq. (3.2.74), we have

$$\begin{aligned}
 & U_{P''}^* \delta_{P''} (\delta \xi)_{P''}^{K-1} SYG(IY) + \delta_{P''} (\delta \xi)_{P''}^{K-1} SYG(IY) d_{P''} (P'_P - P'_E) \\
 & - U_{W''}^* \delta_{W''} (\delta \xi)_{W''}^{K-1} SYG(IY) - \delta_{W''} (\delta \xi)_{W''}^{K-1} SYG(IY) d_{W''} (P'_W - P'_P) \\
 & + (U_{\xi}^*)_{P'} (\delta \xi)_{P'}^{K-1} SXG(IX) + (\delta \xi)_{P'}^{K-1} SXG(IX) d_{P'} (P'_P - P'_N) - \\
 & (U_{\xi}^*)_{S'} (\delta \xi)_{S'}^{K-1} SXG(IX) - (\delta \xi)_{S'}^{K-1} SXG(IX) d_{S'} (P'_S - P'_P) = 0
 \end{aligned}$$

from which we can write

$$a_P \ P'_P = a_E \ P'_E + a_W \ P'_W + a_N \ P'_N + a_S \ P'_S + B \quad (3.2.91)$$

where

$$a_E = d_{P''} \delta_{P''} (\delta \xi)_{P''}^{K-1} SYG(IY)$$

$$a_W = d_W \cdot \delta_W \cdot (\delta \xi)^{K-1}_W \text{ SYG(IY)}$$

$$a_N = d_{P*} (\delta \xi)^{K-1}_{P*} \text{SXG(IX)} \quad (3.2.92)$$

$$a_S = d_S, \quad (\delta\xi)_S^{K-1} \quad SXG(IX)$$

$$a_P = a_E + a_W + a_N + a_S$$

$$B = - (U_{\xi}^*)_{P'} (\delta \xi)_{P'}^{K-1} S X G(I_X) + (U_{\xi}^*)_{S'} (\delta \xi)_{S'}^{K-1} S X G(I_X)$$

$$= U_P^* \delta_P (\delta \xi)_P^{K-1} S(Y) + U_W^* \delta_W (\delta \xi)_W^{K-1} S(Y)$$

( 3.2.93 )

and where  $d_{P''}$ ,  $d_{W''}$ ,  $d_P$ , and  $d_S$ , are given by Eqs. (3.2.84), (3.2.86a), (3.2.89), and (3.2.90) respectively.

The direct solution of Eq. (3.2.91) for all the  $P'$  values on the line IX in Fig. 6 can be obtained with one application of the Thomas algorithm by suitably guessing the off-line dependent

variable values. Such a line-by-line solution is the basis of an iteration scheme that solves along each IX-line and then along each IY-line, and repeats the pattern until convergence is achieved. The rate of convergence of such a scheme depends crucially on the treatment of the off line values of the dependent variable.

Let us suppose that in the current iteration Eq. (3.2.91) is to be solved along an IX line, sweeping in the direction of increasing IX. Now according to Patankar's suggestion [7] the available estimate of  $P'_E$  is from the previous iteration i.e.  $[P'_E]^O$ , but according to Van Doormaal and Raithby [12] the best estimate of  $P'_E$  is

$$P'_E = [P'_E]^O + (\theta - 1) (P'_E - [P'_E]^O)$$

$$\approx [P'_E]^O + (\theta - 1) (P'_P - [P'_P]^O)$$

where  $\theta$  is a relaxation parameter such that for  $\theta = 1$ ,  $P'_E$  is taken as  $[P'_E]^O$ . The optimal value of  $\theta$  depends upon the problem. In general,  $1 \leq \theta < 2$ . The best available estimate of  $P'_W$  is that obtained from the just completed solution along the (IX - 1) line. It has been observed that Van Doormaal and Raithby's approximation for off-line values accelerates the rate of convergence. Therefore, with Van Doormaal and Raithby's approximation Eq. (3.2.91) takes the form

$$(a_P - (\theta-1) a_E) P'_P = a_S P'_S + a_N P'_N + a_W P'_W + a_E \{ [P'_E]^O - (\theta-1) [P'_P]^O \} + B \quad (3.2.94)$$

A similar estimation is made for solution along an IY-line.

### 3.3 Discretized Equations for the Non-Symmetric Channel

Following the same procedure as in Sec. 3.2, the following equations are obtained for the non-symmetric channel.

#### a) Discretization of U-momentum equation

The U-momentum equation [Eq. (2.4.15) with  $\varphi = U$ ] can be written in discretized form as

$$a_{P''} U_{P''} = a_{E''} U_{E''} + a_{W''} U_{W''} + a_{N''} U_{N''}$$

$$+ a_{S''} U_{S''} + \{ SYG(IY) \} (P_P - P_E) + Sb \quad (3.3.1)$$

$$\text{where } Sb = S + \int_{\Psi} \beta \frac{\partial P}{\partial \xi} d\eta \, d\xi \quad (3.3.2)$$

$$\text{with } S = \left[ \left( \frac{\beta}{Re} \frac{\partial U}{\partial \xi} \right)_P - \left( \frac{\beta}{Re} \frac{\partial U}{\partial \xi} \right)_E \right] SYG(IY)$$

$$+ \left[ \left( \frac{\beta}{Re} \frac{\partial U}{\partial \eta} \right)_{S''} - \left( \frac{\beta}{Re} \frac{\partial U}{\partial \eta} \right)_{N''} \right] SXU(IX) \quad (3.3.3)$$

The coefficients in Eq. (3.3.1) are given by Eq. (3.2.16a) where the convective and diffusive fluxes are expressed as

Convective flux :

$$F_E = U_E SYG(IY), \quad F_P = U_P SYG(IY) \quad (3.3.4)$$

$$F_{n''} = (U_\xi)_{n''} SXU(IX), \quad F_{s''} = (U_\xi)_{s''} SXU(IX)$$

Diffusive flux :

$$D_E = \frac{1}{Re} \frac{SYG(IY)}{DXU(IXP1)}, \quad D_P = \frac{1}{Re} \frac{SYG(IY)}{DXU(IX)}$$

$$D_{n''} = \frac{1}{Re} \alpha_{n''} SXU(IX)/DYG(IYP1) \quad (3.3.5)$$

$$D_{s''} = \frac{1}{Re} \alpha_{s''} SXU(IX)/DYG(IY)$$

Using the same assumptions as in Sec. 3.2, the discretized form of  $S_b$  becomes

$$S_b = S_{UW} - S_{UE} + S_{US} - S_{UN} + S_{UP} \quad (3.3.6)$$

where

$$S_{UW} = \frac{\beta_p}{2Re} (U_{N''} - U_{S''} + U_{NW''} - U_{SW''}) \frac{SYG(IY)}{Y(IYP1) - Y(IYM1)} \quad (3.3.7)$$

$$S_{UE} = \frac{1}{2} \frac{\beta_E}{Re} (U_{N''} - U_{S''} + U_{NE''} - U_{SE''}) \frac{SYG(IY)}{Y(IYP1) - Y(IYM1)} \quad (3.3.8)$$

$$S_{US} = \frac{\beta_s''}{Re} [U_{SE''} - U_{SW''} + (U_{E''} - U_{W''} - U_{SE''} \\ + U_{SW''}) \frac{\frac{1}{2} SYG(IYM1)}{DYG(IY)}] \frac{SXU(IX)}{XU(IXP1) - XU(IXM1)} \quad (3.3.9)$$

$$S_{UN} = \frac{\beta_n''}{Re} [U_{E''} - U_{W''} + (U_{NE''} - U_{NW''} - U_{E''} + U_{W''}) \\ \frac{\frac{1}{2} SYG(IY)}{DYG(IYP1)}] \frac{SXU(IX)}{XU(IXP1) - XU(IXM1)} \quad (3.3.10)$$

$$S_{UP} = \beta_p'' [P_N - P_S + (P_{NE} - P_{SE} - P_N + P_S) \frac{\frac{1}{2} SXG(IX)}{SXU(IX)}] \frac{SYG(IY) SXU(IX)}{Y(IYP1) - Y(IYM1)} \quad (3.3.11)$$

∴ The complete source term in the U-momentum equation is

$$S_u = S_b + \{SYG(IY)\} (P_p - P_E) \\ = S_c'' + S_p'' U_p'' \quad (3.3.12)$$

$$\text{where } S_c'' = S_b + SYG(IY)(P_p - P_E) \quad (3.3.13)$$

$$S_p'' = 0 \quad (3.3.14)$$

With these, Eq. (3.3.1) may be expressed as

$$(a_P - S_{P''}) U_{P''} = a_E'' U_{E''} + a_W'' U_{W''} + a_N'' U_{N''} + a_S'' U_{S''} + S_C'' \quad (3.3.15)$$

b) Discretization of  $U_\xi$ -momentum equation :

The  $U_\xi$ -momentum equation [Eq. (2.4.25) with  $\varphi = U_\xi$ ]

can be discretized as

$$\begin{aligned} a_P (U_\xi)_P &= a_E (U_\xi)_E + a_W (U_\xi)_W + a_N (U_\xi)_N \\ &+ a_S (U_\xi)_S + \{\alpha_P, SXG(IX)\} (P_P - P_N) + Sb \end{aligned} \quad (3.3.16)$$

where  $Sb$  is given by

$$\begin{aligned} Sb &= S + \int_V \beta \frac{\partial P}{\partial \eta} d\eta d\xi - \int_V U^2 \frac{d^2 \delta}{d\eta^2} d\eta d\xi \\ &+ \frac{1}{Re} \int_V U \frac{d^3 \delta}{d\eta^3} d\eta d\xi + \frac{2}{Re} \int_V \frac{\partial U}{\partial \eta} \frac{d^2 \delta}{d\eta^2} d\eta d\xi \\ &- \frac{2}{Re} \int_V \beta \frac{\partial U}{\partial \xi} \frac{d^2 \delta}{d\eta^2} d\eta d\xi \end{aligned} \quad (3.3.17)$$

$$\begin{aligned} \text{with } S &= \left[ \left( \frac{\beta}{Re} \frac{\partial U_\xi}{\partial \xi} \right)_W - \left( \frac{\beta}{Re} \frac{\partial U_\xi}{\partial \xi} \right)_E \right] SYV(IX) \\ &+ \left[ \left( \frac{\beta}{Re} \frac{\partial U_\xi}{\partial \eta} \right)_P - \left( \frac{\beta}{Re} \frac{\partial U_\xi}{\partial \eta} \right)_N \right] SXG(IX) \end{aligned} \quad (3.3.18)$$

The coefficients  $a_E$ ,  $a_W$ ,  $a_N$ ,  $a_S$ , and  $a_P$ , in Eq. (3.3.16) are given by Eq. (3.2.32) where the convective and diffusive fluxes are :

Convective flux :

$$F_{e'} = U_{e'} SYV(IY), \quad F_w = U_w SYV(IY) \quad (3.3.19)$$

$$F_N = (U_\xi)_N SXG(IX), \quad F_P = (U_\xi)_P SXG(IX)$$

Where  $U_{e'}$ ,  $U_w$ ,  $(U_\xi)_N$ , and  $(U_\xi)_P$  are obtained from Eqs. (3.2.34) and (3.2.35).

Diffusive flux :

$$D_{e'} = \frac{1}{Re} \frac{SYV(IY)}{DXG(IXP1)}, \quad D_w = \frac{1}{Re} \frac{SYV(IY)}{DXG(IX)} \quad (3.3.20)$$

$$D_N = \frac{1}{Re} \alpha_N \frac{SXG(IX)}{DYV(IYP1)}, \quad D_P = \frac{1}{Re} \alpha_P \frac{SXG(IX)}{DYV(IY)}$$

Discretization form of  $S_b$  :

$$S_b = SVW - SVE + SVS - SVN + SVP1 - SVP2 \\ + SVP3 + SVP4 - SVP5 \quad (3.3.21)$$

where

$$SVW = \frac{\beta_w}{Re} [(U_\xi)_{NW} - (U_\xi)_{SW} + \{(U_\xi)_N - (U_\xi)_S \\ - (U_\xi)_{NW} + (U_\xi)_{SW}\} \frac{\frac{1}{2} SXG(IXM1)}{DXG(IX)}] \frac{SYV(IY)}{YV(IYP1) - YV(IYM1)} \quad (3.3.22)$$

$$SVE = \frac{\beta_{e'}}{Re} [(U_\xi)_N - (U_\xi)_S + \{(U_\xi)_{NE} - (U_\xi)_{SE} \\ - (U_\xi)_N + (U_\xi)_S\} \frac{\frac{1}{2} SXG(IX)}{SXU(IX)}] \frac{SYV(IY)}{YV(IYP1) - YV(IYM1)} \quad (3.3.23)$$

$$SVS = \frac{1}{2} \frac{\beta_P}{Re} [(U_\xi)_E - (U_\xi)_W + (U_\xi)_{SE} - (U_\xi)_{SW}]$$

$$\frac{SXG(IX)}{X(IXP1) - X(IXM1)} \quad (3.3.24)$$

$$SVN = \frac{1}{2} \frac{\beta_N}{Re} [(U_\xi)_E - (U_\xi)_W + (U_\xi)_{NE} - (U_\xi)_{NW}]$$

$$\frac{SXG(IX)}{X(IXP1) - X(IXM1)} \quad (3.3.25)$$

$$SVP1 = \beta_P [ P_E - P_W + (P_{NE} - P_{NW} - P_E + P_W) \frac{\frac{1}{2} SYG(IY)}{DYG(IYP1)} ]$$

$$\frac{SXG(IX) SYV(IY)}{X(IXP1) - X(IXM1)} \quad (3.3.26)$$

$$SVP2 = U_P^2 \left( \frac{d^2 \delta}{d\eta^2} \right)_P SXG(IX) SYV(IY) \quad (3.3.27)$$

$$SVP3 = \frac{1}{Re} U_P \left( \frac{d^3 \delta}{d\eta^3} \right)_P SXG(IX) SYV(IY) \quad (3.3.28)$$

$$SVP4 = \frac{2}{Re} \left( \frac{\partial U}{\partial \eta} \right)_P \left( \frac{d^2 \delta}{d\eta^2} \right)_P SXG(IX) SYV(IY) \quad (3.3.29)$$

$$SVP5 = \frac{2}{Re} \left( \frac{\partial U}{\partial \xi} \right)_P \left( \frac{d^2 \delta}{d\eta^2} \right)_P SXG(IX) SYV(IY) \quad (3.3.30)$$

where  $U_P$ ,  $\left( \frac{\partial U}{\partial \eta} \right)_P$ , and  $\left( \frac{\partial U}{\partial \xi} \right)_P$  are given by Eqs. (3.2.47), (3.2.50) and (3.2.52) respectively.

The complete source term in the  $U_\xi$ -momentum equation is

$$S_{U_\xi} = S_b + \alpha_P SXG(IX) (P_P - P_N)$$

$$= S_C + S_P (U_\xi)_P \quad (3.3.31)$$

$$\text{where } S_C = S_b + \alpha_P \cdot SXG(IX) (P_P - P_N) \quad (3.3.32)$$

$$S_P = 0.0 \quad (3.3.33)$$

with these, Eq. (3.3.16) may be expressed as

$$\begin{aligned} (a_P, -S_P) (U_\xi)_P &= a_E (U_\xi)_E + a_W (U_\xi)_W \\ &\quad + a_N (U_\xi)_N + a_S (U_\xi)_S + S_C, \end{aligned} \quad (3.3.34)$$

c) Discretization of energy equation :

The energy equation [Eq. (2.4.15) with  $\varphi = H$ ] can be discretized as

$$a_P H_P = a_E H_E + a_W H_W + a_N H_N + a_S H_S + S \quad (3.3.35)$$

where  $S$  is given by

$$\begin{aligned} S &= \left[ \left( \frac{\beta}{P_e} \frac{\partial H}{\partial \xi} \right)_W - \left( \frac{\beta}{P_e} \frac{\partial H}{\partial \xi} \right)_E \right] SYG(IY) \\ &\quad + \left[ \left( \frac{\beta}{P_e} \frac{\partial H}{\partial \eta} \right)_S - \left( \frac{\beta}{P_e} \frac{\partial H}{\partial \eta} \right)_N \right] SXG(IX) \end{aligned} \quad (3.3.36)$$

The coefficients  $a_W$ ,  $a_E$ ,  $a_S$ ,  $a_N$  and  $a_P$  of Eq. (3.3.35) are given by Eq. (3.2.63), where the convective and diffusive fluxes are given by

Convective flux :

$$F_e = U_P \cdot SYG(IY), \quad F_w = U_W \cdot SYG(IY), \quad (3.3.37)$$

$$F_s = (U_\xi)_S \cdot SXG(IX), \quad F_n = (U_\xi)_N \cdot SXG(IX)$$

Diffusive flux :

$$D_e = \frac{1}{Pe} \frac{SYG(IY)}{DXG(IXP1)}, \quad D_w = \frac{1}{Pe} \frac{SYG(IY)}{DXG(IX)}, \quad (3.3.38)$$

$$D_n = \frac{1}{Pe} \alpha_n \frac{SXG(IX)}{DYG(IYP1)}, \quad D_s = \frac{1}{Pe} \alpha_s \frac{SXG(IX)}{DYG(IY)}$$

The discretized form of source term S is given by

$$S = SHW - SHE + SHS - SHN \quad (3.3.39)$$

where

$$SHW = \frac{\beta_w}{Pe} [H_{NW} - H_{SW} + (H_N - H_S - H_{NW} + H_{SW}) \\ \times \frac{\frac{1}{2} SXG(IXM1)}{DXG(IX)}] \frac{SYG(IY)}{Y(IYP1) - Y(IXM1)} \quad (3.3.40)$$

$$SHE = \frac{\beta_e}{Pe} [H_N - H_S + (H_NE - H_SE - H_N + H_S) \frac{\frac{1}{2} SXG(IX)}{DXG(IXP1)}] \frac{SYG(IY)}{Y(IYP1) - Y(IXM1)} \quad (3.3.41)$$

$$SHS = \frac{\beta_s}{Pe} [H_{SE} - H_{SW} + (H_E - H_W - H_{SE} + H_{SW}) \\ \times \frac{\frac{1}{2} SYG(IXM1)}{DYG(IY)}] \frac{SXG(IX)}{X(IXP1) - X(IXM1)} \quad (3.3.42)$$

$$SHN = \frac{\beta_n}{Pe} [H_E - H_W + (H_NE - H_{NW} - H_E + H_W) \\ \times \frac{\frac{1}{2} SYG(IY)}{DYG(IYP1)}] \frac{SXG(IX)}{X(IXP1) - X(IXM1)} \quad (3.3.43)$$

The complete source term in this case is

$$S_H = S \\ = S_C + S_P H_P \quad (3.3.44)$$

where  $S_C = S$  and  $S_P = 0$  (3.3.45)

with these, Eq. (3.3.35) may be written as

$$(a_P - S_P)H_P = a_E H_P + a_W H_W + a_S H_S + a_N H_N + S_C \quad (3.3.46)$$

d) Discretization of continuity equation :

The discretized form of continuity equation [Eq.(2.4.18)] is

$$U_e SYG(IY) + (U_\xi)_n SXG(IX) - U_w SYG(IY) - (U_\xi)_s SXG(IX) = 0 \quad (3.3.47)$$

e) Pressure-correction equation :

The velocity-correction equations are given by Eqs. (3.2.85), (3.2.86), (3.2.87), and (3.2.88), where  $d_{P''}$ ,  $d_{W''}$ ,  $d_S$ , and  $d_P$ , are given by

$$d_{P''} = \frac{SYG(IY)}{D_{P''} - \sum a_{nb}} , \quad d_{W''} = \frac{SYG(IY)}{D_{W''} - \sum a_{nb}} \quad (3.3.48)$$

$$d_S = \alpha_S \frac{SXG(IX)}{D_S - \sum a_{nb}} , \quad d_P = \alpha_P \frac{SXG(IX)}{D_P - \sum a_{nb}}$$

and the pressure correction equation is given by  $P = P^* + P'$ , where  $P'$  is obtained from equation

$$(a_P - (\theta-1) a_E) P'_P = a_S P'_S + a_N P'_N + a_W P'_W + a_E \{ [P'_E]^O - (\theta-1) [P'_P]^O \} + B \quad (3.3.49)$$

where

$$a_E = d_P, \text{ SYG(IX)} , \quad a_W = d_W, \text{ SYG(IY)} ,$$

$$a_N = d_P, \text{ SXG(IX)} , \quad a_S = d_S, \text{ SXG(IX)} \quad (3.3.50)$$

$$a_P = a_E + a_W + a_N + a_S$$

and

$$B = -(U_{\xi}^*)_P, \text{ SXG(IX)} + (U_{\xi}^*)_S, \text{ SXG(IX)}$$

$$- U_P^*, \text{ SYG(IY)} + U_W^*, \text{ SYG(IY)} \quad (3.3.51)$$

## Chapter 4

### RESULTS AND DISCUSSION

Results for both developing and fully-developed region in a short wavelength sinusoidal symmetric and non-symmetric channel and a short wavelength converging-diverging pipe are presented in terms of computer generated profiles as shown in Figs. 11 to 71. Figs. 11 to 29 show the behaviour of the various quantities for the symmetric channel. Similarly, Figs. 30 to 52 and Figs. 53 to 71 depict the behaviour of the same quantities for the pipe and for the non-symmetric channel respectively. All earlier studies of flow through such ducts are restricted to the fully developed flow in a long wavelength channel or pipe of small wall amplitude whereas the present analysis is for a short wavelength channel and pipe with sufficiently large amplitude. Also results are obtained for both the developing and the fully developed region. That is why the present results are not compared with any previous results. From the nature of the profiles, however, it is felt that the present numerical procedure can predict the flow through such ducts quite accurately.

The numerical work was performed for a dimensionless wall amplitude LAMBDA ( $\lambda/L$ ) = 0.10, 0.20, and 0.25. The Prandtl number was fixed at 0.72 (for air), while the Reynolds number,  $Re$ , was given values of 100 and 500. Non-uniform grid

spacing was employed through factors  $F_1$  and  $F_2$  as shown in the Appendix in both directions. Solutions were obtained for a prescribed wall enthalpy only.

Though it takes about 10 cycles for the flow to get fully developed, the figures depict only the first few cycles and the last two cycles. Due to symmetry, as in the case of symmetric channel, the figures show the profiles in the upper half of the flow domain only. In the figures the solid boundary of the channels is drawn using a very small number of points. Hence these boundaries have not been represented exactly in the figures.

#### 4.1 Symmetric Channel :

Figs. 11 to 13 show the behaviour of the dimensionless velocity components  $U$  and  $V$  and the velocity vector  $\vec{U}$  for a dimensionless wall amplitude  $\lambda/L = 0.10$  and  $Re = 100$ . Similarly Figs. 15 to 17, Figs. 19 to 21, and Figs. 23 to 25 depict the behaviour of the same quantities for  $\lambda/L = 0.10$  and  $Re = 500$ ,  $\lambda/L = 0.20$  and  $Re = 100$ , and  $\lambda/L = 0.25$  and  $Re = 100$  respectively. It is observed that the negative  $V$ -component at the minimum cross-section and the positive  $V$ -component at the maximum cross-section increases with  $Re$ . This is due to the effect of inertia [3].

It can be easily observed that the velocity components  $U$  and  $V$  are affected significantly by the parameter  $\lambda$ . It is seen from the Figs. 11 and 13 that for  $\lambda/L = 0.10$  and  $Re = 100$

there is no separation of flow. But when  $Re$  increases to 400, it was found that the flow begins to separate as  $\frac{\partial U}{\partial Y}$  at the wall tends to zero. From Figs. 15, one finds a small back flow near the channel wall for  $\lambda/L = 0.10$  and  $Re = 500$ . The corresponding separation point (S) and reattachment point (R) are also shown in Fig. 15.

A comparison of Figs. 11, 15, 19, and 23 shows that as the amplitude  $\lambda/L$  increases, the separation point moves upstream and the reattachment point moves down-stream. Similar effect has also been observed for an increase in  $Re$ . Therefore, the separated flow region grows with wall amplitude as well as with  $Re$ . From Fig. 27 it is evident that for  $\lambda/L = 0.20$  and  $Re = 500$  the back flow becomes stronger as well as more extensive. Moreover for higher  $\lambda/L$  and  $Re$ , separated flow occurs in the converging portion of the channel as well.

From Figs. 14, 18, 22, and 26 we can make out the behaviour of the dimensionless fluid enthalpy for the same combinations of  $\lambda/L$  and  $Re$  respectively. From these figures we notice that as the wall amplitude  $\lambda/L$  is increased or the Reynolds number  $Re$  is decreased the difference between the fluid enthalpy and the wall enthalpy decreases substantially. Out of these two parameters the non-dimensional parameter  $\lambda/L$  has the strongest effect in reducing this difference. Therefore, the length required to reach the wall enthalpy in the flow field decreases with increase of  $\lambda/L$  and with decrease

of  $Re$ . From a careful inspection of the same figures it is seen that a point of inflection appears in the enthalpy profiles in the separated flow region whereas in the non-separated region the enthalpy profile is almost parabolic.

Fig. 28(a,b) and 29(a,b) show the dimensionless pressure distribution in the downstream direction for the same  $\lambda/L$  and  $Re$ . A simple analysis of Figs. 28 and 29 makes it possible to express this distribution as

$$P(X) = -f(X) + p'(X)$$

where  $p'(x)$  behaves in the periodic fashion from cycle to cycle and  $f(x)$  is nearly linear in the developing region and linear in the fully-developed region. The percycle pressure drop  $\Delta P$  in the fully developed region is same for each cycle, e.g. for  $\lambda/L = 0.10$  and  $Re = 100$ ,  $\Delta P = -0.090$ . This per-cycle pressure drop increases with increase of wall amplitude. The variation of pressure in the  $Y$ -direction is negligible and has therefore not been shown.

#### 4.2 For Pipe

Figs. 30 to 32, Figs. 34 to 36, Figs. 38 to 40, Figs. 42 to 44, and Figs. 46 to 48 show the behaviour of the dimensionless velocity components  $U$  and  $V$  and velocity vector  $\vec{U}$  for  $\lambda/L = 0.10$  and  $Re = 100$ ,  $\lambda/L = 0.10$  and  $Re = 500$ ,  $\lambda/L = 0.20$  and  $Re = 100$ ,  $\lambda/L = 0.20$  and  $Re = 500$ , and  $\lambda/L = 0.25$  and  $Re = 100$  respectively. Similar to that for the symmetric channel, the negative  $V$ -component at the minimum cross-section and the positive

$V$ -component at the maximum cross-section increases with  $Re$ . In this case the effect of  $Re$  on the separated flow is stronger than that in the case of the symmetric channel. Here the flow begins to separate even at  $\lambda/L = 0.10$  and  $Re = 100$  (of Fig. 30) since  $\partial U / \partial Y \rightarrow 0$  at some locations, e.g., at  $X = 8.94$  near the wall. When the Reynolds number increases from 100 to 500 with the wall amplitude held constant, a slightly larger back flow than that in the case of the symmetric channel is observed at some locations, e.g., at  $X = 2.78, 8.94$  in Fig. 34. Here also, as in the symmetric channel, a similar conclusion can be drawn about the effect of  $\lambda/L$  and  $Re$  on separated flow by comparing the Figs. 30, 34, 38, 42, and 46. It is also observed that the back flow in this case is more stronger and extensive than that for the symmetric channel.

Figs. 33, 37, 41, 45, and 49 depict the dimensionless enthalpy  $H$  for the same combinations of  $\lambda/L$  and  $Re$ . Here also, the enthalpy is affected by the  $\lambda/L$  and  $Re$  in a similar way as in the case of the symmetric channel. However, the length required to reach the wall value is smaller than that for the symmetric channel. The point of inflection in the enthalpy profiles is also observed in the separated flow regions.

Figs. 50 to 52 represent the distribution of non-dimensional pressure  $P$  in the  $X$ -direction for the same values of  $\lambda/L$  and  $Re$ . The pressure  $P(X)$  also varies in a similar fashion as in a symmetric channel. However the per-cycle

pressure drop  $\Delta P$  in this case is higher e.g. for  $\lambda/L = 0.10$  and  $Re = 100$ ,  $\Delta P = -0.248$ . As earlier,  $\Delta P$  in the fully developed region is the same for each cycle and increases with increase of wall amplitude. Again the variation of pressure in the Y-direction is negligible and has not been shown.

It appears that the circular geometry enhances various effects in comparison to the plane-geometry.

#### 4.3 For non-symmetric Channel

Figs. 53 to 55, Figs. 57 to 59, Figs. 61 to 63, and Figs. 65 to 67 show the behaviour of the dimensionless velocity components U and V and the velocity vector  $\vec{U}$  for  $\lambda/L = 0.10$  and  $Re = 100$ ,  $\lambda/L = 0.10$  and  $Re = 500$ ,  $\lambda/L = 0.20$  and  $Re = 100$ , and  $\lambda/L = 0.20$  and  $Re = 500$  respectively. A comparison between Figs. 54 and 58 shows that the negative V-component at  $X = 15.50$ ,  $17.50$ , etc. increases with increase of Reynolds number. This is due to the effect of inertia [3]. From Figs. 55, 57, 63, and 67 it is observed that the resultant velocity  $\vec{U}$  is retarded near the lower boundary and accelerated near the upper boundary when the flow is in the downward direction but this behaviour is reversed when the flow is in the upward direction. Due to this behaviour flow separates near the upper boundary in one section whereas it separates near the lower boundary in the adjacent section. It is also seen from the same figures that the Reynolds number has a significant effect on the above phenomenon.

From Figs. 53, 57, and 61 it is observed that for  $\lambda/L = 0.10$  and  $Re = 100, 500$ , and for  $\lambda/L = 0.20$  and  $Re = 100$  there is no separation in the flow field. But when  $Re$  increases to 500 with  $\lambda/L = 0.20$ , a small back flow near the wall is observed. The effect of  $Re$  and  $\lambda/L$  on the separated flow is similar to that in the symmetric channel.

Figs. 56, 60, 64, and 68 depict the non-dimensional enthalpy  $H$  for the same  $\lambda/L$  and  $Re$ . Here also, as in the symmetric channel or pipe, the enthalpy is affected by  $\lambda/L$  and  $Re$  in a similar manner. Point of inflection is also observed in the separated region.

Figs. 69(a,b) and 70(a,b) show the distribution of non-dimensional pressure  $P$  in the  $X$ -direction for the same values of  $\lambda/L$  and  $Re$ . Here, the pressure  $P$  varies almost in a linear fashion. For  $\lambda/L = 0.20$  and  $Re = 500$ , slight fluctuation is observed in the distribution. These fluctuation increases with increase of  $\lambda/L$  and  $Re$ . Per-cycle pressure drop  $\Delta P$  in the fully developed region is same, e.g. for  $\lambda/L = 0.10$ , and  $Re = 100$ ,  $\Delta P = -0.288$  and it increases with increase of amplitude. In the  $Y$ -direction a slight variation of pressure is observed in the developing region whereas in the fully-developed region this variation is negligible as shown in Fig. 71 for  $\lambda/L = 0.20$  and  $Re = 100$ .

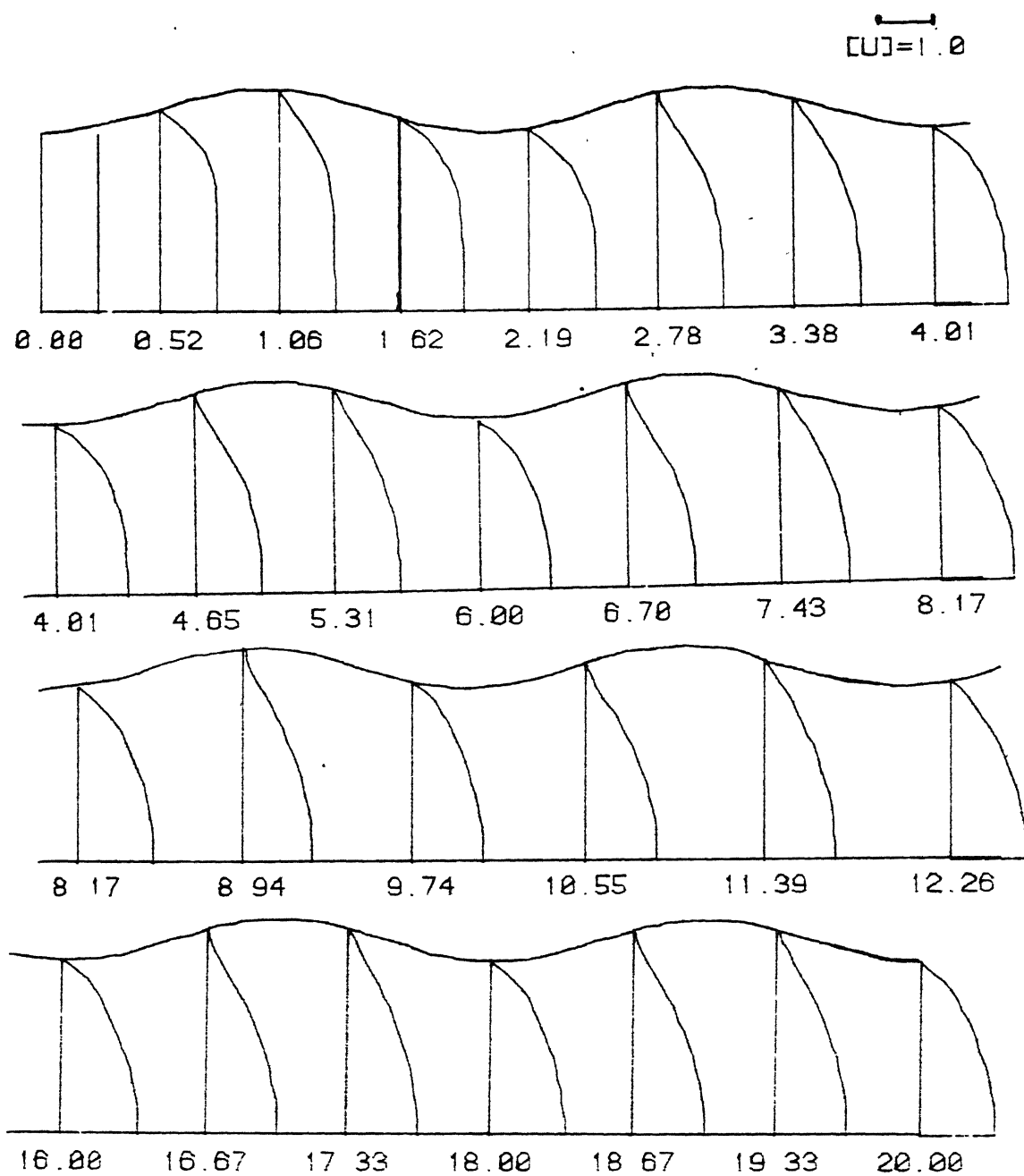
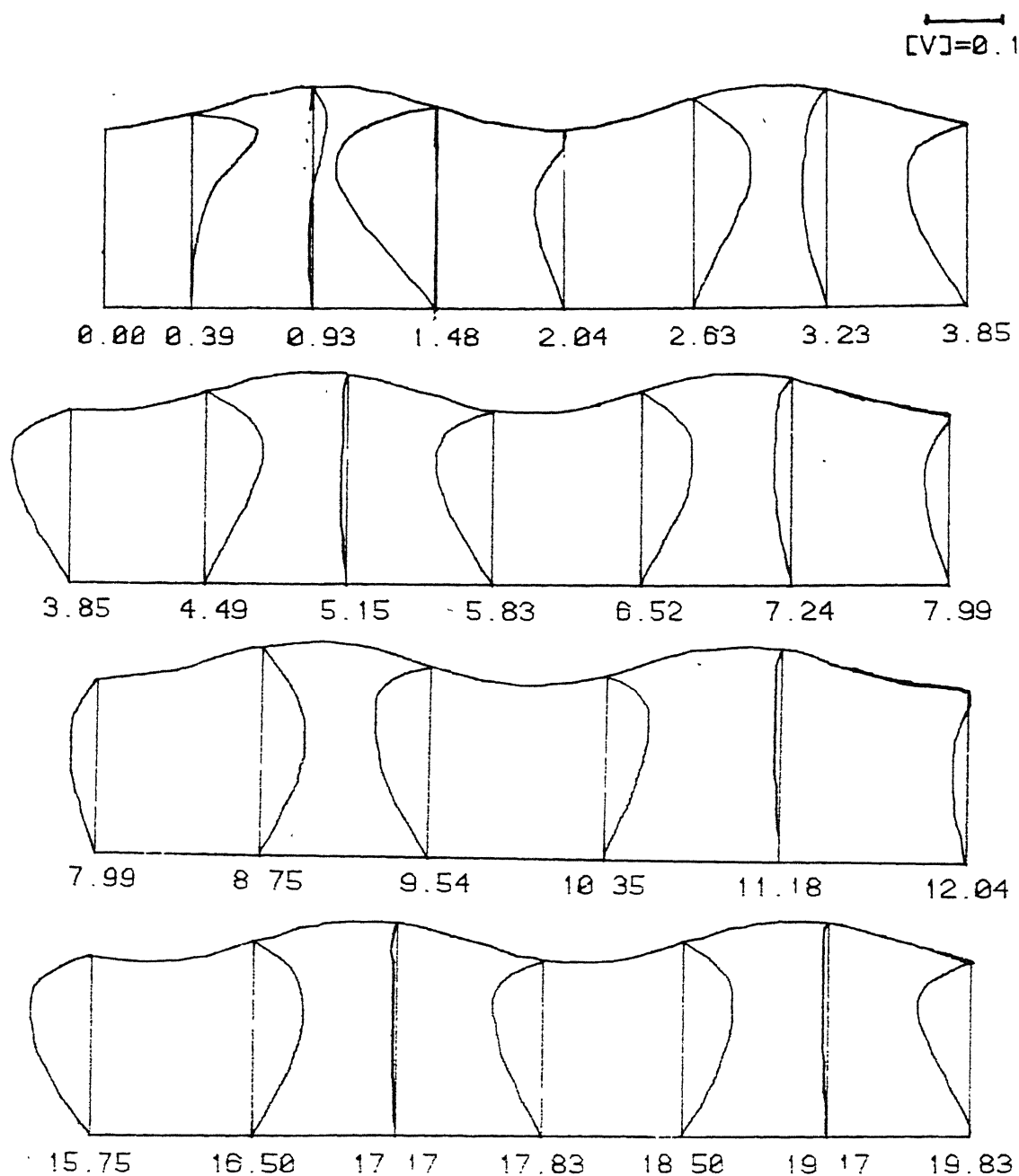


FIG.11 U-VELOCITY PROFILES FOR A SYM. CHANNEL  
WITH LAMBDA=0.10 AND  $Re=100$



**FIG.12** V-VELOCITY PROFILES FOR A SYM. CHANNEL  
WITH LAMBDA=0.10 AND Re=100

$\left[\frac{U}{U_0}\right] = 1.0$

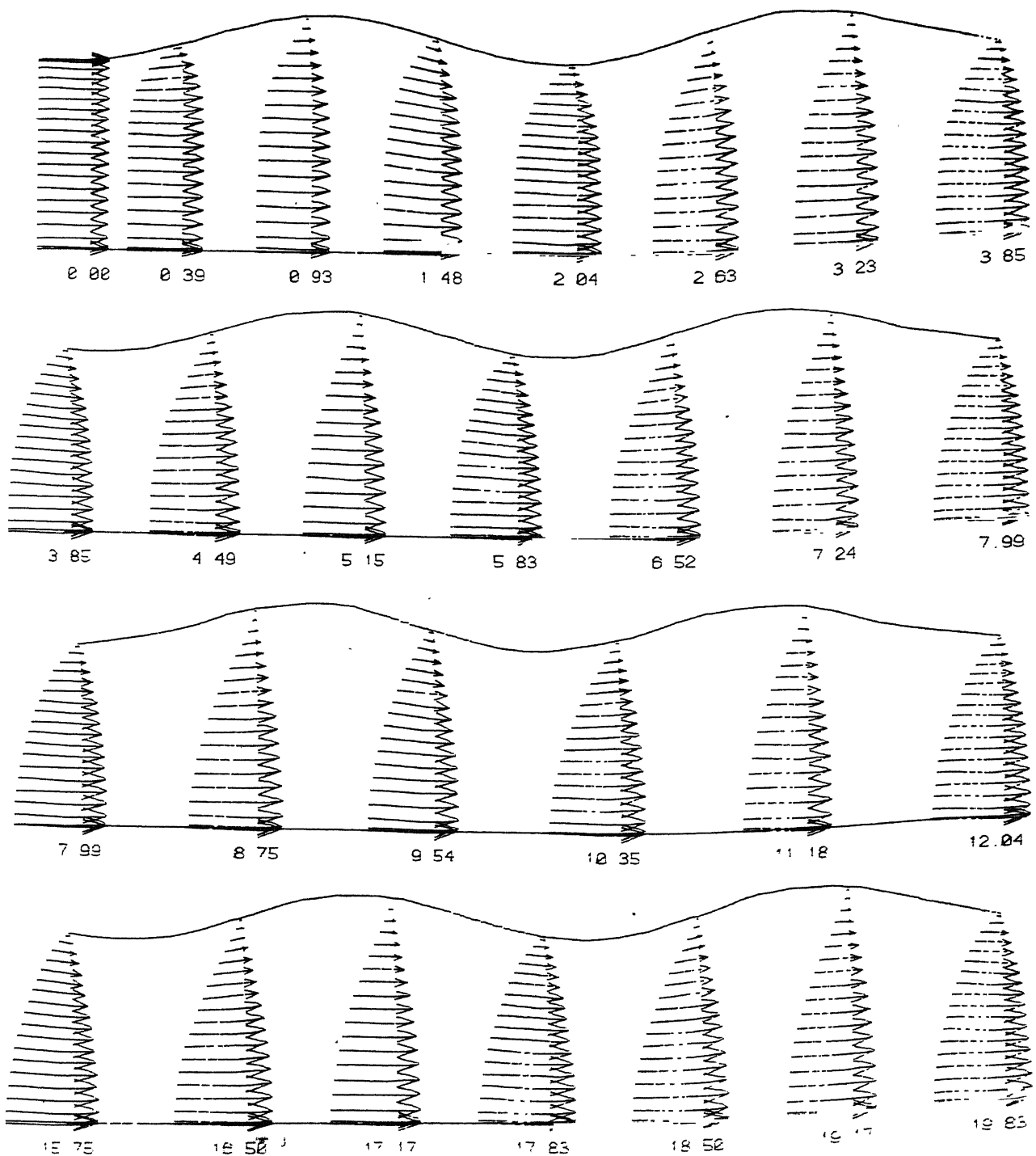


FIG.13 VELOCITY VECTORS IN A SYM. CHANNEL  
WITH LAMBDA=2 10 AND Re=102

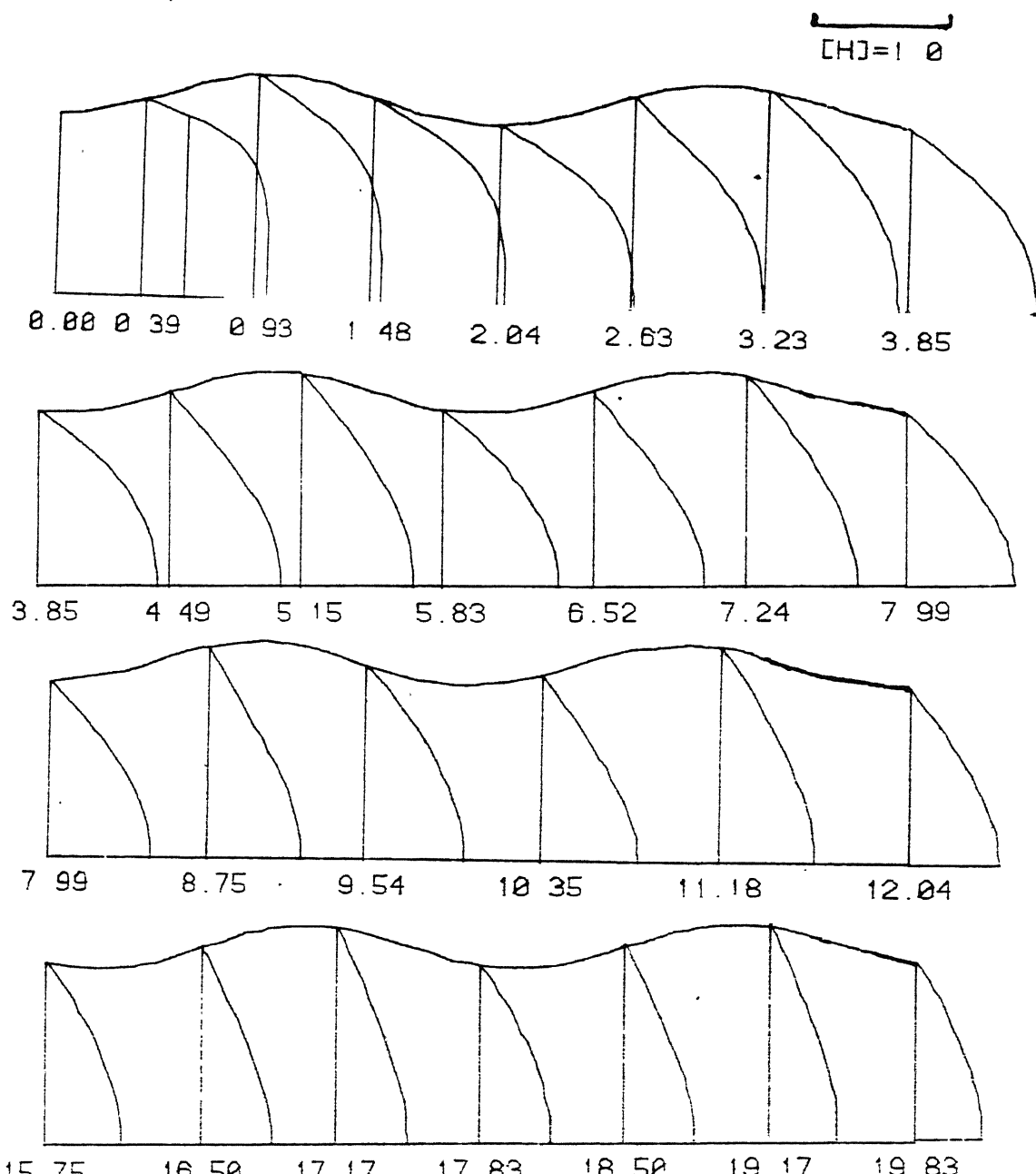
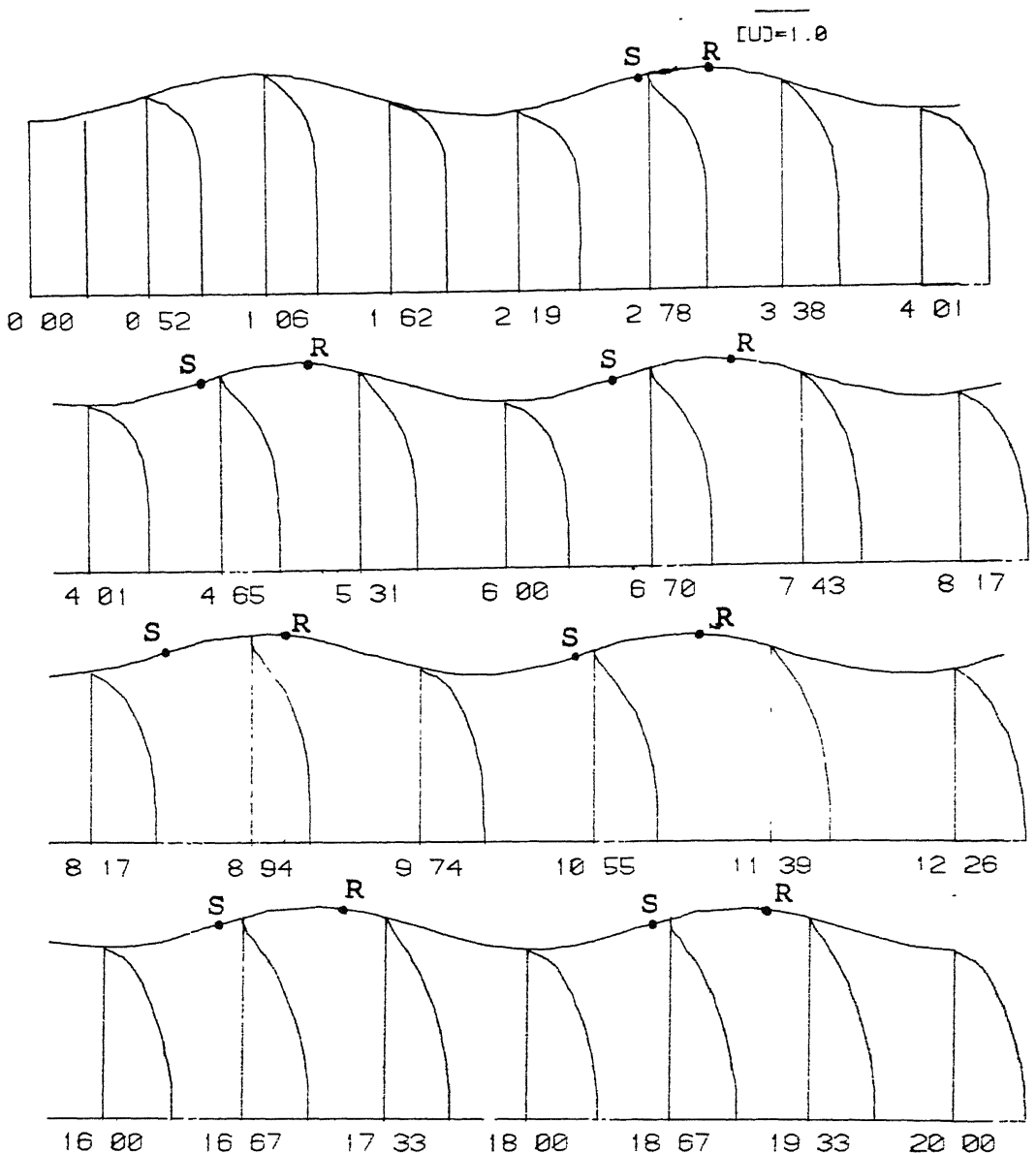
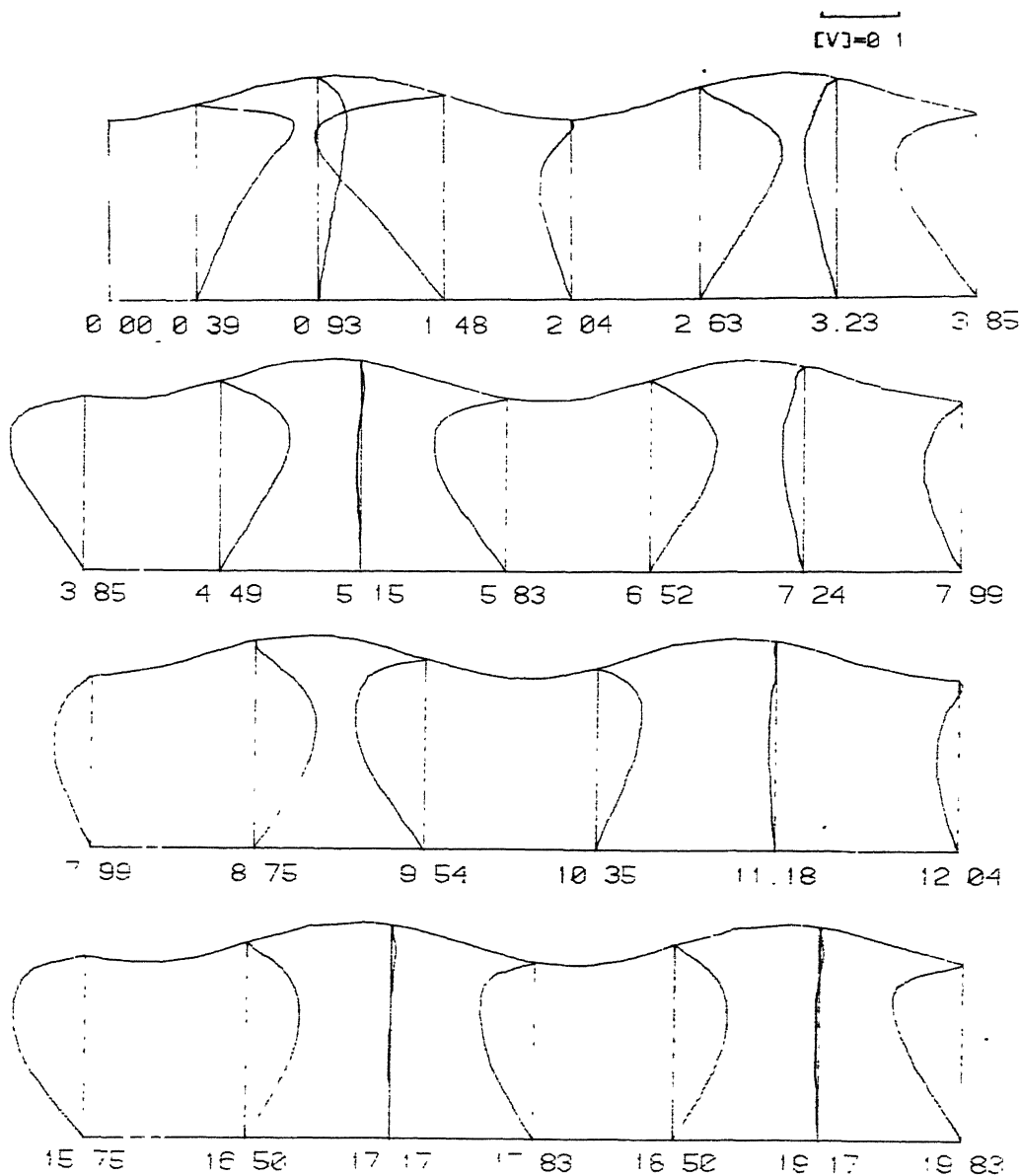


FIG.14 ENTHALPY PROFILES FOR A SYM. CHANNEL  
WITH LAMBDA=0.10 AND Re=100



**FIG.15 :** U-VELOCITY PROFILES FOR A SYM CHANNEL  
WITH LAMBDA=0.10 AND Re=500



**FIG.16** V-VELOCITY PROFILES FOR A SYM. CHANNEL  
WITH LAMBDA4=0.18 AND Re=500

1  
0.00-1.0

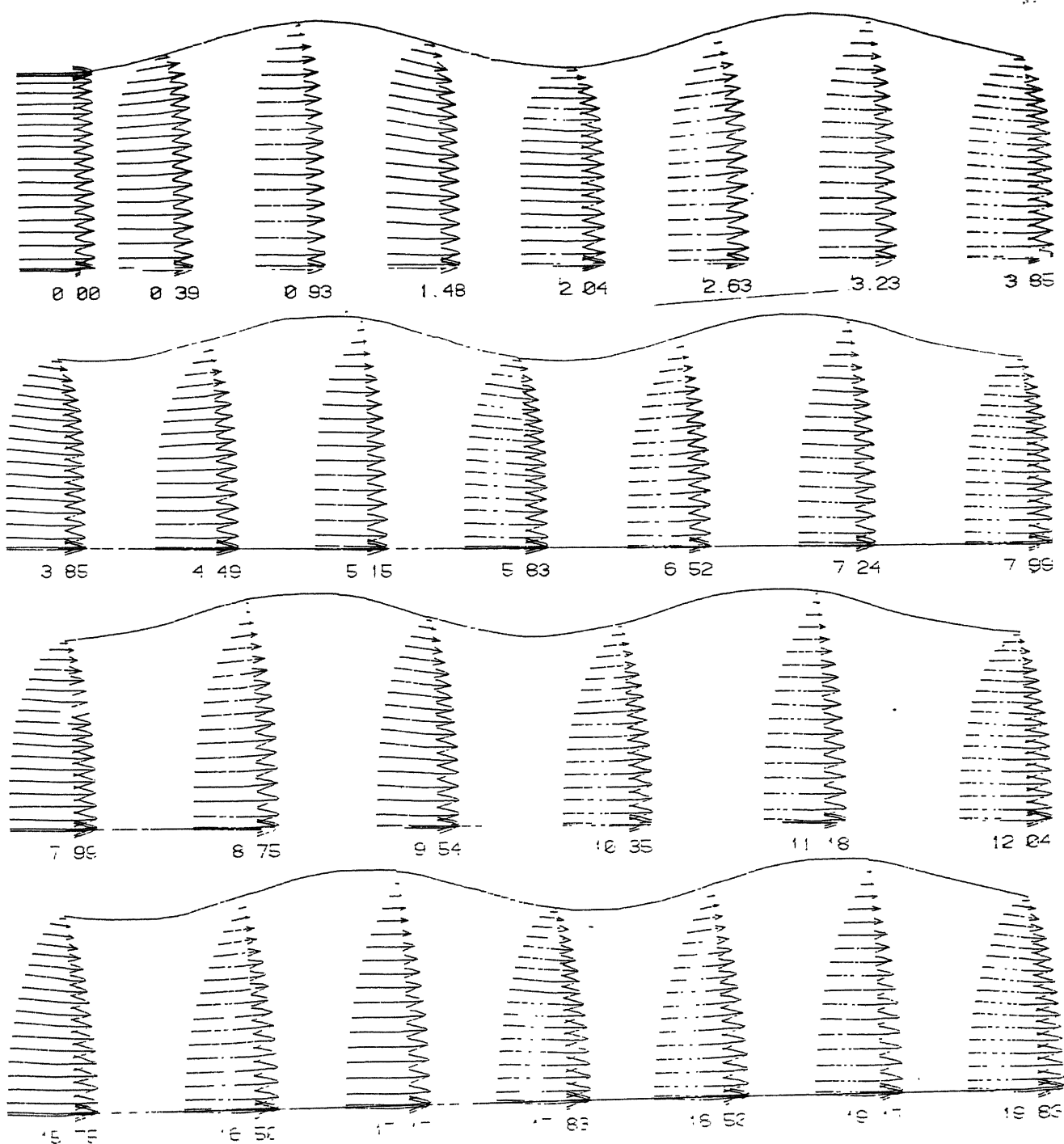
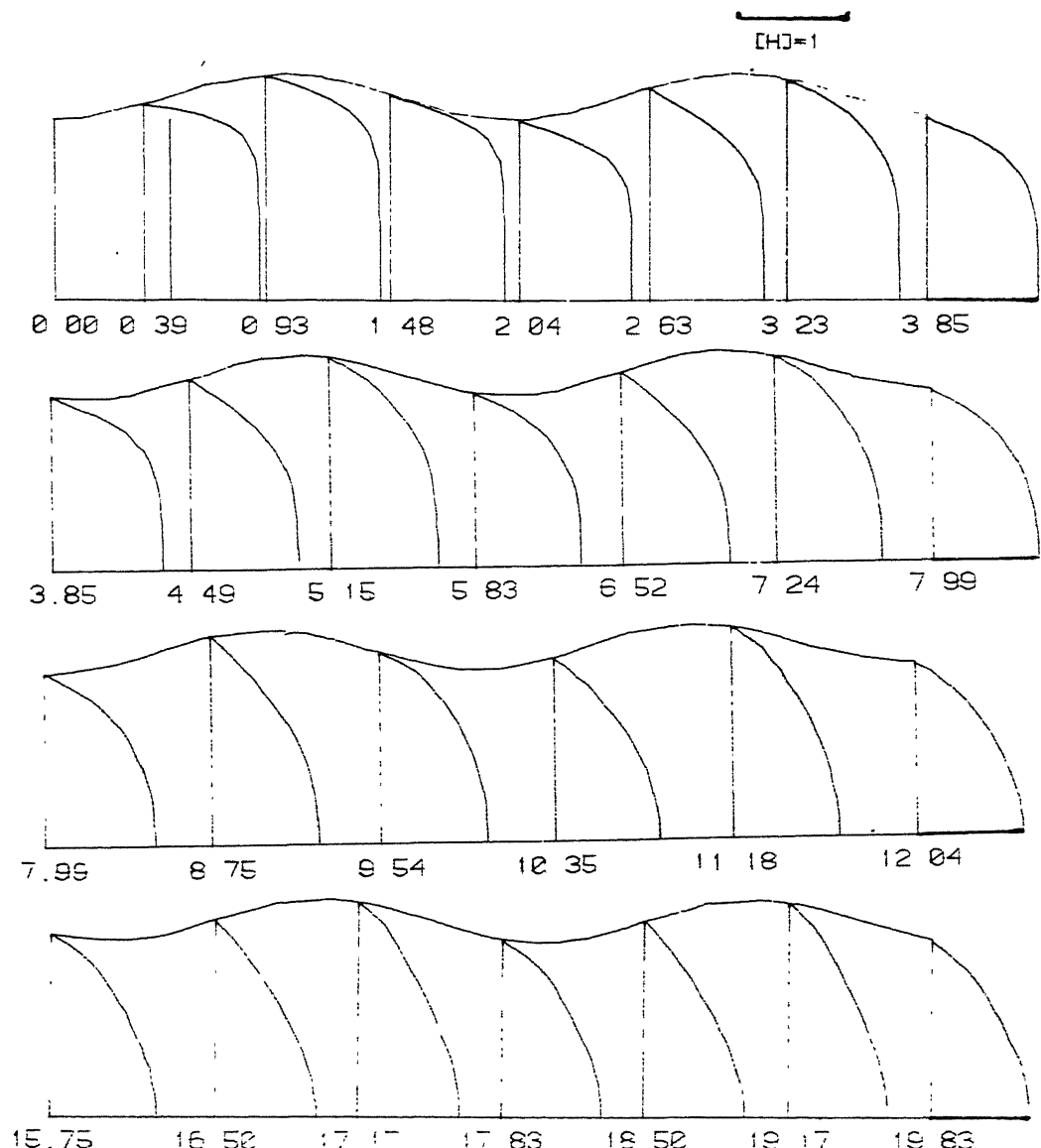
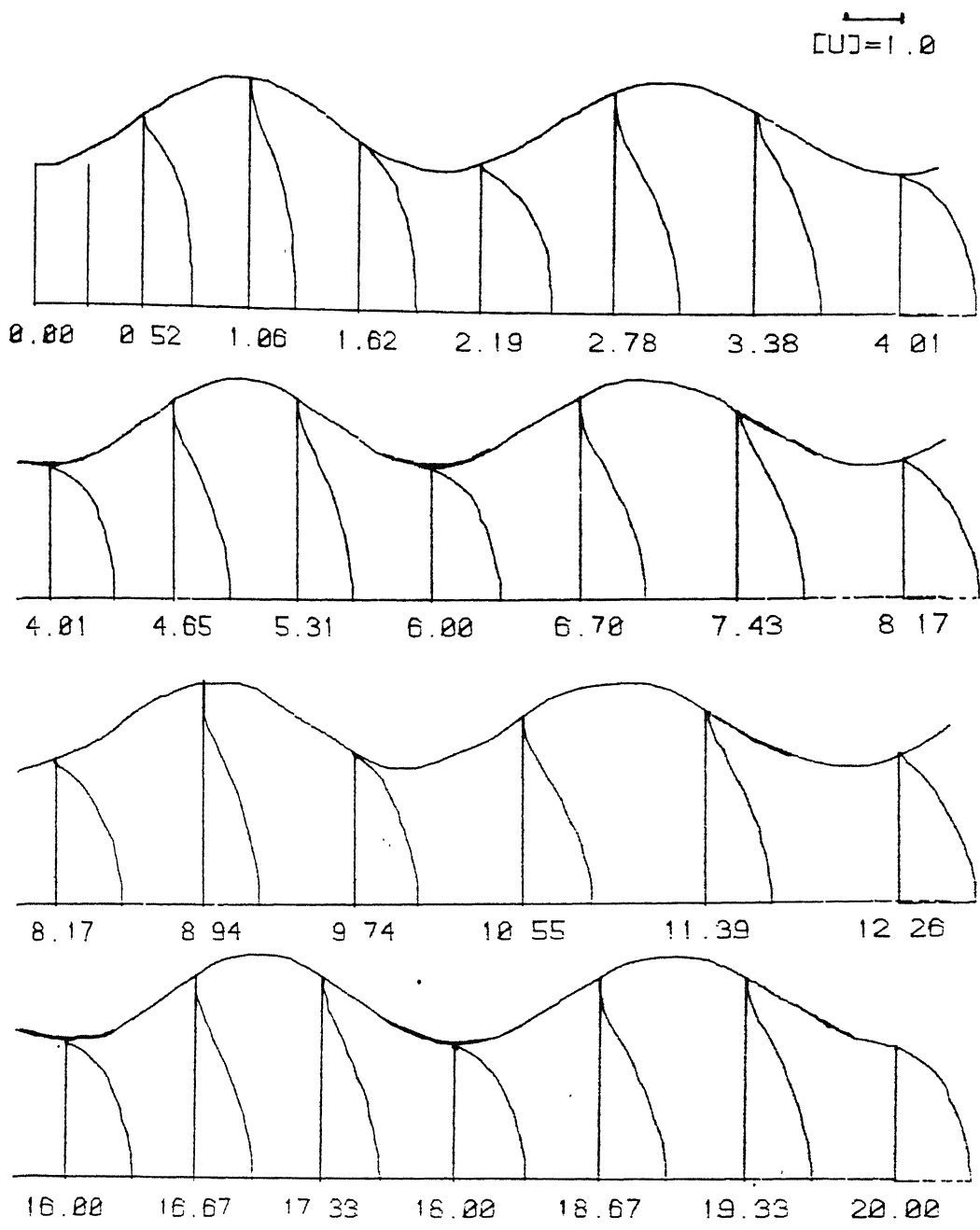


FIG 17 VELOCITY VECTORS IN S-CHANNE  
WITH LAMBDA=0.18 AND Re=500



**FIG.18 ENTHALPY PROFILES FOR A SYM. CHANNEL  
WITH  $\lambda_{MBD}=0.12$  AND  $Re=500$**



**FIG.19** U-VELOCITY PROFILES FOR A SYM CHANNEL  
WITH LAMBDA=0.20 AND Re=100.

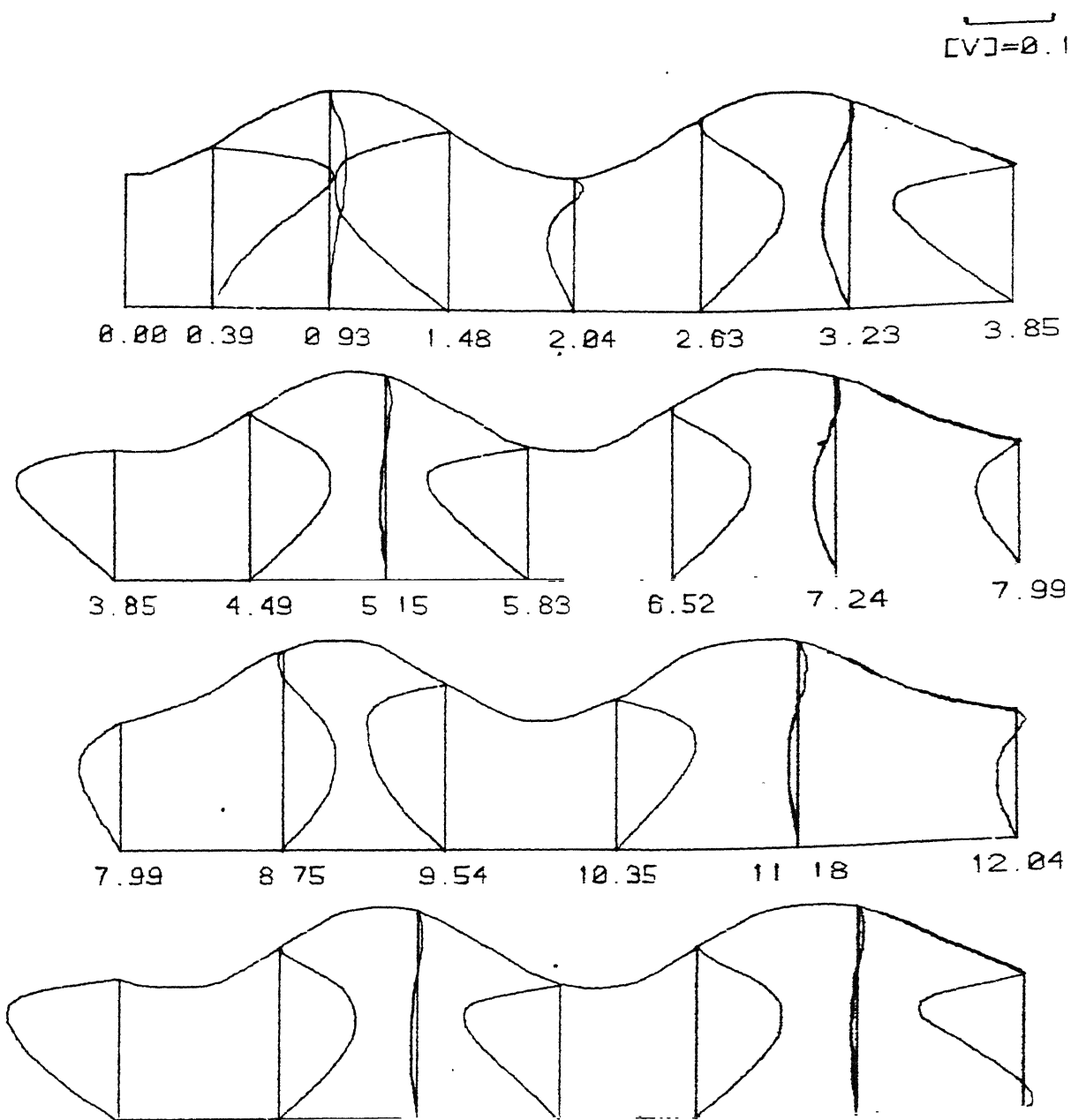


FIG.20 V-VELOCITY PROFILES FOR A SYM. CHANNEL  
WITH  $\lambda=0.20$  AND  $Re=100$ .

$\|U\|=1.0$

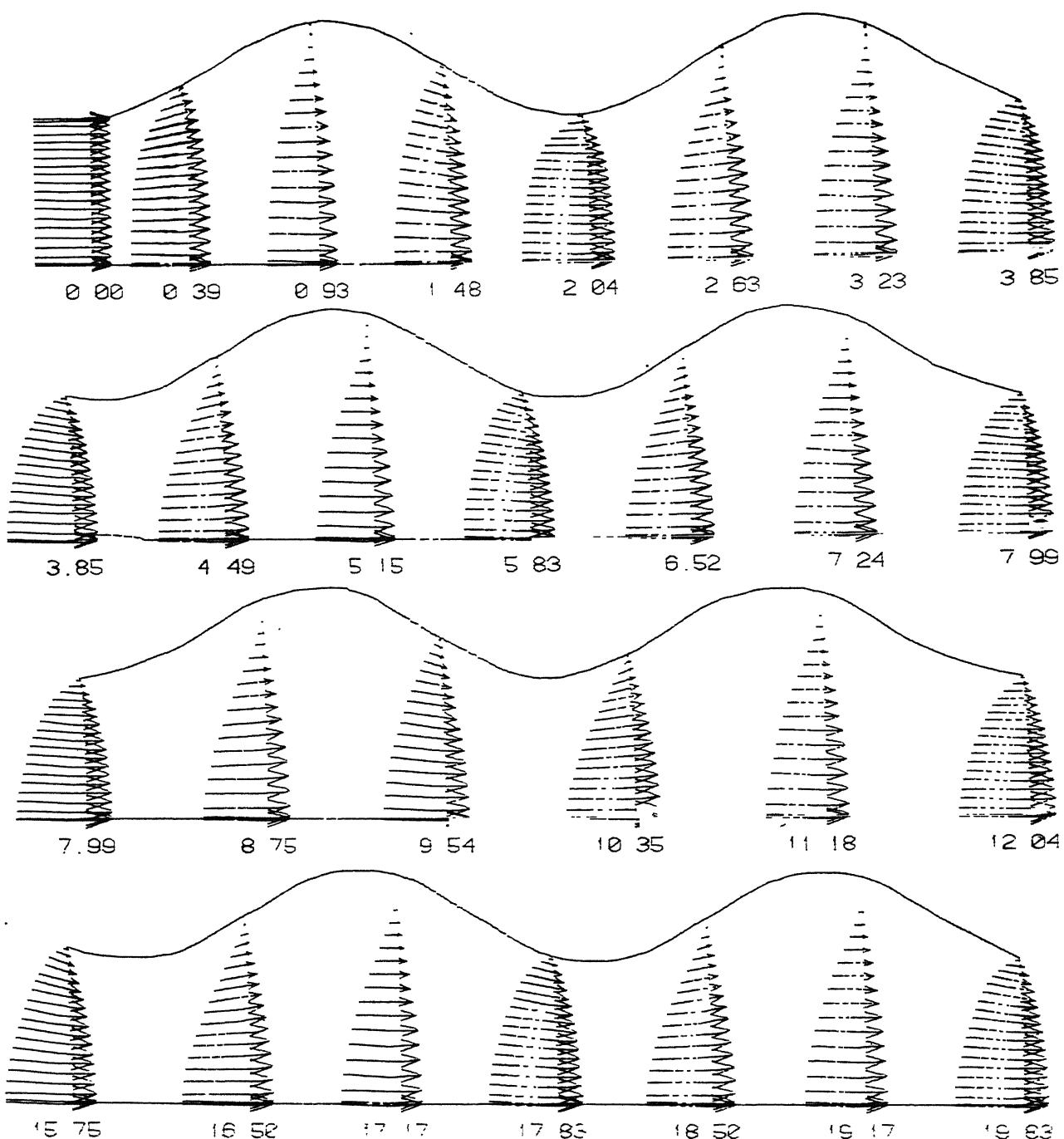
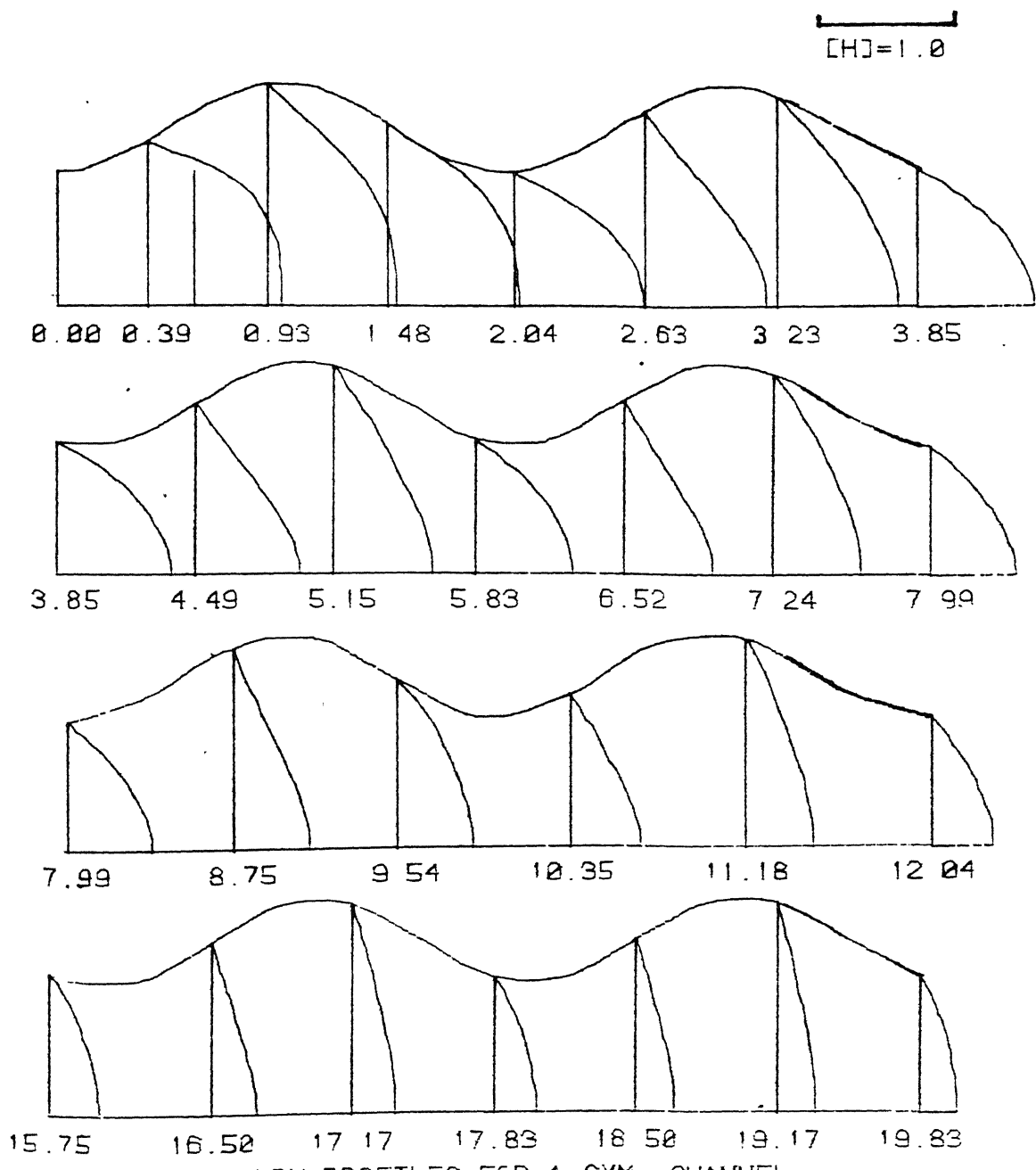


FIG.21 VELOCITY VECTORS IN A SYM CHANNEL  
WITH LAMBDA=8.20 AND Re=102



**FIG.22 ENTHALPY PROFILES FOR A SYM. CHANNEL  
WITH LAMBDA=0.20 AND Re=100.**

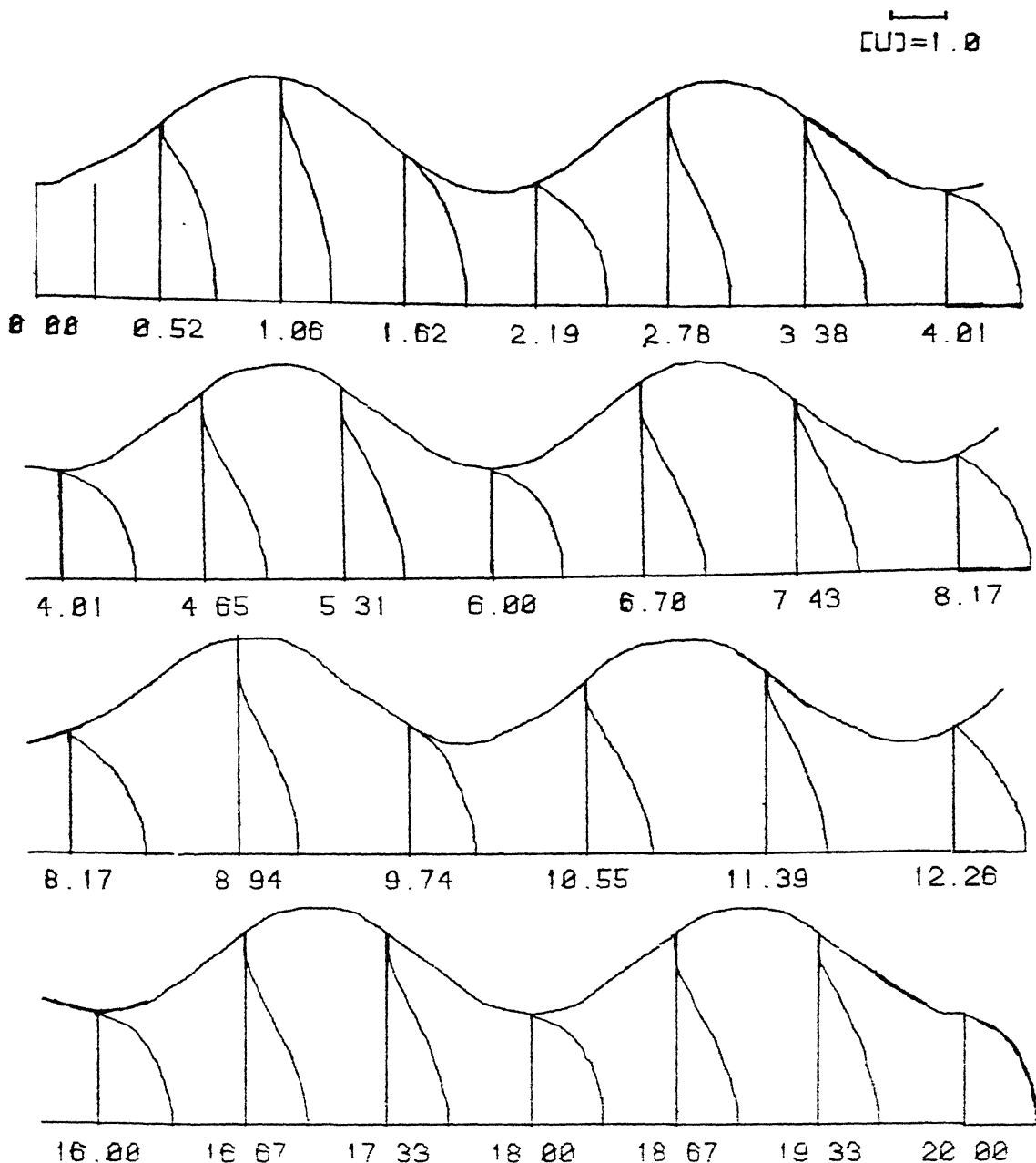


FIG.23 U-VELOCITY PROFILES FOR A SYM.. CHANNEL  
WITH LAMBDA=0.25 AND Re=100.

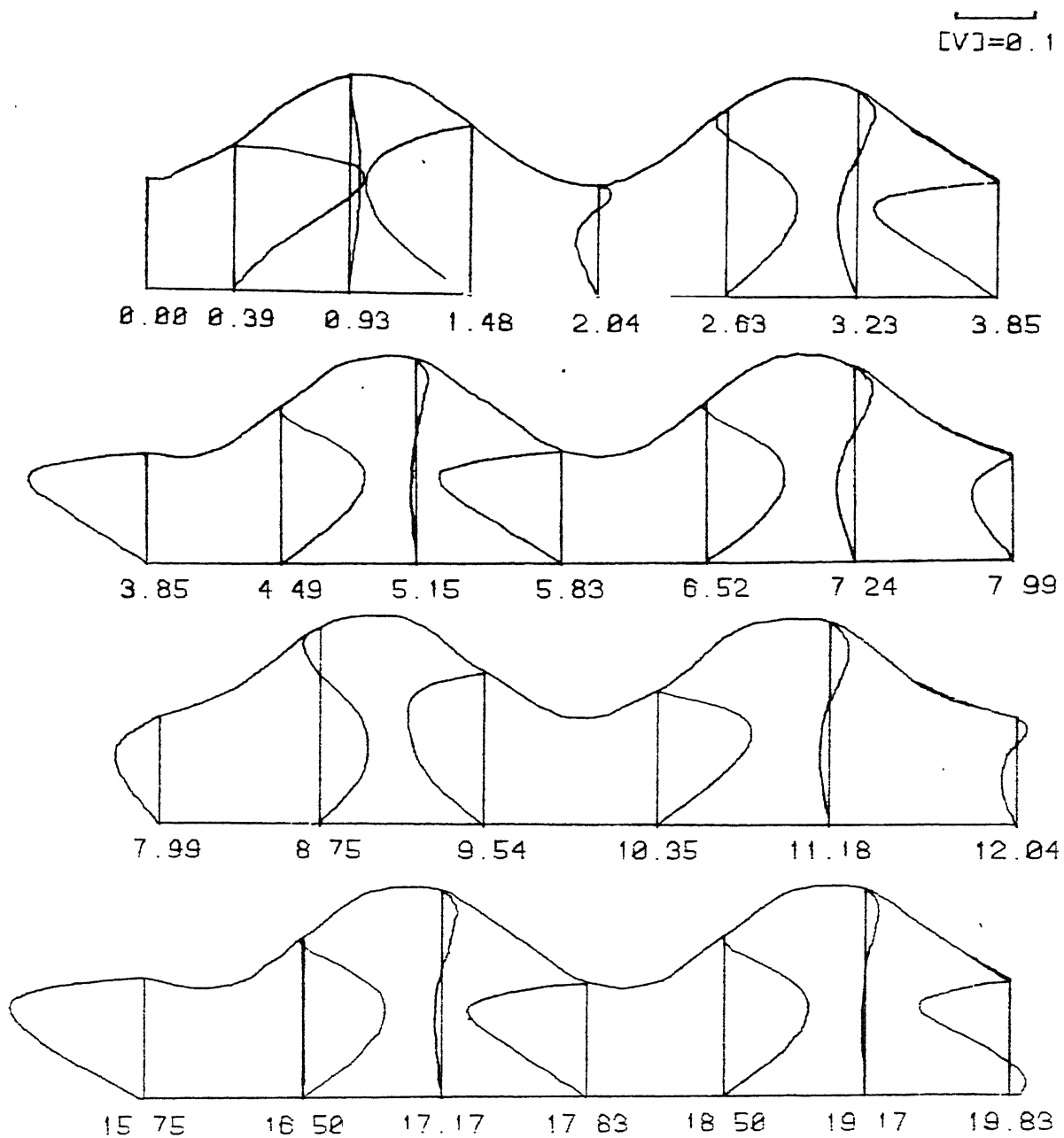


FIG.24 V-VELOCITY PROFILES FOR A SYM. CHANNEL  
WITH LAMBDA=0.25 AND Re=100.

$\text{L} = 1.0$

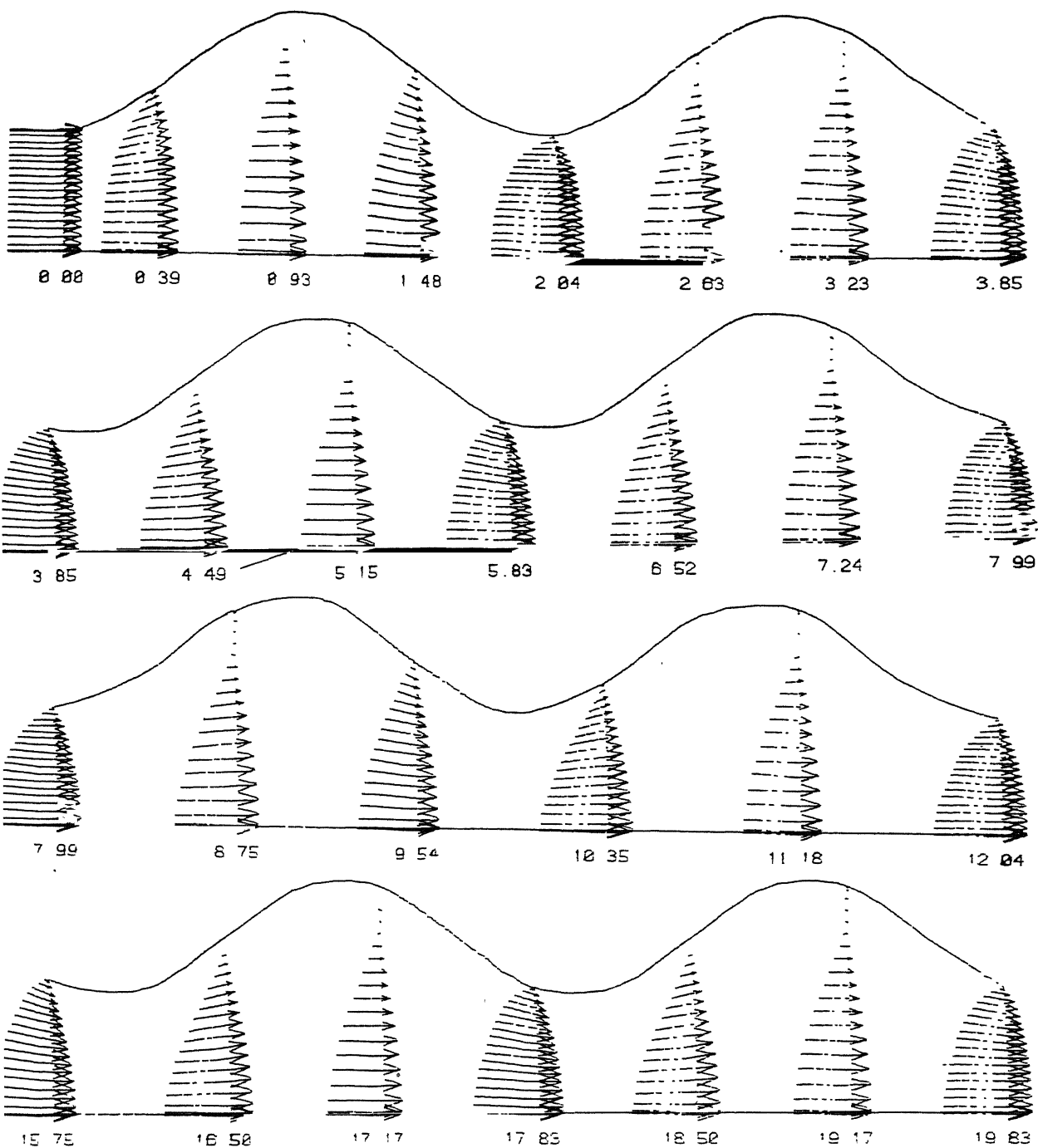


FIG.25 VELOCITY VECTORS IN A SYM CHANNEL  
WITH LAMBDA=0.25 AND Re=102

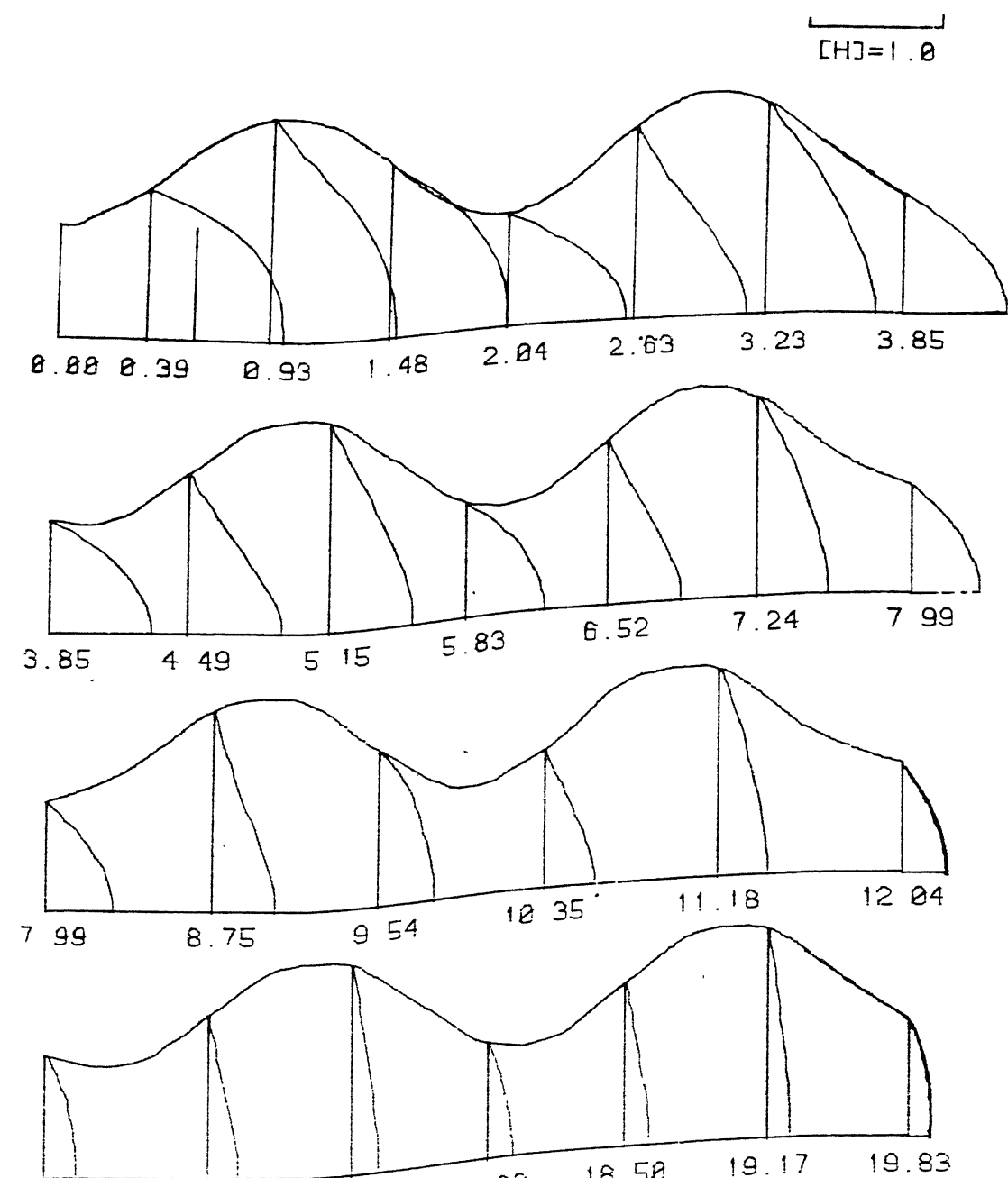


FIG. 26 ENTHALPY PROFILES FOR A SYM. CHANNEL

WITH LAMBDA=0.25 AND Re=100

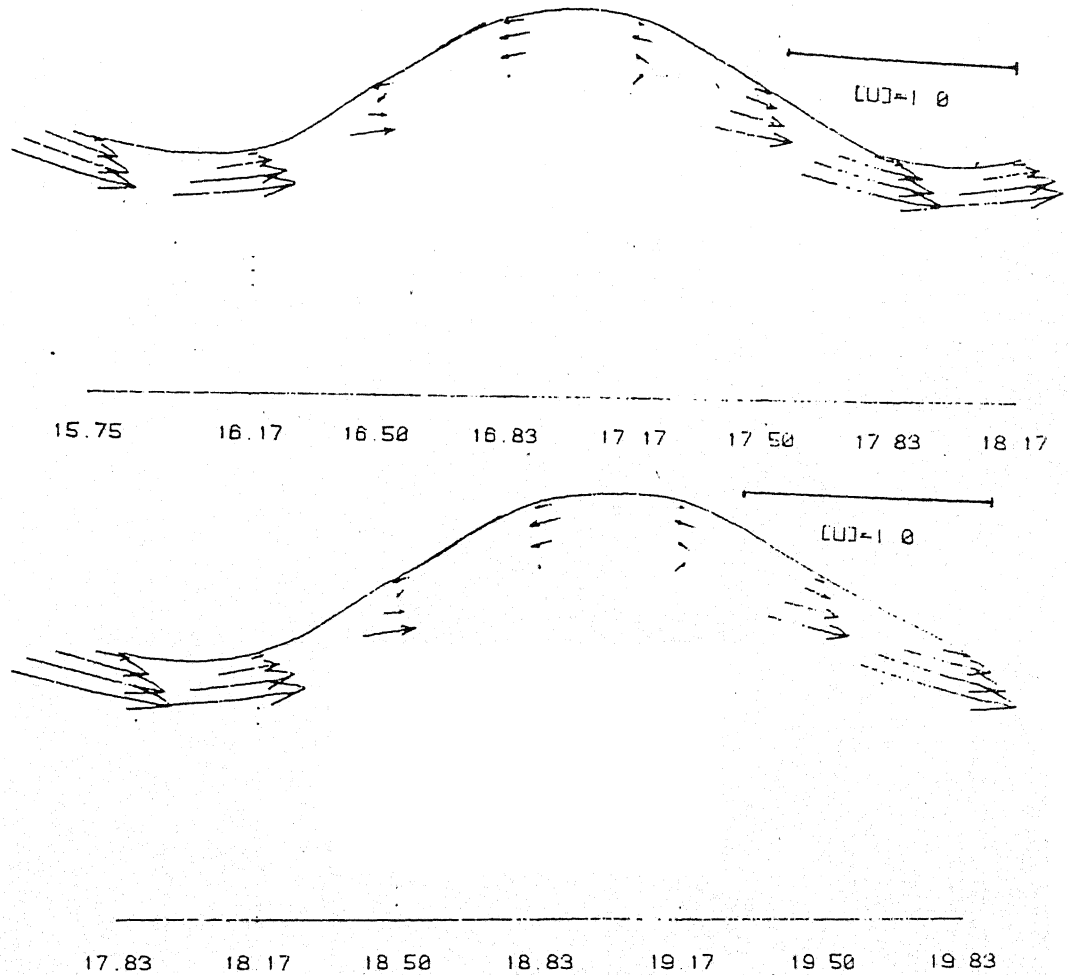


FIG. 27 VELOCITY VECTORS IN A SYM CHANNEL

WITH LAMBDA=0.20 AND  $Re=500$ .

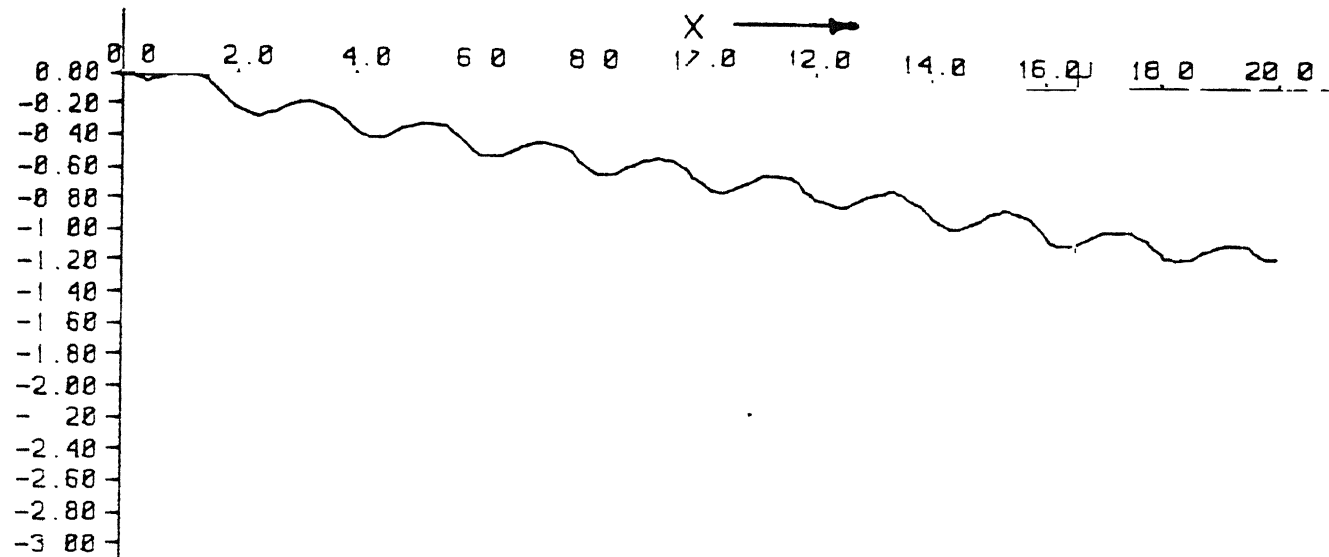


FIG.28a

PRESSURE DISTRIBUTION ALONG X FOR A SYM CHANNEL  
WITH LAMBDA=0.10 AND  $Re=100$

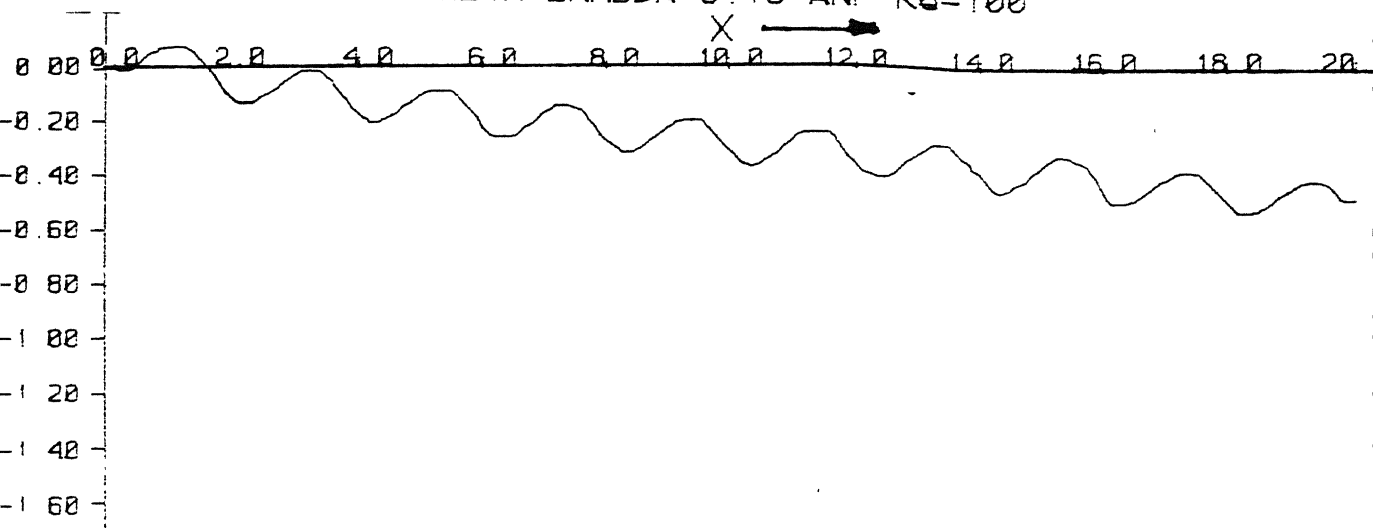


FIG.28b

PRESSURE DISTRIBUTION ALONG X FOR A SYM. CHANNEL  
WITH LAMBDA=0.10 AND  $Re=500$

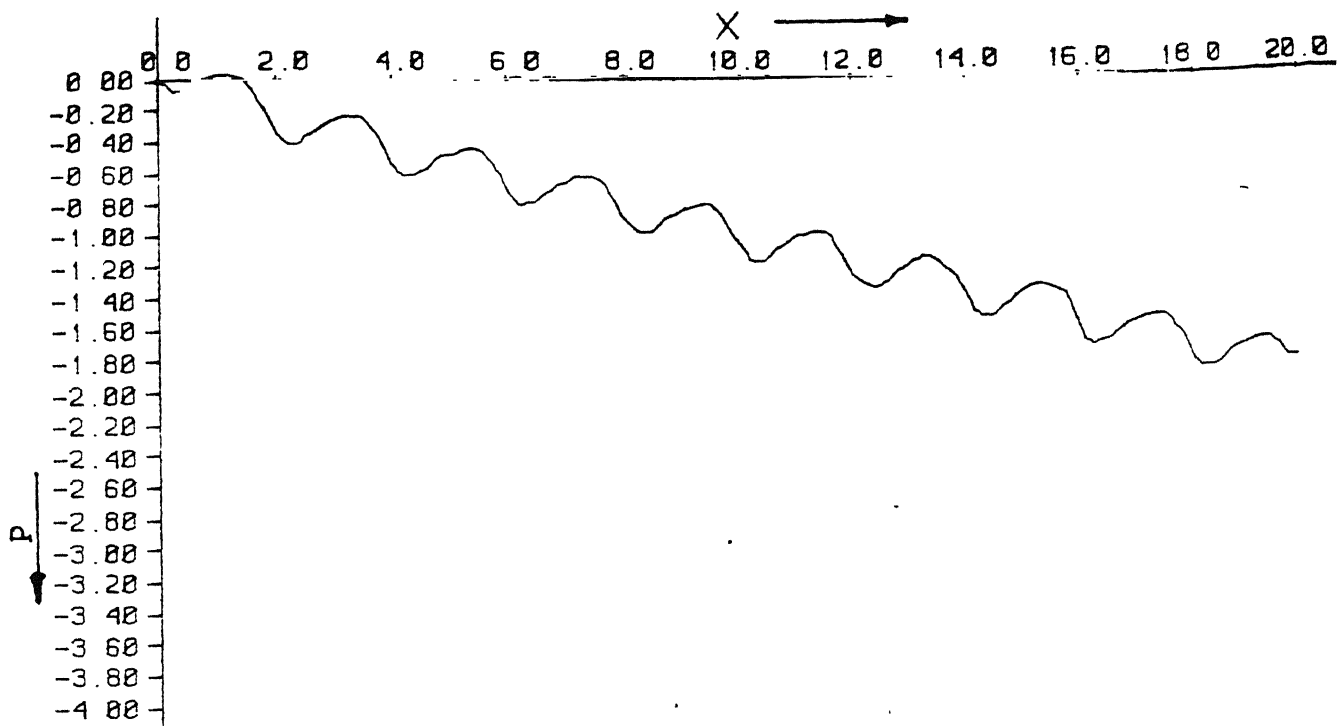


FIG. 29a

PRESSURE DISTRIBUTION ALONG X FOR A SYM. CHANNEL  
WITH LAMBDA=0.20 AND  $Re=100$

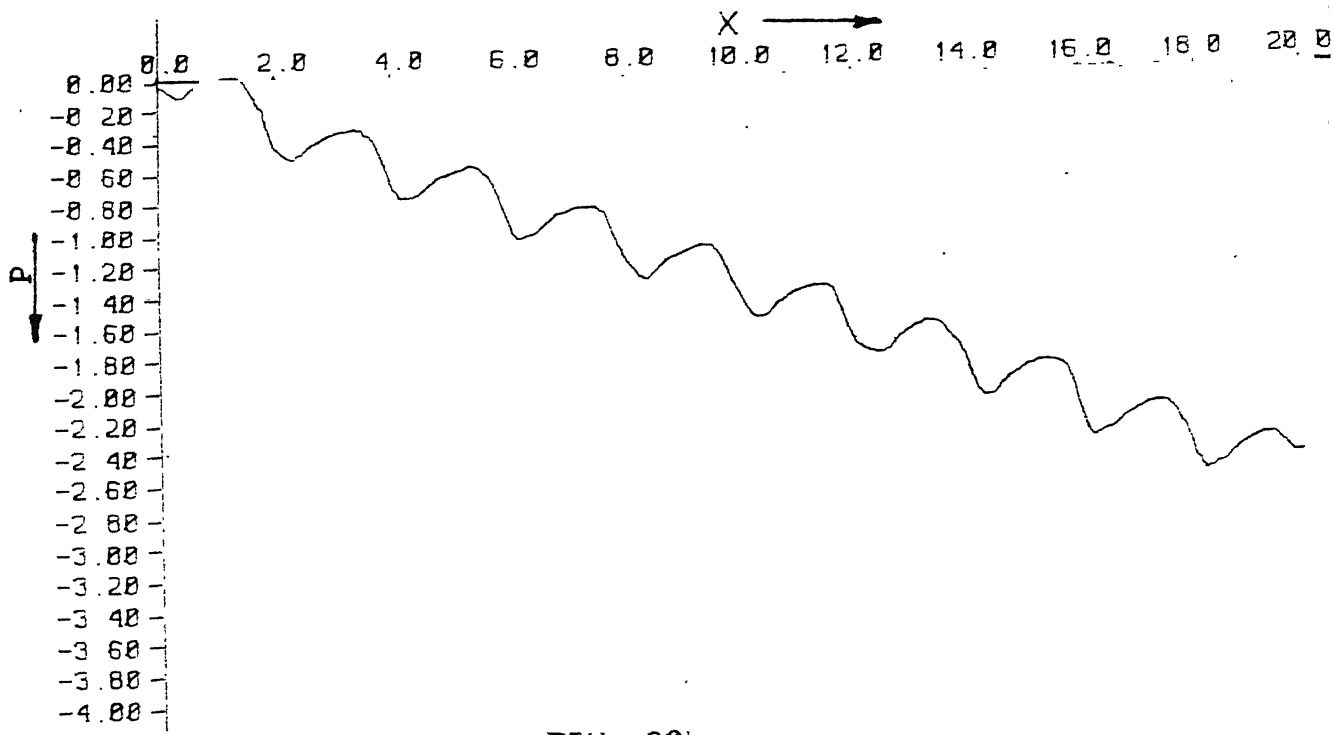


FIG. 29b

PRESSURE DISTRIBUTION ALONG X FOR A SYM. CHANNEL  
WITH LAMBDA=0.25 AND  $Re=100$

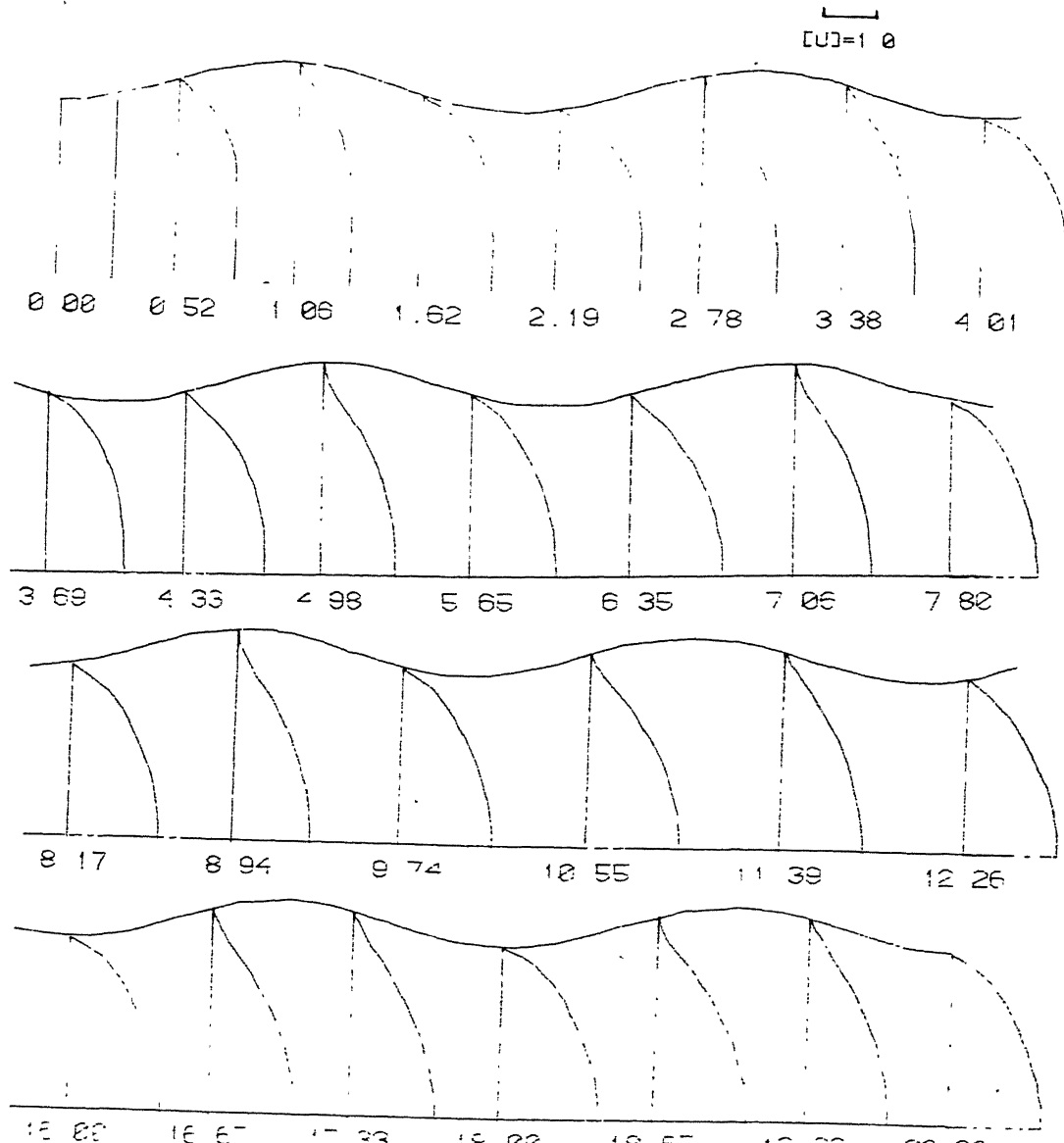


FIG.30 - VELOCITY PROFILES FOR A PIPE  
WITH  $\lambda_{MB4}=2.18$  AND  $Re=100$

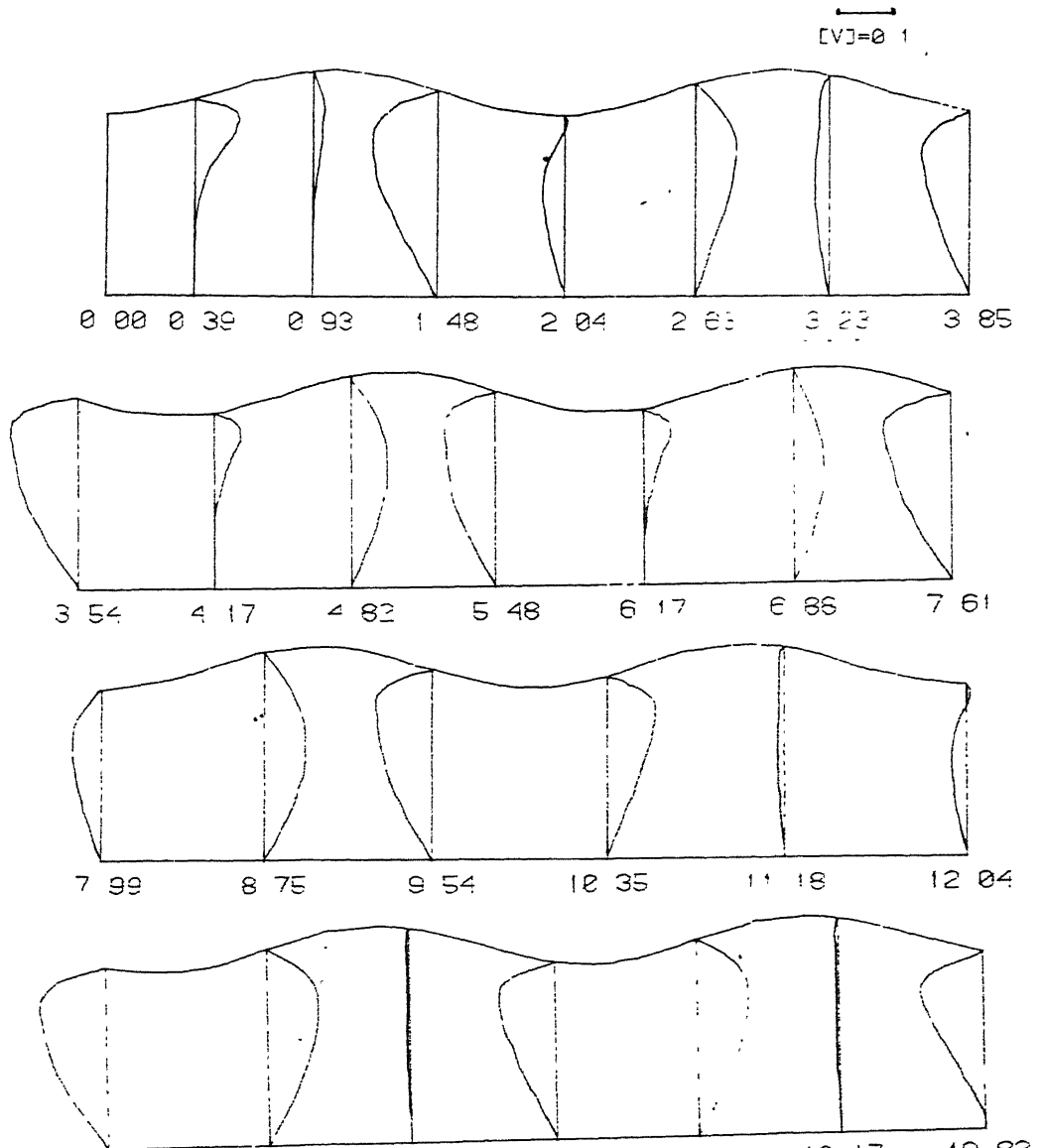


FIG. 31 V-VELOCITY PROFILES FOR A PIPE  
WITH  $\Lambda = 0.12$  AND  $R_e = 100$

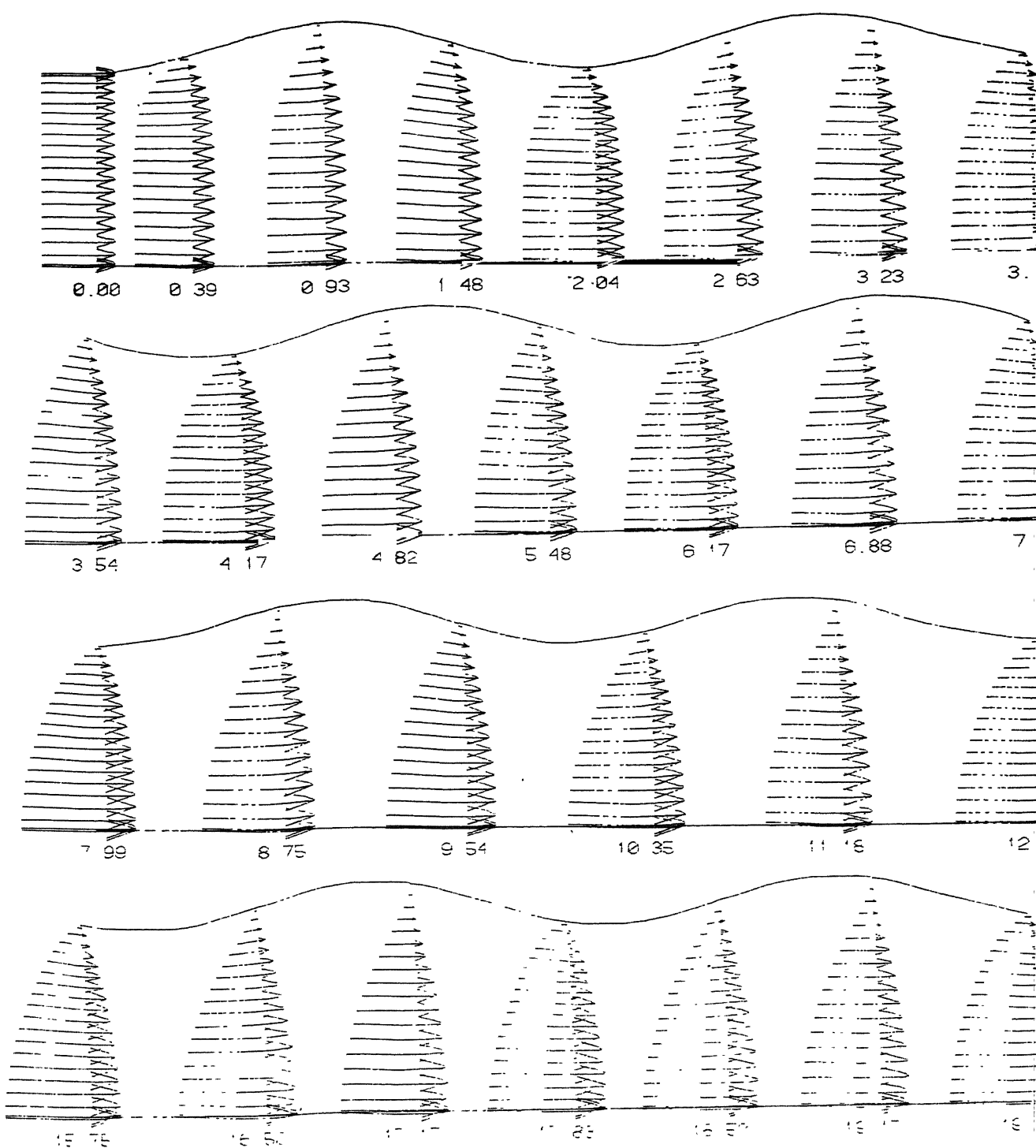


FIG.32 VELOCITY VECTORS IN A PIPE  
 $Re = 1000$ ,  $L/D = 6$ ,  $10^3 \text{ L/D}$ ,  $R_e = 10^3$

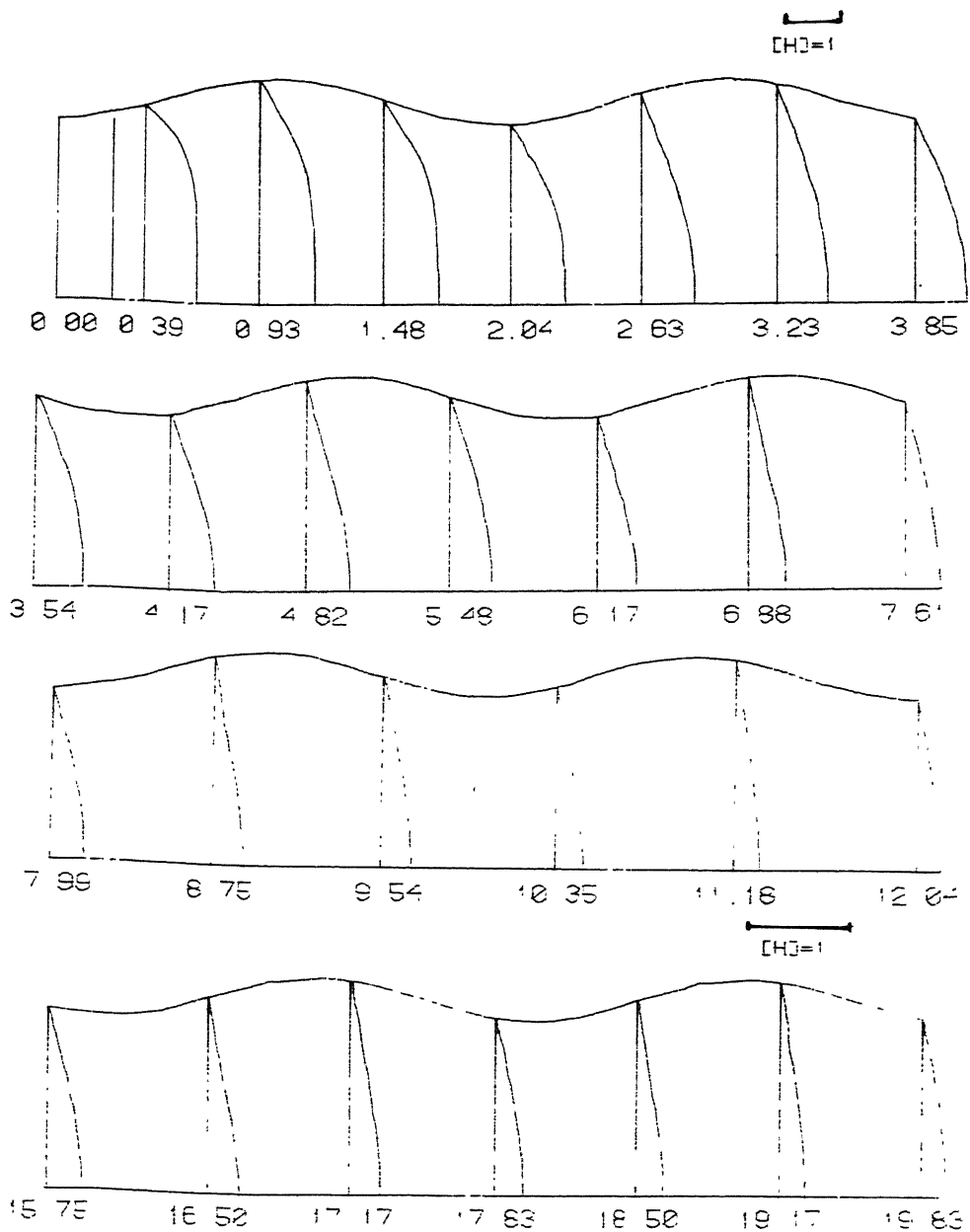


FIG.33 ENTHALPY PROFILES FOR A PIPE  
WITH  $\lambda = 0.10$  AND  $Re = 100$

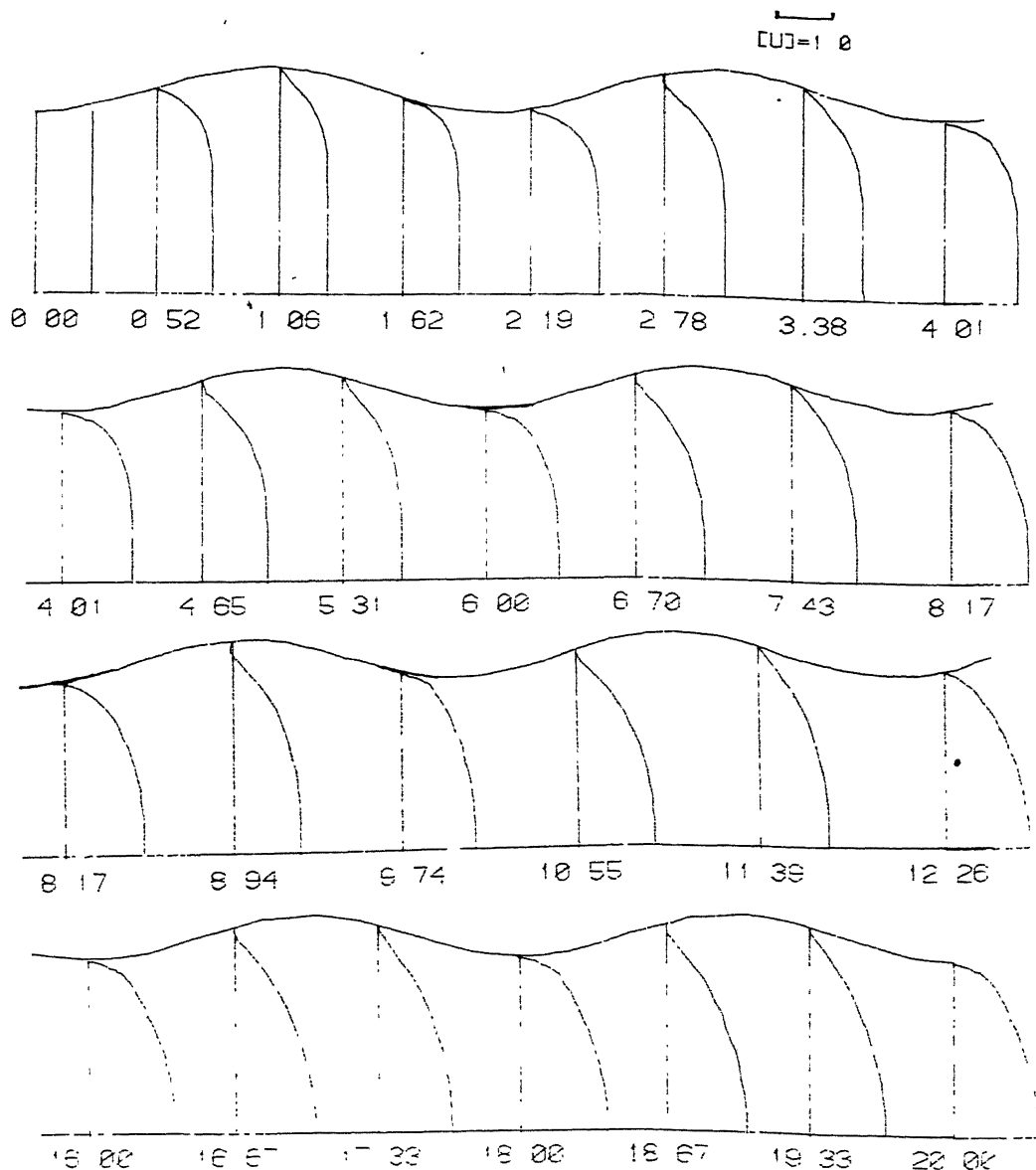


FIG. 34. VELOCITY PROFILES FOR A PIPE  
WITH  $\lambda/\text{D} = 2.18$  AND  $Re = 500$

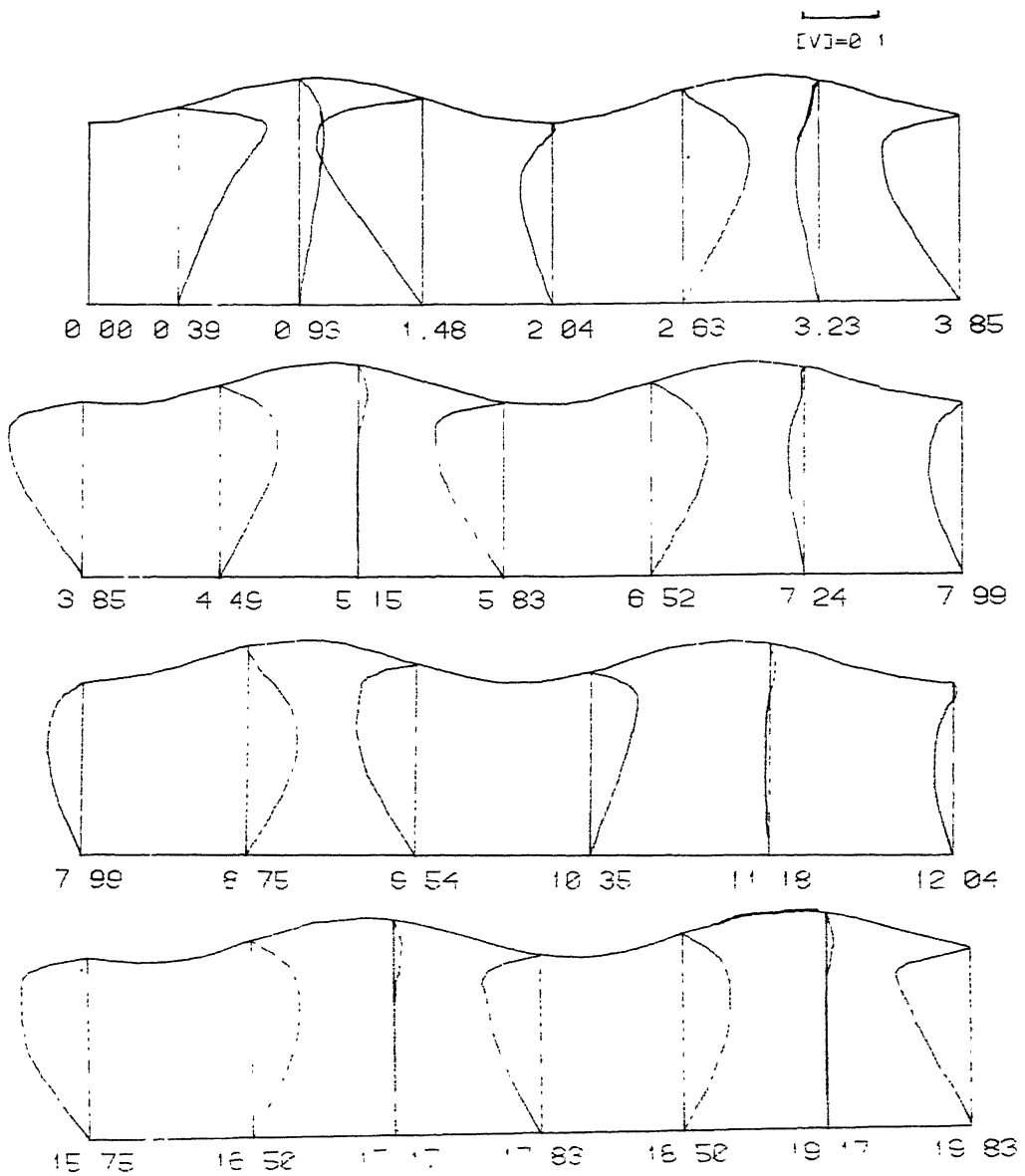


FIG.35. VELOCITY PROFILES FOR A PIPE  
WITH  $\lambda=0.10$  AND  $R_e=500$

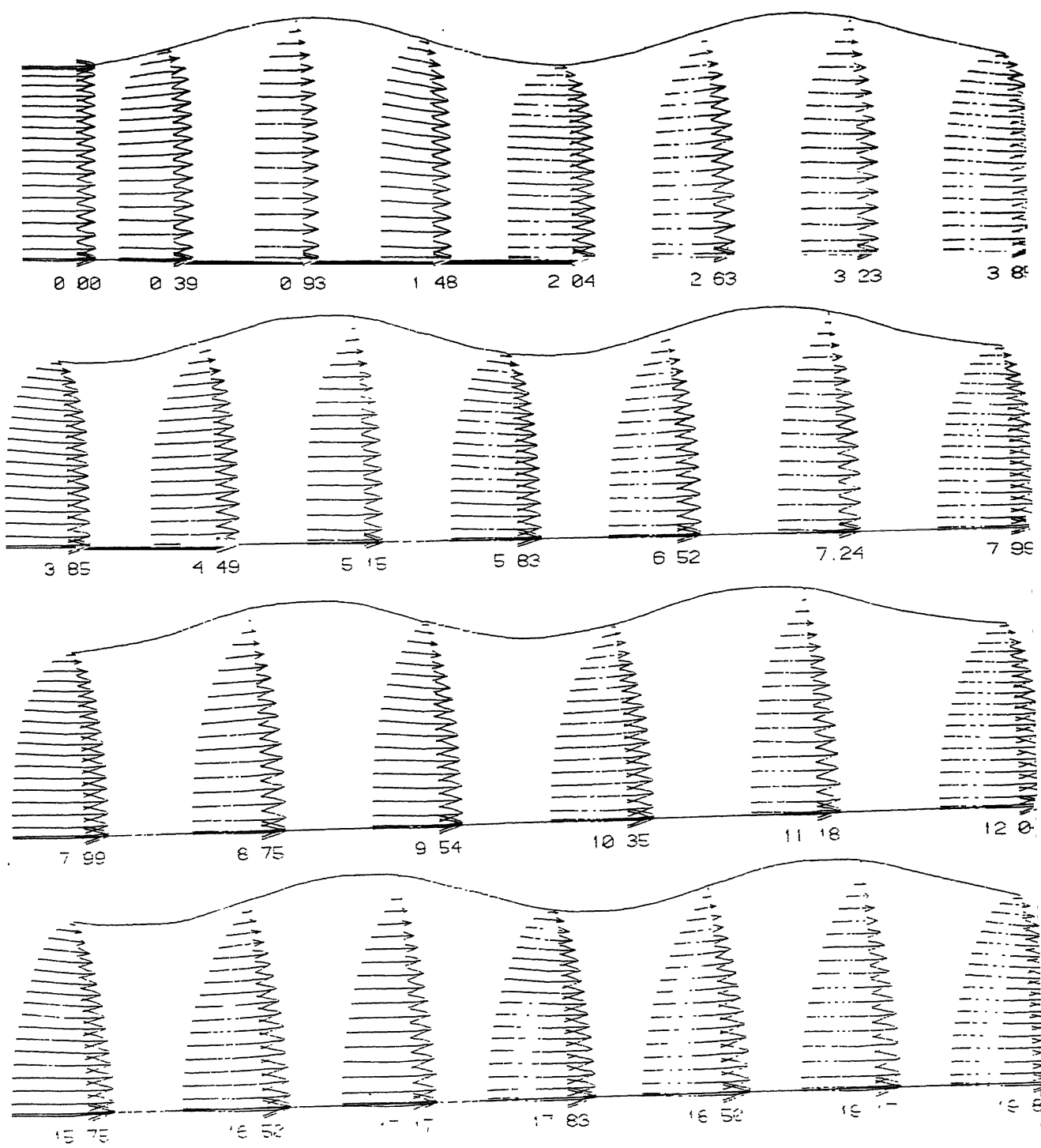


FIG. 36 VELOCITY VECTORS IN L PIPE  
WITH  $\lambda_{BL} = 0.12$  AND  $Re = 500$

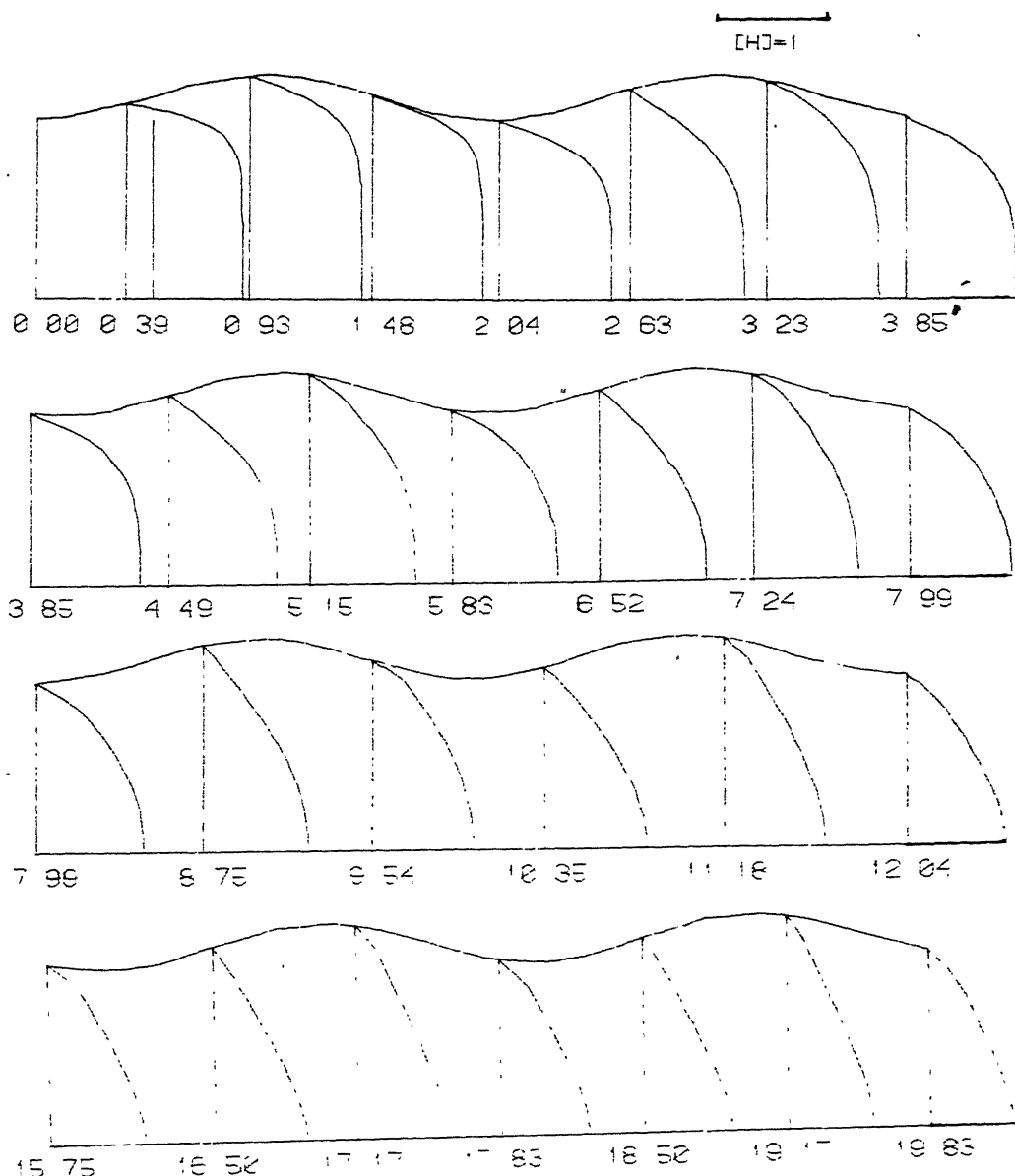


FIG.37 STREAMWISE PROFILES FOR A PIPE  
 $w_1 = 14.524 = 2.12$  AND  $Re = 500$

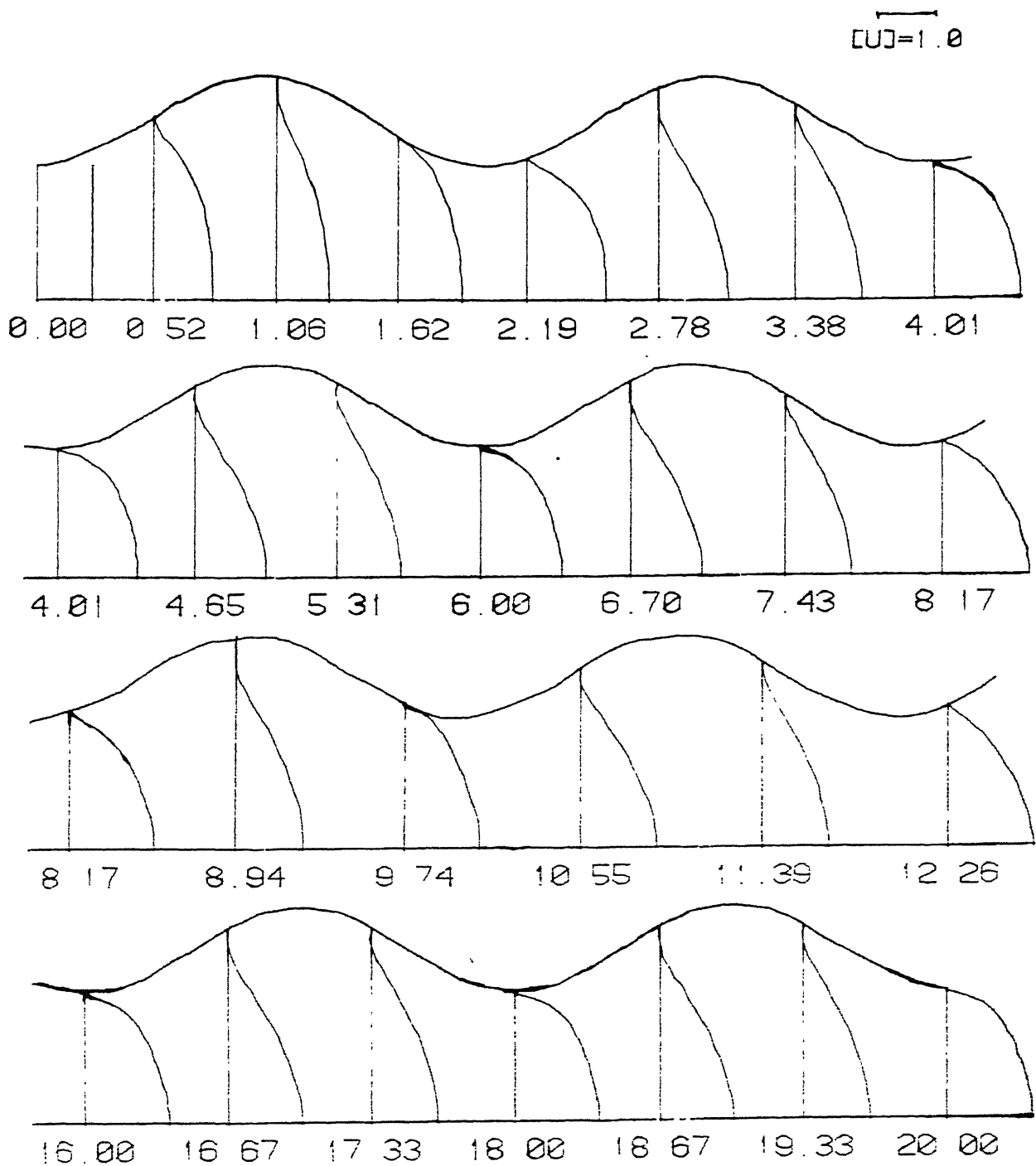
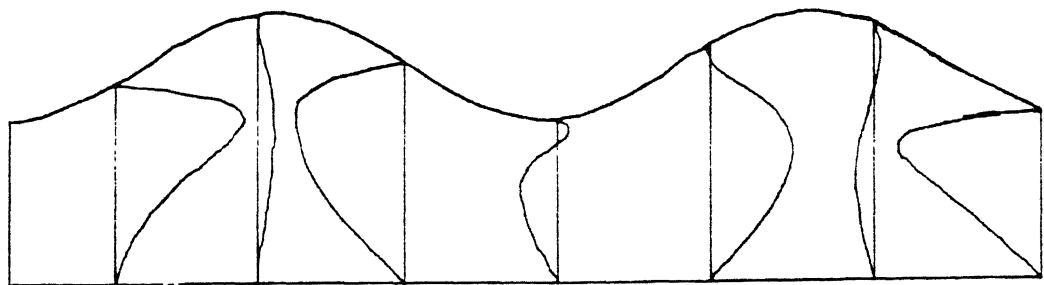
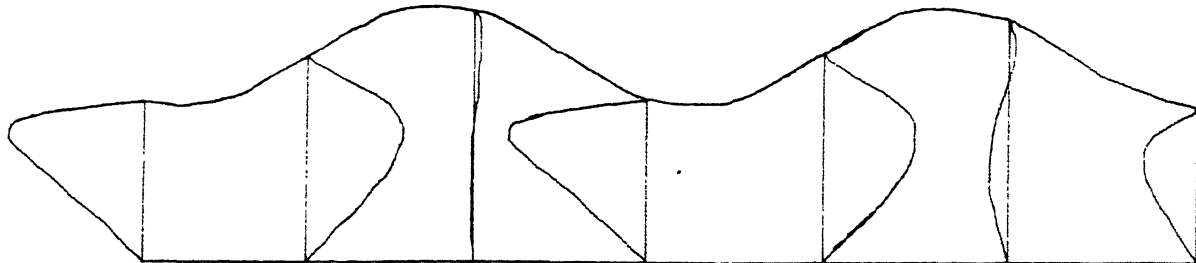


FIG.38 U-VELOCITY PROFILES FOR A PIPE  
WITH LAMBDA=0.28 AND Re=100

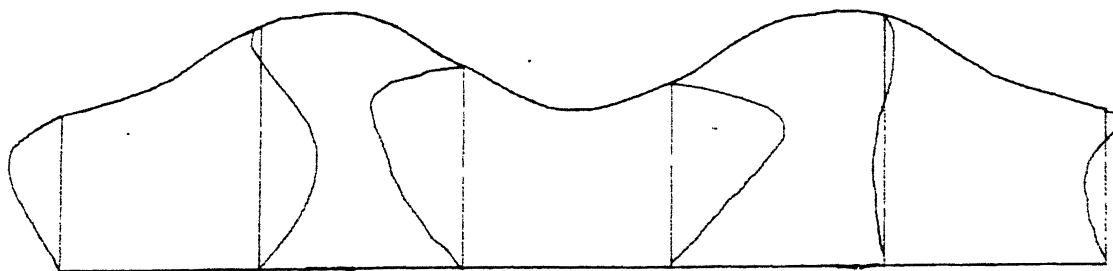
$\overline{V} = 0$



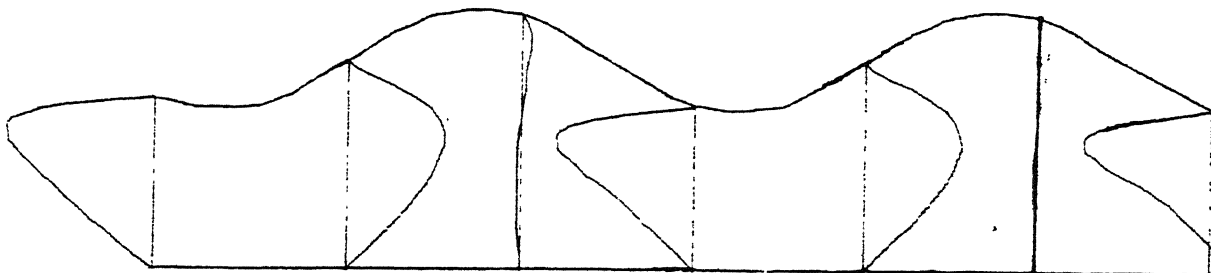
0 00 0.39 0.93 1.48 2.04 2.63 3.23 3.85



3.85 4.49 5.15 5.83 6.52 7.24 7.99



7.99 8.75 9.54 10.35 11.18 12.04



15.75 16.50 17.17 17.83 18.50 19.17 19.83

FIG.39 V-VELOCITY PROFILES FOR A PIPE  
WITH LAMBDA=0.28 AND Re=100

[ $\vec{U}_0 = 1 \text{ e}$ ]

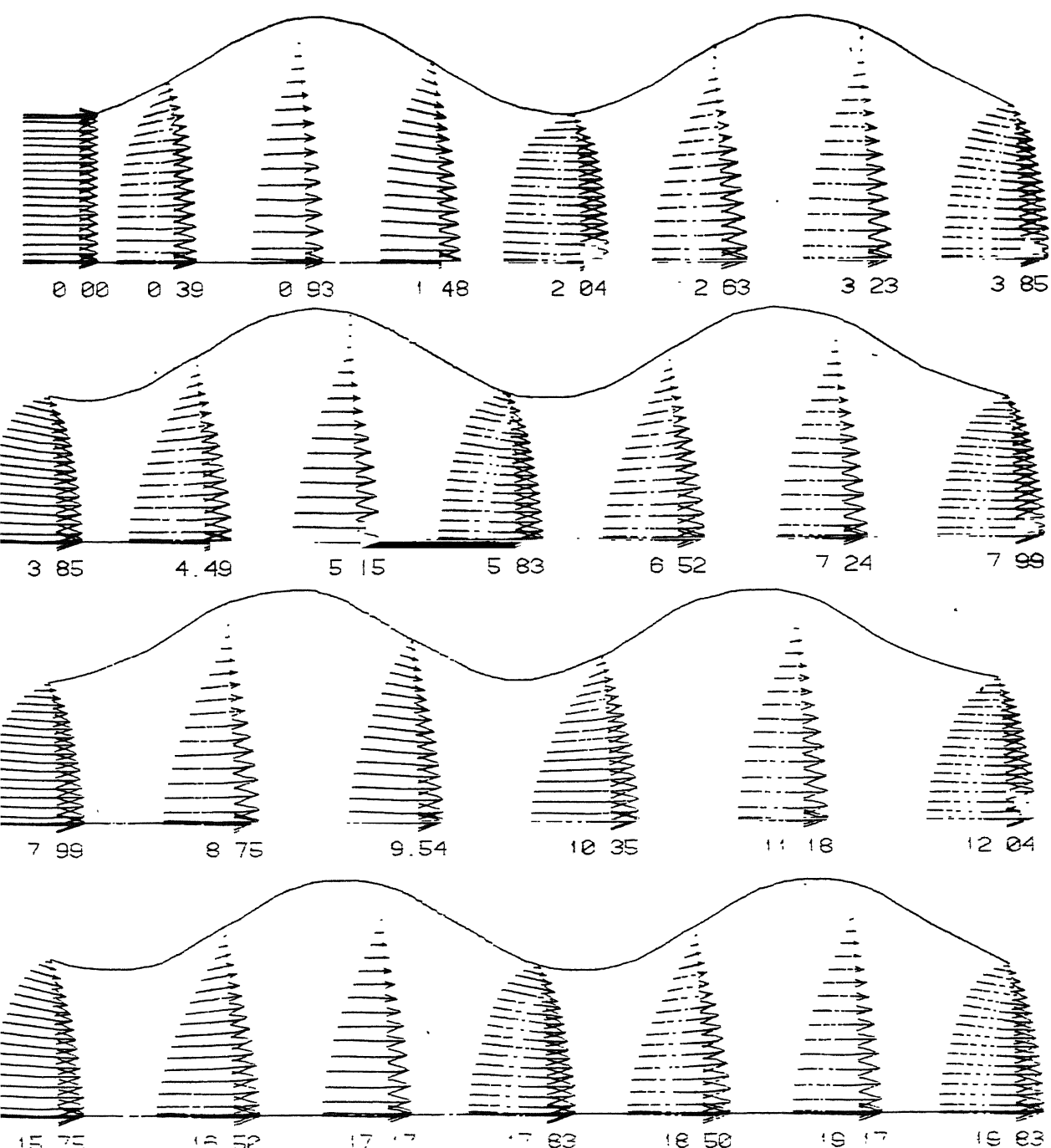


FIG. 40 VELOCITY VECTORS IN A PIPE  
WITH  $\lambda_{ABD4}=0.20$  AND  $Re=100$

$[H]=1.$

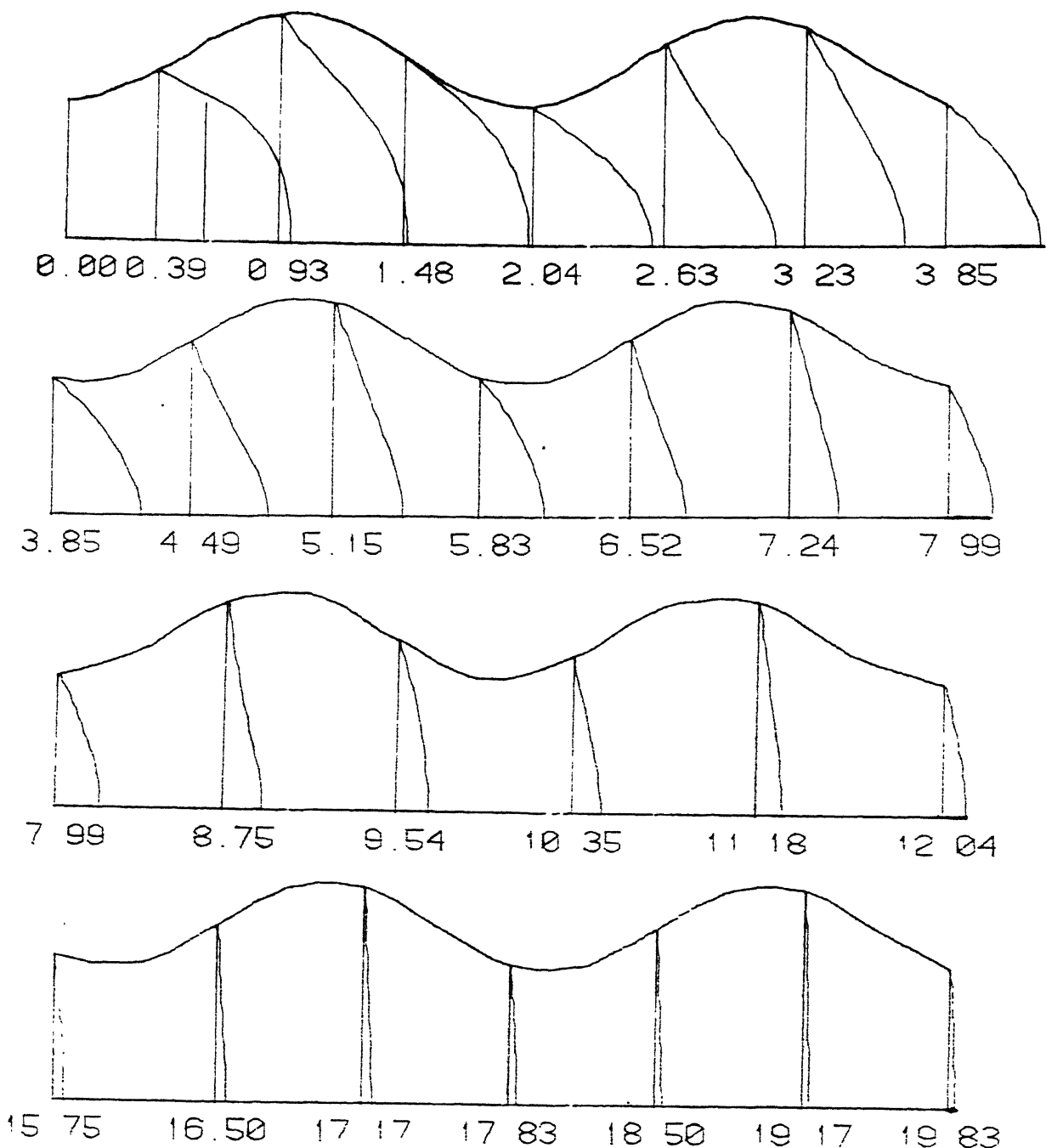


FIG.41 ENTHALPY PROFILES FOR A PIPE  
WITH LAMBDA=0.20 AND Re=100

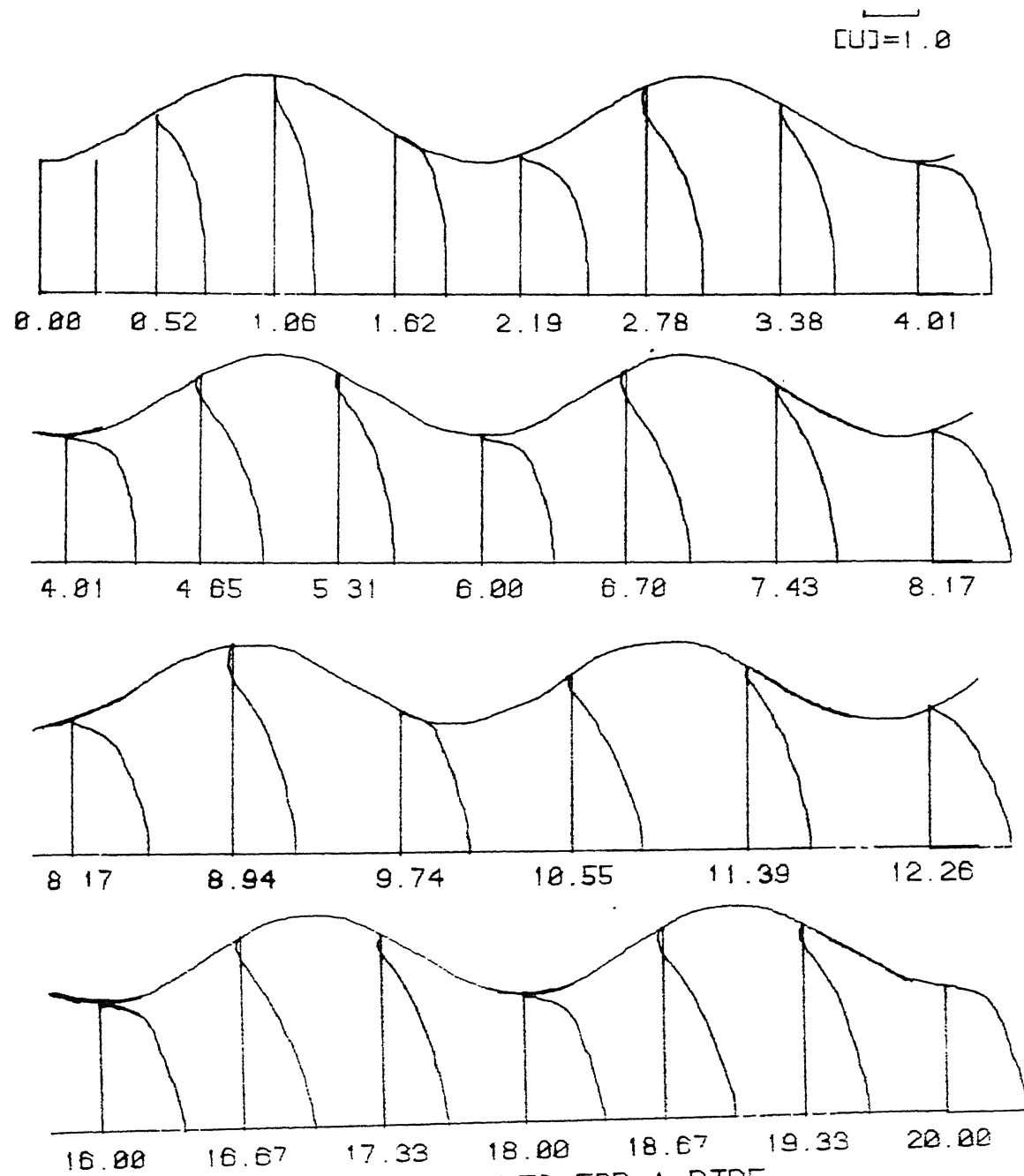


FIG.42 U-VELOCITY PROFILES FOR A PIPE  
WITH LAMBDA=0.20 AND Re=500

$[V]=0$  1

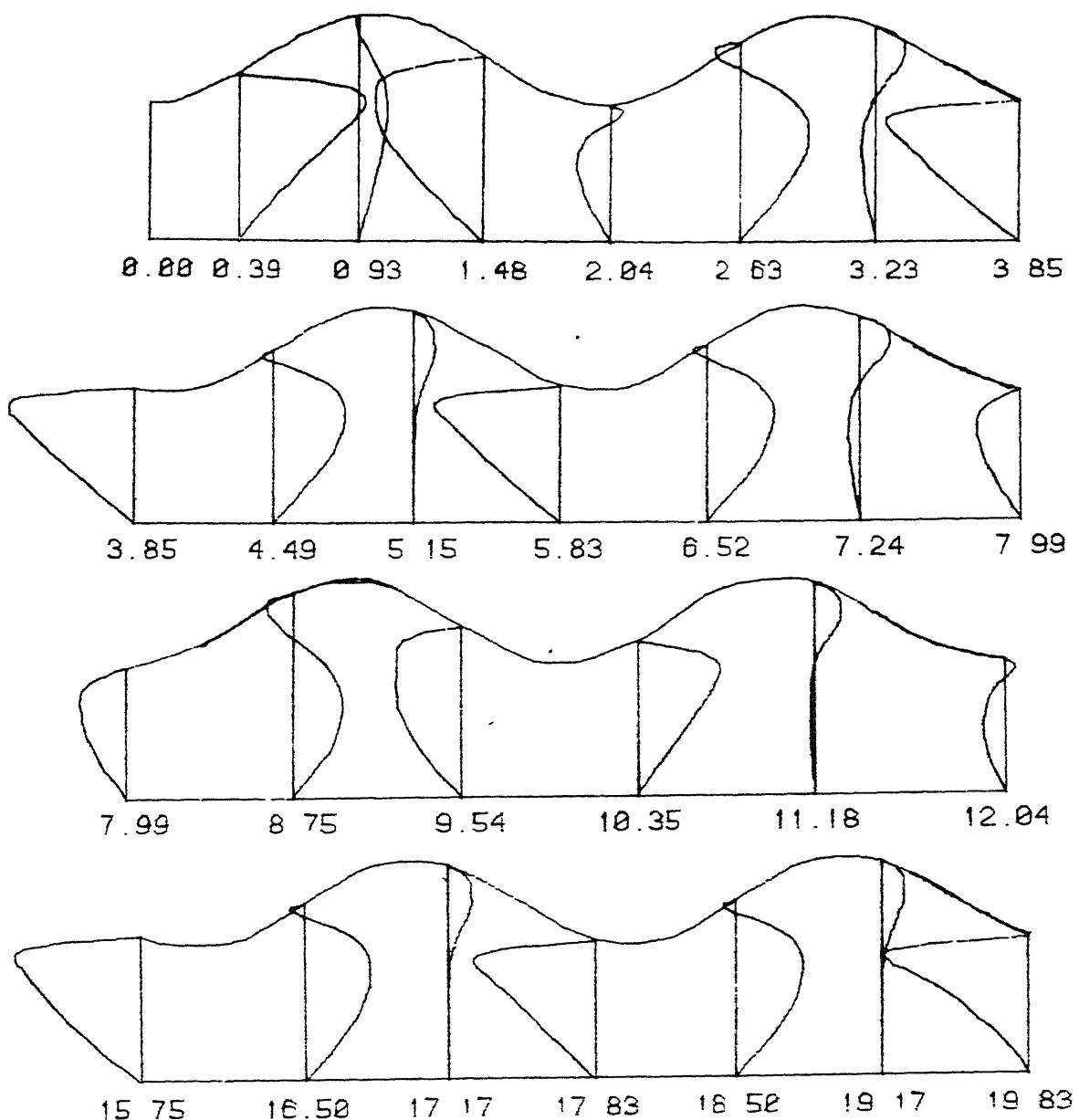


FIG. 43 V-VELOCITY PROFILES FOR A PIPE  
WITH  $\lambda=0.28$  AND  $Re=500$ .

$\lambda = 0$

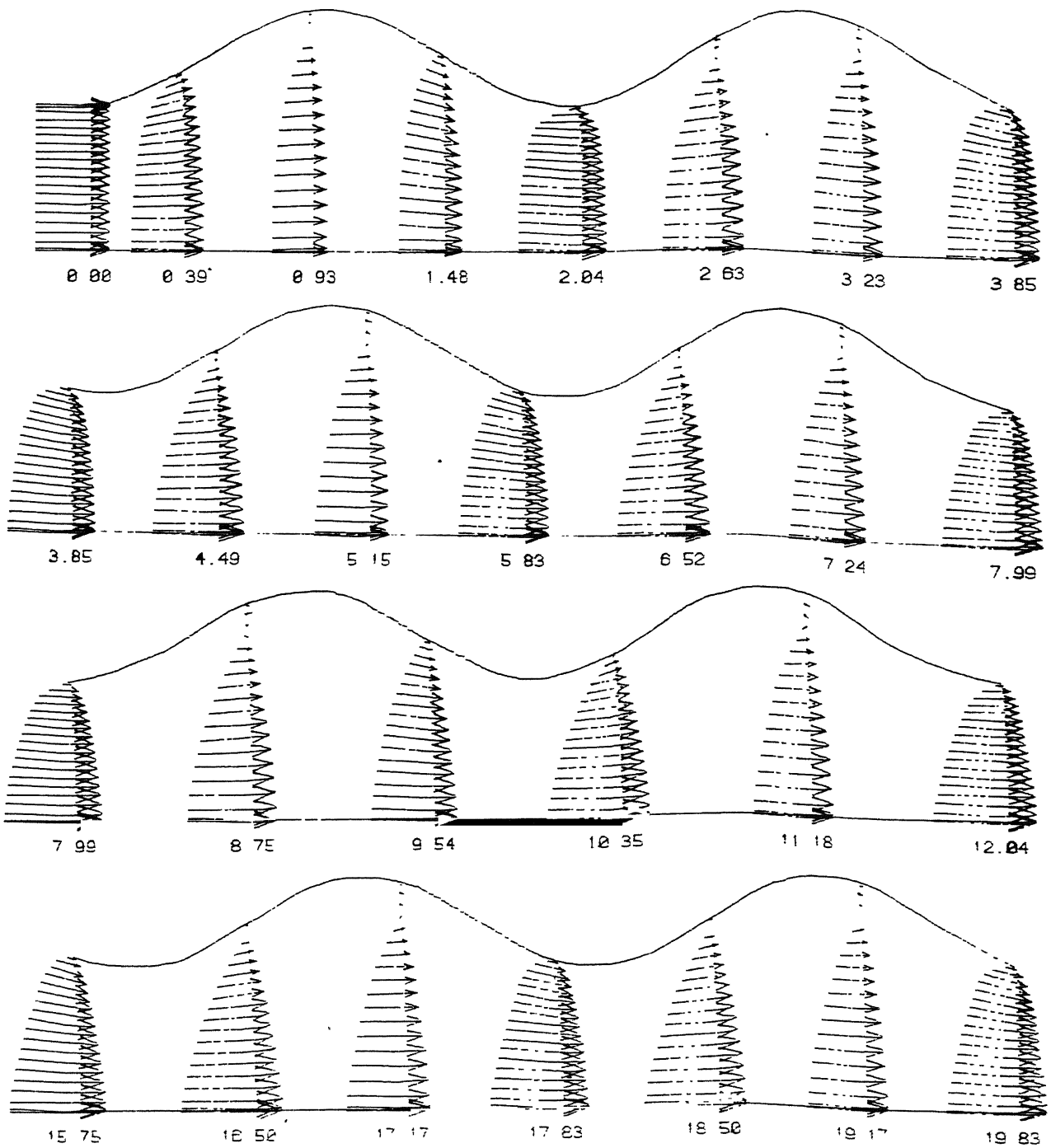


FIG.44 VELOCITY VECTORS IN A PIPE  
WITH  $\lambda = 0.28$  AND  $Re=502$

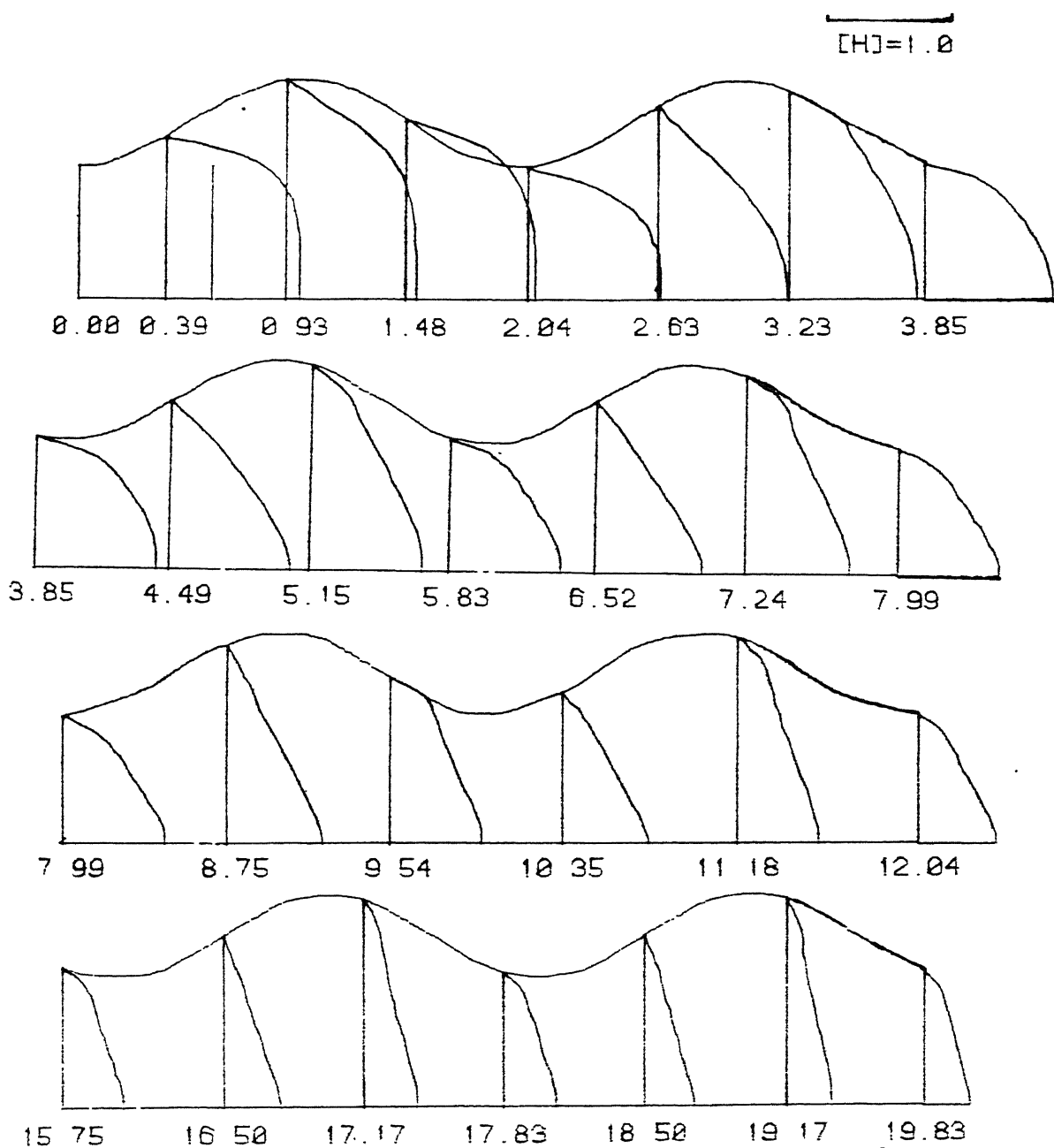


FIG.45 ENTHALPY PROFILES FOR A PIPE  
WITH LAMBDA=0.20 AND Re=500

$[U] = 1 \text{ m/s}$

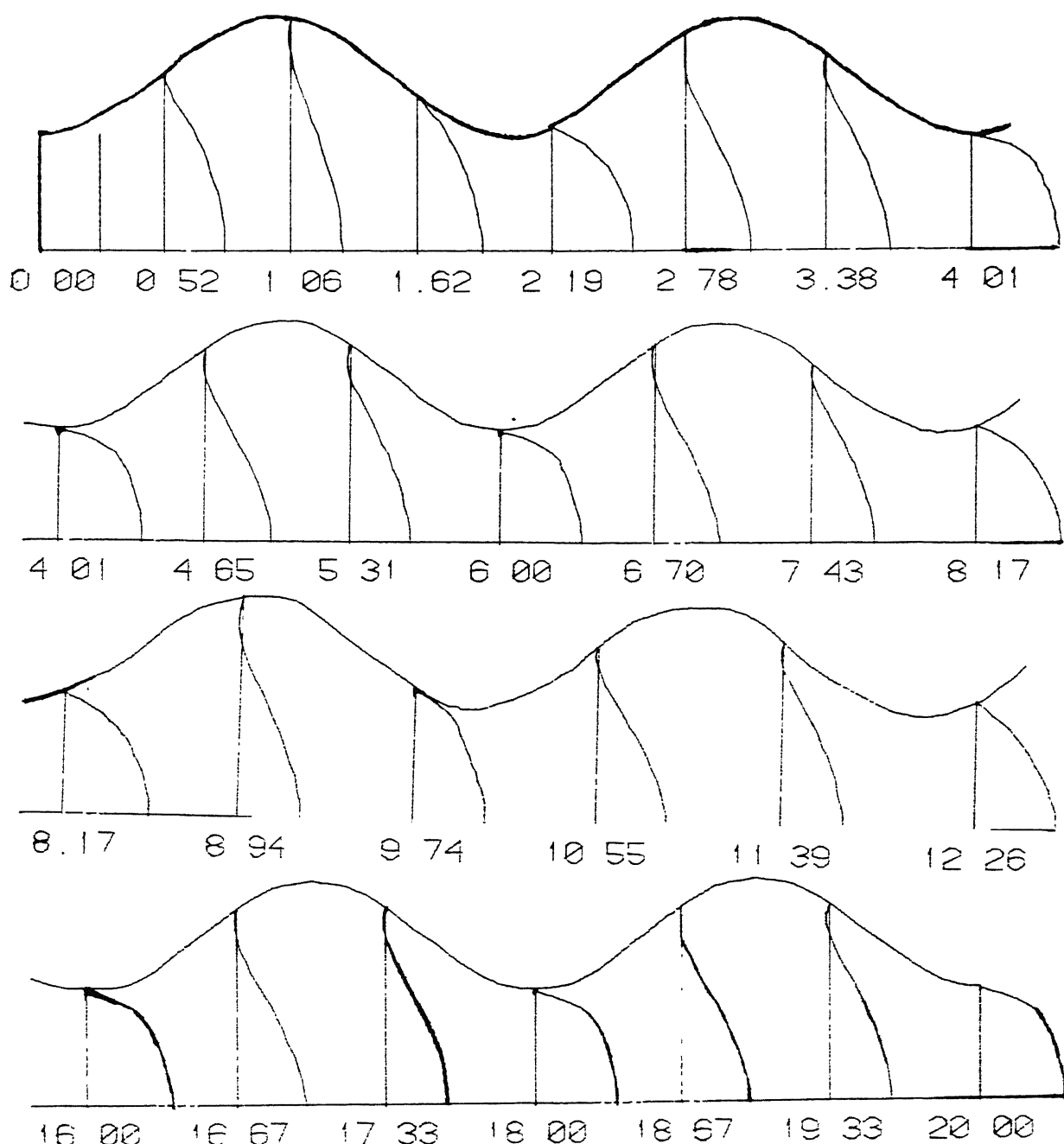


FIG.46 U-VELOCITY PROFILES FOR A PIPE  
WITH  $\lambda = 0.25$  AND  $Re = 100$

$\Delta V = 0.1$

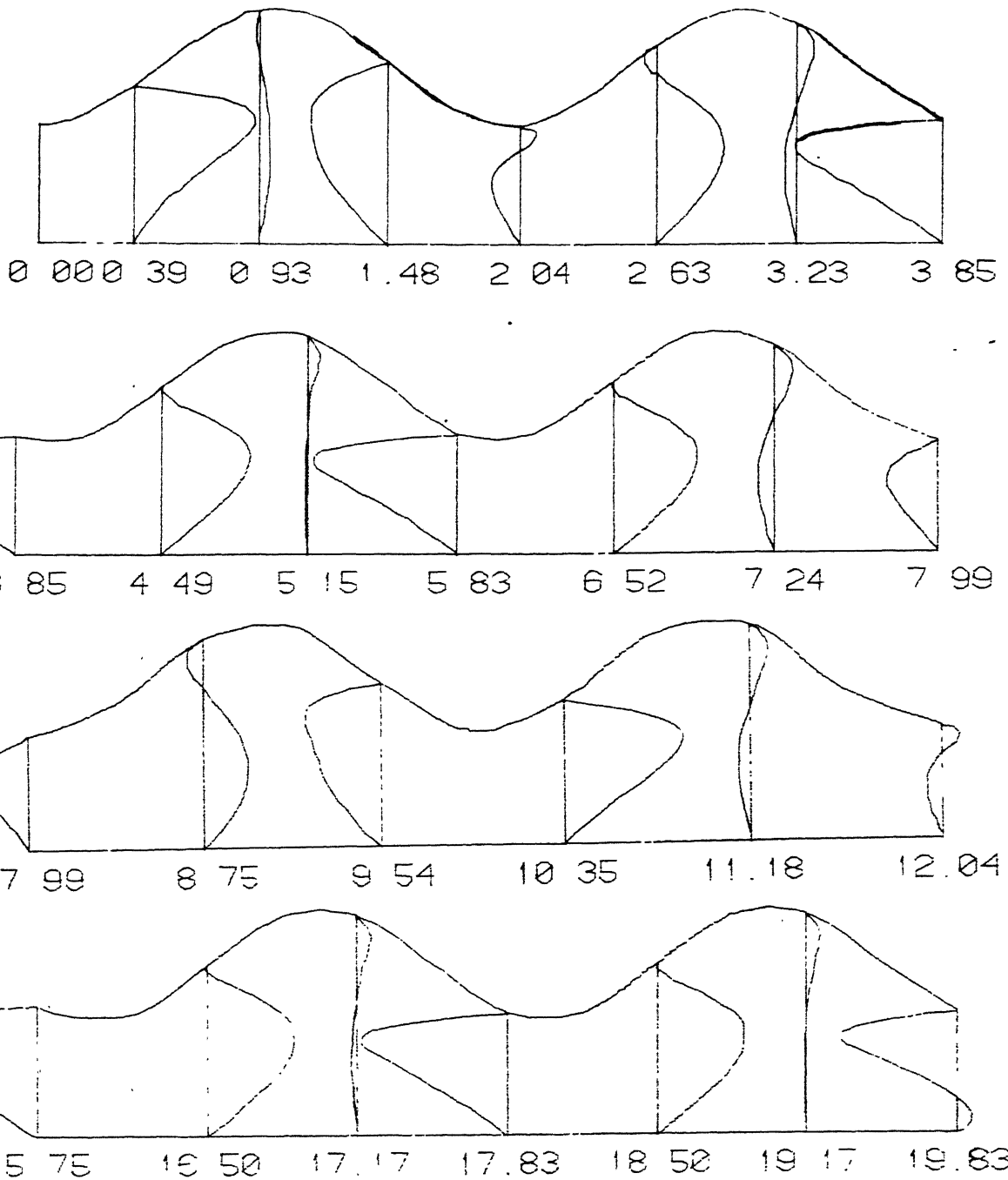


FIG.47 V-VELOCITY PROFILES FOR A PIPE  
WITH  $\lambda = 0.25$  AND  $Re = 100$

$\frac{U}{U_0} = 1.0$

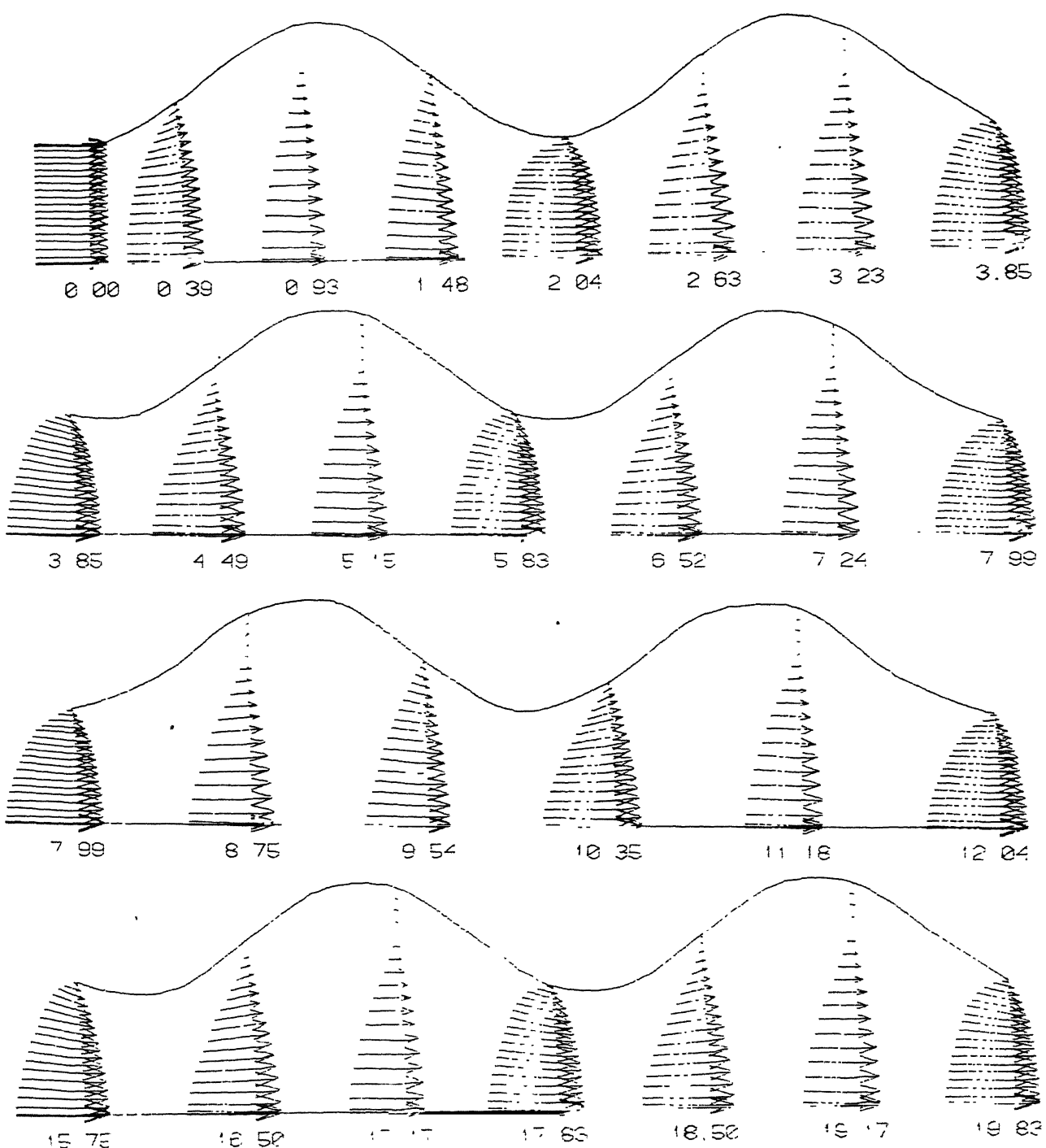


FIG.48 VELOCITY VECTORS IN A PIPE

WEYL NUMBER=2.25 AND  $Re=100$

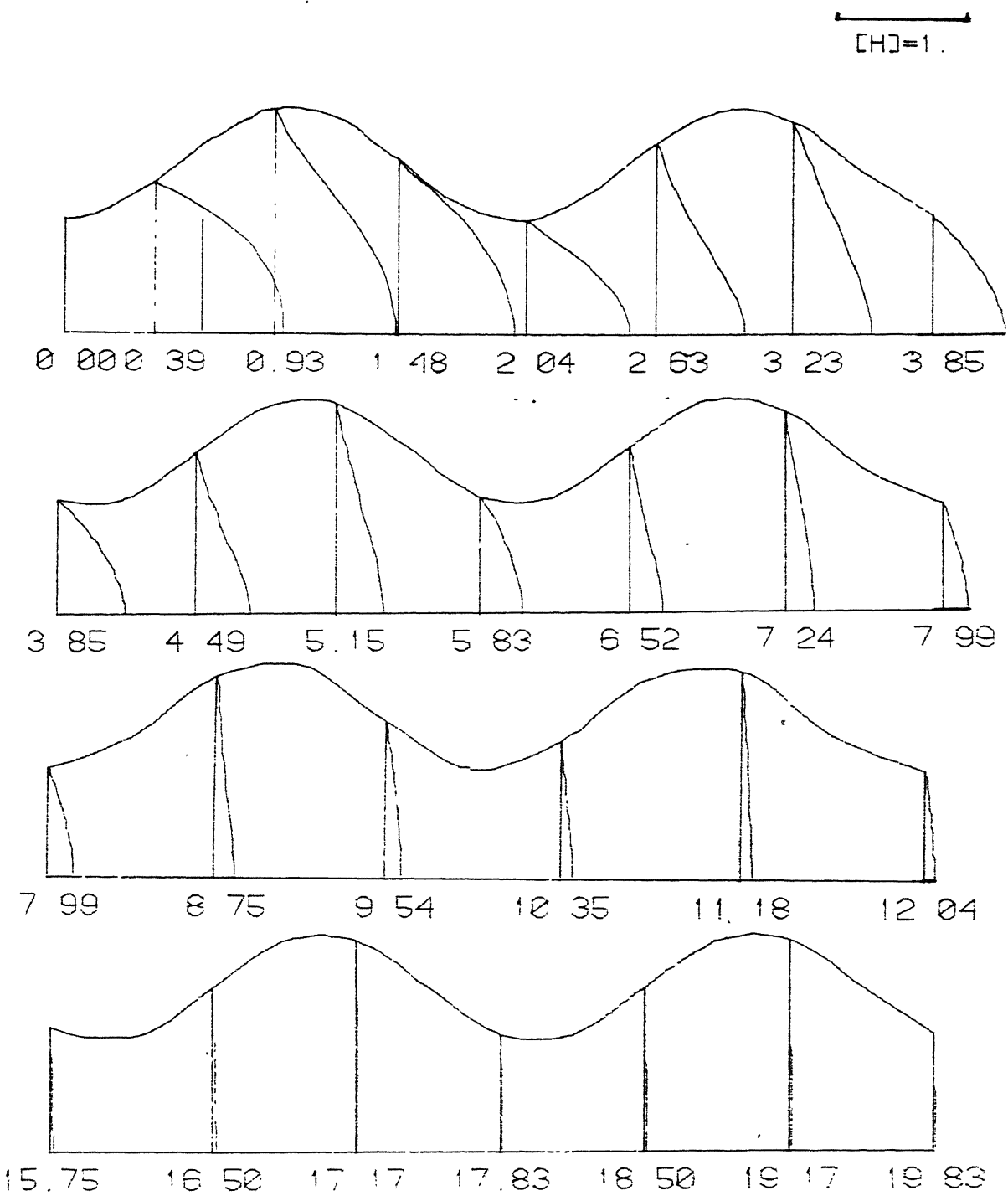


FIG. 49 ENTHALPY PROFILES FOR A PIPE  
WITH  $\lambda = 0.25$  AND  $Re = 100$

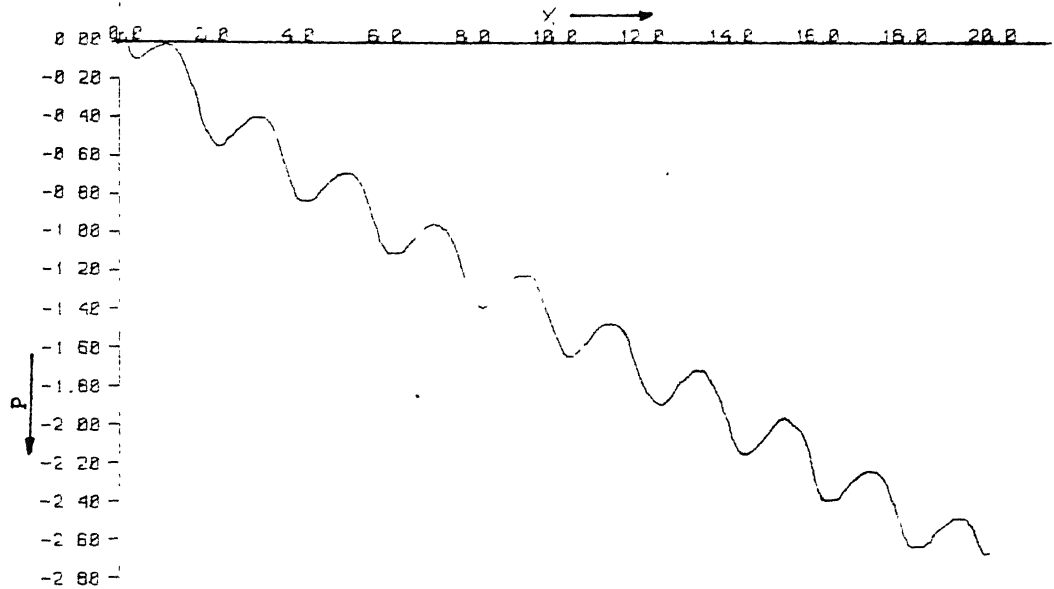


FIG.50a PRESSURE DISTRIBUTION ALONG X FOR A PIPE  
WITH LAMBDA=0.10 AND  $Re=100$

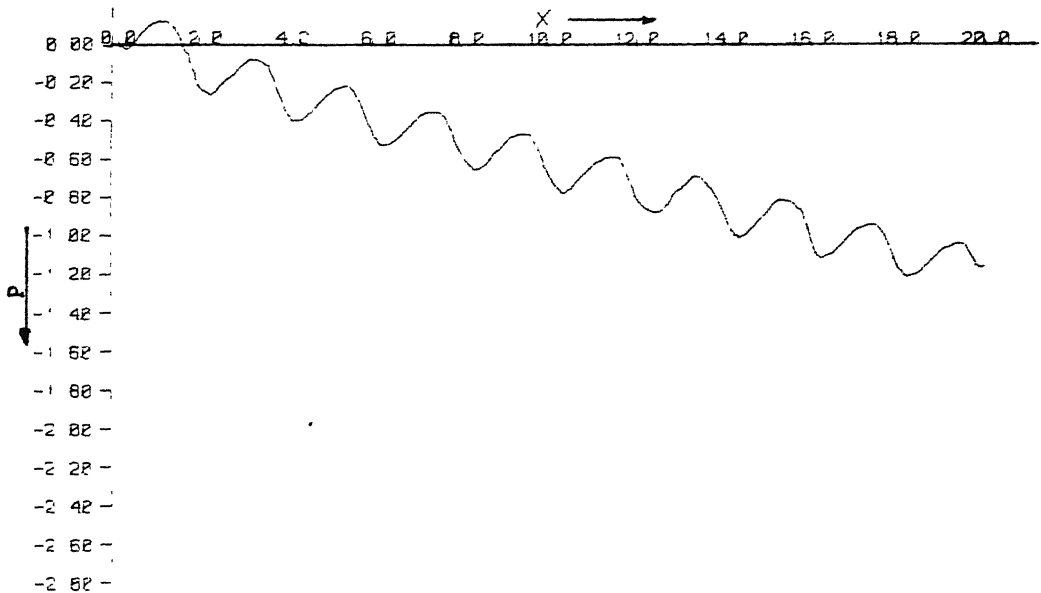


FIG.50b PRESSURE DISTRIBUTION ALONG X FOR A PIPE  
WITH LAMBDA=0.10 AND  $Re=500$

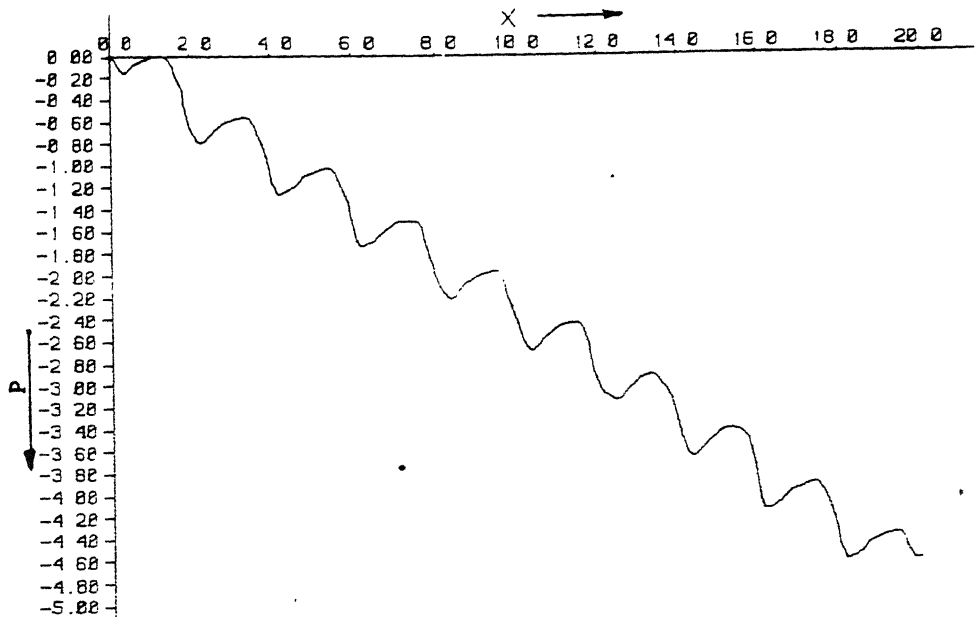


FIG.51a PRESSURE DISTRIBUTION ALONG X FOR A PIPE  
WITH LAMBDA=0.20 AND  $Re=100$

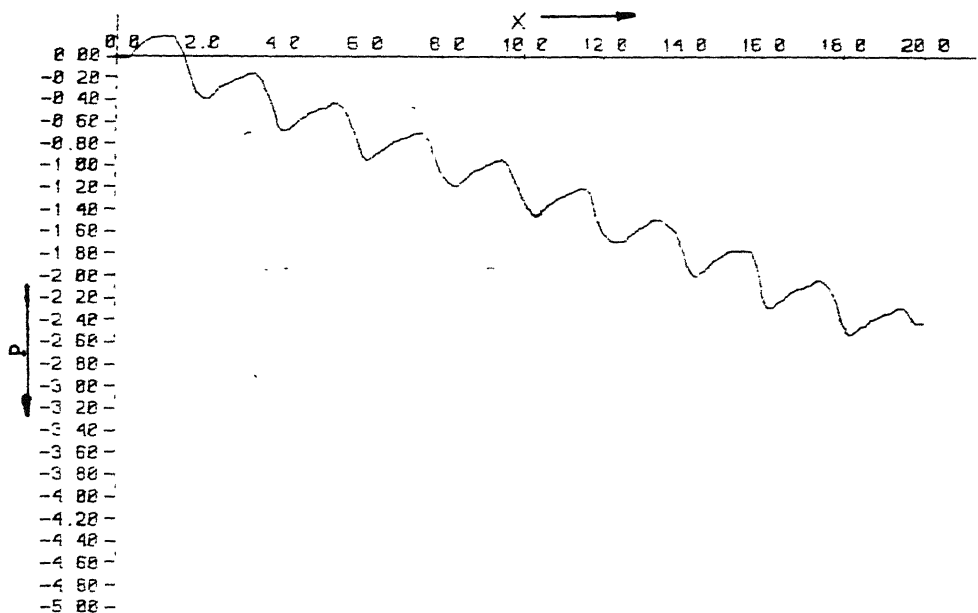


FIG.51b PRESSURE DISTRIBUTION ALONG X FOR A PIPE  
WITH LAMBDA=0.20 AND  $Re=500$

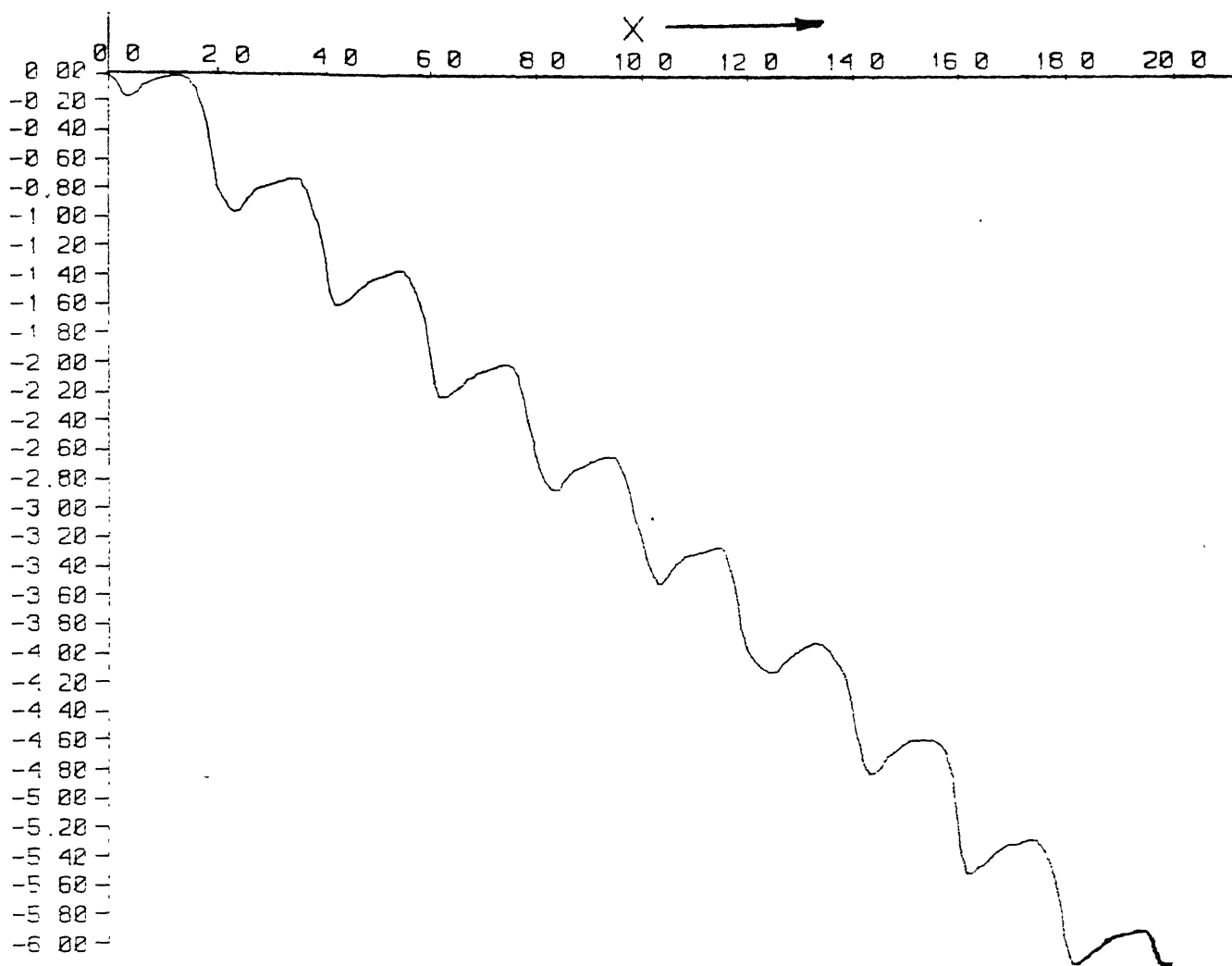
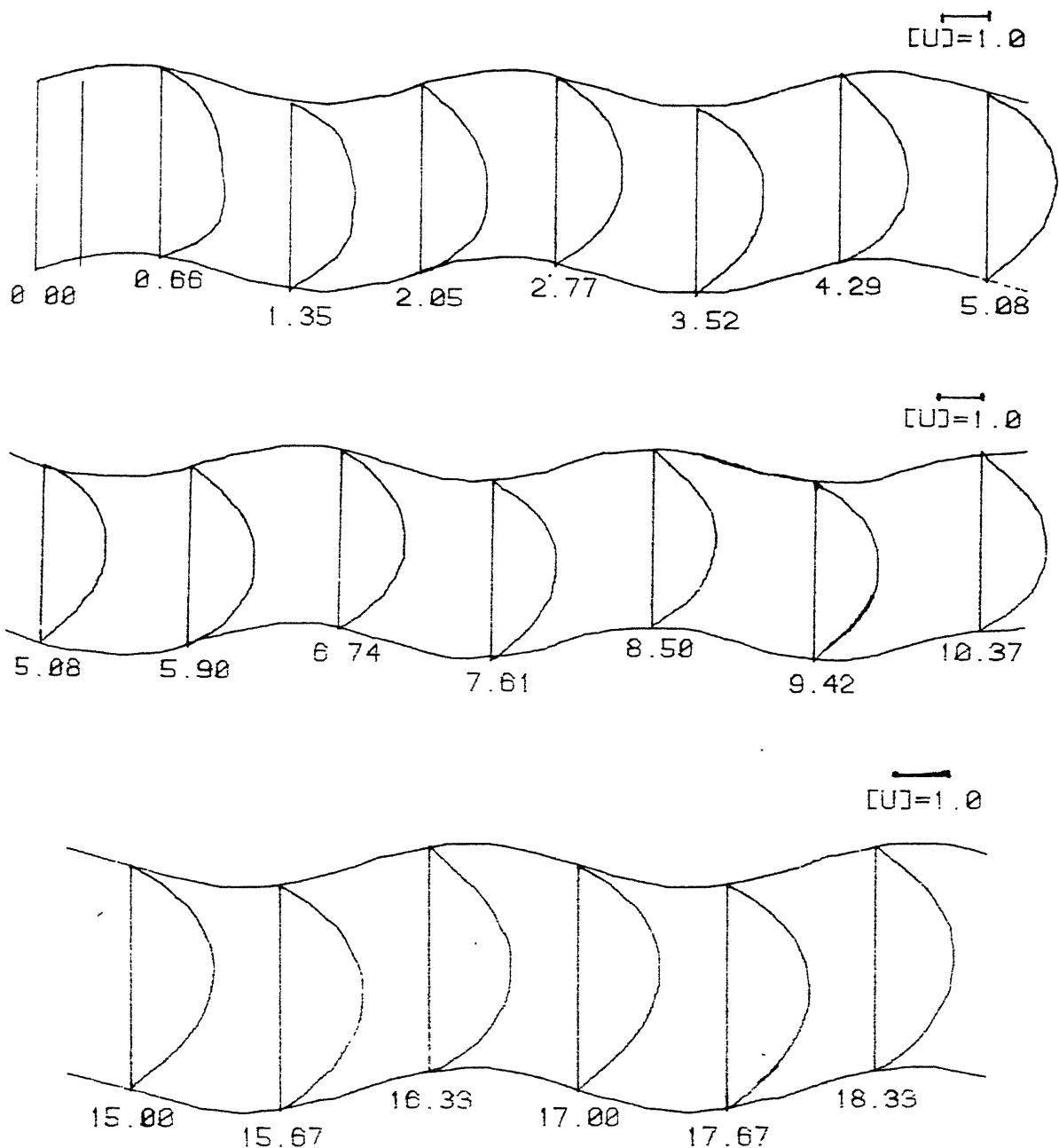


FIG.52 PRESSURE DISTRIBUTION ALONG X FOR A PIPE  
WITH LAMBDA=0.25 AND  $Re=100$



**FIG.53** U-VELOCITY PROFILES FOR A NON-SYM. CHANNEL  
WITH LAMBDA=0.10 AND Re=100.

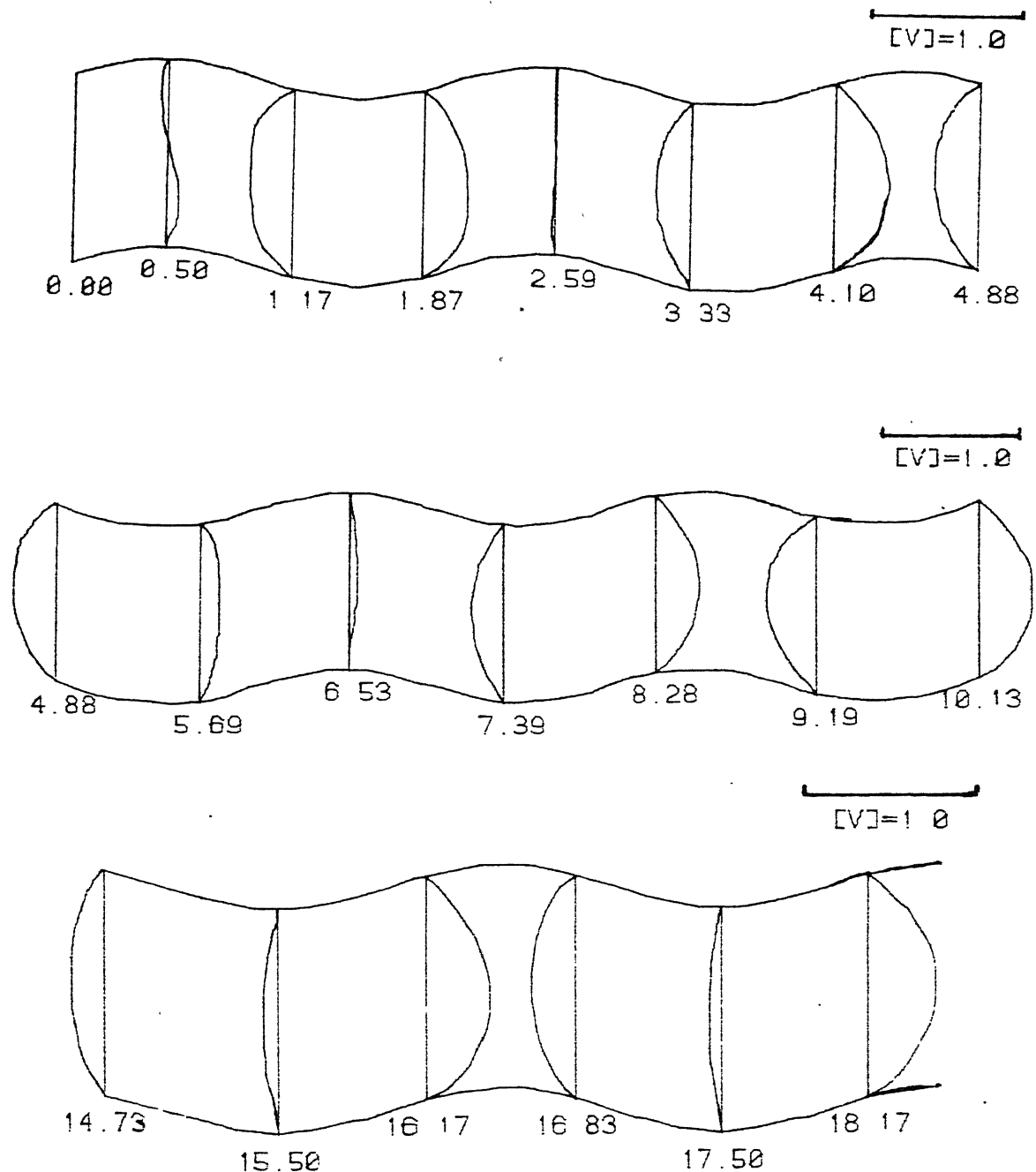


FIG. 54 V-VELOCITY PROFILES FOR A NON-SYM CHANNEL  
WITH LAMBDA=0.10 AND Re=100

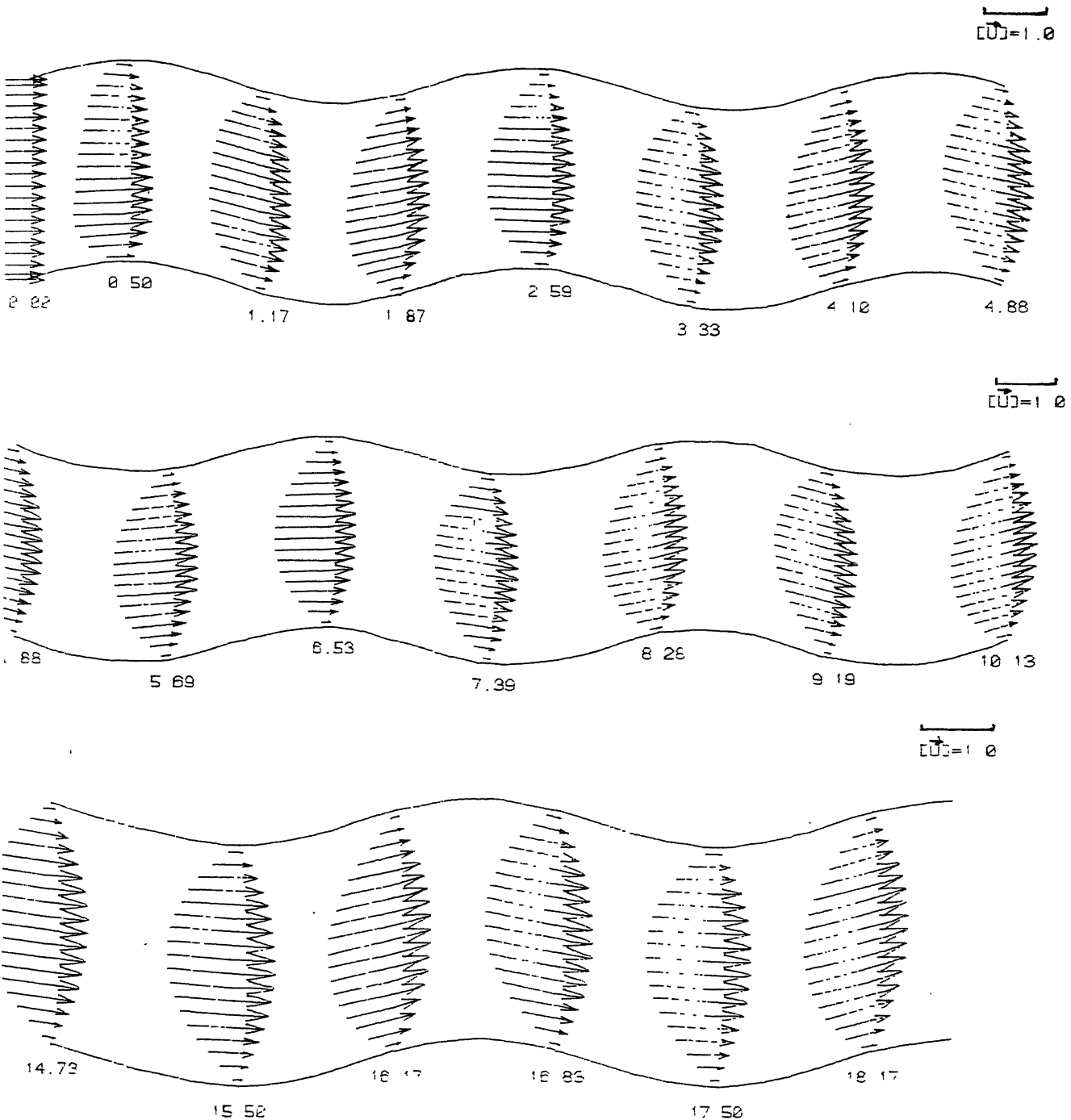


FIG.55 VELOCITY VECTORS IN A NON-SYM CHANNEL  
WITH LAMBDA=0.10 AND Re=100

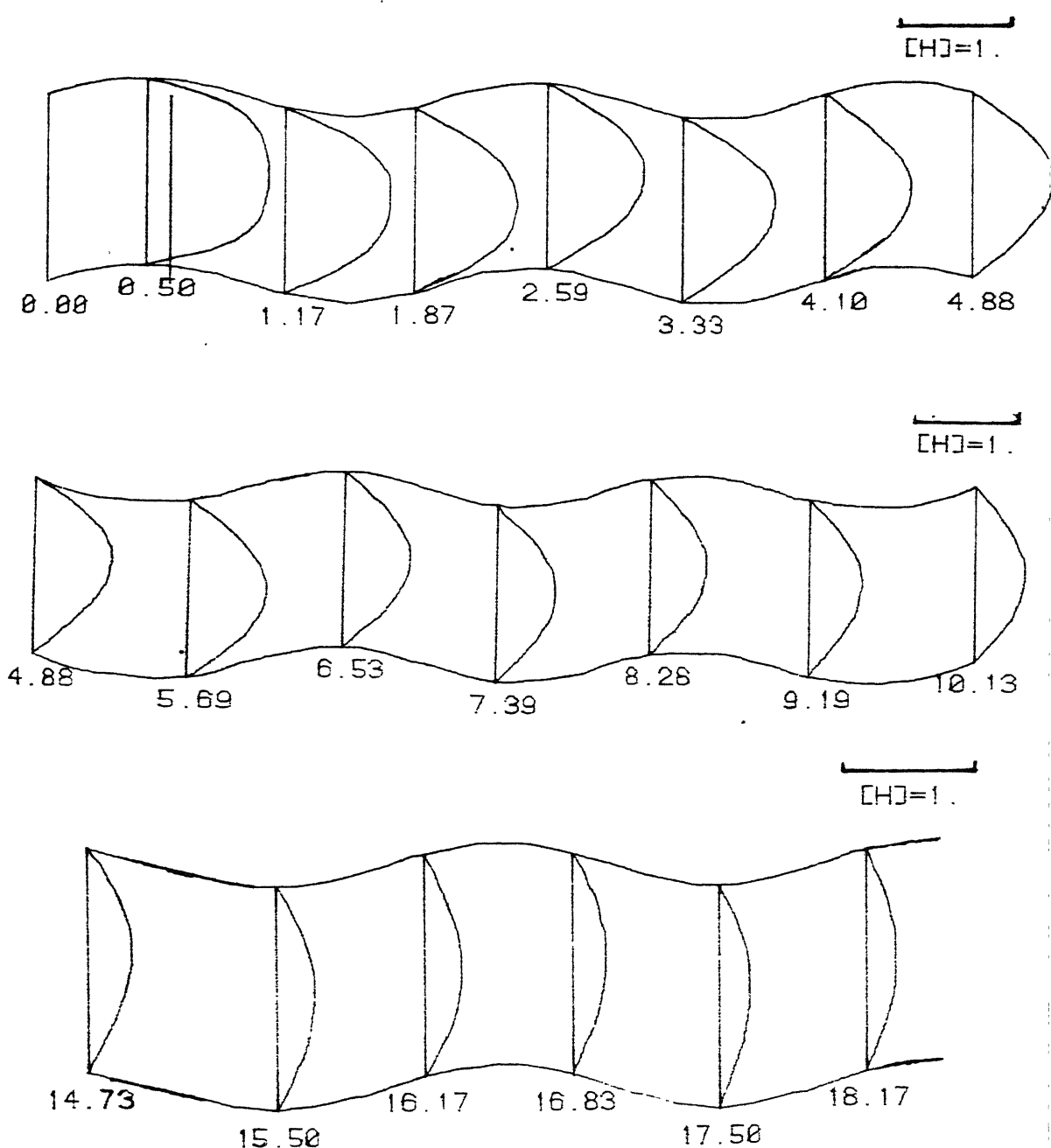
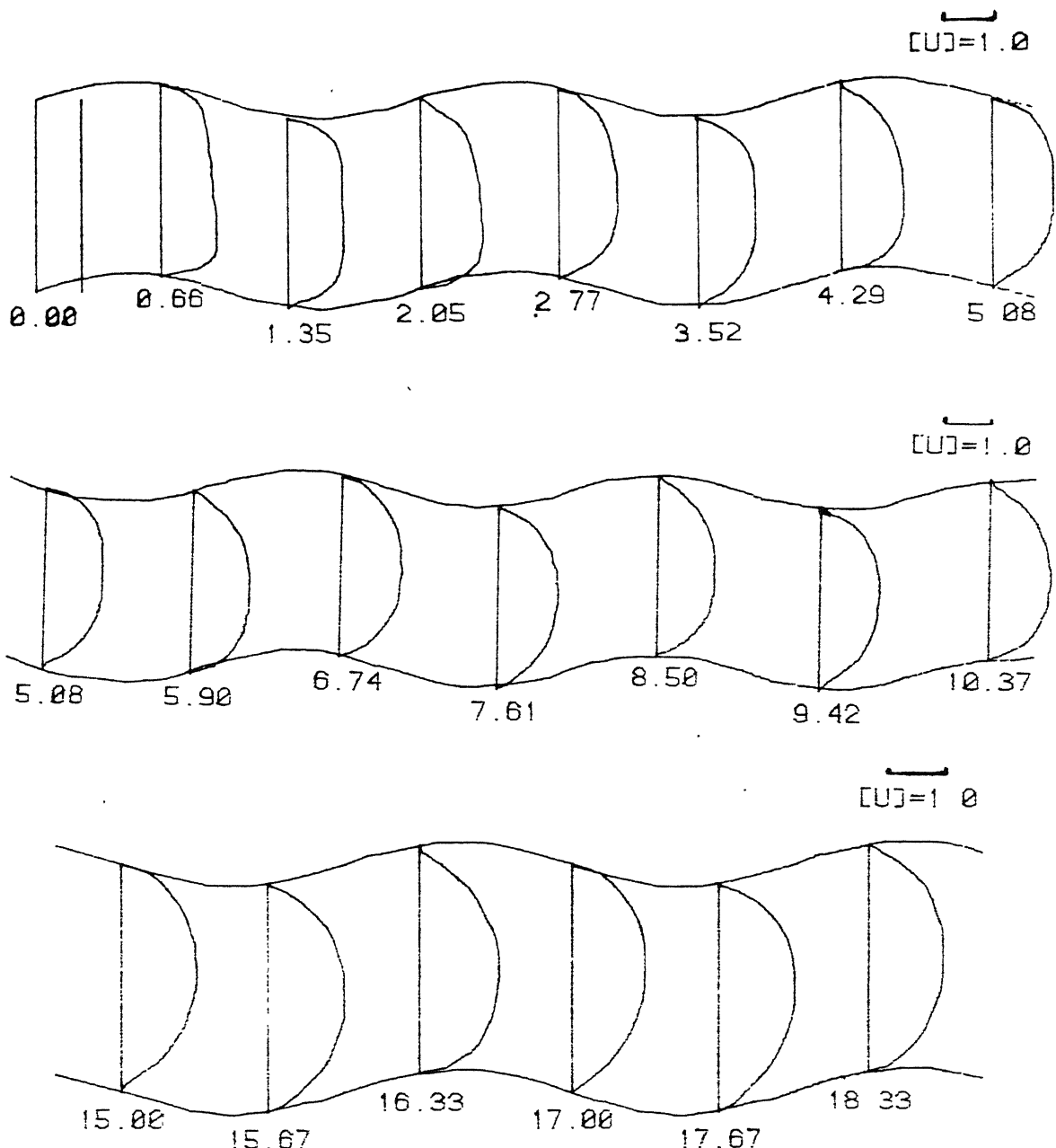


FIG. 56 ENTHALPY PROFILES FOR A NON-SYM. CHANNEL  
WITH  $\lambda=0.10$  AND  $Re=100$ .



**FIG. 57** U-VELOCITY PROFILES FOR A NON-SYM. CHANNEL WITH  $\lambda=0.10$  AND  $R_e=500$ .

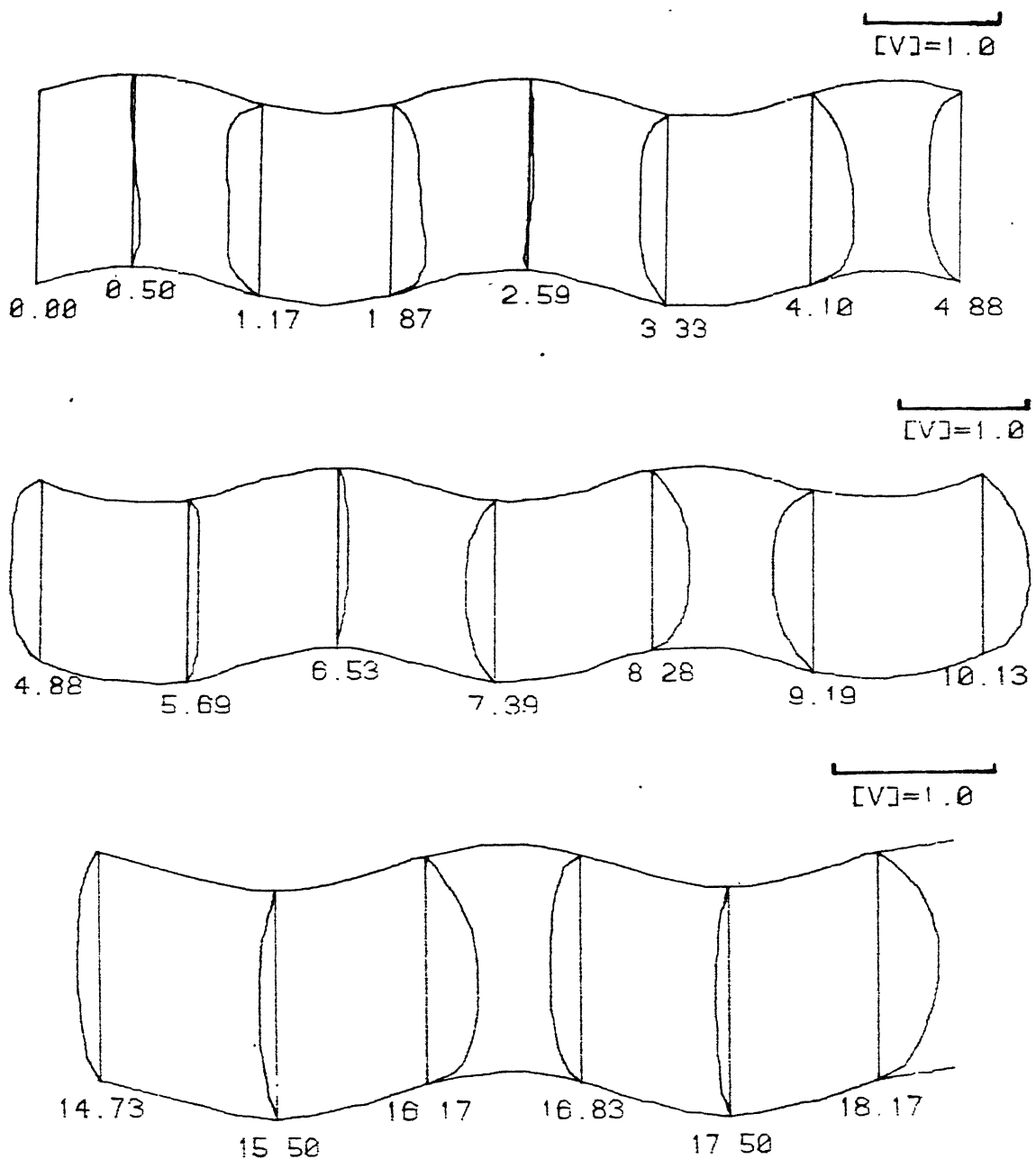


FIG. 58 V-VELOCITY PROFILES FOR A NON-SYM. CHANNEL  
WITH LAMBDA=0.10 AND Re=500

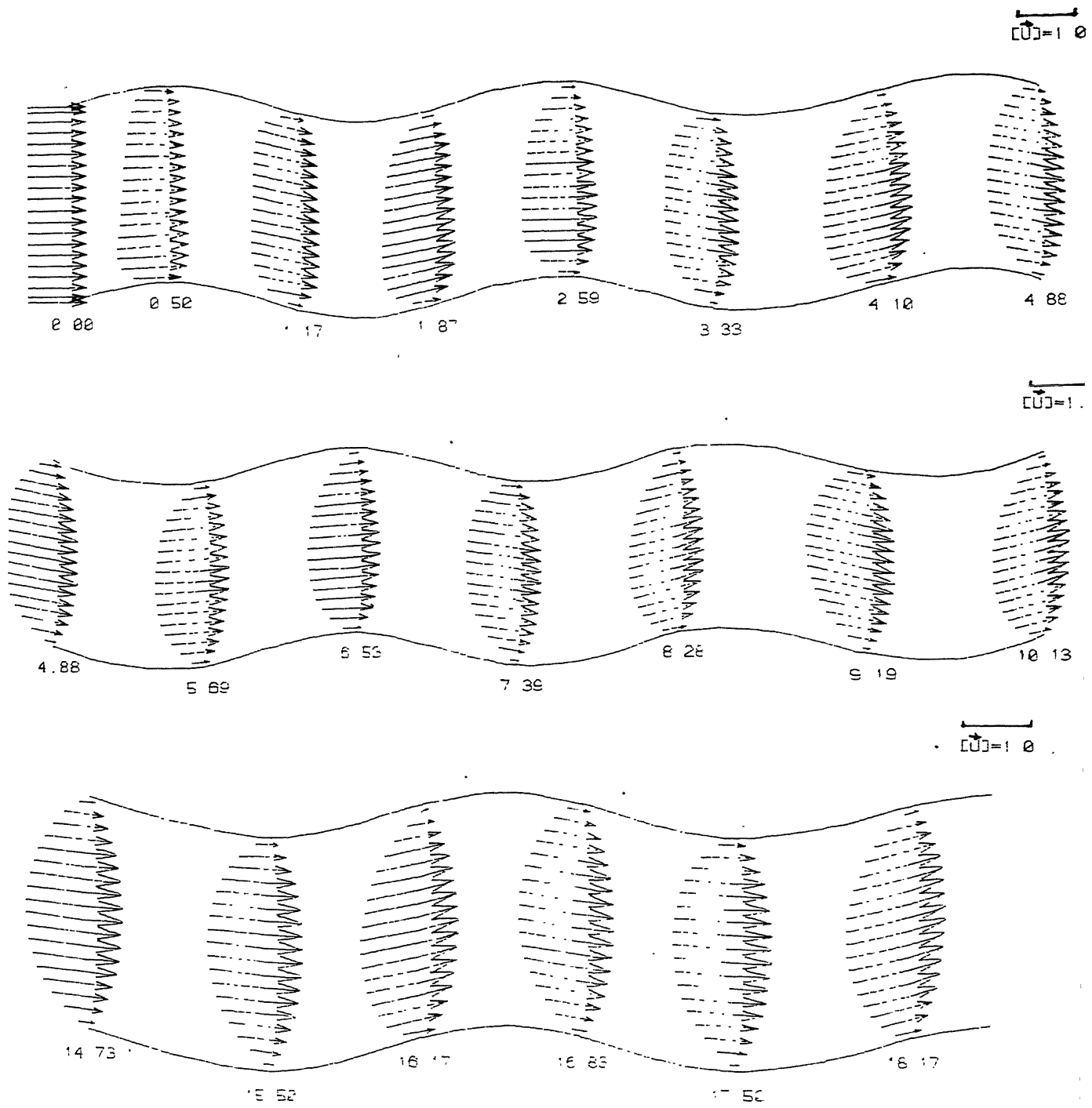
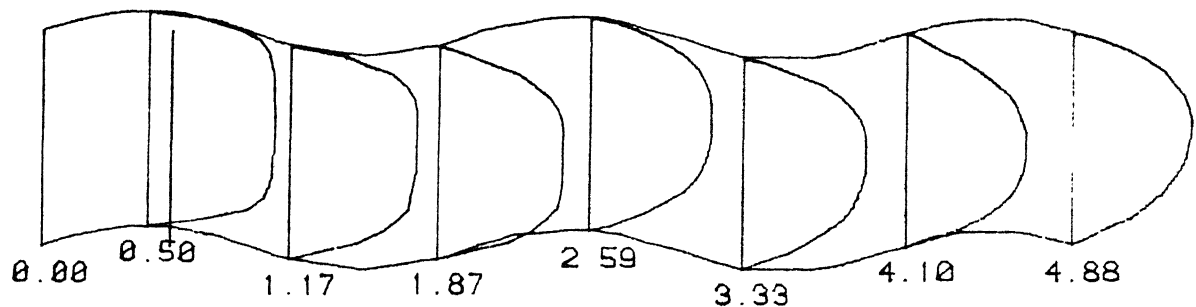
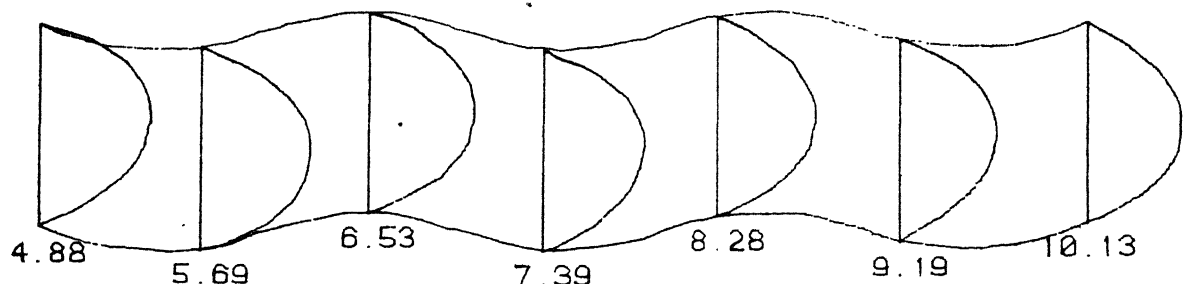


FIG.59 VELOCITY VECTORS IN A NON-SYM CHANNEL  
WITH  $\Lambda=0.10$  AND  $Re=500$

135  
[H]=1.



[H]=1



[H]=1.

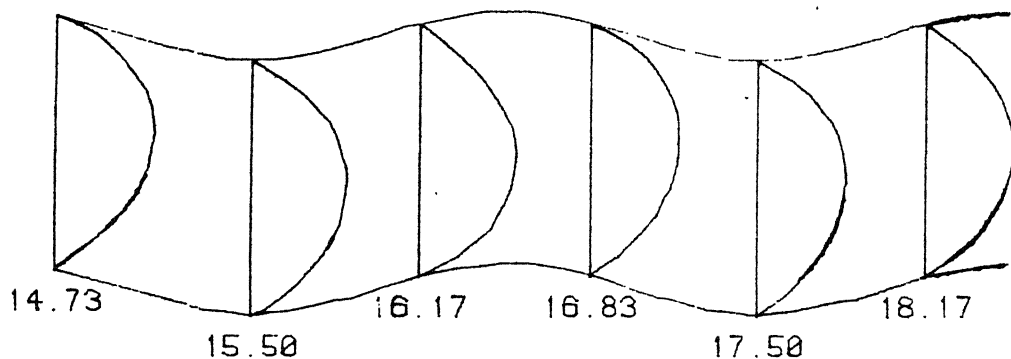


FIG. 60 ENTHALPY PROFILES FOR A NON-SYM CHANNEL WITH LAMBDA=0.10 AND  $Re=500$ .

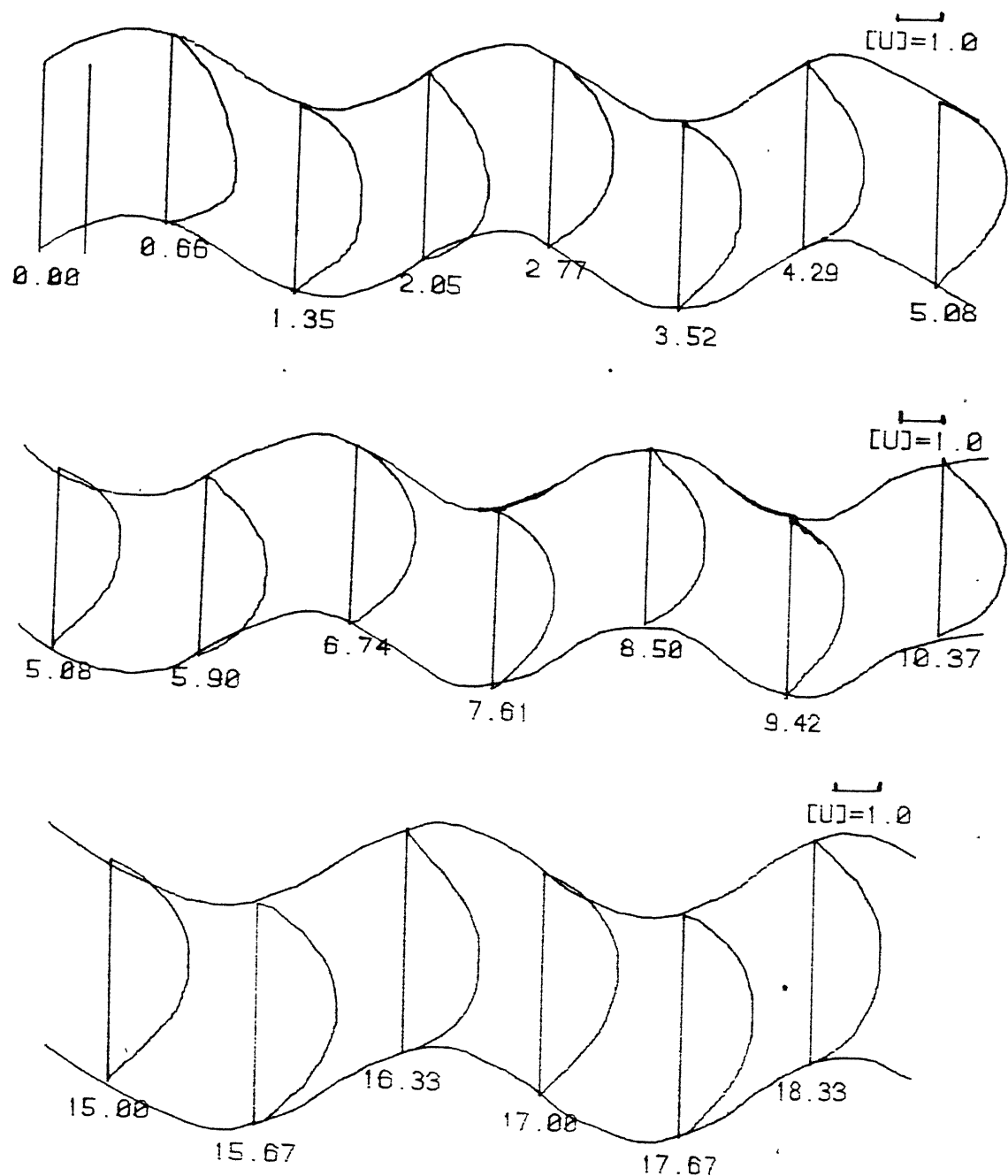


FIG. 61 U-VELOCITY PROFILES FOR A NON-SYM. CHANNEL  
WITH LAMBDA=0.20 AND  $R_e=100$

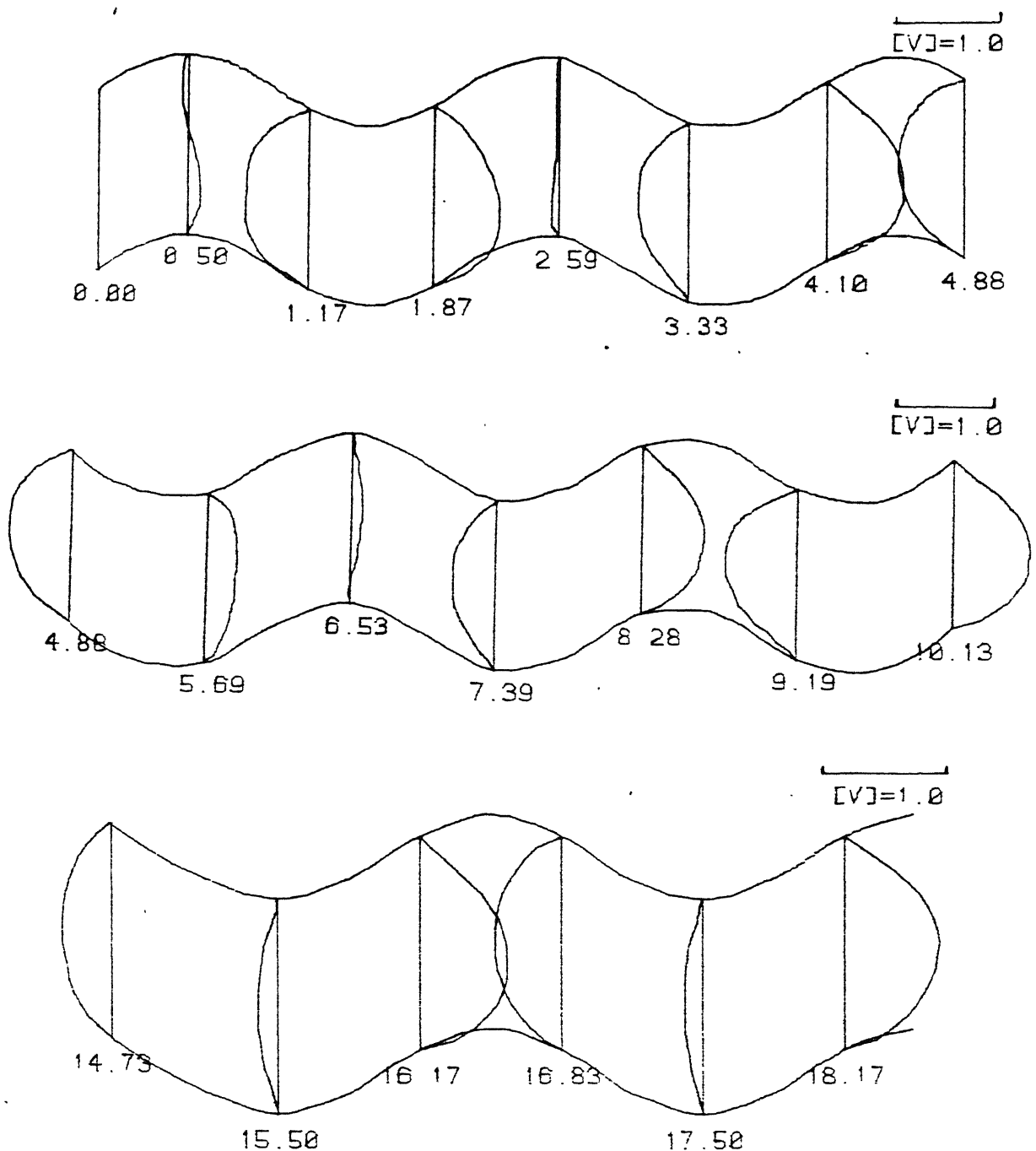


FIG. 62 V-VELOCITY PROFILES FOR A NON-SYM. CHANNEL  
WITH LAMBDA=0.20 AND Re=100.

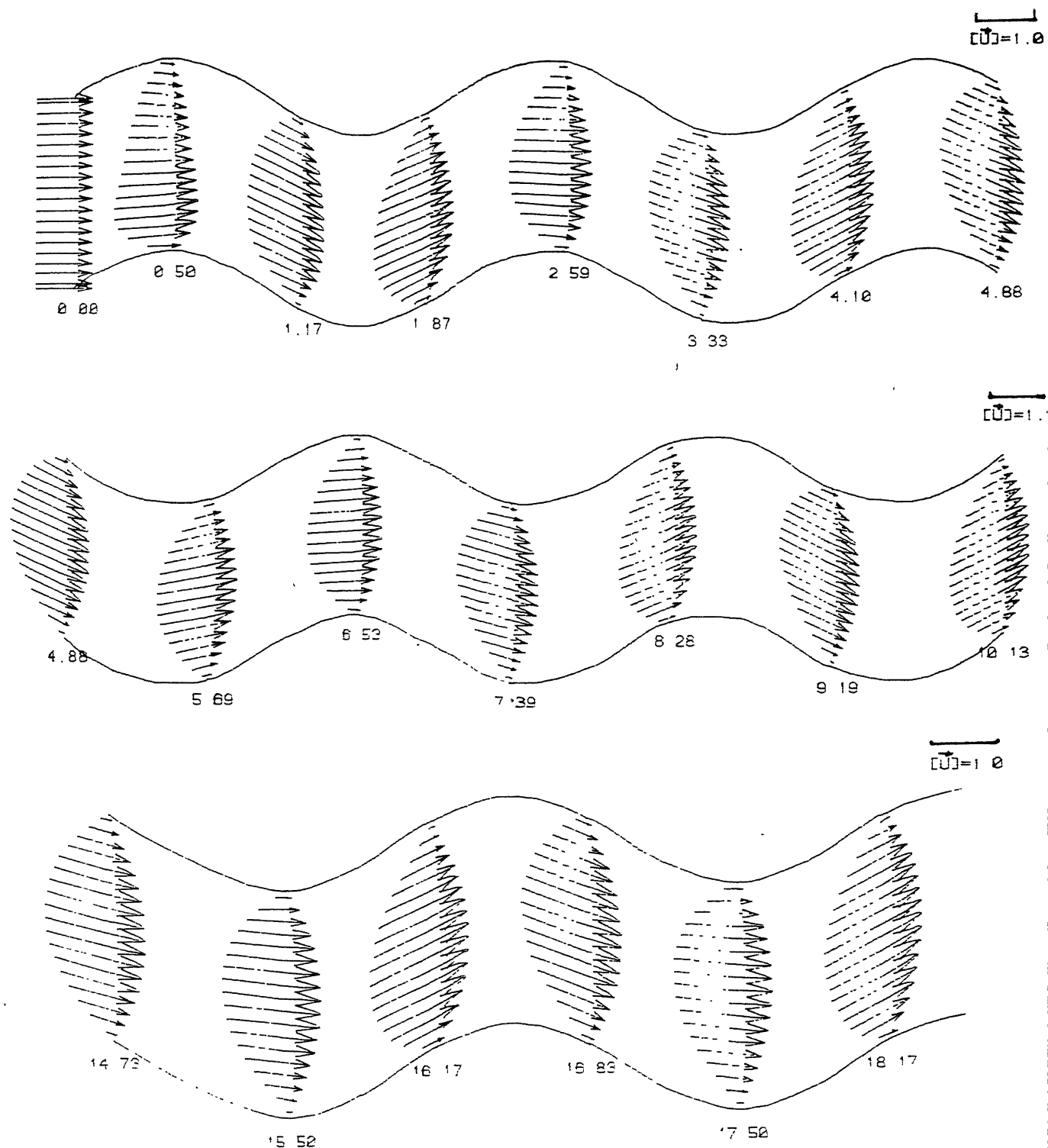


FIG. 63 VELOCITY VECTORS IN A NON-SYM CHANNEL  
WITH LAMBDA=0.20 AND Re=100

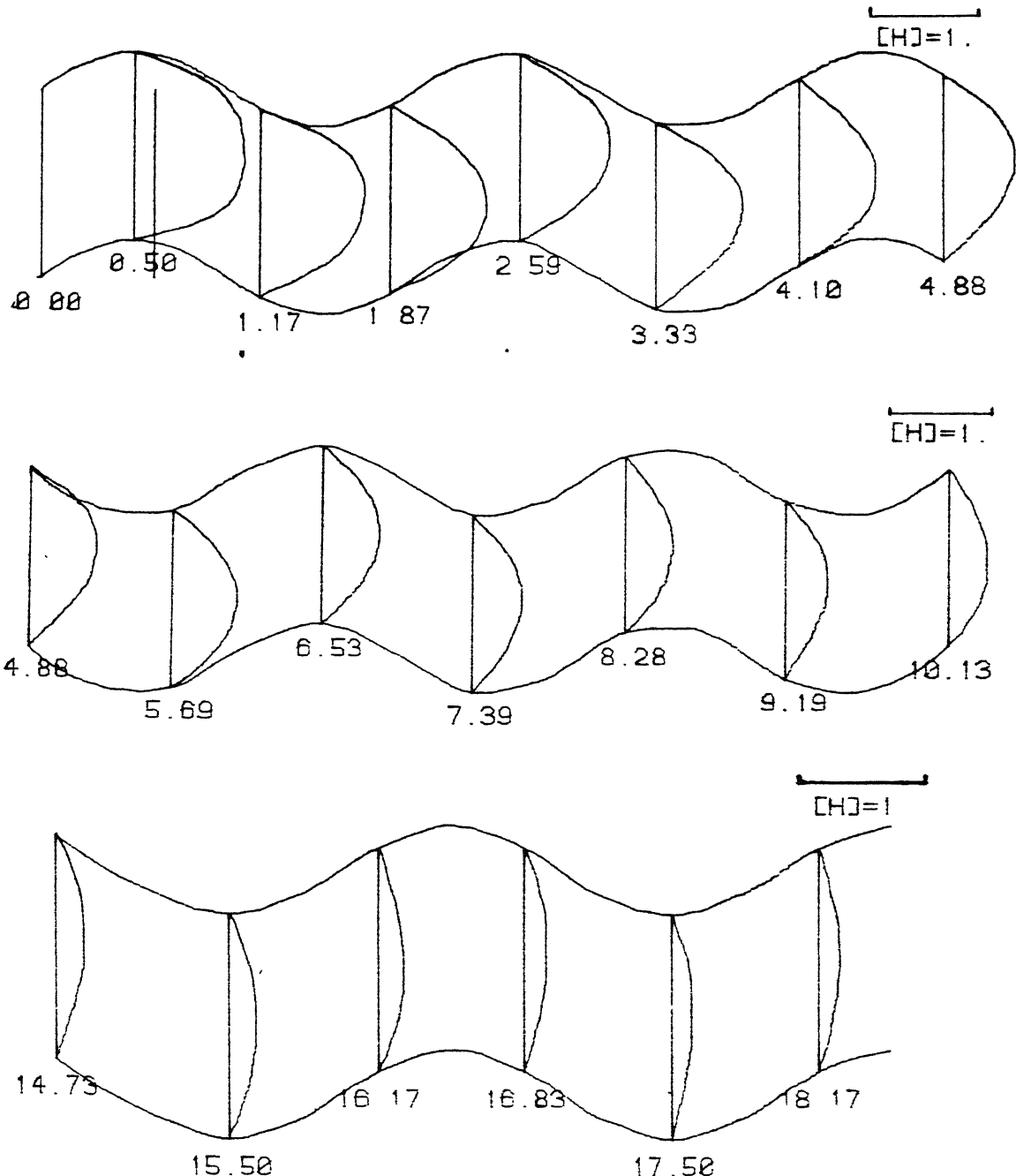


FIG.64 ENTHALPY PROFILES FOR A NON-SYM. CHANNEL  
WITH  $\lambda=0$   $20$  AND  $Re=100$ .

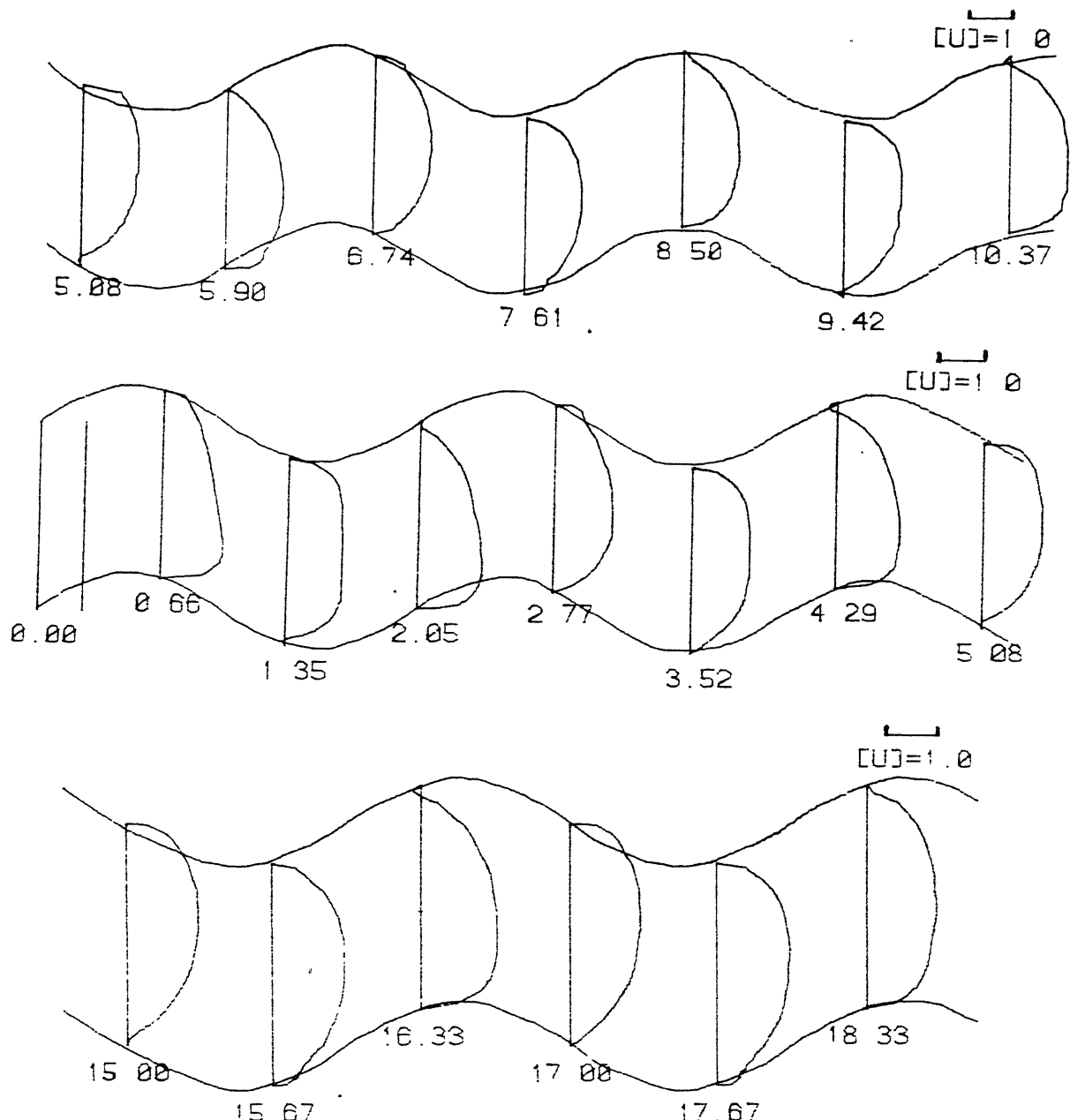


FIG. 65 U-VELOCITY PROFILES FOR A NON-SYM. CHANNEL  
WITH LAMBDA=0.20 AND Re=500.

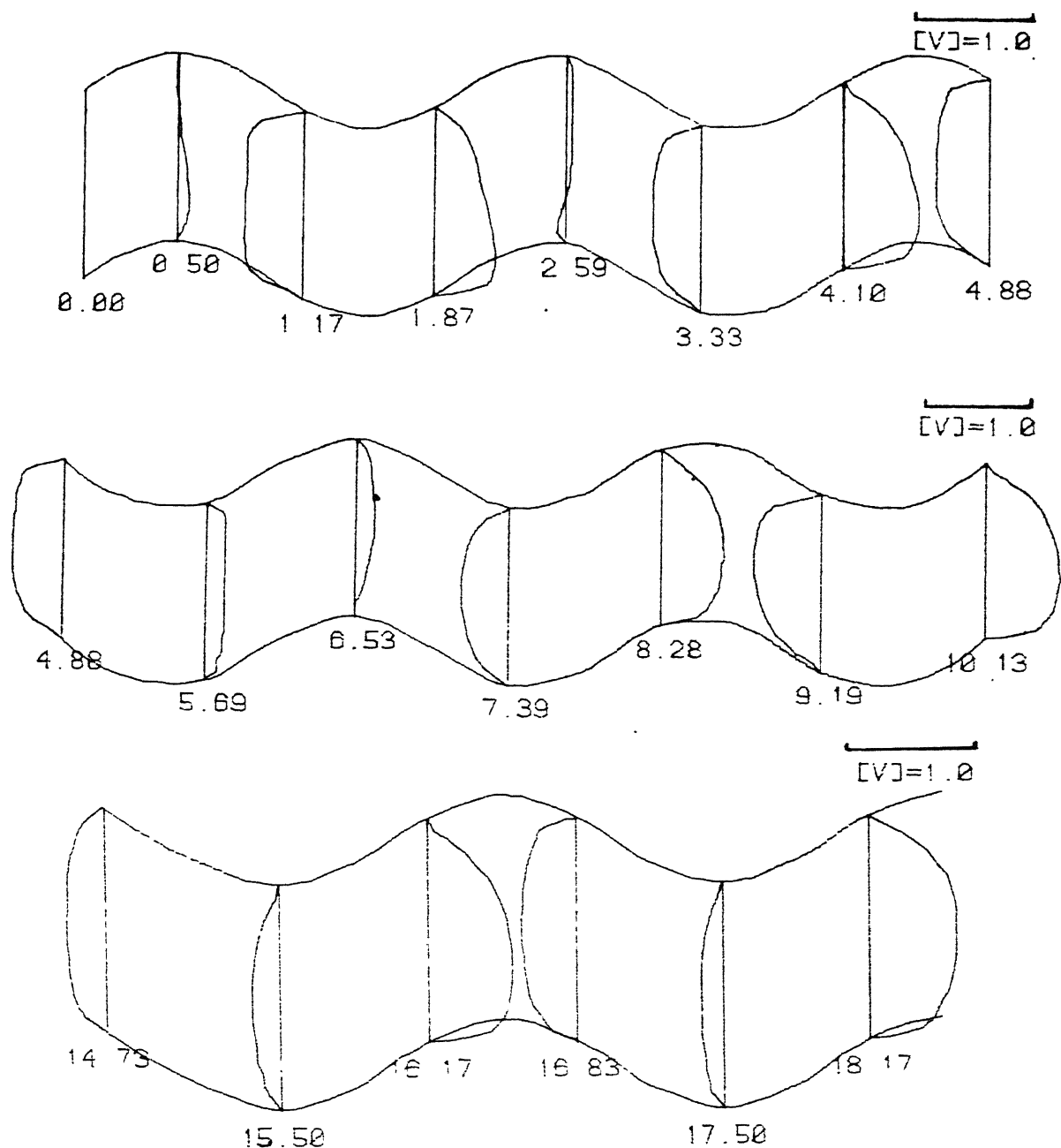


FIG. 66 V-VELOCITY PROFILES FOR A NON-SYM. CHANNEL  
WITH LAMBDA=0.20 AND  $Re=500$

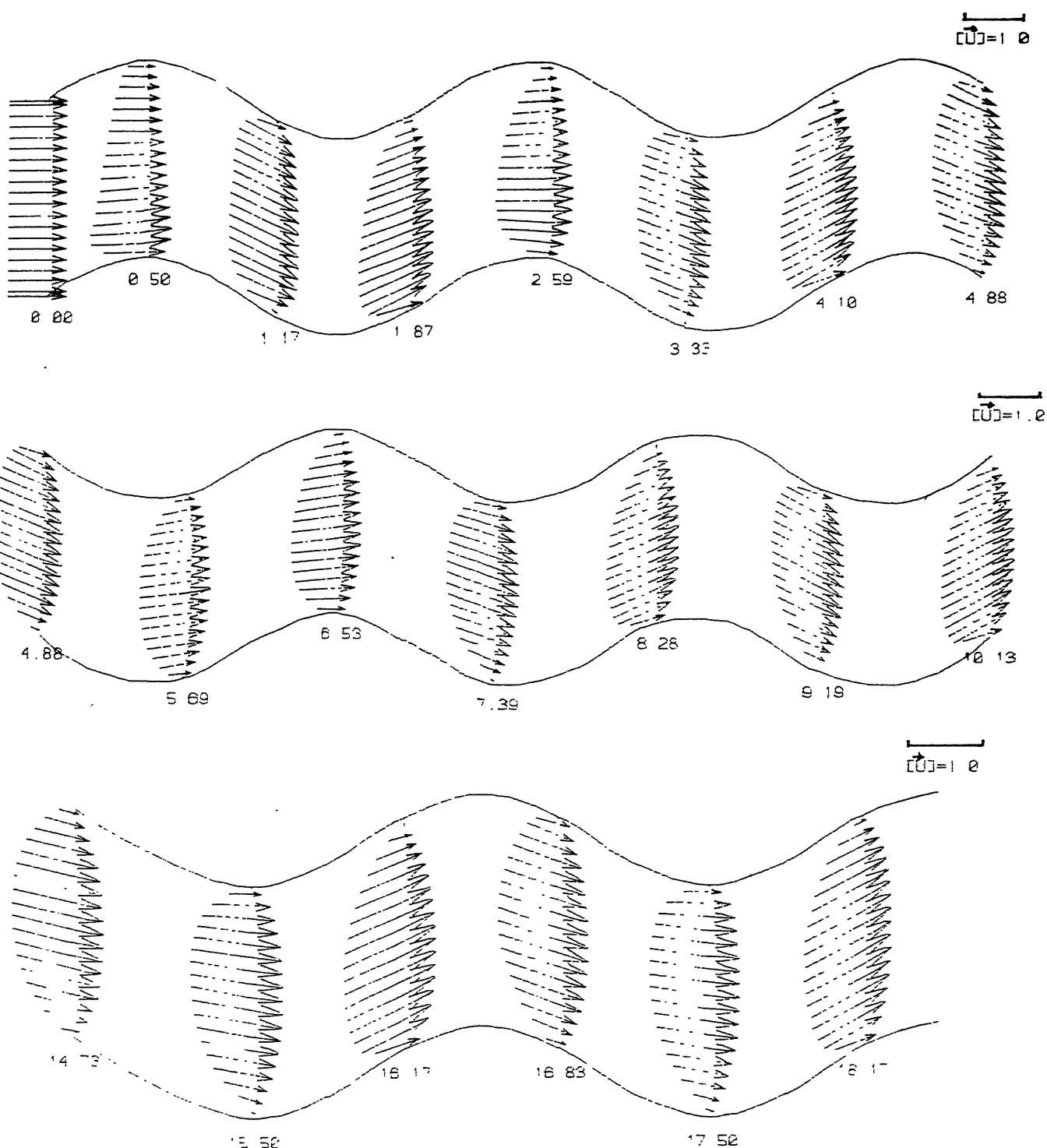


FIG. 67 VELOCITY VECTORS IN A NON-SYM CHANNEL  
WITH LAMBDA=2.20 AND Re=500

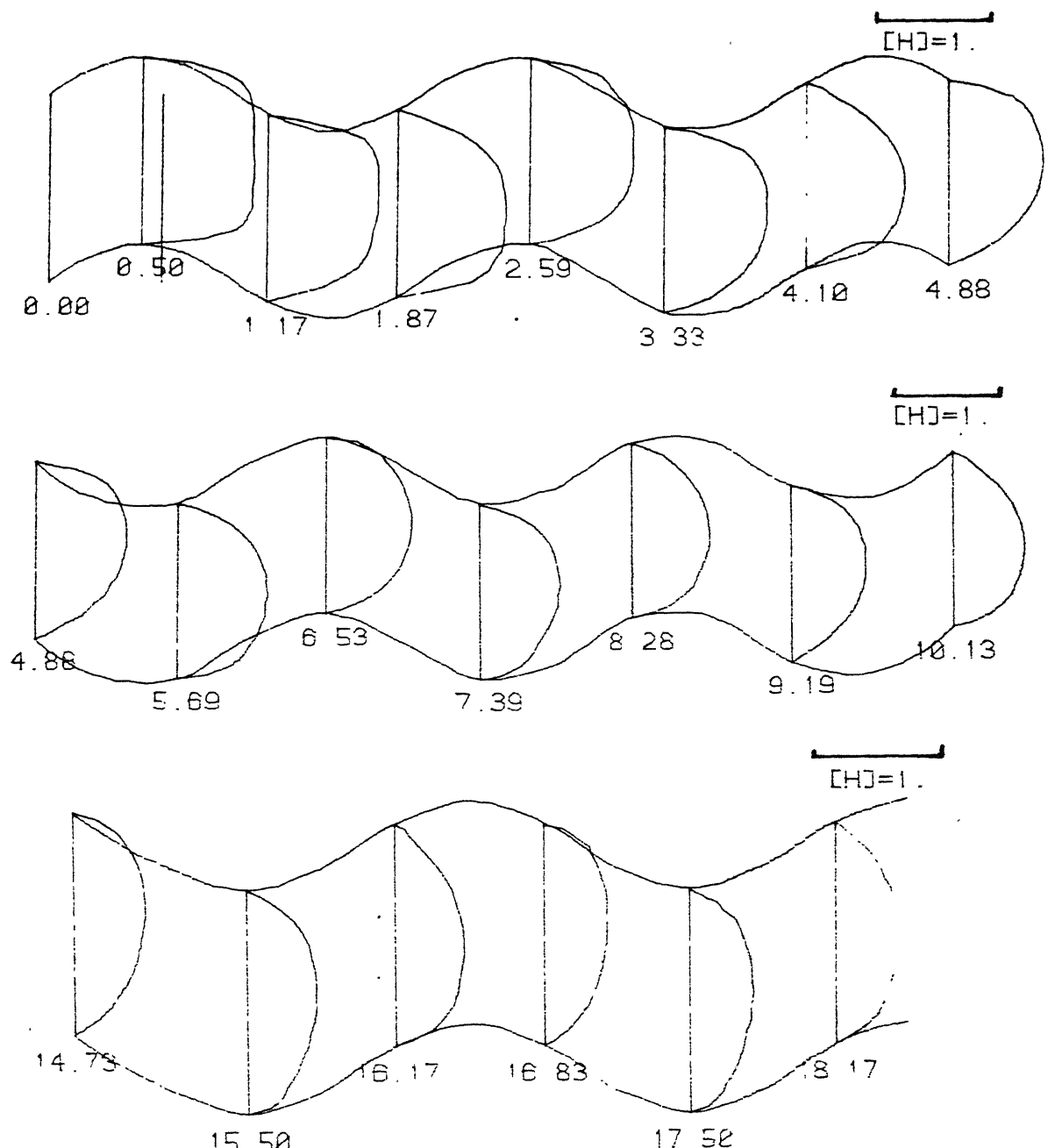


FIG. 68 ENTHALPY PROFILES FOR A NON-SYM. CHANNEL  
WITH  $\lambda=0.20$  AND  $Re=500$

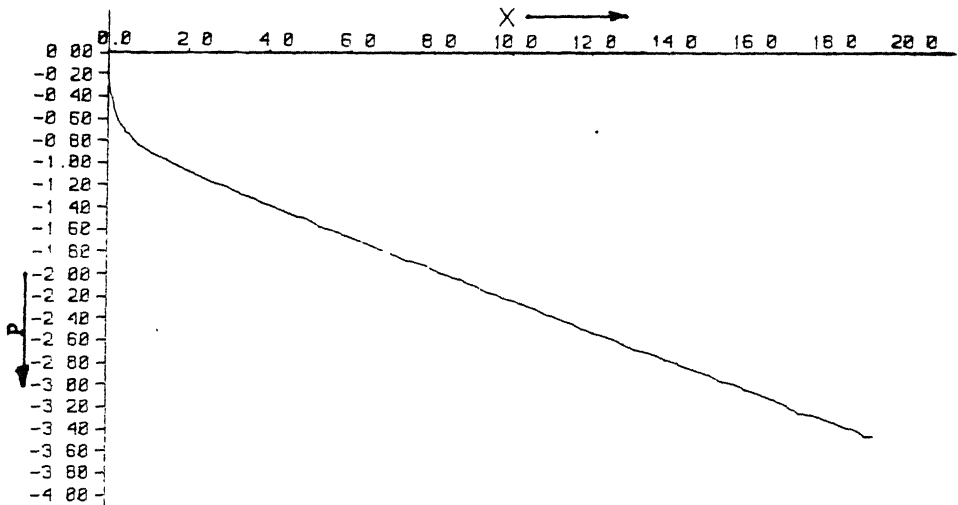


FIG. 69a  
PRESSURE DISTRIBUTION ALONG X FOR A NON-SYM CHANNEL  
WITH LAMBDA=0.12 AND Re=100

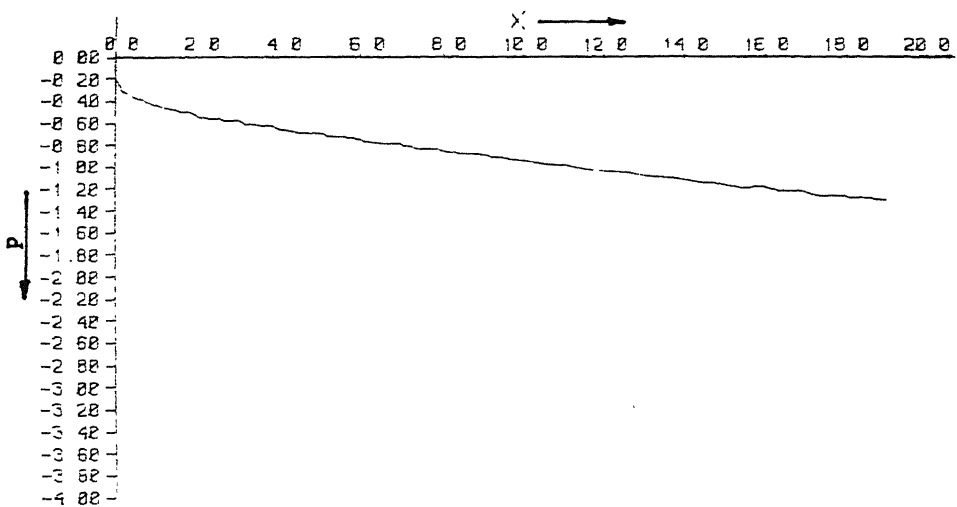


FIG. 69b.  
PRESSURE DISTRIBUTION ALONG X FOR A NON-SYM CHANNEL  
WITH LAMBDA=0.12 AND Re=500

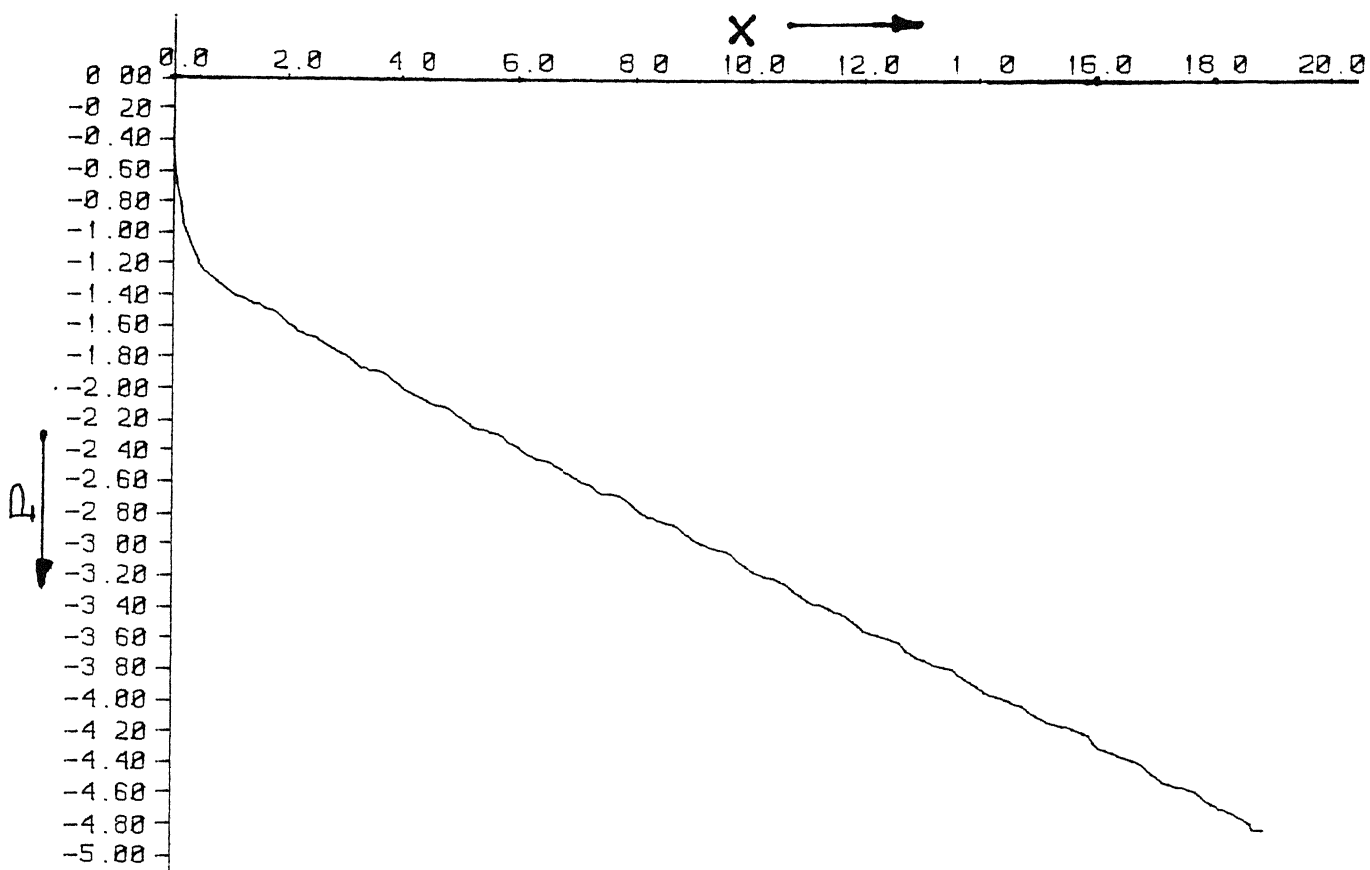


FIG. 70a  
PRESSURE DISTRIBUTION ALONG X FOR A NON-SYM. CHANNEL  
WITH LAMBDA=0.20 AND  $Re=100$ .

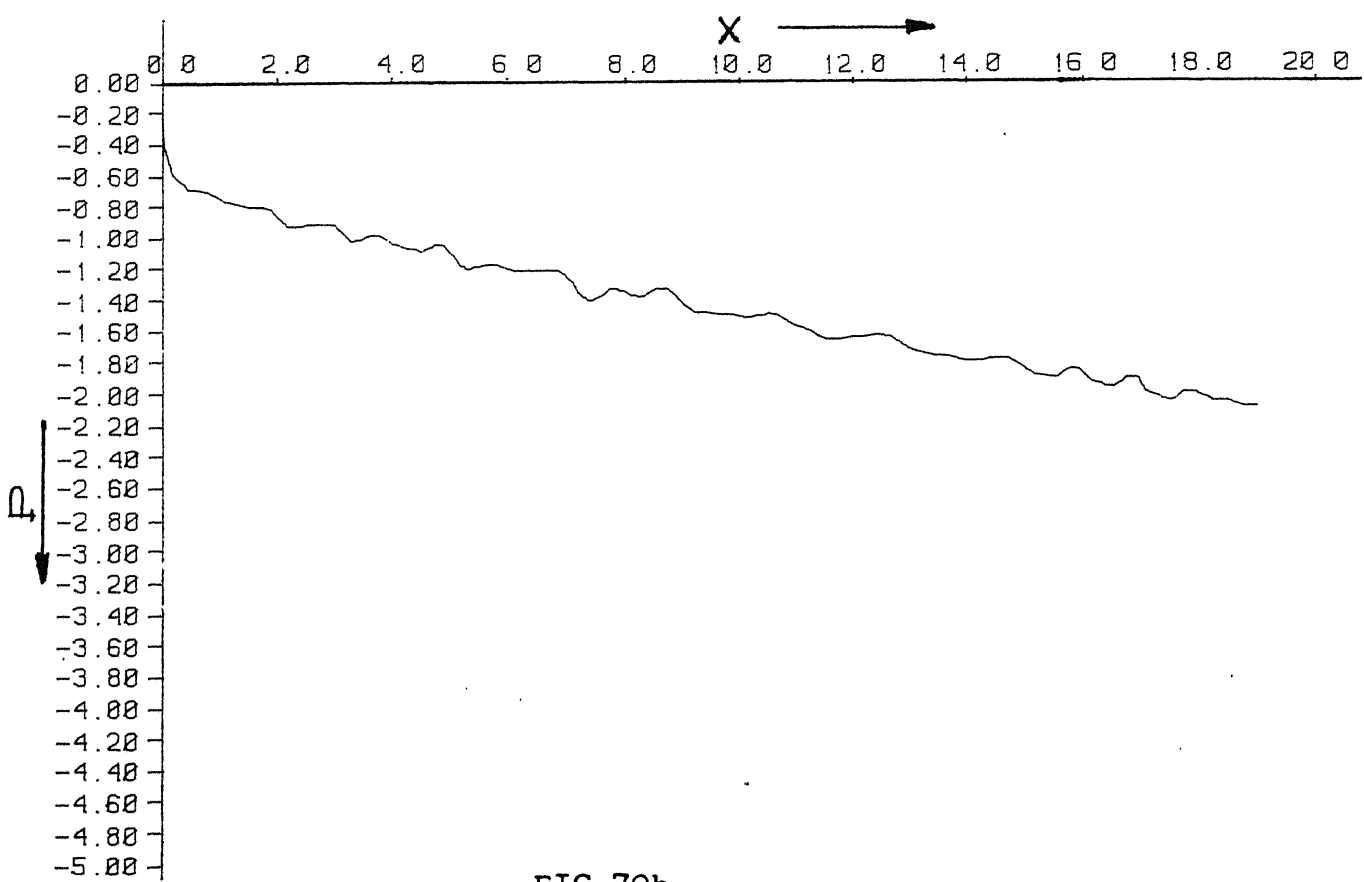
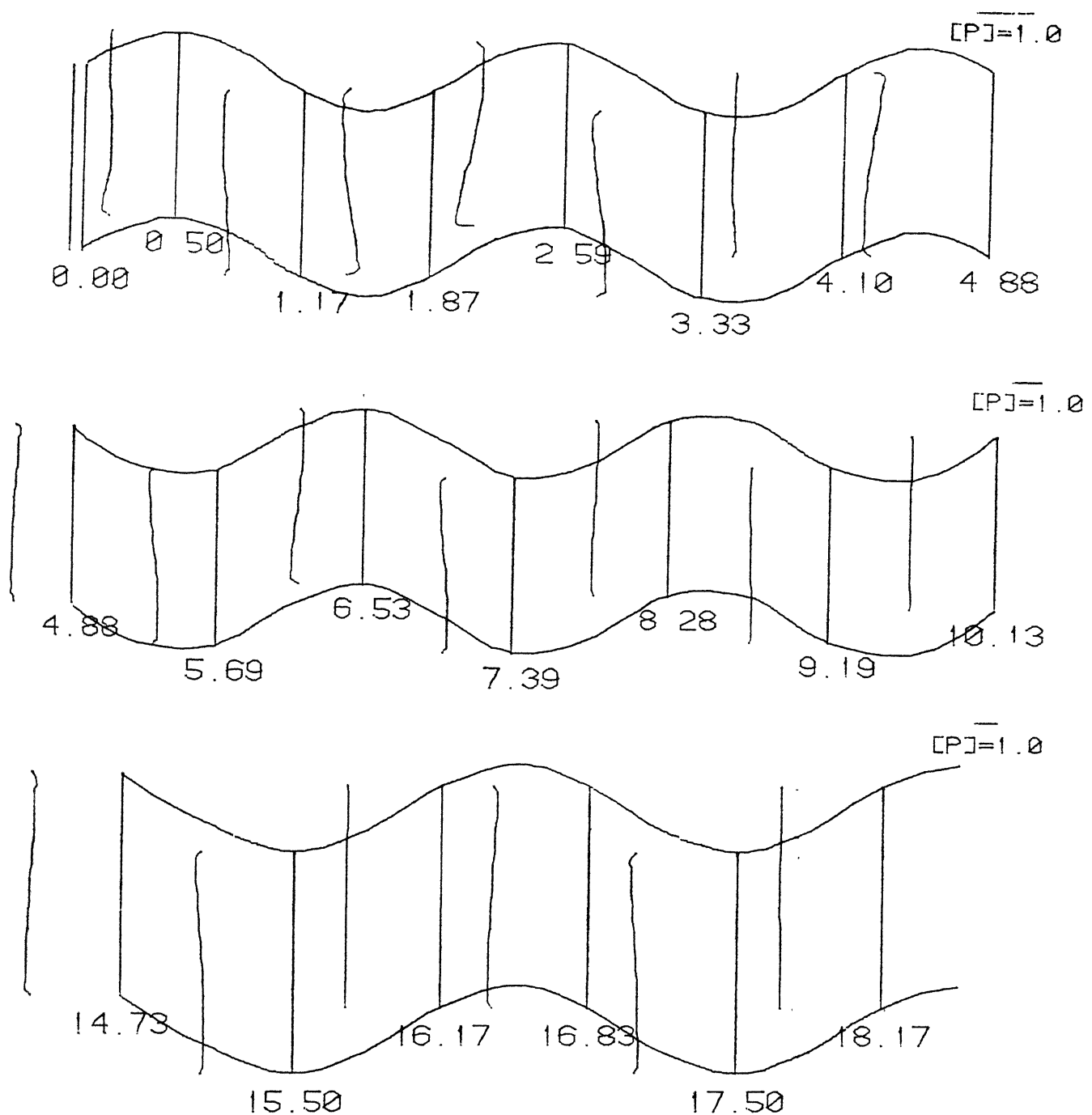


FIG. 70b  
PRESSURE DISTRIBUTION ALONG X FOR A NON-SYM. CHANNEL  
WITH LAMBDA=0.20 AND  $Re=500$ .



PRESSURE DISTRIBUTION ALONG Y FOR A NON-SYM. CHANNEL  
WITH LAMBDA=0.20 AND Re=100.

## Chapter 5

### CONCLUSION

In the present work an analysis has been performed for the solution of two-dimensional laminar, viscous flow through symmetric as well as non-symmetric channels and through converging and diverging pipes. Suitable non-orthogonal algebraic coordinate transformations are used that map the physical irregular domain into a rectangular one. The conservation equations are derived on a control volume basis that ensures global as well as local conservation of mass, momentum and energy. Also, velocity components  $U$  and  $U_\xi$  are used as the primary dependent variables in the momentum equations. Since those components are normal to the control volume faces, evaluation of the mass flow ( $F$ ) and convective fluxes ( $D$ ) passing through the faces is facilitated.

In order to obtain the solution, the discretized conservation equations are solved using the SIMPLEC algorithm [12] which reduces solution cost reasonably. Further reduction in the solution cost has been achieved by using the methodology set forth in [12] for the solution of pressure correction equation. The computer code developed is extremely general in that it can be easily modified to consider turbulent flow and variable fluid properties.

Results found for a fixed  $Pr$  and for various values of  $Re$  and  $\lambda/L$  show the following :

1. In all the cases under consideration, the separated flow region grows with increase of  $Re$  and  $\lambda/L$ .
2. In the case of a symmetric channel or pipe, the separated flow region extends mainly in the diverging portion but for higher  $Re$  and  $\lambda/L$  it occurs in the converging portion as well.
3. In the case of a non-symmetric channel, the resultant velocity  $\vec{U}$  is retarded near the lower boundary and accelerated near the upper boundary when the flow is in the downward direction but this behaviour is reversed when the flow is in the upward direction. Due to this flow separates near the upper boundary in one section while it separates near the lower boundary in the adjacent section.
4. In the case of a symmetric channel or pipe, variation of pressure in the Y-direction is negligible but in the case of a non-symmetric channel this variation is perceptible in the developing region.
5. The distribution of pressure in the X-direction can be express as

$$P(x) = -f(x) + p'(x)$$

where  $p'(x)$  behaves in a periodic fashion from cycle to cycle, and  $f(x)$  is nearly linear in the developing region and linear in the fully developed region for a symmetric channel or pipe. For a non-symmetric channel, however,  $P(x)$  is almost linear throughout.

6. Per-cycle pressure drop  $\Delta P$  in the fully developed region is constant for each cycle and it increases with increase of  $Re$  and  $\lambda/L$ .
7. A point of inflection is observed in the enthalpy profiles in the separated region whereas in the non-separated region this distribution is almost parabolic.
8. In the case of symmetric channel or pipe, the negative V-component at the minimum cross-section and positive V-component at the maximum cross-section increases with  $Re$ . This is due to the effect of inertia [3].
9. In general, the circular geometry enhances the various effects compared to the plane geometry.

## APPENDIX

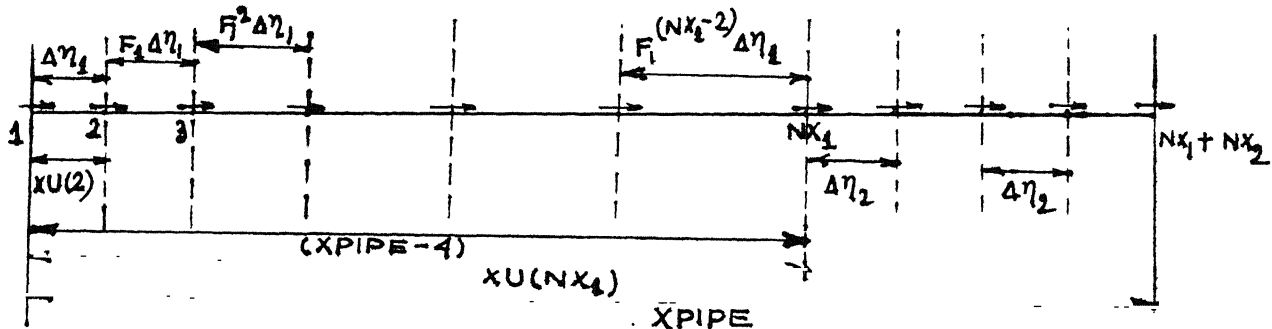
### Discretization of Domain Using $F_1$ and $F_2$ Factor

Here the factors  $F_1$  and  $F_2$  are used for the purpose to generate a non-uniform grid spacing in both the directions. Where

$F_1$  = Expansion factor for grid step-length in the  $\eta$ -direction

$F_2$  = Contraction or expansion factor for grid step-length in the  $\xi$ -direction.  $F_2 \leq 1$  for symmetric channel or pipe and  $F_2 \geq 1$  for non-Symmetric Channel.

#### i) Discretization in the $\eta$ -direction



$$XU(NX_1) = \Delta\eta_1 + F_1 \Delta\eta_1 + \dots + F_1^{(NX_1-2)} \Delta\eta_1$$

$$= \frac{F_1^{(NX_1-1)} - 1}{F_1 - 1} \Delta\eta_1 = f_1 \Delta\eta_1$$

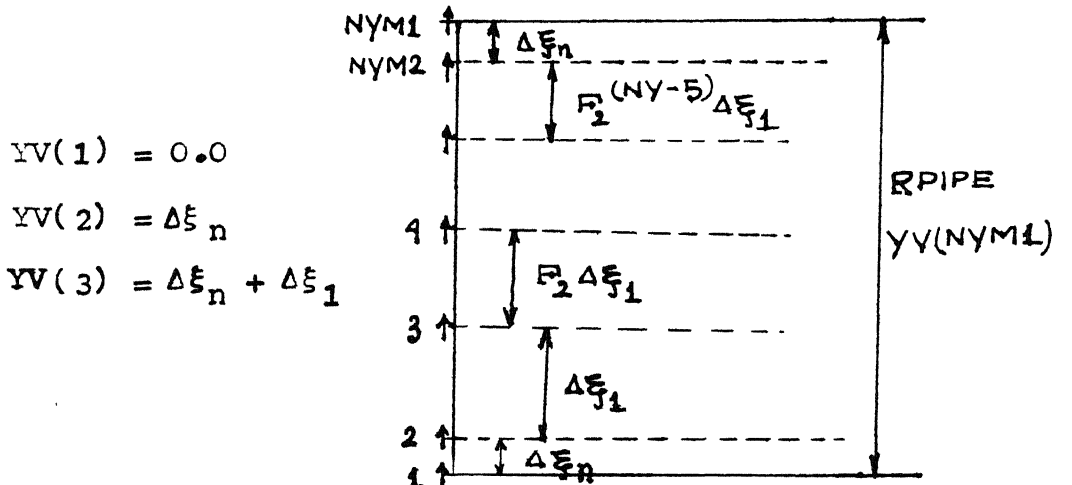
$$\Delta\eta_1 = \frac{XU(NX_1)}{f_1} = \frac{(XPIPE - 4)}{f_1}$$

$$\text{where } f_1 = \frac{F_1^{(NX_1-1)} - 1}{F_1 - 1}$$

$$\Delta \eta_2 = 4/NX_2.$$

ii) Discretization in the  $\xi$ -direction

a) For symmetric channel or pipe



$$YV(1) = 0.0$$

$$YV(2) = \Delta \xi_n$$

$$YV(3) = \Delta \xi_n + \Delta \xi_1$$

$$YV(NYM1) = \Delta \xi_n + YV(NYM2)$$

$$= \Delta \xi_n + \Delta \xi_n + (1 + F_2 + \dots + F_2^{(NYM5)}) \Delta \xi_1$$

$$= 2\Delta \xi_n + \frac{1 - F_2^{NYM4}}{1 - F_2} \Delta \xi_1$$

$$\text{Let } \Delta \xi_n = \frac{1}{2} (F_2^{NYM5} \Delta \xi_1)$$

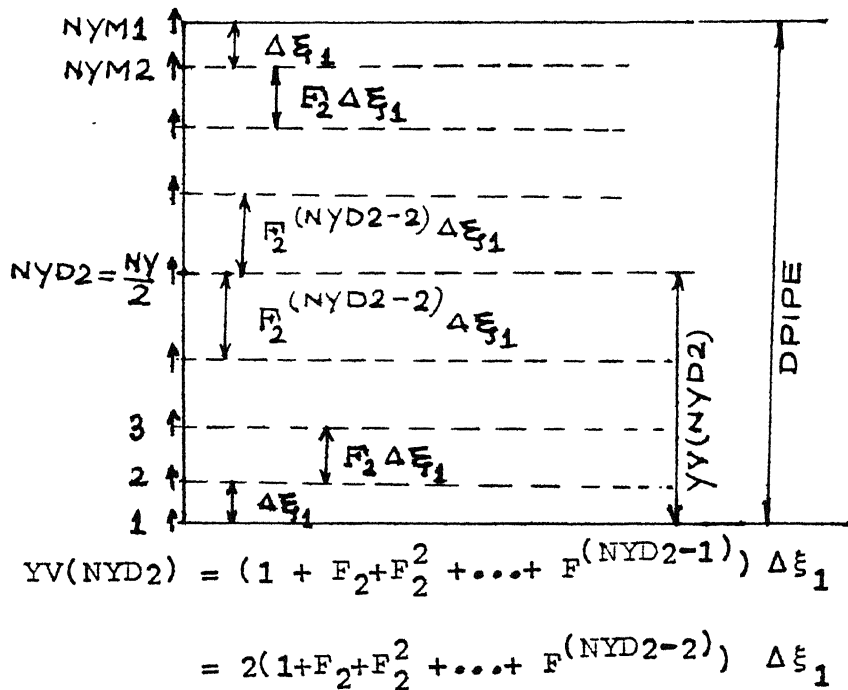
$$\therefore RPIPE = \{F_2^{NYM5} + \frac{1 - F_2^{NYM4}}{1 - F_2}\} \Delta \xi_1$$

$$= f_2 \Delta \xi_1$$

$$\therefore \Delta \xi_1 = RPIPE/f_2$$

$$\text{where } f_2 = F_2^{NYM5} + \frac{1 - F_2^{NYM4}}{1 - F_2}.$$

b) For non-symmetric channel



$$\text{DPipe} = 2 \frac{F^{(\text{NYD2}-1)} - 1}{F_1 - 1} \Delta \xi_1$$

$$= f_2 \Delta \xi_1$$

$$\therefore \Delta \xi_1 = \text{DPipe}/f_2$$

$$\text{where } f_2 = 2 \frac{F^{(\text{NYD2}-1)} - 1}{F_2 - 1}$$

REFERENCES

1. J.C. Burns and T. Parkes, Peristaltic motion, *J. Fluid Mech.*, Vol. 29, PP. 405-416, 1967.
2. S. Tsangaris and E. Leiter, Analytical solutions for weakly-stenosed channels at low Reynolds numbers, *Proc. 1st Int. Conf. Mech. Med. and Biol.*, PP. 289-292, 1978.
3. S. Tsangaris and E. Leiter, On laminar steady flow in sinusoidal channels, *J. Engg. Math.*, Vol. 18, PP. 89-103, 1984.
4. I.J. Sobey, On flow through furrowed channels, Part 1 : Calculated flow patterns, *J. Fluid Mech.*, Vol. 96, PP. 1-26, 1980.
5. K. Vajravelu, Fluid flow and heat transfer in horizontal wavy channels, *Acta Mechanica*, Vol. 35, PP. 245-258, 1980.
6. A.T. Prata and E.M. Sparrow, Heat transfer and fluid flow characteristics for an annulus of periodically varying cross section, *Numerical Heat Transfer*, Vol. 7, PP. 285-304, 1984.
7. S.V. Patankar, *Numerical Heat Transfer and Fluid Flow*, Hemisphere, Washington, D.C., 1980.
8. D.C. Belinfante, On viscous flow in a pipe with constrictions, *Proceed. Cambr. Phil. Soc. (Math. and Phil. Soc.)*, Vol. 58, PP. 405-416, 1962.
9. S.T. Hsu and J.F. Kennedy, Turbulent flow in wavy pipes, *J. Fluid Mech.*, Vol. 47, PP. 481-502, 1972.
10. K.D. Stephanoff, I.J. Sobey, and B.J. Belhouse, On flow through furrowed channels, Part 2 : Observed flow patterns, *J. Fluid Mech.*, Vol. 96, PP. 27-32, 1980.
11. M. Faghri, E.M. Sparrow, and A.T. Prata, Finite-difference solutions of convection-diffusion problems in irregular domains, using a nonorthogonal coordinate transformation, *Numerical Heat Transfer*, Vol. 7, PP. 183-209, 1984.
12. J.P. Van Doormaal and G. Raithby, *Numerical Heat Transfer*, Vol. 7, PP. 147-163, 1984.